

FOR REFERENCE

DO NOT BE TAKEN FROM THIS ROOM

**SCATTERING OF ACOUSTIC WAVES  
BY CYLINDERS WITH ARBITRARY CROSS SECTIONS  
T-MATRIX FORMULATION**

by

BORA GÜNGÖR

B.S. in M.E., Middle East Technical University, 1981

Bogazici University Library



14

39001100315251

Submitted to the Institute for Graduate Studies in  
Science and Engineering in partial fulfillment of  
the requirements for the degree of  
Master of Science  
in  
Mechanical Engineering

Boğaziçi University

1984

SCATTERING OF ACOUSTIC WAVES  
BY CYLINDERS WITH ARBITRARY CROSS SECTIONS  
T-MATRIX FORMULATION

APPROVED BY

Doç. Dr. Ahmet Ceranoğlu  
(Thesis Supervisor)

Ahmet Ceranoğlu

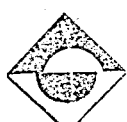
Prof. Dr. Akın Tezel

Akin Tezel

Prof. Dr. Attila Aşkar

Attila Aşkar

DATE OF APPROVAL 22/6/1984



181959

### ACKNOWLEDGEMENTS

I would like to thank Doç.Dr. Ahmet Ceranoğlu, Prof.Dr. Akın Tezel and Prof. Dr. Attila Aşkar for their sincere cooperation and excellent support throughout this work.

SCATTERING OF ACOUSTIC WAVES  
BY CYLINDERS WITH ARBITRARY CROSS SECTIONS  
T-MATRIX FORMULATION

ABSTRACT

In this work, the scattering of steady-state acoustic waves from arbitrarily shaped obstacles in an infinite medium is studied using the T-matrix method. The problem is examined for the two dimensional case where the obstacle is a cylindrical rigid inclusion or a cavity. An acoustic plane wave is considered to be incident on the obstacle.

In the solution of the problem, both incident and scattered wave fields are expanded in series of the circular basis wave functions. The scattered wave field is then evaluated through a transition matrix (T-matrix) which relates the unknown coefficients of the scattered wave series to the coefficients of the incident wave.

Numerical results pertaining to circular, elliptical, rectangular and triangular cross sections are obtained. The results are presented in graphical form and found to be in good agreement compared with the some known exact or approximate solutions available in the literature.

AKUSTİK DALGALARIN  
RASTGELE KESİTLİ SİLİNDİRLERDEN SAÇILIMI  
T-MATRİS FORMULASYONU

KISA ÖZET

Bu çalışmada, akustik dalgaların sonsuz bir ortamda rastgele şekilli engellerden saçılımını, T-matris metodu kullanılarak ele alınmıştır. Problem, iki boyutta, silindirik rüjüt cisimler ve boşluklar için incelenmiştir. Engel üzerine gelen dalganın akustik bir düzlem dalga olduğu düşünülmüştür.

Problemin çözümünde, hem gelen hem de saçılan dalga alanları, dairesel temel dalga fonksiyonları cinsinden seri olarak açılmaktadır. Saçılan dalga alanı, saçılan dalga serisinin katsayılarını gelen dalga serisinin katsayılarına bağlayan bir geçiş matrisi (T-matris) vasıtasiyla hesaplanmaktadır.

Dairesel, eliptik, dikdörtgen ve üçgen kesitli silindirik şekiller için nümerik sonuçlar elde edilmiştir. Sonuçlar, grafikler halinde gösterilmiş ve literatürdeki bazı bilinen kesin veya yaklaşık çözümlerle uyuştuğu görülmüştür.

## TABLE OF CONTENTS

	<u>Page</u>
ACKNOWLEDGEMENTS	iii
ABSTRACT	iv
KISA ÖZET	v
LIST OF FIGURES	viii
LIST OF SYMBOLS	xii
 I. INTRODUCTION	1
 II. THE THEORY OF ACOUSTIC WAVES	4
2.1 Equations of Hydrodynamics	4
2.2 Harmonic Wave Motion in Acoustic Fields	6
2.3 Solution of the Helmholtz Equation	7
2.3.1 Acoustic Plane Wave	8
2.3.2 General Solution	9
 III. T-MATRIX FORMULATION	12
3.1 Basis Wave Functions	12
3.2 Orthogonality of the Basis Functions	15
3.3 Wave Function Expansions	21
3.3.1 The Incident Wave Field	23
3.3.2 The Scattered Wave Field	25
3.4 Boundary Conditions	28
3.4.1 Neumann Type Boundary Condition	28
3.4.2 Dirichlet Type Boundary Condition	29
3.5 The Transition Matrix	30
3.6 Structure of the Q-Matrix	31

	<u>Page</u>
3.7 Properties of the T-Matrix	34
3.8 Presentation of the Scattered Wave Field	35
3.8.1 Near Field Solutions	37
3.8.2 Far Field Solution	38
3.8.3 Total Scattering Cross Section	40
IV. NUMERICAL EVALUATIONS	41
4.1 General Procedure for the Evaluation of the Q-Matrix Elements	42
4.2 Creation of the T-Matrix	48
4.3 Numerical Examples	49
4.3.1 Circular Cylinders	50
4.3.2 Elliptical Cylinders	51
4.3.3 Rectangular Cylinders	52
4.3.4 Triangular Cylinders	54
V. CONCLUSIONS	56
APPENDIX A. SIMPSON'S APPROXIMATE INTEGRATION FORMULA	124
APPENDIX B. ANALYTICAL EXPRESSIONS FOR THE ELEMENTS OF THE Q-MATRIX	126
APPENDIX C. NUMERICAL EXPRESSIONS FOR THE ELEMENTS OF THE Q-MATRIX	128
APPENDIX D. COMPUTER PROGRAM LISTING	131
BIBLIOGRAPHY	170
REFERENCES NOT CITED	172

## LIST OF FIGURES

	<u>Page</u>
FIGURE 2.1 Representation of a plane wave incidence	8
FIGURE 3.1 Geometry of an infinite cylindrical obstacle	14
FIGURE 3.2 Geometry for a constant cross sectional scatterer	17
FIGURE 3.3 Geometry for a plane wave incidence on a cylindrical scatterer	22
FIGURE 4.1 Geometrical representation of the unit normal vector	43
FIGURE 4.2 Boundary subdivision	46
FIGURE 4.3 Interval subdivision	48
FIGURE 4.4 Geometry for the circular cylindrical scatterer	50
FIGURE 4.5 Boundary geometry of the elliptic cylinder	51
FIGURE 4.6 Boundary geometry of the round cornered rectangular cylinder	52
FIGURE 4.7 Boundary geometry of the triangular cylinder	55
FIGURE 4.8 Velocity potential distribution, $ u^s/A $ , at the boundary of a rigid circular inclusion due to the scattered wave field	61
FIGURE 4.9 Far field amplitude, $ f/A $ , due to the scattered wave field from a rigid circular inclusion	63
FIGURE 4.10 Far field amplitude, $ f/A $ , due to the scattered wave field from a circular cavity	65

	<u>Page</u>
FIGURE 4.11 Velocity potential distribution, $ u^s/A $ , at the boundary of a rigid elliptical inclusion due to the scattered wave field for $\alpha = 0^\circ$ and $b/a = 0.5$	67
FIGURE 4.12 Velocity potential distribution, $ u^s/A $ , at the boundary of a rigid elliptical inclusion due to the scattered wave field for $\alpha = 0^\circ$ and $b/a = 2.0$	69
FIGURE 4.13 Far field amplitude, $ f/A $ , due to the scattered wave field from a rigid elliptical inclusion for $b/a = 0.5$	71
FIGURE 4.14 Far field amplitude, $ f/A $ , due to the scattered wave field from a rigid elliptical inclusion for $b/a = 2.0$	73
FIGURE 4.15 Far field amplitude, $ f/A $ , due to the scattered wave field from a rigid elliptical inclusion for $b/a = 5.0$	75
FIGURE 4.16 Far field amplitude, $ f/A $ , due to the scattered wave field from an elliptical cavity for $b/a = 0.5$	77
FIGURE 4.17 Far field amplitude, $ f/A $ , due to the scattered wave field from an elliptical cavity for $b/a = 2.0$	79
FIGURE 4.18 Far field amplitude, $ f/A $ , due to the scattered wave field from an elliptical cavity for $b/a = 5.0$	81
FIGURE 4.19 Velocity potential distribution, $ u^s/A $ , at the boundary of a rigid rectangular inclusion due to the scattered wave field for $\alpha = 0^\circ$ , $r_c/a = 0.1$ and $b/a = 0.5$	83
FIGURE 4.20 Velocity potential distribution, $ u^s/A $ , at the boundary of a rigid rectangular inclusion due to the scattered wave field for $\alpha = 0^\circ$ , $r_c/a = 0.1$ and $b/a = 2.0$	85
FIGURE 4.21 Effect of the corner radius on the far field amplitude, $ f/A $ , due to the scattered wave field from a rigid rectangular inclusion for $\alpha = 0^\circ$ and $b/a = 1.0$	87

Page

FIGURE 4.22	Effect of the corner radius on the far field amplitude, $ f/A $ , due to the scattered wave field from a rigid rectangular inclusion for $\alpha = 0^\circ$ and $b/a = 0.5$	88
FIGURE 4.23	Far field amplitude, $ f/A $ , due to the scattered wave field from a rigid rectangular inclusion for $r_c/a = 0.1$ and $b/a = 1.0$	89
FIGURE 4.24	Far field amplitude, $ f/A $ , due to the scattered wave field from a rigid rectangular inclusion for $r_c/a = 0.1$ and $b/a = 0.5$	91
FIGURE 4.25	Far field amplitude, $ f/A $ , due to the scattered wave field from a rigid rectangular inclusion for $r_c/a = 0.1$ and $b/a = 2.0$	93
FIGURE 4.26	Far field amplitude, $ f/A $ , due to the scattered wave field from a rigid rectangular inclusion for $r_c/a = 0.1$ and $b/a = 5.0$	95
FIGURE 4.27	Far field amplitude, $ f/A $ , due to the scattered wave field from a rigid rectangular inclusion for $r_c/a = 0.1$ and $b/a = 10.0$	97
FIGURE 4.28	Effect of the corner radius on the far field amplitude, $ f/A $ , due to the scattered wave field from a rectangular cavity for $\alpha = 0^\circ$ and $b/a = 1.0$	99
FIGURE 4.29	Effect of the corner radius on the far field amplitude, $ f/A $ , due to the scattered wave field from a rectangular cavity for $\alpha = 0^\circ$ and $b/a = 0.5$	100
FIGURE 4.30	Far field amplitude, $ f/A $ , due to the scattered wave field from a rectangular cavity for $r_c/a = 0.1$ and $b/a = 1.0$	101
FIGURE 4.31	Far field amplitude, $ f/A $ , due to the scattered wave field from a rectangular cavity for $r_c/a = 0.1$ and $b/a = 0.5$	103
FIGURE 4.32	Far field amplitude, $ f/A $ , due to the scattered wave field from a rectangular cavity for $r_c/a = 0.1$ and $b/a = 2.0$	104
FIGURE 4.33	Far field amplitude, $ f/A $ , due to the scattered wave field from a rectangular cavity for $r_c/a = 0.1$ and $b/a = 5.0$	106

	<u>Page</u>
FIGURE 4.34 Far field amplitude, $ f/A $ , due to the scattered wave field from a rectangular cavity for $r_c/a = 0.1$ and $b/a = 10.0$	108
FIGURE 4.35 Velocity potential distribution, $ u^s/A $ , at the boundary of a rigid triangular inclusion due to the scattered wave field for $\alpha = 0^\circ$ and $\beta = 60^\circ$	109
FIGURE 4.36 Far field amplitude, $ f/A $ , due to the scattered wave field from a rigid triangular inclusion for $\beta = 60^\circ$	111
FIGURE 4.37 Far field amplitude, $ f/A $ , due to the scattered wave field from a rigid triangular inclusion for $\beta = 30^\circ$	113
FIGURE 4.38 Far field amplitude, $ f/A $ , due to the scattered wave field from a rigid triangular inclusion for $\beta = 0.001^\circ$	115
FIGURE 4.39 Far field amplitude, $ f/A $ , due to the scattered wave field from a triangular cavity for $\beta = 60^\circ$	117
FIGURE 4.40 Far field amplitude, $ f/A $ , due to the scattered wave field from a triangular cavity for $\beta = 30^\circ$	119
FIGURE 4.41 Far field amplitude, $ f/A $ , due to the scattered wave field from a triangular cavity for $\beta = 0.001^\circ$	121

## LIST OF SYMBOLS

$A$	Constant amplitude factor of the incident wave
$a_m^\sigma, a_m$	Coefficients of the series representing the incident wave field
$\tilde{a}$	Coefficient vector for the incident wave with elements $a_m$
$a, b$	Half major and minor axes for elliptical and rectangular geometries
$B$	Bulk modulus of the medium
$c$	Wave speed
$c_s$	A constant multiplication factor associated with the Simpson's integration
$c_m^\sigma, c_m$	Coefficients of the series representing the scattered wave field
$\tilde{c}$	Coefficient vector for the scattered wave with elements $c_m$
$\underline{e}_1, \underline{e}_2$	Unit vectors along the $x$ and $y$ directions of the Cartesian coordinate system
$\underline{e}_r, \underline{e}_\theta$	Unit radial and tangential vectors in polar coordinate system
$f$	Farfield amplitude of the scattered wave field
$h$	Height of an isosceles triangle along its symmetry axis
$H_n$	$n$ -th order cylindrical Hankel function of the first kind
$J_n$	$n$ -th order cylindrical Bessel function of the first kind
$k, \underline{k}$	Wave number and wave normal vector, respectively

$\hat{n}$	Unit outward normal vector along the boundary of the scatterer
$\partial/\partial n$	Directional derivative along the unit normal $\hat{n}$
N	Number of the boundary segments used in the numerical evaluation of the boundary integrals
p	Pressure
P	Order of the Simpson's rule used in the numerical integrations
$\hat{Q}_{\approx}$	A matrix with elements involving integrals over the boundary of the scatterer
$\hat{Q}_{\approx}$	Real part of the $\hat{Q}$ -matrix
$\hat{Q}_{\approx}^{11}, \hat{Q}_{\approx}^{12}, \hat{Q}_{\approx}^{21}, \hat{Q}_{\approx}^{22}$	Submatrices of the $\hat{Q}$ -matrix
$Q_{jm}^{\sigma\nu}, Q_{jm}^{\nu\sigma}$	Elements of the $\hat{Q}$ -matrix
$(r, \theta)$	Coordinates of a point in circular polar coordinate system
$\underline{r}$	Position vector in polar coordinate system
$r_{iq}, \theta_{iq}, q=0, \dots, P$	Coordinates of the integration points on the i-th boundary segment
$r_c$	Corner radius of a round cornered rectangle
S	Boundary of the cross section of an infinite cylinder
$S_+, S_\infty$	Two arbitrary circular curves enclosing S
$r_+, r_\infty$	Radii of the curves $S_+, S_\infty$
$\Delta S_i, i = 1, \dots, N$	i-th boundary segment along S
$\hat{T}_{\approx}$	Transition matrix (T-matrix)
$\hat{T}_{\approx}^{11}, \hat{T}_{\approx}^{12}, \hat{T}_{\approx}^{21}, \hat{T}_{\approx}^{22}$	Submatrices of the T-matrix
$u^i, u^S, u^-$	Incident, scattered and total wave fields outside the scatterer, respectively
$u^+$	Total wave field at the boundary of the scatterer
$\underline{v}$	Velocity field

$w_q$ , $q = 0, \dots, P$	Weighing factors associated with the Simpson's formula
$(x, y, z)$	Coordinates of a point in Cartesian coordinate system
$Y_n$	n-th order cylindrical Bessel function of the second kind
$\alpha$	Incidence angle of a plane wave
$\alpha_m^\sigma, \alpha_m$	Coefficients of the series representing the wave field at the surface of the scatterer
$\tilde{\alpha}$	Coefficient vector for the surface wave field with elements $\alpha_m$
$\beta$	Tip angle for the isosceles triangular cross section
$\delta_{mn}$	Kronecker delta
$\varepsilon_n$	Neumann factor
$\Delta\theta_i$	i-th angular interval associated with $S_i$
$\theta_{a_i}, \theta_{b_i}$	Lower and upper angles of the i-th angular interval
$\lambda$	Wavelength
$\rho$	Density distribution in the medium
$\rho_0$	Equilibrium density of the medium
$\sigma_{tot}$	Total scattering cross section
$\phi$	Velocity potential function
$\psi$	Spatial part of the velocity potential function
$\psi_n^\sigma, \hat{\psi}_n, \hat{\psi}_n^\sigma, \hat{\psi}_n$	Basis functions for two-dimensional scalar waves
$\tau_n^\sigma$	Angular part of the basis functions
$\omega$	Angular frequency

## I. INTRODUCTION

When a wave propagating in an unbounded homogeneous medium encounters an obstacle immersed in the medium, its propagation path changes and while a portion of it is reflected back into the medium as a secondary wave emitted by the obstacle the other part of it, if the obstacle is not a cavity, is refracted into the body of the obstacle. The radiation of these secondary waves from the obstacle is called scattering. The obstacle may be a cavity or an inclusion with physical properties differing from those of the surrounding medium.

Scattering and diffraction problems have become increasingly important in the recent years, particularly in the areas of remote sensing, seismic exploration, oil technology, underwater sound detection and especially in non-destructive testing of materials where the scattered wave form is used to identify the shapes and the sizes of the material defects such as voids, cracks or inclusions.

In solving the scattering problems, especially where explicit numerical results are desired, four methods are extensively employed in the literature. These are method of separation-of-variables, variational method, integral equation method and the transition matrix (T-matrix) method which has been recently developed [1].

The method of separation of variables is usually employed in finding exact analytical solutions for only a class of objects bounded by quadric surfaces, [2-5]. Hence, the method restricts the shape of the scatterer to simple geometries, like sphere, circular and elliptic cylinders, such that their boundary geometries can be expressed conveniently in separable coordinates. The variational method is another method used in the scattering problem solutions and, from the theoretical point of view, it is applicable for arbitrary boundary geometries, [3,6,7]. However, this method especially for general geometries, requires the evaluation of repeated surface or volume integrals with singular kernels. Thus this method is also restricted to relatively simple geometries. The third method, namely the integral equation method, consists of approximating an integral over the surface of the scatterer by a finite sum and then computing the quantities like displacements, velocity potentials at many discrete points by solving the resulting system of equations numerically, [8]. In previous years, several applications of this approach have appeared in the literature [6,9-11].

The latest method developed for the solution of the wave scattering problems is the T-matrix method which was first introduced by Waterman [1] for acoustic waves and reformulated by Pao [12] for elastic waves. The method starts directly with the Helmholtz integral formula, and uses either cylindrical or spherical wave functions for bodies of arbitrary shape. Both incident and scattered waves are represented as a series of the common wave functions, known as the basis functions. The unknown coefficients of the scattered wave series are then related by a transition matrix (T-matrix) to the coefficients of the incident

wave, [1,12]. The elements of the T-matrix are integrals of basis functions and their normal derivatives over the bounding surface of the scatterer, which can be evaluated numerically even for bodies of complex geometry.

The key feature of the method lies in the fact that the T-matrix is fixed for a specific boundary type and geometry and wave number of the incident wave. Hence, once it is created, the scattered field quantities at various regions of the medium for different incidence angles of the impinging wave can be calculated. The method, comparing with the variational and integral equation techniques, has also a computational advantage because the integrals involved in the formulation are only single surface integrals with no singularities in their integrands. In the recent years, several applications of T-matrix approach to the scattering of acoustic and elastic waves by finite elliptic cylinders [13,14], spheroids [14], finite circular cylinders [15], infinite strips [1,16] have verified the power of the method.

In this work, we have considered the scattering of the plane acoustic waves by infinite cylinders. The near and far field results for cavity and rigid inclusion cases are presented. A brief review of the governing equations for acoustic fields is given in Chapter 2. In Chapter 3, formulation of the transition matrix for the scattering problem is given. The numerical methods employed in the solutions are discussed in Chapter 4 where solutions to specific problems are also given. Results pertaining to circular, elliptical, rectangular and triangular geometries are presented in polar graphical form.

## II. THE THEORY OF ACOUSTIC WAVES

In this section, the reduction of the general equations of hydrodynamics to the Helmholtz reduced wave equation describing the motion of the harmonic disturbances in a fluid is discussed briefly. Also, a general solution of the Helmholtz equation is given for polar coordinates.

### 2.1 EQUATIONS OF HYDRODYNAMICS

To study the wave propagation in a fluid medium, the starting equations are the hydrodynamical equations of motion due to Euler [17]:

$$\rho \left[ \frac{\partial \underline{v}}{\partial t} + \underline{v} \cdot \nabla \underline{v} \right] = -\nabla p , \quad (2.1)$$

$$\frac{\partial \rho}{\partial t} + \nabla \cdot (\rho \underline{v}) = 0 , \quad (2.2)$$

$$p = p(\rho) , \quad (2.3)$$

where  $\rho$  is the density,  $p$  is the pressure and  $\underline{v}$  is the fluid velocity vector at any point. This set of equations, which are valid for an ideal fluid, is complete and consists of the equation of motion (2.1), the equation of continuity (2.2), and the equation of state (2.3).

Whenever a disturbance is created at any point inside the fluid it will propagate throughout the medium. In order to obtain the

governing equations of motion regarding the propagation of this disturbance, one assumes that the relative perturbations from the initial equilibrium state are small, that is,

$$\frac{\rho'}{\rho_0} = \frac{\rho - \rho_0}{\rho_0} \sim \mu, \quad \frac{p'}{p_0} = \frac{p - p_0}{p_0} \sim \mu, \quad (2.4)$$

where  $\rho_0$  and  $p_0$  are the equilibrium density and pressure, respectively, while  $\mu$  is some small parameter denoting the variations from the equilibrium values. Under these conditions, the fluid velocity  $v$  with which the fluid particles oscillate is a small quantity of the order of  $\mu$  relative to the propagation speed of the disturbance. This is the case, actually, in acoustics. Since, acoustical wave lengths are long, the variations in the velocity field,  $v$ , are very small quantities. Thus, neglecting the term  $v \cdot \nabla v$  in Eq. (2.1), we get

$$\rho \frac{\partial v}{\partial t} = -\nabla p. \quad (2.5)$$

Substitution of the expressions  $\rho = \rho_0 + \rho'$  and  $p = p_0 + p'$  into the Eqs. (2.5), (2.2) and (2.3) yields

$$\rho_0 \frac{\partial v}{\partial t} = -\nabla p', \quad (2.6)$$

$$\frac{\partial \rho'}{\partial t} + \rho_0 \nabla \cdot v = 0, \quad (2.7)$$

$$p' = \frac{dp}{dp'} \rho' \quad (2.8)$$

where we have neglected the terms involving the products of the perturbed quantities. For the reduction of this set to a single equation, it is convenient to introduce a scalar function  $\phi$  such that

$$\underline{v} = \nabla\phi \quad (2.9)$$

The function  $\phi$  in the above equation is called the velocity potential. Then, Eqs. (2.6) and (2.7) yields

$$p' = -\rho_0 \frac{\partial\phi}{\partial t}, \quad (2.10)$$

$$\frac{\partial p'}{\partial t} + \rho_0 \nabla^2\phi = 0 \quad (2.11)$$

Eliminating the variables  $p'$  and  $\rho'$  from the above equations, we obtain the equation of motion of the disturbance,

$$\frac{\partial^2\phi}{\partial t^2} - c^2 \nabla^2\phi = 0 \quad (2.12)$$

This is a scalar wave equation describing the motion of a disturbance in an acoustic field where the propagation speed of the disturbance is  $c$ ,

$$c = \sqrt{dp/d\rho} \quad , \quad (2.13)$$

or, in general  $c$  can also be written in the form

$$c = \sqrt{B/\rho_0} \quad , \quad (2.14)$$

where  $B$  is the bulk modulus of the fluid.

## 2.2 HARMONIC WAVE MOTION IN ACOUSTIC FIELDS

Considering a disturbance which is harmonic in time and has a circular frequency of  $\omega$ , one can write the velocity potential as

$$\phi(x, y, z, t) = \psi(x, y, z) e^{-i\omega t}, \quad (2.15)$$

where  $\psi$  is the spatial part of the velocity potential function,  $\phi$ .

Substituting Eq. (2.15) into Eq. (2.12) and rearranging the terms, we get

$$\nabla^2\psi + k^2\psi = 0 \quad , \quad (2.16)$$

where  $k = \omega/c$  is the wave number. Eq. (2.16) is known as the Helmholtz reduced wave equation and describes the motion of the acoustic harmonic waves in a fluid medium.

It should also be noted that use of the velocity potential formulation is indeed a convenient way for acoustic wave propagation. However,  $\phi$  is not a measurable quantity like velocity or pressure but it is possible to obtain such quantities from it. For example, substitution of Eq. (2.15) into (2.10) yields

$$p = p_0 + i\omega p_0 \phi \quad . \quad (2.17)$$

### 2.3 SOLUTION OF THE HELMHOLTZ EQUATION

Since throughout this work scattering of the plane waves by infinite cylinders with constant cross-sections will be studied and the wave normals of the incident waves which will be considered are perpendicular to the axes of the cylinders, the dimensionality of the problem reduces to two and it is convenient to obtain the solution of the Helmholtz equation in polar coordinates.

### 2.3.1 Acoustic Plane Wave

A harmonic plane wave of magnitude  $A$  propagating in an acoustic field can be expressed as

$$\phi(\underline{r}, \theta, t) = A e^{i(\underline{k} \cdot \underline{r} - \omega t)} \quad (2.18)$$

Note that we can write the vectors  $\underline{r}$  and  $\underline{k}$  as

$$\underline{r} = r(\cos\theta \underline{e}_1 + \sin\theta \underline{e}_2) ; \quad r = |\underline{r}| , \quad (2.19)$$

$$\underline{k} = k(\cos\alpha \underline{e}_1 + \sin\alpha \underline{e}_2) ; \quad k = |\underline{k}| = \omega/c , \quad (2.20)$$

respectively. In this case, Eq. (2.18) can be written as

$$\phi = A e^{ikr \cos(\theta - \alpha)} e^{-i\omega t} , \quad (2.21)$$

where  $\theta$  and  $\alpha$  are the angles that the vectors  $\underline{r}$  and  $\underline{k}$  make with the  $x$ -axis and  $\underline{e}_1$ ,  $\underline{e}_2$  are the unit vectors along the  $x$  and  $y$  directions of the Cartesian coordinate system (Fig. 2.1).

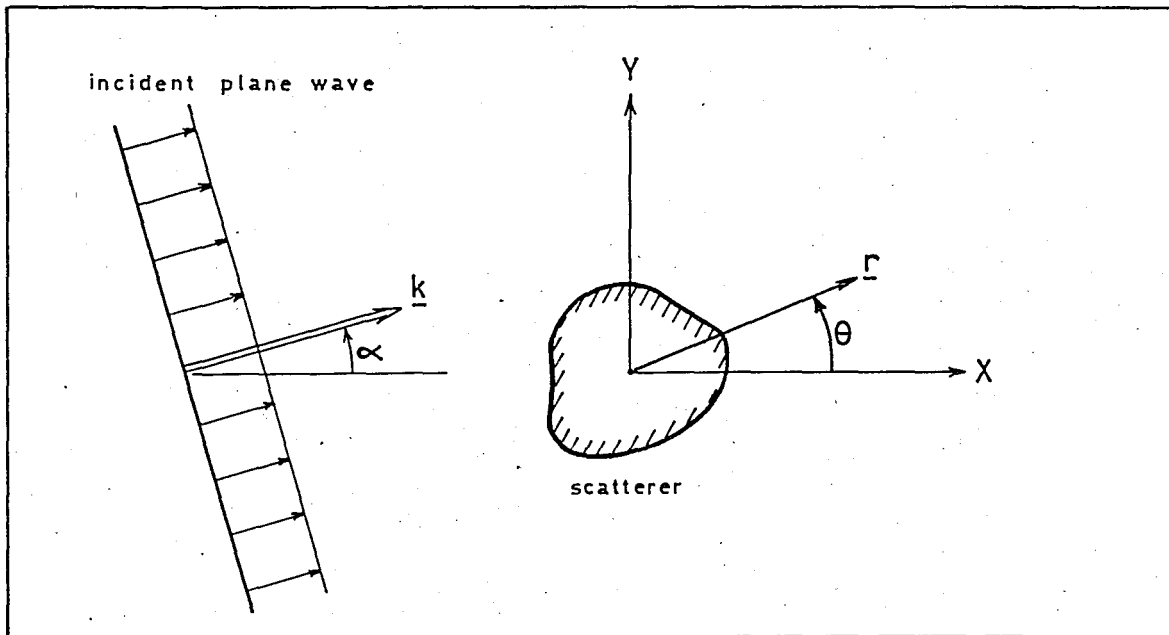


Figure 2.1 - Representation of a plane wave incidence.

Comparing Eq. (2.21) with Eq. (2.15) one can write the spatial part of  $\phi$  as

$$\psi(r, \theta) = Ae^{ikrcos(\theta-\alpha)} \quad (2.22)$$

Note that  $\psi$  given by Eq. (2.22) does satisfy the Helmholtz equation, Eq. (2.16).

### 2.3.2 General Solution

In polar coordinates, the Laplacian operator,  $\nabla^2$ , is given as

$$\nabla^2 = \frac{1}{r} \frac{\partial}{\partial r} \left( r \frac{\partial}{\partial r} \right) + \frac{1}{r^2} \frac{\partial^2}{\partial \theta^2}, \quad (2.23)$$

thus, Eq. (2.16) takes the form

$$\frac{1}{r} \frac{\partial}{\partial r} \left( r \frac{\partial \psi}{\partial r} \right) + \frac{1}{r^2} \frac{\partial^2 \psi}{\partial \theta^2} + k^2 \psi = 0 \quad (2.24)$$

The most common method used in obtaining the general solution of Eq. (2.24) is the method of separation-of-variables where a solution of the form

$$\psi(r, \theta) = R(r)T(\theta) \quad (2.25)$$

is assumed. Upon substitution of the above solution into Eq. (2.24) one can show that the latter equation reduces to two separate equations of the form

$$r^2 \frac{d^2 R}{dr^2} + r \frac{dR}{dr} + (k^2 r^2 - n^2)R = 0, \quad (2.26)$$

$$\frac{d^2T}{d\theta^2} + n^2 T = 0 \quad (2.27)$$

Eq. (2.26) is the well-known Bessel's Differential Equation and has its solution either as

$$R = A_n J_n(kr) + B_n Y_n(kr), \quad (2.28)$$

or,

$$R = A_n H_n^{(1)}(kr) + B_n H_n^{(2)}(kr). \quad (2.29)$$

$J_n(kr)$  and  $Y_n(kr)$  are known as the  $n$ -th order cylindrical Bessel functions of the first and second kind while  $H_n^{(1)}(kr)$  and  $H_n^{(2)}(kr)$  are the  $n$ -th order Hankel functions of the first and second kind, respectively. The unknown constants  $A_n$  and  $B_n$  are to be determined from the boundary conditions impending on the problem.

The solution of Eq. (2.27) can be written as

$$T = e^{\pm in\theta} = \begin{pmatrix} \cos(n\theta) \\ \sin(n\theta) \end{pmatrix} \quad (2.30)$$

Hence, combining the solutions (2.28), (2.29), (2.30) and the time factor  $\exp[-i\omega t]$ , one obtains the general solution as

$$\phi(r, \theta, t) = [A_n I_n^{(1)}(kr) + B_n I_n^{(2)}(kr)] \begin{pmatrix} \cos(n\theta) \\ \sin(n\theta) \end{pmatrix} e^{-i\omega t}, \quad (2.31)$$

where  $I_n^{(1)}$  and  $I_n^{(2)}$  are the cylindrical Bessel or Hankel functions of the first and second kind, depending on the physics of the problem.

If a wave progressing through a medium encounters an obstacle immersed in the medium, scattering phenomenon takes place and the wave field becomes different from what it would have been in the absence of the obstacle. In general, the solution to the scattering problem of an acoustic wave propagation in an infinite fluid medium, requires the solution of the Helmholtz equation satisfying the boundary conditions prescribed over a discontinuity surface, called scatterer. In order to solve this problem, the usual method of attack is to try to satisfy the boundary conditions impending on the problem so as to obtain an exact solution directly from the general solution (Eq. 2.31) obtained by the method of separation-of-variables. However, this type of approach is successful only if the geometry of the curve  $S$  representing the boundary of the scatterer is such that  $S$  coincides with an orthogonal curvilinear coordinate system in which the Helmholtz equation separates. Hence, the analytical solutions are possible only for simple geometries like circular and elliptic cylinders. Exact solutions are available for circular cylinders using circular polar coordinates and Bessel functions, and for elliptic cylinders using elliptic coordinates and Mathieu functions. Thus, for general boundary geometries one of the various approximation techniques must be employed in the solution of the scattering problems. The transition matrix formulation, shortly called T-matrix method, is the latest technique developed for this purpose.

### III. T-MATRIX FORMULATION

In the wave scattering problems, as stated in the previous section, the complexity of the boundary geometry of the scatterer necessitates the use of a numerical method to obtain an approximate solution. In the evaluation of the scattered wave field, especially at the far field, the T-matrix method is highly efficient and powerful computational procedure. It uses, depending on the dimensionality of the problem, only cylindrical or spherical wave functions even for bodies of arbitrary shape.

In the formulation, both incident and scattered waves are expanded in series of the common wave functions, known as the basis functions, satisfying the Helmholtz equation (Eq. 2.16). The unknown coefficients of the scattered wave series are then related to the coefficients of the incident wave by a transition matrix, called T-matrix.

#### 3.1 BASIS WAVE FUNCTIONS

A class of solutions for Helmholtz reduced wave equation is the wave functions in circular polar coordinates,

$$\psi_n^\sigma(r, \theta) = (\epsilon_n)^{1/2} H_n^{(1)}(kr) \tau_n^\sigma(\theta); \quad n = 0, 1, \dots, \infty \quad , (3.1)$$

where  $H_n^{(1)}(kr)$  is the cylindrical Hankel function of the first kind,  $\tau_n^\sigma$  is given by

$$\tau_n^\sigma(\theta) = \begin{cases} \cos(n\theta) & \text{for } \sigma = 1 \\ \sin(n\theta) & \text{for } \sigma = 2 \end{cases}, \quad (3.2)$$

and  $\varepsilon_n$  is the Neumann factor,

$$\varepsilon_n = \begin{cases} 1 & \text{for } n = 0 \\ 2 & \text{for } n > 0 \end{cases} \quad (3.3)$$

Equation (3.1) can be written from the general solution (2.31) by simply setting,  $I_n^{(1)}(kr) \rightarrow H_n^{(1)}(kr)$ ,  $B_n \rightarrow 0$ .

Assuming a time dependency of the form

$$\phi(r, \theta, t) = \psi_n^\sigma e^{-i\omega t}, \quad (3.4)$$

$\phi$  represents an outgoing cylindrical wave with respect to the origin of a coordinate system located as shown in Fig. 3.1. Using the function  $H_n^{(2)}(kr)$  in Eq. (3.4) would give the functional form of an incoming wave. However, if  $H_n^{(1)}(kr)$  is replaced by  $J_n(kr)$ , the cylindrical Bessel function of the first kind, we get the expression for a standing wave,

$$\hat{\psi}_n^\sigma(r, \theta) = (\varepsilon_n)^{\frac{1}{2}} J_n(kr) \tau_n^\sigma(\theta); \quad n = 0, 1, \dots, \infty \quad (3.5)$$

One should also note that  $\hat{\psi}_n^\sigma$  is the regular part of  $\psi_n^\sigma$  given by Eq. (3.1), and it corresponds to the real part of the latter when  $kr$  is real. The functions  $\psi_n^\sigma$  and  $\hat{\psi}_n^\sigma$  are called the basis wave functions for two dimensional scalar waves.

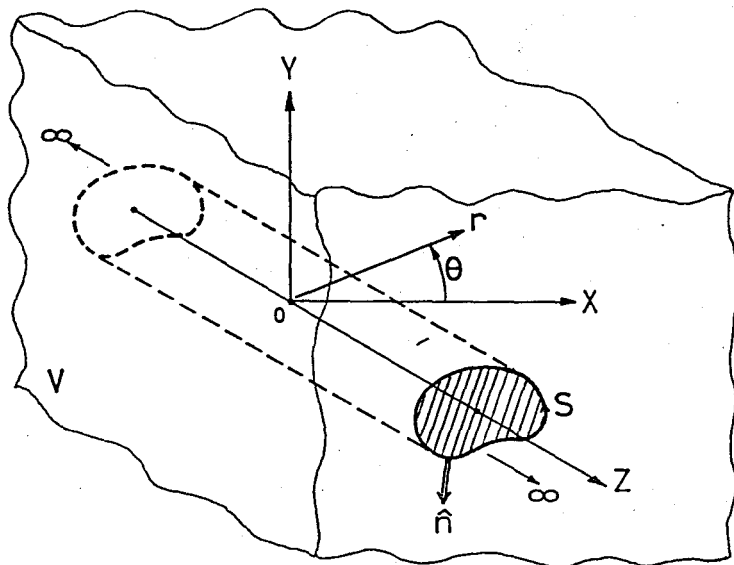


Figure 3.1 - Geometry of an infinite cylindrical obstacle.

Recalling the orthogonality relations for the trigonometric functions,

$$\int_0^{2\pi} \cos(m\theta) \cos(n\theta) d\theta = \frac{2\pi}{(\varepsilon_m \varepsilon_n)^{\frac{1}{2}}} \delta_{mn}, \quad (3.6)$$

$$\int_0^{2\pi} \sin(m\theta) \sin(n\theta) d\theta = \frac{2\pi}{(\varepsilon_m \varepsilon_n)^{\frac{1}{2}}} \delta_{mn}, \quad (3.7)$$

$$\int_0^{2\pi} \cos(m\theta) \sin(n\theta) d\theta = 0, \quad (3.8)$$

where  $\varepsilon_m, \varepsilon_n$  are the Neumann factors and  $\delta_{mn}$  is the Kronecker delta, one can write orthonogonality relation for  $\tau_n^\sigma(\theta)$  over a closed curve as

$$(\varepsilon_m \varepsilon_n)^{\frac{1}{2}} \int_0^{2\pi} \tau_m^\sigma \tau_n^\nu d\theta = 2\pi \delta_{mn} \quad \text{for } \sigma = \nu \quad . \quad (3.9)$$

Since, only the Hankel functions of the first kind will be utilized in the rest of the work, to simplify the writing the superscript (1) appearing on  $H_n(kr)$  will be omitted.

### 3.2 ORTHOGONALITY OF THE BASIS FUNCTIONS

From the divergence theorem, it can be shown that two arbitrary scalar functions  $u(x, y, t)$  and  $v(x, y, t)$  satisfy the Green's second identity [18],

$$\oint_C \left( u \frac{\partial v}{\partial n} - v \frac{\partial u}{\partial n} \right) dS = \iint_{A_s} (u \nabla^2 v - v \nabla^2 u) dA \quad . \quad (3.10)$$

The  $u$  and  $v$  and their first and second derivatives are continuous in a two-dimensional region of area  $A_s$  bounded by the closed curve  $C$ . The  $\partial u / \partial n = \hat{n}$ .  $\nabla u$  is the directional derivative along a unit normal  $\hat{n}$  which is pointed outward from the curve  $C$ . So far no restriction has been imposed on  $u$  and  $v$  except the conditions of continuity.

Let  $u$  or  $v$  represent a scalar wave, satisfying the Helmholtz equation written in the form

$$(\nabla^2 + k_1^2)u = 0 \quad , \quad (\nabla^2 + k_2^2)v = 0 \quad . \quad (3.11)$$

A time factor  $\exp(-i\omega t)$  is assumed for the wave. When both  $u$  and  $v$  have the same wave number, i.e.,  $k_1 = k_2 = k = \omega/c$ , the area integral on the right hand side of Eq. (3.10) vanishes identically and we have

$$\int_C \left( u \frac{\partial v}{\partial n} - v \frac{\partial u}{\partial n} \right) dS = 0 \quad (3.12)$$

This result is valid for any two functions  $u$  and  $v$ , so long as they satisfy the same wave equation, and the aforementioned conditions of continuity. For acoustic waves,  $u$  and  $v$  are the usual velocity potentials.

For the problem of scattering by an infinite cylindrical boundary, consider the geometry shown in Fig. 3.2, where the curve  $S$  represents the boundary of the scatterer while  $S_+$  and  $S_\infty$  are somewhat arbitrary circular curves outside the scatterer. By utilizing Eqs. (3.9) and (3.12), the following orthonogonality conditions can be established for the basis wave functions over the circle  $S_+$ :

$$\int_{S_+} \left( \hat{\psi}_p \frac{\partial \hat{\psi}_q}{\partial n} - \hat{\psi}_q \frac{\partial \hat{\psi}_p}{\partial n} \right) dS = 0 \quad , \quad (3.13)$$

$$\int_{S_+} \left( \psi_p \frac{\partial \psi_q}{\partial n} - \psi_q \frac{\partial \psi_p}{\partial n} \right) dS = 0 \quad , \quad (3.14)$$

$$\int_{S_+} \left( \psi_p \frac{\partial \psi_q}{\partial n} - \hat{\psi}_q \frac{\partial \hat{\psi}_p}{\partial n} \right) dS = (-4i) \delta_{pq} \quad . \quad (3.15)$$

For simplicity in writing, only the subscript which indicates the order of the Bessel functions is retained, that is,

$$\psi_p \equiv \psi_p^\sigma \quad , \quad \psi_q \equiv \psi_q^\nu \quad , \quad \text{etc.} \quad (3.16)$$

The proof of the first condition is rather simple. Let the region  $A_S$  in Eq. (3.10) be bounded externally by the circle  $S_+$  of radius  $r = r_+$

as shown in Fig. 3.2. Note that both  $\hat{\psi}_p$  and  $\hat{\psi}_q$  and their normal derivatives are continuous within  $S_+$ , that is,  $J_{p,q}(kr)$  have no singularity inside  $S_+$ , and furthermore they satisfy the wave equation (3.11) with  $k_1 = k_2 = k$ . Thus, Eq. (3.13) is a special case of (3.12) with  $u = \hat{\psi}_p$  and  $v = \hat{\psi}_q$ .

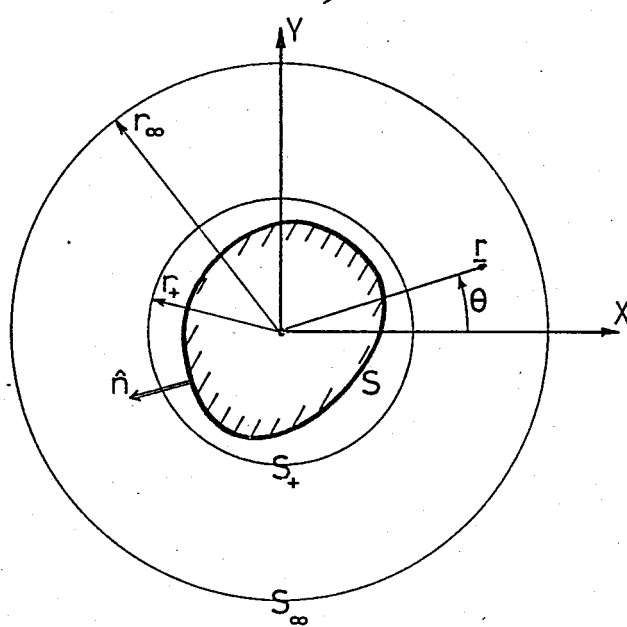


Figure 3.2 - Geometry for a constant cross-sectional scatterer.

The same proof, however, cannot be applied to the functions  $\psi_p$  and  $\psi_q$  because the origin  $r = 0$  is a singularity point for  $H_{p,q}(kr)$ . For the proof of Eq. (3.14), we consider a region bounded internally by  $S_+$  ( $r = r_+$ ) and externally by  $S_\infty$  ( $r = r_\infty$ ), (Fig. 3.2). Within this region, both  $\psi_{p,q}$  and  $\partial\psi_{p,q}/\partial n$  are regular, and Eq. (3.12) reduces to

$$-\int_{S_+} (\psi_p \frac{\partial \psi_p}{\partial n} - \psi_q \frac{\partial \psi_p}{\partial n}) ds + \int_{S_\infty} (\psi_p \frac{\partial \psi_q}{\partial n} - \psi_q \frac{\partial \psi_p}{\partial n}) ds = 0, \quad (3.17)$$

where we have replaced  $u$  and  $v$  by  $\psi_p$  and  $\psi_q$ , respectively. Note that, while the outer normal along  $S_+$  is in the negative direction of the unit radial vector  $e_r$ , it is in the positive direction along  $S_\infty$ . The negative sign in front of the integral along  $S_+$  is introduced because the normal derivative  $\partial/\partial n$  is taken to be in the direction of  $+e_r$  along both curves.

It is seen immediately that both integrals in the above equation vanish identically when  $p = q$ . When  $\psi_p$  differs from  $\psi_q$ , it can be shown that each integral vanishes due to the orthogonality condition given by Eq. (3.9). To show this, note that  $\partial/\partial n = \partial/\partial r$  and  $ds = rd\theta$  along the circular curves  $S_+$  and  $S_\infty$ , and

$$\frac{\partial \psi_p}{\partial r} = (\epsilon_p)^{\frac{1}{2}} \tau_p^\sigma(\theta) \frac{\partial H_p(kr)}{\partial r} = (\epsilon_p)^{\frac{1}{2}} \tau_p^\sigma k H'_p(kr), \quad (3.18)$$

$$\frac{\partial \psi_q}{\partial r} = (\epsilon_q)^{\frac{1}{2}} \tau_q^\nu(\theta) \frac{\partial H_q(kr)}{\partial r} = (\epsilon_q)^{\frac{1}{2}} \tau_q^\nu k H'_q(kr), \quad (3.19)$$

where primes denote derivatives of the Hankel functions with respect to their argument. Substitution of these into the integral along  $S_+$  in Eq. (3.17) yields

$$\begin{aligned} \int_{S_+} (...) ds &= \int_{S_+} [(\epsilon_p)^{\frac{1}{2}} \tau_p^\sigma (\epsilon_q)^{\frac{1}{2}} \tau_q^\nu H_p(kr) k H'_q(kr) \\ &\quad - (\epsilon_q)^{\frac{1}{2}} \tau_q^\nu (\epsilon_p)^{\frac{1}{2}} \tau_p^\sigma H_q(kr) k H'_p(kr)] ds. \end{aligned} \quad (3.20)$$

Since  $r \neq r(\theta)$ , one can write the above equation in the form

$$\int_{S_+} (\dots) ds = kr[H_p(kr)H'_q(kr) - H_q(kr)H'_p(kr)][(\epsilon_p \epsilon_q)^{\frac{1}{2}} \int_0^{2\pi} \tau_p^\sigma \tau_q^\nu d\theta]. \quad (3.21)$$

One can see that the expression in the second bracket is the same as that given by Eq. (3.9). Thus the integral over  $S_+$  vanishes if  $p \neq q$ . Going through a very similar procedure, one can show that the integral over  $S_\infty$  also vanishes for  $p \neq q$ . This completes the proof of Eq. (3.14). From this proof it is seen that the circle  $S_+$  can be replaced by any other circular curve, not necessarily centered at the origin of the coordinate system.

To prove Eq. (3.15), let the region of interest be the same region as in the preceding case and let  $u = \psi_p$  and  $v = \hat{\psi}_q$  in Eq. (3.12). Since they are continuous within that region, we can write

$$\int_{S_+} (\psi_p \frac{\partial \hat{\psi}_q}{\partial n} - \hat{\psi}_q \frac{\partial \psi_p}{\partial n}) ds = \int_{S_\infty} (\psi_p \frac{\partial \hat{\psi}_q}{\partial n} - \hat{\psi}_q \frac{\partial \psi_p}{\partial n}) ds. \quad (3.22)$$

Again, if  $p \neq q$ , one can show by giving a similar proof as for Eq. (3.17) that the integrals in the above expression vanish. However, they do not, when  $p = q$ .

To evaluate the integral on the right-hand side, let  $S_\infty$  recede to infinity. The asymptotical expressions for  $\psi_p$  and  $\hat{\psi}_q$  as  $r \rightarrow \infty$  are [2]

$$\psi_p = (\epsilon_p)^{\frac{1}{2}} H_p(kr) \tau_p^\sigma \stackrel{\infty}{\approx} (\epsilon_p)^{\frac{1}{2}} \tau_p^\sigma \sqrt{2/\pi kr} e^{i(kr - \pi_p)}, \quad (3.23)$$

$$\hat{\psi}_q = (\epsilon_q)^{\frac{1}{2}} J_q(kr) \tau_q^\nu \stackrel{\infty}{\approx} (\epsilon_q)^{\frac{1}{2}} \tau_q^\nu \sqrt{2/\pi kr} \cos(kr - \pi_q), \quad (3.24)$$

where  $\pi_p = (2p + 1)\pi/4$ . Recalling that, [2],

$$\frac{\partial H_p(kr)}{\partial r} = kH'_p(kr) = \frac{k}{2}[H_{p-1}(kr) - H_{p+1}(kr)] , \quad (3.25)$$

$$\frac{\partial J_q(kr)}{\partial r} = kJ'_q(kr) = \frac{k}{2}[J_{q-1}(kr) - J_{q+1}(kr)] , \quad (3.26)$$

and as  $r \rightarrow \infty$ ,

$$H_{p\pm 1}(kr) \rightarrow \pm i\sqrt{2/\pi kr} e^{i(kr-\pi_p)} , \quad (3.27)$$

$$J_{q\pm 1}(kr) \rightarrow \pm \sqrt{2/\pi kr} \sin(kr-\pi_q) , \quad (3.28)$$

the asymptotic expressions for  $\partial\psi_p/\partial r$  and  $\partial\hat{\psi}_q/\partial r$  can be written as

$$\frac{\partial\psi_p}{\partial r} \underset{\infty}{\approx} ik\sqrt{2/\pi kr} e^{i(kr-\pi_p)} (\epsilon_p)^{\frac{1}{2}} \tau_p^\sigma , \quad (3.29)$$

$$\frac{\partial\hat{\psi}_q}{\partial r} \underset{\infty}{\approx} -k\sqrt{2/\pi kr} \sin(kr-\pi_q) (\epsilon_q)^{\frac{1}{2}} \tau_q^\nu . \quad (3.30)$$

Substituting the expressions (3.23), (3.24), (3.29) and (3.30) into Eq. (3.22), one obtains

$$\begin{aligned} \int_{S_+} (\psi_p \frac{\partial\hat{\psi}_q}{\partial n} - \hat{\psi}_q \frac{\partial\psi_p}{\partial n}) ds &= \int_{S_\infty} \left( -\frac{2i}{\pi r} \right) [(\epsilon_p \epsilon_q)^{\frac{1}{2}} \tau_p^\sigma \tau_q^\nu e^{i(kr-\pi_p)}] \\ &\quad \times [\cos(kr-\pi_q) - i \sin(kr-\pi_q)] ds \\ &= \int_0^{2\pi} \left( -\frac{2i}{\pi r} \right) [(\epsilon_p \epsilon_q)^{\frac{1}{2}} \tau_p^\sigma \tau_q^\nu e^{i(\pi_q - \pi_p)}] r d\theta \end{aligned}$$

$$\begin{aligned}
 &= \left[ -\frac{2i}{\pi} \right] \left[ (\epsilon_p \epsilon_q)^{\frac{1}{2}} \int_0^{2\pi} \tau_p^\sigma \tau_q^\nu d\theta \right] [e^{i(\pi_q - \pi_p)}] \\
 &= \left[ -\frac{2i}{\pi} \right] [2\pi \delta_{pq}] [e^{i(\pi_q - \pi_p)}] \\
 &= -4i\delta_{pq} \tag{3.31}
 \end{aligned}$$

This completes the proof of the third orthogonality condition (3.15).

### 3.3 WAVE FUNCTION EXPANSIONS

Consider a cylindrical inclusion of cross-sectional area  $A_c$ , bounded by a closed curve  $S$ , and let a plane wave  $u^i(r, \theta) \exp(-i\omega t)$  be incident upon this inclusion, as shown in Fig. 3.3. Then, the total wave field  $u(r, \theta)$  in the medium will be composed of two parts; the incident wave,  $u^i$ , and the scattered wave,  $u^s$ , i.e.,

$$u(r, \theta) = u^i(r, \theta) + u^s(r, \theta) \tag{3.32}$$

For notational convenience, the time factor  $\exp(-i\omega t)$  will be suppressed in the rest of the work.

Both incident and scattered waves can be expanded into a series of the basis functions in the form

$$u^i = A \sum_m \hat{a}_m \hat{\psi}_m , \quad u^s = A \sum_m c_m \psi_m , \tag{3.33}$$

where  $A$  is the constant amplitude factor of the incident wave,  $a_m$  are the incident wave coefficients which can be determined uniquely for a given incident wave type, and  $c_m$  are the unknown coefficients of the scattered wave. The coefficients  $c_m$ , as will be shown, can be determined

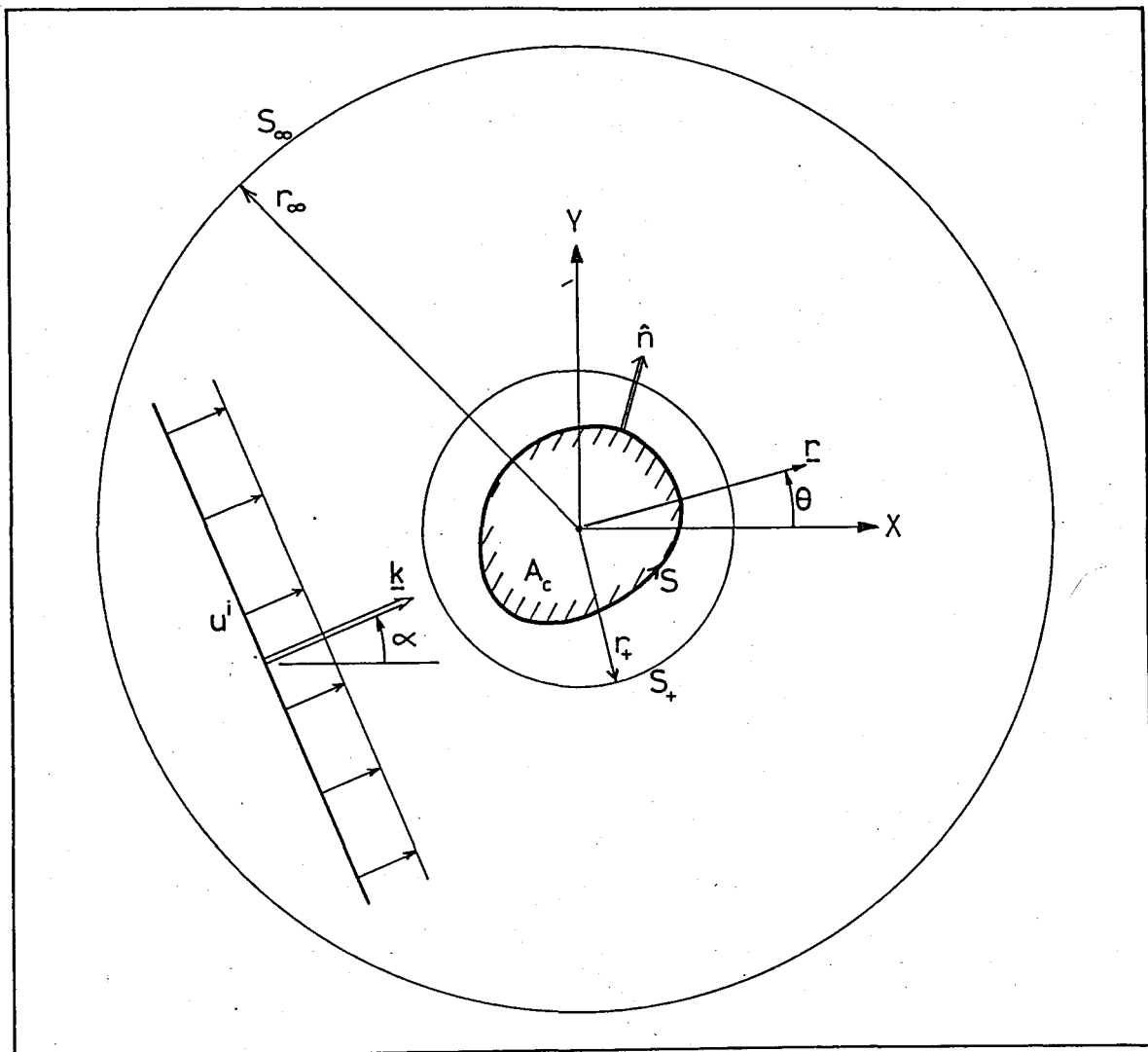


Figure 3.3 - Geometry for a plane wave incidence on a cylindrical scatterer.

by making use of a transition matrix (T-matrix) which relates to  $c_m$  to  $a_m$  by

$$c_m = \sum T_{mn} a_n \quad (3.34)$$

### 3.3.1 The Incident Wave Field

Any known incident wave can be expanded into a series of the basis functions  $\psi_m$  as defined by Eqs. (3.5) and (3.16), [12],

$$u^i(r, \theta) = A \sum_m a_m \hat{\psi}_m(r, \theta) \equiv A \sum_{m=0}^{\infty} \sum_{\sigma=1}^2 a_m^{\sigma} \hat{\psi}_m^{\sigma}, \quad r < r_{\infty}. \quad (3.35)$$

Since,  $\hat{\psi}_m$  are regular at the origin ( $r = 0$ ), taken to be inside the surface  $S$ , the series converges uniformly within a large circle  $S_{\infty}$  of radius, say,  $r_{\infty}$ . For plane incident waves,  $S_{\infty}$  is at the infinity.

In Eq. (3.35) and in the following equations, for the simplicity in writing, the double sum will be represented by a single index and summation. Since the index  $m$  is an abbreviation for the two indices  $m$  and  $\sigma$ , the symbol  $\Sigma$  means summation on  $\sigma$  from 1 (even) to 2 (odd) and  $m$  from 0 to  $\infty$ .

Consider a plane incident wave with its wave normal perpendicular to the axis of the scatterer, as shown in Fig. 3.3. This wave can be represented by

$$u^i = Ae^{ikrcos(\theta-\alpha)} \quad (3.36)$$

as defined in section (2.3.1), where the time factor has been omitted. If the plane wave expression given in Eq. (3.36) is expanded into a series as defined by Eq. (3.35) then the coefficients  $a_m^{\sigma}$  can be determined as explained below.

Trigonometric Fourier series expansion of an even function  $f(x)$ , in the interval  $-L \leq x \leq L$  is given by

$$f(x) = \sum_{n=0}^{\infty} \epsilon_n \frac{a_n}{2} \cos \frac{n\pi x}{L}, \quad (3.37)$$

where  $\epsilon_n$  is the Neumann factor, and

$$a_n = \frac{1}{L} \int_0^{2L} f(x) \cos \frac{n\pi x}{L} dx, \quad n = 0, 1, \dots, \infty \quad (3.38)$$

If we now consider the function  $f(x)$  to be of the form  $e^{iz\cos\beta}$  where we have replaced  $x$  by  $\beta$ . If this function is defined in the interval  $-\pi \leq \beta \leq \pi$  then its Fourier series expansion is

$$e^{iz\cos\beta} = \sum_{n=0}^{\infty} \epsilon_n \frac{a_n}{2} \cos(n\beta), \quad (3.39)$$

where

$$a_n = \frac{1}{\pi} \int_0^{2\pi} e^{iz\cos\beta} \cos(n\beta) d\beta. \quad (3.40)$$

Recalling the integral representation of the Bessel functions [19],

$$2\pi i^n J_n(z) = \int_0^{2\pi} e^{iz\cos\beta} \cos(n\beta) d\beta, \quad (3.41)$$

equation (3.39) can be written as

$$e^{iz\cos\beta} = \sum_{n=0}^{\infty} \epsilon_n i^n J_n(z) \cos(n\beta) \quad (3.42)$$

In order to obtain the Fourier series expansion of the expression given by Eq. (3.36) one then has to replace  $z$  by  $kr$  and  $\beta$  by  $(\theta - \alpha)$  in Eq. (3.42). Doing so one gets

$$\begin{aligned}
 e^{ikr\cos(\theta-\alpha)} &= \sum_{n=0}^{\infty} \epsilon_n i^n J_n(kr) \cos[n(\theta-\alpha)] \\
 &= \sum_{n=0}^{\infty} \epsilon_n i^n J_n(kr) [\cos(n\theta)\cos(n\alpha) + \sin(n\theta)\sin(n\alpha)]. \quad (3.43)
 \end{aligned}$$

Rearranging Eq. (3.43) as

$$e^{ikr\cos(\theta-\alpha)} = \sum_{n=0}^{\infty} \sum_{\sigma=1}^2 [(\epsilon_n)^{\frac{1}{2}} i^n J_n(kr) \frac{\cos(n\theta)}{\sin(n\theta)}] [(\epsilon_n)^{\frac{1}{2}} i^n \frac{\cos(n\alpha)}{\sin(n\alpha)}] \quad (3.44)$$

and then comparing with Eq. (3.35), the coefficients  $a_m^\sigma$  of the incident plane wave are found to be

$$a_m^\sigma = (\epsilon_m)^{\frac{1}{2}} i^m \begin{cases} \cos(m\alpha) & ; \sigma = 1 \\ \sin(m\alpha) & ; \sigma = 2 \end{cases} \quad (3.45)$$

### 3.3.2 The Scattered Wave Field

The scattered wave field can be expanded into a series in terms of the functions  $\psi_m$ , i.e.,

$$u^s(r, \theta) = A \sum c_m \psi_m(r, \theta) \equiv A \sum_{m=0}^{\infty} \sum_{\sigma=1}^2 c_m^\sigma \psi_m^\sigma, \quad r \geq r_+. \quad (3.46)$$

Note that  $\psi_m$  are regular outside the region enclosed by the curve  $S$ , the boundary of the inclusion. Thus, the above series converges uniformly outside and on a circle  $S_+$ , enclosing the inclusion (Fig. 3.3). The radius  $r_+$  of  $S_+$  is yet unspecified, and it can be ascertained when the unknown coefficients  $c_m$  are found.

To determine  $c_m$ , consider a region which is bounded internally by  $S$ , and externally by  $S_+$ . Furthermore, to apply Eq. (3.12) for that region, let  $v$  be  $\hat{\psi}_m$ , and  $u$  be the total wave field as defined in Eq. (3.32), that is

$$u(r, \theta) = u^i(r, \theta) + u^s(r, \theta) ; \quad (r \text{ inside } S_+, \text{ outside } S). \quad (3.47)$$

At the boundary  $S$  one writes

$$u(r, \theta) = u^+ , \frac{\partial u(r, \theta)}{\partial n} = \frac{\partial u^+}{\partial n} ; \quad (r \text{ on } S) . \quad (3.48)$$

Both  $u^+$  and  $\partial u^+ / \partial n$  are unknown quantities at the surface  $S$ , where (+) indicates that we approach  $S$  from the positive direction of  $\hat{n}$ .

Substituting Eqs. (3.35), (3.46) into (3.47) and evaluating it on  $S_+$  we get

$$u(r, \theta) = A \sum a_j \hat{\psi}_j(r, \theta) + A \sum c_j \psi_j(r, \theta); \quad (r \text{ on } S_+) . \quad (3.49)$$

Since both series are uniformly convergent on the surface (circle)  $S_+$ , one can differentiate them term by term to obtain

$$\frac{\partial u(r, \theta)}{\partial n} = A \sum a_j \frac{\partial \hat{\psi}_j(r, \theta)}{\partial n} + A \sum c_j \frac{\partial \psi_j}{\partial n}; \quad (r \text{ on } S_+) . \quad (3.50)$$

Substitution of the expressions (3.48), (3.49) and (3.50) into Eq. (3.12) where the contour  $C$  is made out of two curves,  $S$  and  $S_+$ , gives

$$\begin{aligned} \int_S \left( u^+ - \hat{\psi}_m \frac{\partial u^+}{\partial n} \right) ds - \int_{S_+} A \left[ \left( \sum_j a_j \hat{\psi}_j + \sum_j c_j \psi_j \right) \frac{\partial \hat{\psi}_m}{\partial n} \right. \\ \left. - \hat{\psi}_m \left( \sum_j a_j \frac{\partial \hat{\psi}_j}{\partial n} + \sum_j c_j \frac{\partial \psi_j}{\partial n} \right) \right] ds = 0 . \end{aligned} \quad (3.51)$$

Rearranging the above expression, we get

$$\begin{aligned} \int_S (u^+ \frac{\partial \hat{\psi}_m}{\partial n} - \hat{\psi}_m \frac{\partial u^+}{\partial n}) ds &= A \sum_j a_j \left[ \int_{S_+} (\hat{\psi}_j \frac{\partial \hat{\psi}_m}{\partial n} - \hat{\psi}_m \frac{\partial \hat{\psi}_j}{\partial n}) ds \right] \\ &\quad + A \sum_j c_j \left[ \int_{S_+} (\psi_j \frac{\partial \hat{\psi}_m}{\partial n} - \hat{\psi}_m \frac{\partial \psi_j}{\partial n}) ds \right]. \end{aligned} \quad (3.52)$$

The integral associated with  $a_j$  vanishes according to the orthogonality condition (3.13), and that with  $c_j$  is the same as the integral in Eq. (3.15). Hence the right-hand side of the preceding equation reduces to  $A \sum c_j (-4i \delta_{jm})$ , yielding

$$\int_S (u^+ \frac{\partial \hat{\psi}_m}{\partial n} - \hat{\psi}_m \frac{\partial u^+}{\partial n}) ds = -4i A c_m. \quad (3.53)$$

Similarly, replacing  $v$  in Eq. (3.12) by  $\psi_m$ , and applying the orthogonality conditions (3.14) and (3.15), one obtains

$$\int_S (u^+ \frac{\partial \psi_m}{\partial n} - \psi_m \frac{\partial u^+}{\partial n}) ds = 4i A a_m. \quad (3.54)$$

Equation (3.53) states that the unknown coefficients  $c_m$  of the series representation for the scattered wave is determined by an integral of the surface sources,  $u^+$  and  $\partial u^+/\partial n$ , over the boundary of the scatterer. These two sources,  $u^+$  and  $\partial u^+/\partial n$ , are not independent of each other and are related by Eq. (3.54) where  $a_m$  are known.

The unknown quantities,  $u^+$  and  $\partial u^+/\partial n$ , are to be determined from prescribed boundary conditions.

### 3.4 BOUNDARY CONDITIONS

In connection with the above formulations, two boundary conditions are of great importance in scattering problems, namely the Neumann and Dirichlet boundary conditions.

#### 3.4.1 Neumann Type Boundary Condition

In the case where the inclusion is a rigid one, the normal component of the velocity field should vanish on the boundary, i.e.,

$$\frac{\partial u^+}{\partial n} = 0 \quad , \quad (3.55)$$

or equivalently, from Eq. (3.47),

$$\frac{\partial u^S}{\partial n} = - \frac{\partial u^i}{\partial n} \quad \text{on } S \quad . \quad (3.56)$$

Such a boundary condition is known as the Neumann type boundary condition.

The other surface quantity  $u^+$ , which is unspecified, can be represented [1] as a series of the regular wave functions  $\hat{\psi}_j$ , that is,

$$u^+ = A \sum_j \alpha_j \hat{\psi}_j \quad , \quad \text{on } S \quad , \quad (3.57)$$

where  $\alpha_j$  are the coefficients of the surface field.

Substitution of Eqs. (3.55) and (3.57) into Eqs. (3.53) and (3.54) yields

$$\sum_j \alpha_j \left[ \int_S \hat{\psi}_j \frac{\partial \hat{\psi}_m}{\partial n} ds \right] = -4ic_m \quad , \quad (3.58)$$

$$\sum_j \alpha_j \left[ \int_S \hat{\psi}_j \frac{\partial \psi_m}{\partial n} ds \right] = 4ia_m \quad . \quad (3.59)$$

The above pair of equations show that both scattered field coefficients  $c_m$  and incident field coefficients  $a_m$  are related to the unknown surface field coefficients  $\alpha_j$ . If the latter are eliminated from these two equations, the  $c_m$  can then be expressed directly in terms of  $a_m$ . Before going into the elimination procedure, it will be better obtain the corresponding pair of equations also for Dirichlet boundary condition.

### 3.4.2 Dirichlet Type Boundary Condition

The Dirichlet boundary condition in acoustic wave scattering corresponds to the case where we have a cavity inside the fluid medium. Thus, the pressure vanishes on the surface of the cavity, i.e.,

$$u^+ = u^i + u^s = 0 \quad , \quad \text{on } S \quad . \quad (3.60)$$

The unspecified surface quantity  $\partial u^+ / \partial n$ , in this case, can be represented [1] as a series in terms of the normal gradients of the regular wave functions, that is,

$$\frac{\partial u^+}{\partial n} = A \sum_j \alpha_j \frac{\partial \hat{\psi}_j}{\partial n} \quad , \quad \text{on } S \quad . \quad (3.61)$$

Equations (3.60) and (3.61) are then substituted into (3.53) and (3.54) to obtain

$$\sum_j \alpha_j \left[ - \int_S \hat{\psi}_m \frac{\partial \hat{\psi}_j}{\partial n} ds \right] = -4ic_m \quad , \quad (3.62)$$

$$\sum_j \alpha_j \left[ - \int_S \hat{\psi}_j \frac{\partial \hat{\psi}_m}{\partial n} ds \right] = 4ia_m \quad (3.63)$$

The above two equations, together with Eqs. (3.58) and (3.59) obtained in the preceding section, form the basis for deriving a transition matrix relating the coefficients  $c_m$  to  $a_m$  directly.

### 3.5 THE TRANSITION MATRIX

One can define two matrices with elements  $Q_{jm}$  and  $\hat{Q}_{jm}$ , which are, in the case of Neumann boundary condition, given by

$$Q_{jm} = \frac{1}{4} \int_S \hat{\psi}_j \frac{\partial \hat{\psi}_m}{\partial n} ds , \quad (3.64)$$

$$\hat{Q}_{jm} = \frac{1}{4} \int_S \hat{\psi}_j \frac{\partial \hat{\psi}_m}{\partial n} ds , \quad (3.65)$$

and in the case of Dirichlet boundary condition, given by

$$Q_{jm} = -\frac{1}{4} \int_S \hat{\psi}_m \frac{\partial \hat{\psi}_j}{\partial n} ds , \quad (3.66)$$

$$\hat{Q}_{jm} = -\frac{1}{4} \int_S \hat{\psi}_m \frac{\partial \hat{\psi}_j}{\partial n} ds . \quad (3.67)$$

As can be easily seen in both cases, the elements of the  $\hat{Q}$  matrix are simply the real part of the elements of the  $Q$  matrix, i.e.,

$$\hat{Q}_{jm} = \operatorname{Re}(Q_{jm}) \quad (3.68)$$

Now, substituting the corresponding  $Q$  and  $\hat{Q}$  matrices into Eqs. (3.58), (3.59), (3.62) and (3.63), we obtain

$$i \sum_j \hat{Q}_{jm} = c_m , \quad (3.69)$$

$$-i \sum_j Q_{jm} = a_m \quad (3.70)$$

The equations (3.69) and (3.70) can then be expressed in matrix form,

$$\hat{Q}^T \underline{\alpha} = \underline{c} , \quad (3.71)$$

$$-Q^T \underline{\alpha} = \underline{a} , \quad (3.72)$$

where  $(t)$  denotes the transpose matrix. Elimination of the unknown surface field coefficient vector  $\underline{\alpha}$  from these two equations yields

$$\underline{c} = -[\hat{Q}^T (Q^T)^{-1}] \underline{a} = T \underline{a} . \quad (3.73)$$

The  $T$  is called transition matrix which relates the scattered wave field directly to the incident wave field. As shown in Ref. [1,20], the  $T$ -matrix is symmetric, i.e.,  $T^T = T$ , it can thus be determined from the relation

$$\hat{Q}^T T = -\hat{Q}^T , \quad (3.74)$$

or,

$$T = -Q^{-1} \hat{Q} \quad (3.75)$$

### 3.6 STRUCTURE OF THE Q-MATRIX

As given in Eqs. (3.63-67), the elements of the  $Q$ -matrix are given by integrals involving basis wave functions and their normal gradients. These integrals are evaluated along the boundary of the scatterer. We

should note that for a given incident wave field (given wave number) the elements of the Q-matrix are fixed when the geometry and the boundary type of the scatterer are given.

In order to understand the structure of the Q-matrix better, one should restore the full index notation of the basis functions, that is,

$$\psi_j(r, \theta) \equiv \psi_j^\sigma(r, \theta) , \quad \psi_m(r, \theta) \equiv \psi_m^\nu(r, \theta) , \text{ etc.} \quad (3.76)$$

With this notation, Eqs. (3.64) and (3.66) take the form

$$Q_{jm}^{\sigma\nu} = \frac{1}{4} \int_S \hat{\psi}_j^\sigma \frac{\partial \psi_m^\nu}{\partial n} ds , \quad (3.77)$$

$$Q_{jm}^{\sigma\nu} = - \frac{1}{4} \int_S \hat{\psi}_m^\nu \frac{\partial \hat{\psi}_j^\sigma}{\partial n} ds , \quad (3.78)$$

respectively. From these expressions one sees that the Q-matrix actually consists of four submatrices, that is,

$$\tilde{Q} = \begin{vmatrix} Q^{11} & Q^{12} \\ Q^{21} & Q^{22} \end{vmatrix} , \quad (3.79)$$

where, in the case of Neumann boundary condition,

$$Q_{jm}^{11} = \frac{1}{4} \int_S \hat{\psi}_j^1 \frac{\partial \psi_m^1}{\partial n} ds , \quad (3.80)$$

$$Q_{jm}^{12} = \frac{1}{4} \int_S \hat{\psi}_j^1 \frac{\partial \psi_m^2}{\partial n} ds , \quad (3.81)$$

$$Q_{jm}^{21} = \frac{1}{4} \int_S \hat{\psi}_j^2 \frac{\partial \psi_m^1}{\partial n} ds , \quad (3.82)$$

$$Q_{jm}^{22} = \frac{1}{4} \int_S \hat{\psi}_j^2 \frac{\partial \psi_m^2}{\partial n} ds , \quad (3.83)$$

and in the case of Dirichlet boundary condition,

$$Q_{jm}^{11} = - \frac{1}{4} \int_S \psi_m^1 \frac{\partial \hat{\psi}_j^1}{\partial n} ds , \quad (3.84)$$

$$Q_{jm}^{12} = - \frac{1}{4} \int_S \psi_m^2 \frac{\partial \hat{\psi}_j^1}{\partial n} ds , \quad (3.85)$$

$$Q_{jm}^{21} = - \frac{1}{4} \int_S \psi_m^1 \frac{\partial \hat{\psi}_j^2}{\partial n} ds , \quad (3.86)$$

$$Q_{jm}^{22} = - \frac{1}{4} \int_S \psi_m^2 \frac{\partial \hat{\psi}_j^2}{\partial n} ds . \quad (3.87)$$

Note that  $\psi_n^\sigma$  and  $\hat{\psi}_n^\sigma$  are given by

$$\hat{\psi}_n^1(r, \theta) = (\epsilon_n)^{\frac{1}{2}} H_n(kr) \cos(n\theta) , \quad (3.88)$$

$$\hat{\psi}_n^2(r, \theta) = (\epsilon_n)^{\frac{1}{2}} H_n(kr) \sin(n\theta) , \quad (3.89)$$

$$\hat{\psi}_n^1(r, \theta) = (\epsilon_n)^{\frac{1}{2}} J_n(kr) \cos(n\theta) , \quad (3.90)$$

$$\hat{\psi}_n^2(r, \theta) = (\epsilon_n)^{\frac{1}{2}} J_n(kr) \sin(n\theta) . \quad (3.91)$$

Depending on the geometry of the scatterer, the Q-matrix has the following properties:

For separable geometries, i.e., for the circle and ellipse, the Q-matrix is symmetric [1], that is,

$$\tilde{Q}^t = \tilde{Q} , \quad (3.92)$$

or in explicit form

$$Q_{jm}^{11} = Q_{mj}^{11}, \quad Q_{jm}^{22} = Q_{mj}^{22}, \quad Q_{jm}^{12} = Q_{mj}^{21}. \quad (3.93)$$

Another important property is that, if the cross-sectional geometry of the scatterer has a mirror symmetry with respect to x-axis, i.e., across the plane  $y = r\sin\theta = 0$ , so that  $r(\theta) = r(2\pi - \theta)$ , then the integrals involving the mixed products of sines and cosines will vanish and we get

$$Q_{jm}^{12} = Q_{jm}^{21} = 0 \quad , \quad (3.94)$$

and for the nonzero matrices,  $\tilde{Q}^{11}$  and  $\tilde{Q}^{22}$ , the integrals are to be evaluated only by considering the half of the boundary.

If the boundary of the scatterer has symmetry with respect to both x and y-axes, then [1],

$$Q_{jm} = 0 \quad \text{if } (j+m) \text{ is odd.} \quad (3.95)$$

Also, for such boundaries, real part of the Q-matrix is symmetric [21], i.e.,

$$\hat{\tilde{Q}}^t = \hat{\tilde{Q}} \quad . \quad (3.96)$$

Note that, for separable geometries both real and imaginary parts are symmetric.

### 3.7 PROPERTIES OF THE T-MATRIX

In the light of the notation of Eq. (3.79), a corresponding block notation can be used for the transition matrix in Eq. (3.75),

$$\begin{matrix} \tilde{T} \\ \approx \end{matrix} = \begin{vmatrix} T^{11} & T^{12} \\ \approx & \approx \\ T^{21} & T^{22} \\ \approx & \approx \end{vmatrix} = - \begin{vmatrix} Q^{11} & Q^{12} \\ \approx & \approx \\ Q^{21} & Q^{22} \\ \approx & \approx \end{vmatrix}^{-1} \times \begin{vmatrix} \hat{Q}^{11} & \hat{Q}^{12} \\ \approx & \approx \\ \hat{Q}^{21} & \hat{Q}^{22} \\ \approx & \approx \end{vmatrix}. \quad (3.97)$$

For the boundaries having mirror symmetry with respect to x-axis, Eq. (3.97) reduces to the two (single) equations

$$\begin{matrix} T^{11} \\ \approx \end{matrix} = - \begin{vmatrix} Q^{11} \\ \approx \end{vmatrix}^{-1} \begin{matrix} \hat{Q}^{11} \\ \approx \end{matrix}, \quad \begin{matrix} T^{22} \\ \approx \end{matrix} = - \begin{vmatrix} Q^{22} \\ \approx \end{vmatrix}^{-1} \begin{matrix} \hat{Q}^{22} \\ \approx \end{matrix}. \quad (3.98)$$

Because of the reciprocity principle and energy-conservation requirements, as shown in Refs. [1] and [20], the T-matrix is always symmetric, i.e.,

$$\begin{matrix} T^t \\ \approx \end{matrix} = \begin{matrix} T \\ \approx \end{matrix}, \quad (3.99)$$

and

$$\begin{matrix} T \\ \approx \end{matrix} \begin{matrix} T^* \\ \approx \end{matrix} = -\text{Re}(T), \quad (3.100)$$

where the asteriks (\*) denotes the complex conjugation and (Re) means the real part. These properties are valid for all geometries and can be used to check the accuracy in the numerical evaluations of the T-matrix.

### 3.8 PRESENTATION OF THE SCATTERED WAVE FIELD

The scattered field coefficients  $c_m$ , which are to be evaluated through the relation (3.73), can be written in a compact form as

$$c_m^\sigma = \sum_{n,v} T_{mn}^{\sigma v} a_n^v, \quad (3.101)$$

or, in block matrix notation,

$$\begin{vmatrix} \tilde{c}^1 \\ \tilde{c}^2 \end{vmatrix} = \begin{vmatrix} \tilde{T}^{11} & \tilde{T}^{12} \\ \tilde{T}^{21} & \tilde{T}^{22} \end{vmatrix} \begin{vmatrix} \tilde{a}^1 \\ \tilde{a}^2 \end{vmatrix} \quad (3.102)$$

One can then write from Eq. (3.101)

$$c_m^1 = \sum_{n=0}^{\infty} T_{mn}^{11} a_n^1 + \sum_{n=1}^{\infty} T_{mn}^{12} a_n^2, \quad m = 0, 1, \dots, \infty, \quad (3.103)$$

$$c_m^2 = \sum_{n=0}^{\infty} T_{mn}^{21} a_n^1 + \sum_{n=1}^{\infty} T_{mn}^{22} a_n^2, \quad m = 1, 2, \dots, \infty, \quad (3.104)$$

where

$$a_n^1 = (\epsilon_n)^{\frac{1}{2}} i^n \cos(n\alpha), \quad a_n^2 = (\epsilon_n)^{\frac{1}{2}} i^n \sin(n\alpha). \quad (3.105)$$

By using the above notation and omitting the time factor, the incident and scattered wave fields can be rewritten as

$$u^i = A \sum_{n=0}^{\infty} (\epsilon_n)^{\frac{1}{2}} J_n(kr) [a_n^1 \cos(n\theta) + a_n^2 \sin(n\theta)], \quad r < \infty, \quad (3.106)$$

$$u^s = A \sum_{n=0}^{\infty} (\epsilon_n)^{\frac{1}{2}} H_n(kr) [c_n^1 \cos(n\theta) + c_n^2 \sin(n\theta)], \quad r \text{ outside } S \quad (3.107)$$

Once the coefficients of the scattered wave field are determined numerically, the scattered field is known. Various field quantities such as the velocity potentials in the near field, surface field potentials, far field amplitudes and scattering cross-sections which are of interest in the acoustic wave scattering problems can then be calculated.

### 3.8.1 Near-field Solutions

The velocity potentials due to the scattered wave field at finite distances from the scatterer can be obtained from Eq. (3.107). In the case where the near-field solutions are concerned, generally the quantity of interest is the distribution of the velocity potential on the boundary of the scatterer due to scattered wave field. However, this distribution can not be evaluated by the T-matrix formulation directly, because the series representing the scattered wave field is not complete on the surface of the scatterer and hence Eq. (3.107) is not valid on  $S$ , [1,12]. The series is complete only on a circular surface, say  $S_+$ , which is outside the scatterer as shown in Fig. 3.3. It is possible to evaluate the velocity potential distribution from the intermediate steps of the T-matrix formulation. For this purpose, one can write, from Eq. (3.47) and (3.48),

$$u^+(r, \theta) = u^i(r, \theta) + u^S(r, \theta) , \quad r \text{ on } S , \quad (3.108)$$

or

$$u^S = u^+ - u^i , \quad r \text{ on } S . \quad (3.109)$$

In the case of Neumann boundary condition, substitution of Eqs. (3.35) and (3.57) into Eq. (3.109) yields

$$u^S = A \sum \alpha_n \hat{\psi}_n - A \sum a_n \hat{\psi}_n , \quad r \text{ on } S , \quad (3.110)$$

where  $u^+$  is the total wave field at the boundary and  $\alpha_n$  are the unknown surface field coefficients. One can immediately see that the unknown coefficients  $\alpha_n$  can be uniquely determined through the Q-matrix by solving the matrix equation (3.72). Substituting the expressions for

$\hat{\psi}_n$  in the above equation and rearranging the terms slightly we get

$$u^S = A \sum_{n=0}^{\infty} (\epsilon_n)^{1/2} J_n(kr) [(\alpha_n^1 - a_n^1) \cos(n\theta) + (\alpha_n^2 - a_n^2) \sin(n\theta)] ,$$

r on S . (3.111)

In the case of Dirichlet boundary condition, however, the scattered wave field on the boundary is simply given by

$$u^S = -u^i , \quad \text{on } S , \quad (3.112)$$

and hence it needs not be evaluated.

It should be noted that, for a circular cylindrical scatterer, the surface field potentials due to scattered wave field can still be determined from Eq. (3.107) directly, because, in this case, the circular surface  $S_+$  can be arbitrarily replaced by S so that the outgoing wave series in Eq. (3.107) is complete also on the boundary of the scatterer.

The near-field results, in fact, have very little practical significance and they are of almost no interest in applications such as non-destructive evaluations, remote sensing etc.

### 3.8.2 Far Field Solution

From the practical point of view, the far field amplitude is the most important quantity to be determined in the acoustic scattering problems.

The expression for the scattered wave field at distances far from the scatterer is obtained from Eq. (3.107) by using the asymptotical

form of the Hankel functions. The asymptotical representation of  $H_n(kr)$  as  $r \rightarrow \infty$  is given by, [2],

$$H_n(kr) \approx \sqrt{2/\pi kr} e^{i[kr - ((2n+1)/4)\pi]} , \quad (3.113)$$

and after simple manipulations, one gets

$$H_n(kr) \approx \sqrt{2/i\pi kr} e^{ikr} i^{-n} . \quad (3.114)$$

Then, substitution of Eq. (3.114) into Eq. (3.107) yields

$$u^S = e^{ikr} \sqrt{2/i\pi kr} A \sum_{n=0}^{\infty} (\varepsilon_n)^{1/2} i^{-n} [c_n^1 \cos(n\theta) + c_n^2 \sin(n\theta)] , \quad r \rightarrow \infty . \quad (3.115)$$

One can also write Eq. (3.115) as

$$u^S = e^{ikr} \sqrt{2/i\pi kr} f(\theta) , \quad (3.116)$$

where  $f(\theta)$  is the far field amplitude describing the angular variation of the scattered field at distances far from the scatterer and it is given by

$$f = A \sum_{n=0}^{\infty} (\varepsilon_n)^{1/2} i^{-n} [c_n^1 \cos(n\theta) + c_n^2 \sin(n\theta)] . \quad (3.117)$$

In the presentation of the scattered wave results, the field quantities given by Eqs. (3.107), (3.111) and (3.117) are first non-dimensionalized through dividing them by the constant amplitude factor of the incident wave  $A$ , and then the angular variations of their norms, i.e.,  $|u^S/A|$ ,  $|f/A|$  versus  $\theta$ , are plotted in polar coordinates for the regions of interest.

### 3.8.3 Total Scattering Cross-Section

In two dimensional wave scattering problems, the total scattering cross-section is defined as the ratio between power generated by the scattered wave over a circle with large radius around the obstacle and the power per unit area generated by the incident wave, and is given by, [13],

$$\sigma^{\text{tot}} = \frac{1}{2\pi} \int_0^{2\pi} \sigma(\theta) d\theta \quad , \quad (3.118)$$

where  $\sigma(\theta)$  is the differential cross-section,

$$\sigma(\theta) = |f(\theta)|^2 \quad . \quad (3.119)$$

The total scattering cross-section can then be written in terms of the scattered wave field coefficients as

$$\sigma^{\text{tot}} = \sum_{n=0}^{\infty} (|c_n^1|^2 + |c_n^2|^2) \quad . \quad (3.120)$$

The above quantity is generally used to check the convergency of the scattered wave field results obtained by the T-matrix formulation and employed in the selection of the T-matrix size to be used in the calculations.

## IV. NUMERICAL EVALUATIONS

This chapter is devoted to the applications of the transition matrix method described in the previous chapter. The examples presented include cylindrical rigid inclusions and cavities with circular, elliptical, rectangular and triangular cross sections. Some of the results obtained have been compared with the known exact and approximate solutions, [9,22].

In the numerical evaluations, an incident plane wave as given by Eq. (3.36) has been considered and both the "near-field" and, mainly, the "far-field" results have been obtained for various angles of incidence. The results have been presented in polar graphical forms, as discussed in sections (3.8.1) and (3.8.2).

The basic steps in the computation of the scattered wave field using T-matrix method can be outlined as follows:

- a) Description of the boundary geometry of the scatterer,
- b) Numerical evaluation of the boundary integrals for the generation of the Q-matrix elements,
- c) Inversion of the Q-matrix and creation of the T-matrix,
- d) Calculation of the scattered field coefficients through T-matrix,

- e) Evaluation of the scattered field for various incidence angles
- f) Check for the convergency of the numerical results by checking the convergency of the series, Eq. (3.120), representing the total scattering cross section.

Note that, if the convergency of the total scattering cross section is found to be insufficient at the end of the calculations, the steps (b) to (f) should be repeated by using a Q-matrix of the larger size.

#### 4.1 GENERAL PROCEDURE FOR THE EVALUATION OF THE Q-MATRIX ELEMENTS

In order to generate the Q-matrix one should evaluate the integrals given by Eqs. (3.77) and (3.78) either analytically or numerically. Analytical evaluation is possible for only circular geometry, because  $r \neq r(\theta)$  for circle and the boundary integrals reduces to simple trigonometric integrals. For general boundary geometries, the boundary integrals are to be evaluated numerically.

In order to illustrate the procedure followed in the computation of the Q-matrix elements, the derivations of the necessary analytical and numerical expressions are presented here for only the  $\tilde{Q}^{11}$  matrix for the rigid inclusion case.

To obtain the elements of the  $\tilde{Q}^{11}$  matrix, first, it is helpful to write Eq. (3.80) with slightly different notation as

$$Q_{jm}^{11} = \frac{1}{4} \int_S [\hat{n} ds \cdot \nabla \psi_m^1(r, \theta)] \hat{\psi}_j^1(r, \theta) , \quad (4.1)$$

where  $\hat{n}$  is the unit normal vector and  $\nabla$  is the gradient operator. To put the above expression into a form which is suitable for numerical calculations we need the explicit expressions for the terms inside the integrand.

Consider Fig. 4.1 for the evaluation of the term  $\hat{n} ds$ . As the incremental quantities  $\Delta s$ ,  $\Delta\theta$ ,  $\Delta r$  become infinitesimally small ( $\epsilon \rightarrow 0$ ), we can write

$$\hat{n} = \underline{e}_r \cos\gamma - \underline{e}_\theta \sin\gamma , \quad (4.2)$$

where  $\underline{e}_r$  and  $\underline{e}_\theta$  are the radial and tangential unit vectors, respectively, and

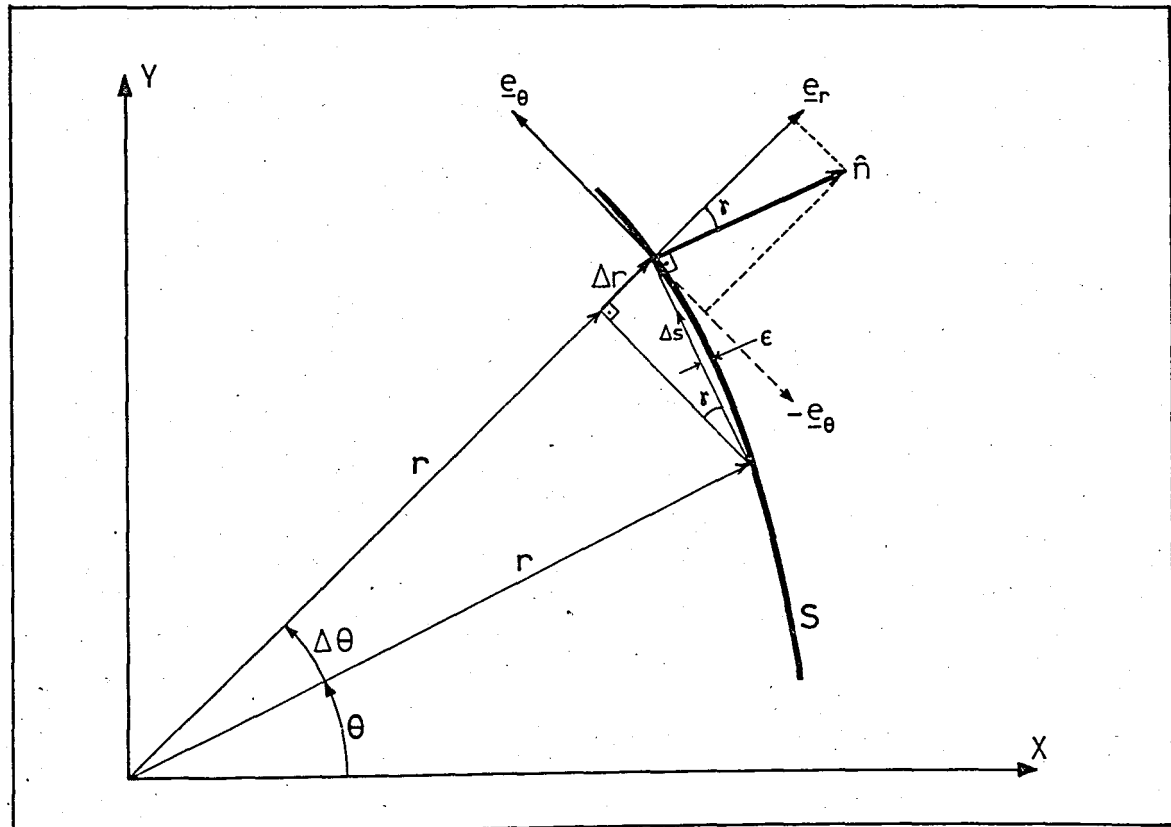


Figure 4.1 - Geometrical representation of the unit normal vector.

$$\cos\gamma = \frac{rd\theta}{ds} , \quad \sin\gamma = \frac{dr}{ds} . \quad (4.3)$$

Hence, from Eqs. (4.2) and (4.3), one obtains

$$\hat{n}ds = rd\theta[\underline{e}_r - \frac{1}{r} \frac{dr}{d\theta} \underline{e}_\theta] . \quad (4.4)$$

As to the term  $\nabla\psi_m^1(r, \theta)$ , using the gradient expression in polar coordinates,

$$\nabla = \frac{\partial}{\partial r} \underline{e}_r + \frac{1}{r} \frac{\partial}{\partial \theta} \underline{e}_\theta , \quad (4.5)$$

one can write

$$\nabla\psi_m^1 = (\epsilon_m)^{1/2} [\underline{e}_r k H_m^1(kr) \cos(m\theta) - \underline{e}_\theta \frac{m}{r} H_m(kr) \sin(m\theta)] . \quad (4.6)$$

Note that

$$\begin{aligned} H_m^1(kr) &= \frac{1}{2} [H_{m-1}(kr) - H_{m+1}(kr)] \\ &= \frac{m}{kr} H_m(kr) - H_{m+1}(kr) , \end{aligned} \quad (4.7)$$

thus, Eq. (4.6) reduces to

$$\begin{aligned} \nabla\psi_m^1 &= (\epsilon_m)^{1/2} \{ \underline{e}_r k [-\frac{m}{kr} H_m(kr) - H_{m+1}(kr)] \cos(m\theta) \\ &\quad - \underline{e}_\theta \frac{m}{r} H_m(kr) \sin(m\theta) \} . \end{aligned} \quad (4.8)$$

From Eqs. (4.4) and (4.8), one then obtains

$$\hat{n}ds \cdot \nabla \psi_m^1 = (\epsilon_m)^{1/2} r d\theta \left\{ k \left[ \frac{m}{kr} H_m(kr) - H_{m+1}(kr) \right] \cos(m\theta) + \frac{m}{r^2} \frac{dr}{d\theta} H_m(kr) \sin(m\theta) \right\} \quad (4.9)$$

Finally, substituting Eq. (4.9) and corresponding expression for  $\hat{\psi}_j^1$ , i.e., Eq. (3.90), into Eq. (4.1), and also writing  $dr/d\theta$  as  $1/k[d(kr)/d\theta]$ , one gets

$$Q_{jm}^{11} = \frac{(\epsilon_j \epsilon_e)^{1/2}}{4} \int_0^{2\pi} d\theta \{ J_j(kr) \cos j\theta \} \{ [mH_m(kr) - krH_{m+1}(kr)] \cos(m\theta) + \frac{m}{kr} H_m(kr) \sin(m\theta) \frac{d}{d\theta} (kr) \} \quad (4.10)$$

The quantities  $r$  and  $dr/d\theta$  both being functions of  $\theta$ , i.e.,  $r = r(\theta)$ ,  $d[r(\theta)]/d\theta$ , are to be determined from the analytical equations describing the geometry of the boundary of the scatterer of interest. One should also notice that 'r' always occurs as  $kr(\theta)$  in the expression for the Q-matrix elements. Therefore, in the numerical evaluations, it is sufficient to specify the wave number in a non-dimensional form, say  $k\ell$ , where  $\ell$  is a characteristic length in the problem, and the non-dimensional ratios of the geometry parameters such as aspect ratio, corner radius ratio etc.

As stated earlier, in general the angular integrations in Eq. (4.10) which are of the form

$$I = \int_0^{2\pi} F(\theta) d\theta \quad , \quad \text{on } S \quad (4.11)$$

can be carried out only numerically. The first step in the numerical evaluation of these integrals is the subdivision of the boundary  $S$  into  $N$  number of intervals  $\Delta S_i$  each subtending a central angle of  $\Delta\theta_i$ .

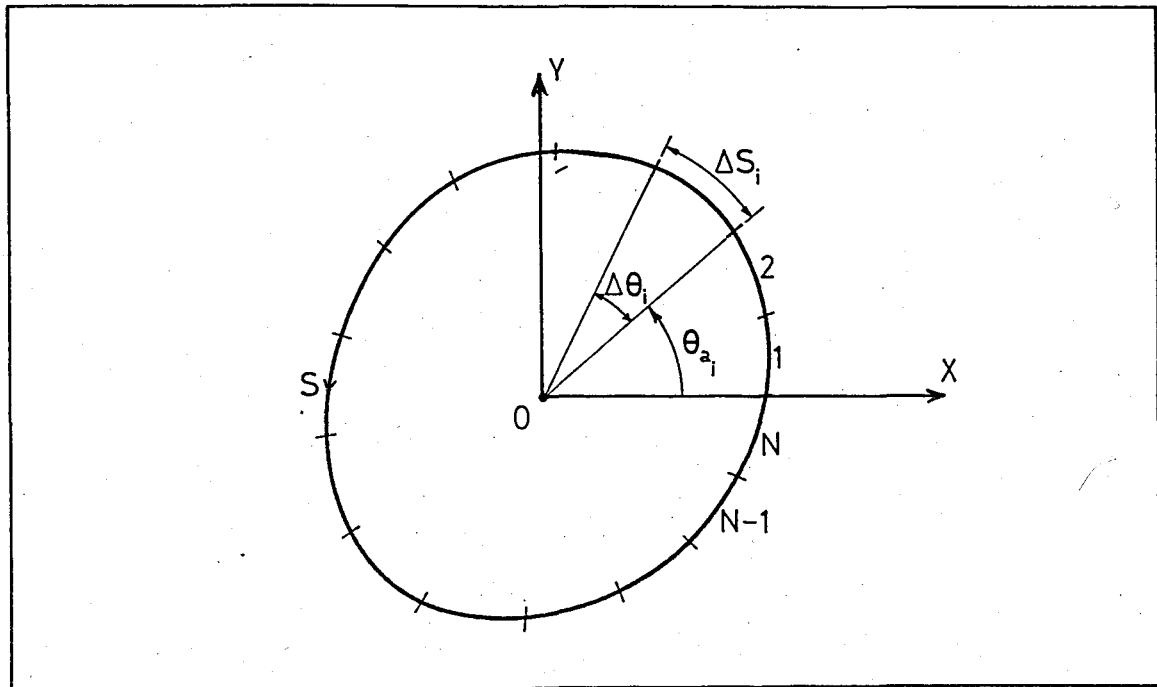


Figure 4.2 - Boundary subdivision.

such that, as shown in Fig. 4.2,

$$\sum_{i=1}^N \Delta S_i = S, \quad \sum_{i=1}^N \Delta\theta_i = 2\pi \quad \dots \quad (4.12)$$

The integral given by Eq. (4.11) can then be written as

$$I = \sum_{i=1}^N \frac{[\int F(\theta) d\theta]}{\Delta\theta_i} \quad , \quad \text{on } S \quad \dots \quad (4.13)$$

Having divided the boundary into  $N$  suitably small segments, one should next approximate the integrals which are to be evaluated separately for each angular interval  $\Delta\theta_i$ . This approximation can be made by using the Simpson's rule of any order. Hence, one can approximate the angular integrals in Eq. (4.13) in the form (see Appendix A)

$$\int_{\Delta\theta_i} F(\theta) d\theta \approx C_s \frac{\Delta\theta_i}{P} \sum_{q=0}^P F(\theta_{a_i} + q[\Delta\theta_i/P]) \times w_q , \quad (4.14)$$

where  $P$  is the order of the Simpson's rule used,  $C_s$  is a constant multiplication factor and  $w_q$  are the weighing factors. Note that,  $C_s$  and  $w_q$  are fixed numbers depending on the order  $P$ . Substituting Eq. (4.14) into (4.13), one gets

$$I \approx \frac{C_s}{P} \sum_{i=1}^N \sum_{q=0}^P \Delta\theta_i F(\theta_{a_i} + q[\Delta\theta_i/P]) w_q , \text{ on } S . \quad (4.15)$$

Finally, applying the above expression to Eq. (4.10) and using the geometrical definitions shown in Fig. 4.3, one obtains the desired numerical expression for the computation of the  $\tilde{Q}^{11}$ -matrix elements,

$$\begin{aligned} Q_{jm}^{11} &\approx \frac{(\varepsilon_j \varepsilon_m)^{\frac{1}{2}}}{4} \frac{C_s}{P} \sum_{i=1}^N \sum_{q=0}^P (\Delta\theta_i) w_q \{ J_j(kr_{iq}) \cos(j\theta_{iq}) \} \\ &\quad \times \{ [mH_m(kr_{iq}) - kr_{iq}H_{m+1}(kr_{iq})] \cos(m\theta_{iq}) \\ &\quad + \frac{m}{kr_{iq}} H_m(kr_{iq}) \sin(m\theta_{iq}) [\frac{d(kr)}{d\theta}]_{iq} \} , \quad r_{iq} \text{ on } S . \end{aligned} \quad (4.16)$$

The analytical and numerical expressions obtained for the other  $Q$ -submatrices, for both rigid inclusion and cavity cases, are given in Appendix B and C.

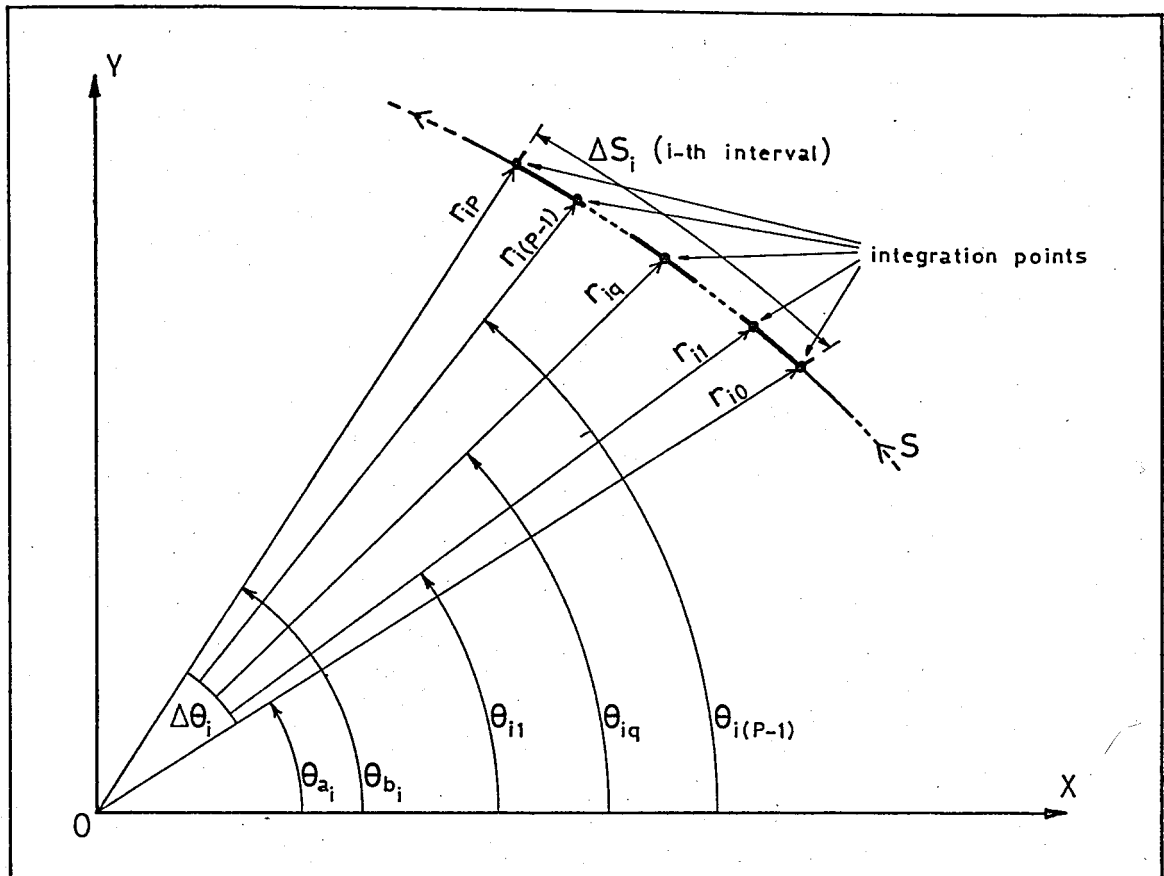


Figure 4.3 - Interval subdivision.

#### 4.2 CREATION OF THE T-MATRIX

After computing the Q-matrix elements according to the procedure outlined in the previous section, one can then create the T-matrix. But, before going into the evaluation of the T-matrix, one should perform the following conditioning on the Q-matrix, [21]. Because of the behaviour of the Hankel functions appearing in the elements of the Q-matrix, the imaginary parts of the elements of the Q-matrix will tend to grow to very large numerical values for the elements above the diagonal. In order to avoid the loss of precision due to the finite

precision arithmetic employed by the digital computers, it is convenient at this point to set the imaginary parts of all the mentioned elements to zero, by Gaussian elimination.

The T-matrix can be evaluated, as discussed earlier, using the matrix equation

$$\tilde{T} = -\tilde{Q}^{-1} \times \hat{\tilde{Q}} \quad (4.17)$$

which first requires the inversion of the Q-matrix directly by using a standard matrix inversion technique. However, from the point of view of numerical accuracy, this evaluation can be performed more effectively by first transforming the Q-matrix to a unitary matrix  $\tilde{Q}_{\text{unit}}$  and then applying the following matrix equation, [20,21],

$$\tilde{T} = -[\tilde{Q}_{\text{unit}}]^{t^*} \times [\hat{\tilde{Q}}_{\text{unit}}] \quad , \quad (4.18)$$

where the symbols 't' and '\*' denote the matrix transpose and the complex conjugate, respectively. This transformation, i.e., Q to  $\tilde{Q}_{\text{unit}}$ , is done by Schmidt orthogonalization [21].

#### 4.3 NUMERICAL EXAMPLES

In this section, the numerical results obtained by the application of the T-matrix method to the cylindrical rigid inclusions and cavities having circular, elliptical, rectangular (round cornered) and triangular (isosceles) cross sectional geometries are presented. The incident wave considered, as stated earlier, is a plane acoustic wave with constant velocity c, angular frequency  $\omega$ , and wavelength  $\lambda = 2\pi/k$ .

The scattered wave field is computed for various non-dimensional wave numbers,  $k\ell$ , and incidence angles,  $\alpha$ .

#### 4.3.1 Circular Cylinders

The equation of the boundary of a circular cylindrical scatterer in polar coordinates is simply

$$r = a \quad , \quad (4.19)$$

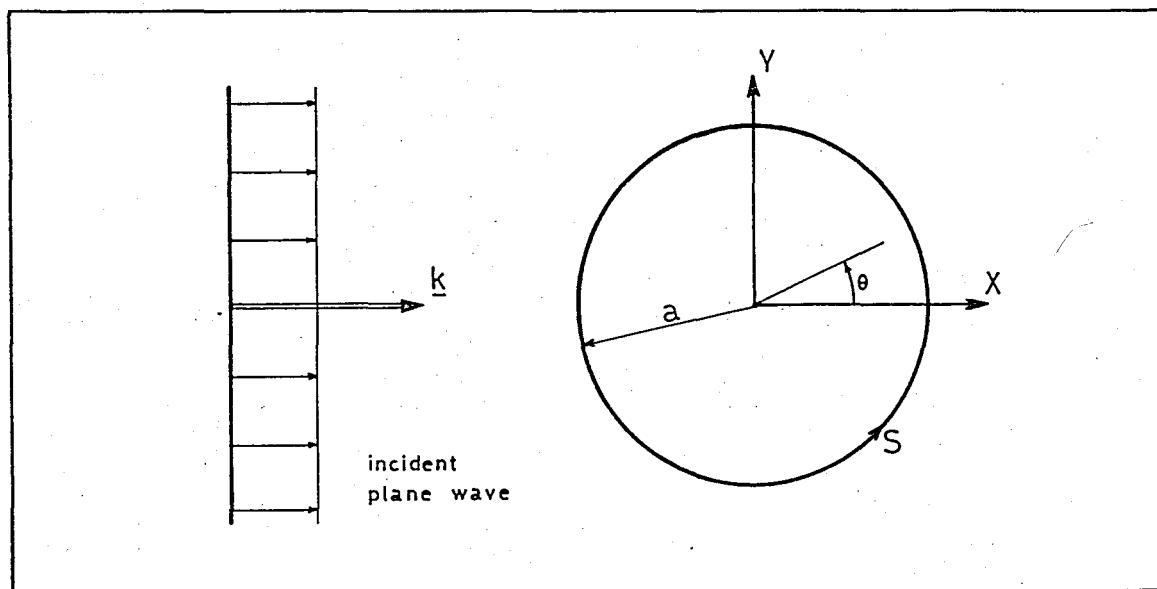


Figure 4.4 - Geometry for the circular cylindrical scatterer.

where  $a$  is the radius of the circle, as shown in Fig. 4.4. From Eq. (4.19) one easily sees that  $r \neq r(\theta)$ , thus,

$$[dr/d\theta] = 0 \quad . \quad (4.20)$$

The polar plots of the scattered field results obtained for the rigid inclusion and cavity cases are presented in Figs. 4.8 to

4.10. Note that, due to the rotational symmetry of the problem, the scattered wave field is to be computed for only zero angle of incidence, i.e., for  $\alpha = 0^\circ$ .

#### 4.3.2 Elliptical Cylinders

For the evaluation of the boundary integrals one needs the equation of the ellipse and the angular variation [ $dr/d\theta$ ], which are given by

$$r(\theta) = a[\cos^2\theta + (b/a)^2\sin^2\theta]^{1/2}, \quad (4.21)$$

$$\frac{dr}{d\theta} = a\{(b/a)[(b/a)^2 - 1]\sin\theta\cos\theta[\sin^2\theta + (b/a)^2\cos^2\theta]^{-3/2}\}, \quad (4.22)$$

where  $2a$  and  $2b$  are the major and minor axes, as shown in Fig. 4.5.

The polar plots of the near and far field results obtained for the rigid inclusion and cavity cases for various  $ka$  values and aspect ratios ( $b/a$ ) are presented in Figs. 4.11 to 4.18.

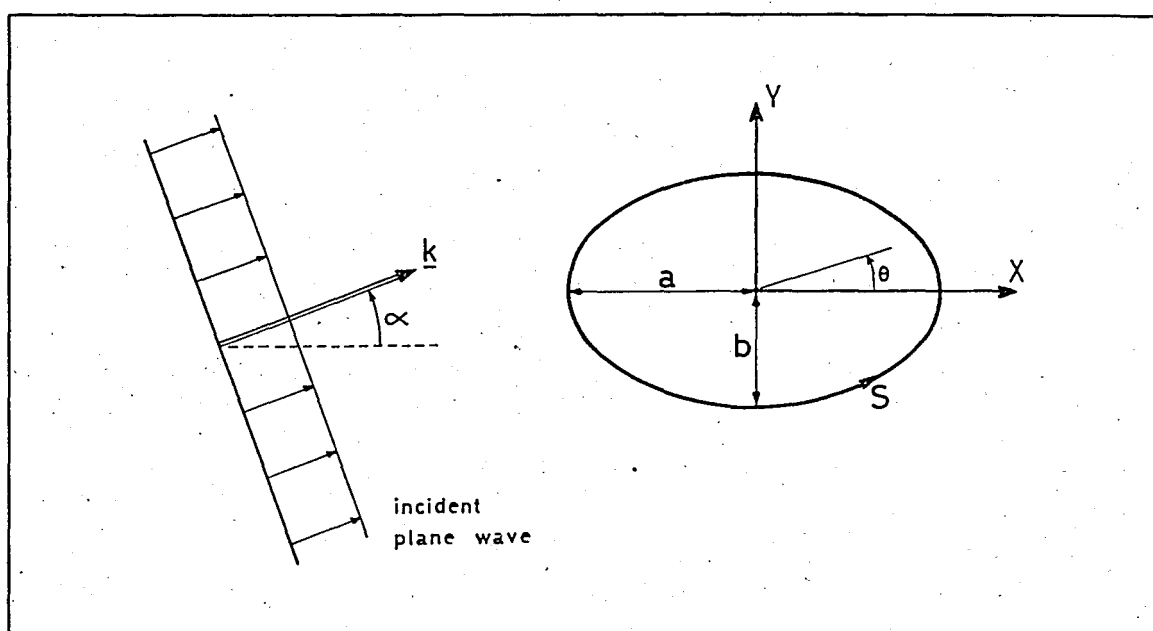


Figure 4.5 - Boundary geometry of the elliptic cylinder.

### 4.3.3 Rectangular Cylinders

In the application of the T-matrix method to rectangular cylinders, a round cornered type rectangular cross section is considered. To describe the boundary geometry, the following geometrical definitions are made first;

$$\gamma = \arctan[(b/a - r_c/a)/(1 - r_c/a)] , \quad (4.23)$$

$$(D/a) = (1 - r_c/a)/\cos\gamma , \quad (4.24)$$

$$\phi_1 = \arctan[b/a - r_c/a] , \quad (4.25)$$

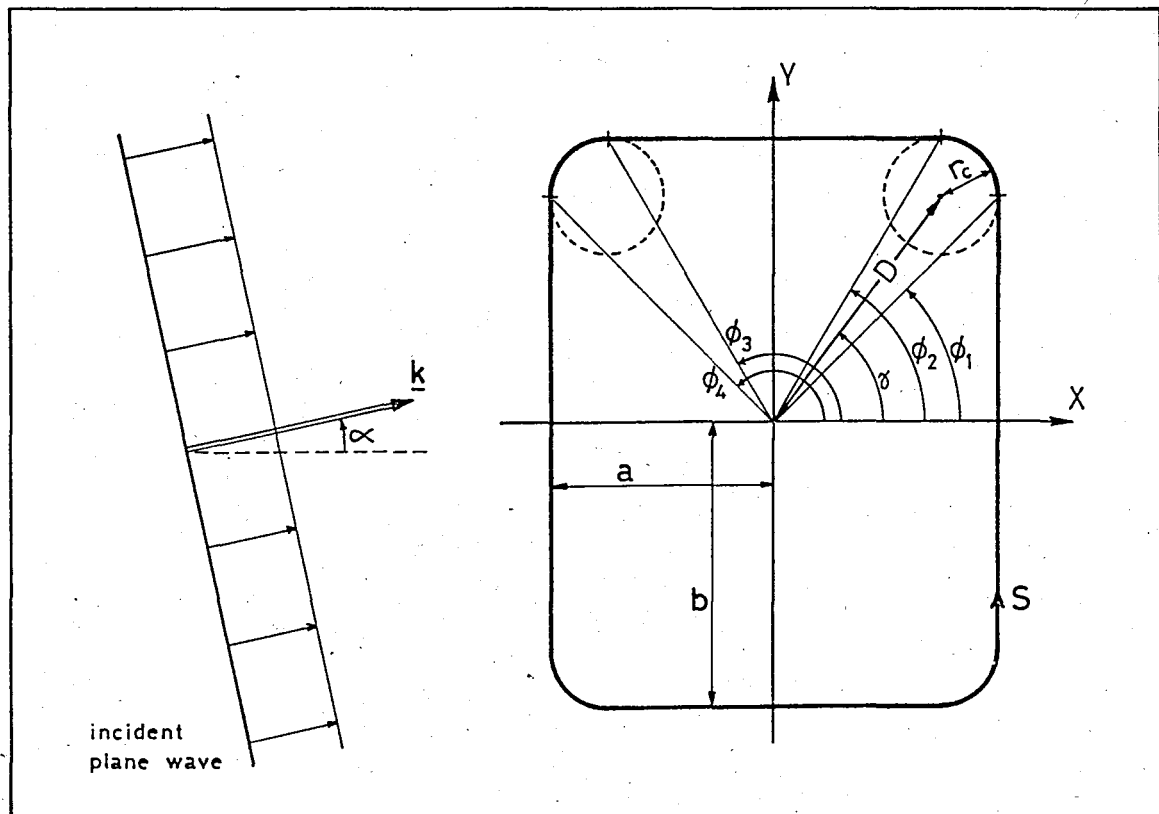


Figure 4.6 - Boundary geometry of the round cornered rectangular cylinder.

$$\phi_2 = \arctan[(b/a)/(1 - r_c/a)] , \quad (4.26)$$

$$\phi_3 = \pi - \phi_2 , \quad \phi_4 = \pi - \phi_1 , \quad (4.27)$$

where  $2a$  and  $2b$  are the width and the length of the rectangle and  $r_c$  is the corner radius, as shown in Fig. 4.6. Employing these definitions one can write the analytical equations of the boundary and the  $(dr/d\theta)$  values in the range  $0 \leq \theta \leq \pi$  as

$$a) \quad r(\theta) = a(1/\cos\theta) ,$$

$$\frac{dr}{d\theta} = a(\sin\theta/\cos^2\theta) \quad \text{for } 0 \leq \theta \leq \phi_1 , \quad (4.28)$$

$$b) \quad r(\theta) = a\{(D/a)\cos(\theta-\gamma) + [(D/a)^2\cos^2(\theta-\gamma) + (r_c/a)^2 - (D/a)^2]^{1/2}\} ,$$

$$\frac{dr}{d\theta} = a\{(D/a)\sin(\gamma-\theta) + (D/a)^2\cos(\gamma-\theta)\sin(\gamma-\theta)$$

$$\times [(D/a)^2\cos^2(\gamma-\theta) + (r_c/a)^2 - (D/a)^2]^{-1/2}\}$$

$$\text{for } \phi_1 \leq \theta \leq \phi_2 , \quad (4.29)$$

$$c) \quad r(\theta) = a[(b/a)/\sin\theta] ,$$

$$\frac{dr}{d\theta} = a[-(b/a)\cos\theta/\sin^2\theta] \quad \text{for } \phi_2 \leq \theta \leq \phi_3 , \quad (4.30)$$

$$d) \quad r(\theta) = a\{(D/a)\cos(\theta+\gamma-\pi) + [(D/a)^2\cos^2(\theta+\gamma-\pi) + (r_c/a)^2 - (D/a)^2]^{1/2}\} ,$$

$$\frac{dr}{d\theta} = a\{(D/a)\sin(\pi-\gamma-\theta) + (D/a)^2\cos(\pi-\gamma-\theta)\sin(\pi-\gamma-\theta)$$

$$\times [(D/a)^2\cos^2(\pi-\gamma-\theta) + (r_c/a)^2 - (D/a)^2]^{-1/2}\}$$

$$\text{for } \phi_3 \leq \theta \leq \phi_4 , \quad (4.31)$$

e)  $r(\theta) = a(-1/\cos\theta)$  ,

$$\frac{dr}{d\theta} = a(-\sin\theta/\cos^2\theta) \quad \text{for } \phi_4 \leq \phi < \pi . \quad (4.32)$$

Note that, the values of  $r$  and  $dr/d\theta$  for the range  $\pi \leq \theta \leq 2\pi$  are computed by first setting  $\theta \rightarrow \theta - \pi$  and then applying again the formulas given in Eqs. (4.28-32).

The polar plots of the scattered wave field results obtained for various  $ka$  values and the ratios  $(b/a)$ ,  $(r_c/a)$  are presented in Figs. 4.19 to 4.34.

#### 4.3.4 Triangular Cylinders

We have also considered a scatterer with cross section in the form of an isosceles triangle, as shown in Fig. 4.7. The expressions for the boundary and  $dr/d\theta$  in the range  $0 \leq \theta < \pi$  are

a)  $r(\theta) = h[1/(3\cos\theta)]$  ,

$$\frac{dr}{d\theta} = h[\sin\theta/(3\cos^2\theta)] \quad \text{for } 0 \leq \theta < \phi , \quad (4.33)$$

b)  $r(\theta) = h\{(2/3)\tan(\beta/2)/[\sin\theta - \cos\theta\tan(\beta/2)]\}$  ,

$$\frac{dr}{d\theta} = h\{(-2/3)\tan(\beta/2)[\cos\theta + \sin\theta\tan(\beta/2)]/[\sin\theta - \cos\theta\tan(\beta/2)]^2\} \quad \text{for } \phi \leq \theta < \pi , \quad (4.34)$$

where the angle  $\phi$  is given by

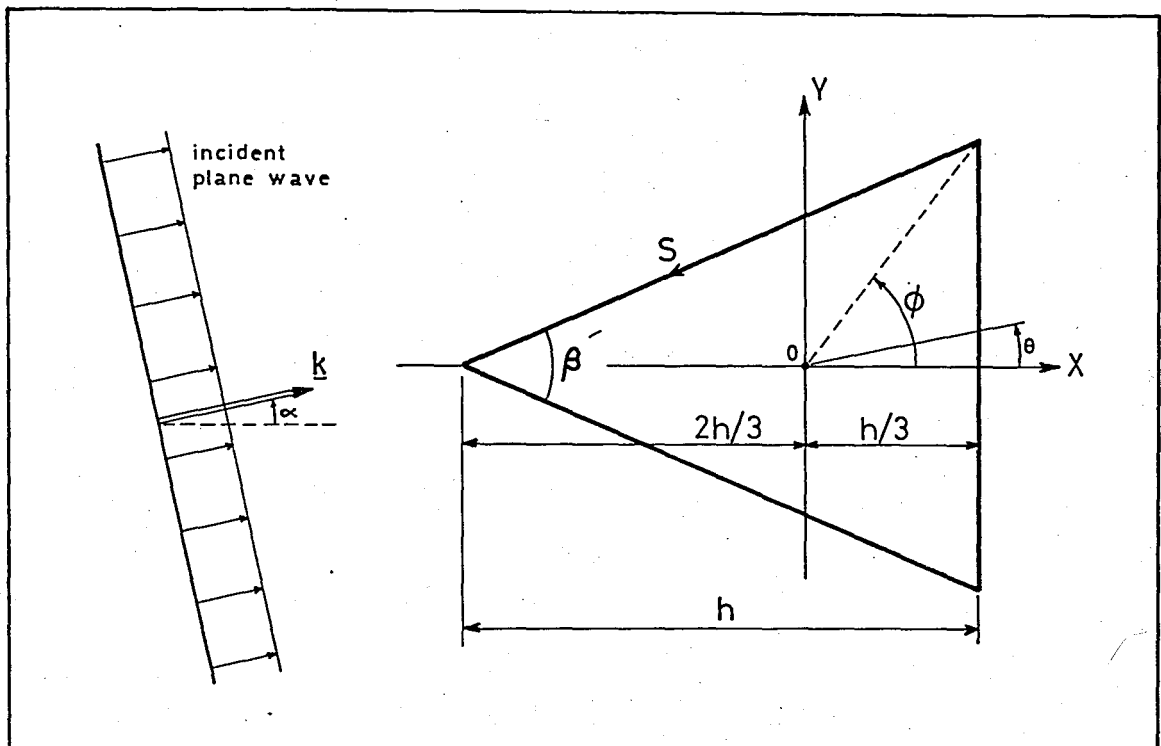


Figure 4.7 - Boundary geometry of the triangular cylinder.

$$\phi = \arctan[3\tan(\beta/2)] \quad . \quad (4.35)$$

Values of  $r(\theta)$  and  $dr/d\theta$ , in the range  $\pi \leq \theta < 2\pi$ , are obtained by setting  $\theta \rightarrow 2\pi - \theta$  in the Eqs. (4.33) and (4.34), and then setting  $dr/d\theta$  to  $-dr/d\theta$ .

The scattered field results obtained for various  $kh$  and  $\beta$  values are presented in Figs. 4.35 to 4.41.

## V. CONCLUSIONS

In this work, the numerical results for acoustic plane waves scattered by circular, elliptical, rectangular and triangular rigid inclusions and cavities have been obtained utilizing the T-matrix method. The results are presented in polar graphical forms. These results are compared with the exact or approximate solutions [9,22], where available. For the rectangular and triangular cylinders, however, because of the unavailability of any result obtained in other studies, no comparison can be made.

In the evaluations of the elements of the Q-matrix, fourth order Simpson's rule is used to perform the angular integrations along the boundaries of the scatterers. Good convergence is obtained using 36 integration steps in the range  $0-\pi$ . For triangular geometry, corners may be thought to give rise to difficulties from the analytical point of view. However, since the integrals are evaluated by considering only discrete points taken within each angular interval, no computational problem is encountered. The symmetry and other numerical properties given by Eqs. (3.92), (3.94) and (3.95) is effectively used to check the accuracy of the numerical procedure followed.

The T-matrix is constructed by inverting the Q-matrix using Gauss-Schmidt orthogonalization technique, as discussed in Section 4.2.

The requirements given by Eqs. (3.99) and (3.100) are first used to check the correctness of the computer program, then they are, together with Eqs. (3.92), (3.94), (3.95), incorporated into the program reducing computing time significantly.

It is observed that the size of the T-matrix to be used is related to the non-dimensional number  $kr_{\max}$ , where  $k$  is the wave number and  $r_{\max}$  is the maximum  $r$  value which is to be encountered along the boundary of the scatterer. In order to be able to obtain sufficiently convergent results, the size of the T-matrix is generally increased in a direct proportion to the non-dimensional number  $kr_{\max}$ . The sufficiency of the matrix size, however, is controlled by checking the convergency of the total scattering cross-section, Eq. (3.120). This check is made up to when the total scattering cross section did not differ by more than at least  $10^{-5}$  per cent. A rough estimate for the size requirement of the T-matrix may be given as  $6 \times 6$  for  $kr_{\max} = 0.1$ ,  $15 \times 15$  for  $kr_{\max} = 1.0$  and  $40 \times 40$  for  $kr_{\max} = 5.0$ .

In the case of scattering by circular cylinders, both near (Fig. 4.8) and far field (Figs. 4.9, 3.10) results are found to be in excellent agreement with the exact solutions for all wave numbers, [22]. This is because of the fact that the basis wave functions given by Eqs. (3.1) and (3.5) are exact expressions for the circle and hence the T-matrix formulation yields exact solutions for the circular cross-sections.

In the case of scattering by elliptical cylinders, the near field results are plotted in Figs. 4.11, 4.12 for the aspect ratios  $b/a = 0.5$  and  $2.0$  and for  $\alpha = 0^\circ$ . In these figures, we observe that for a given incident wave number the angular spectrum of the scattered

field is quite different for two different values of  $b/a$ . In the case of scattered far field amplitudes, some of the results were compared with those obtained in Ref. [9] and found to be in good agreement especially for relatively small wave numbers ( $ka \leq 1.0$ ). The far field results have been obtained for the aspect ratios 0.5, 2.0, 5.0 and for different incidence angles and presented in Figs. 4.13-15 for rigid inclusion, and in Figs. 4.16-18 for cavity. In the case of rigid inclusion, the structure of the polar plots varies quite remarkably for different incidence angles and aspect ratios. Especially for the higher aspect ratios, larger angular peaks are observed in the forward direction. However, for a cavity, we observe that, in contrast to the rigid inclusion, the dependency of the structure of the plots on both incidence angle and aspect ratio is not so significant.

The near field results, Figs. 4.19, 4.20, for scatterers with rectangular cross-section show that the surface field potential distributions, comparing with the circular and elliptical geometries, display sharper maxima and minima for all wave numbers. Although, for low frequencies ( $ka \leq 1.0$ ), the shapes of the plots are somewhat similar to the ones obtained in the elliptical case, the picture is entirely different in the high frequency range. For the far field case, we observe that the field scattered by a rectangular cylinder displays more angular structure than that generated by a circular or elliptical cylinder. The far field results obtained for a rigid inclusion (Figs. 4.21-27) indicate that effects of the aspect ratio and the incidence angle on the shape of the polar plots are relatively strong. These effects are more obvious at higher wave numbers ( $ka > 1.0$ ). On the

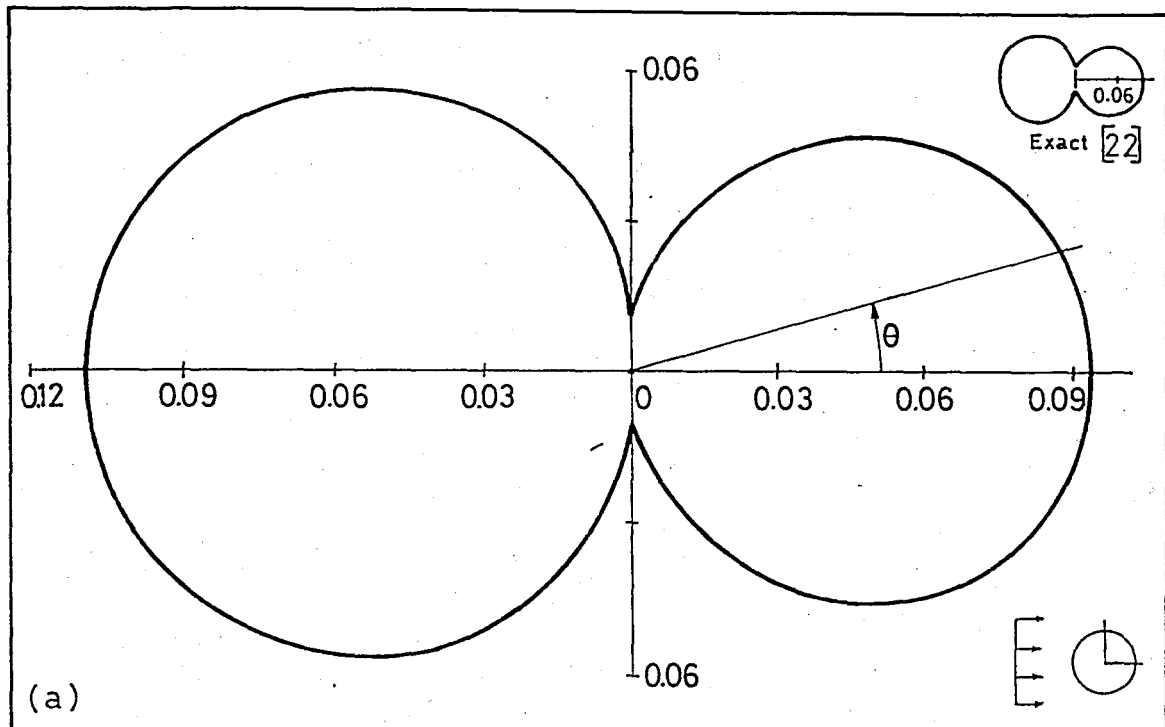
other hand, it is observed that, as shown in Figs. 4.21, 4.22 (rigid inclusion) and in Figs. 4.28, 4.29 (cavity), effect of the corner radius ratio,  $r_c/a$  is not significant for a given aspect ratio and the wave number. In this respect, the scattered field results pertaining to the rectangular geometry are presented for  $r_c/a = 0.1$  only. In the case of a cavity (Figs. 4.28-34), as for the rigid inclusion, the structure of the far field plots exhibits similar behaviour with respect to the changes in the aspect ratio, incidence angle, and frequency; however, the curves for the cavity are relatively smooth. A comparison of the far field results obtained for a cavity and a rigid inclusion cases reveals that for identical surface geometries no similarity exists for any given wave number in the range  $0.1 \leq ka \leq 1.0$ . However, at the higher wave numbers the cavity cannot be clearly distinguished from a rigid inclusion.

In the case of cylinders with triangular cross-sections, the near field solution given in Fig. 4.35 are quite different when compared to the previous geometries. This difference may be attributed to the fact that the cross-sectional geometry of the cylinder has only single symmetry axis. The far field results both for cavity and rigid inclusion, Figs. 4.36-41, are given for three different tip angles,  $\beta = 60^\circ, 30^\circ$  and  $0.001^\circ$ . For  $\beta = 60^\circ$  and  $30^\circ$ , we observe that if  $\alpha \neq 0^\circ$  the far field plots are quite similar to the ones obtained for the rectangular cross-sections, while for  $\alpha = 0^\circ$  structure of the plots differs remarkably when compared to the other geometries. Especially at the higher frequencies, for  $\alpha = 0^\circ$  comparably larger angular peaks are observed in the forward scattering than in the

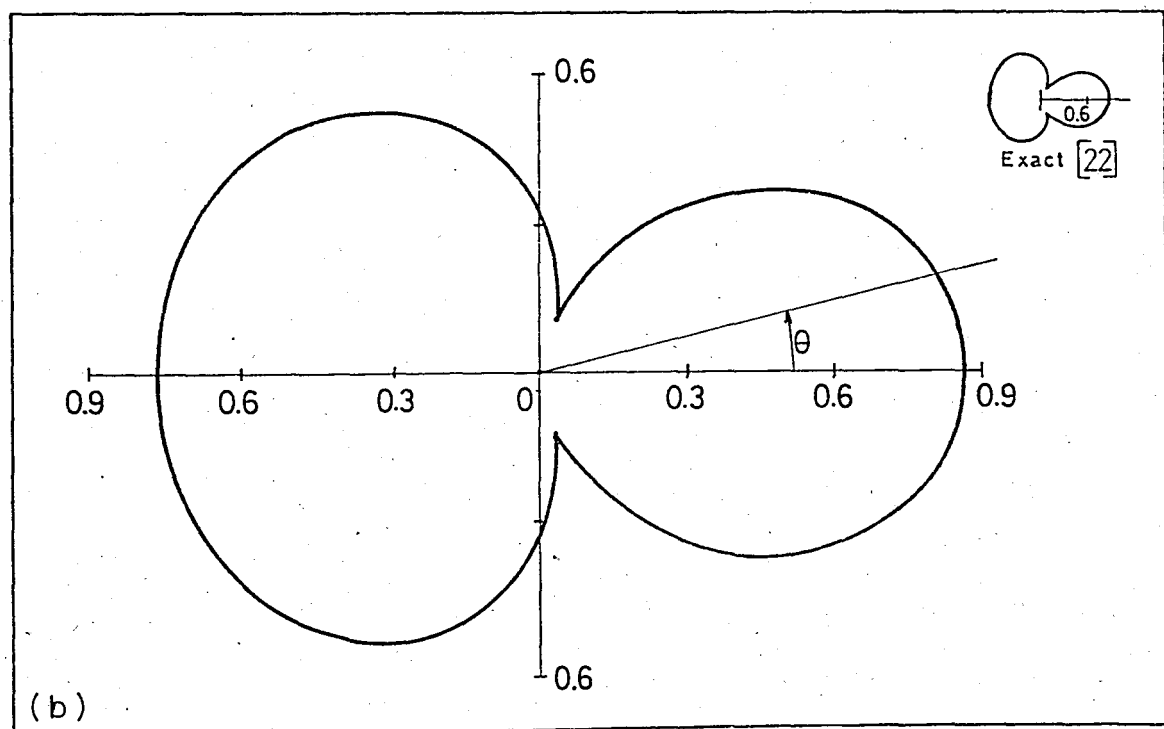
backward scattering. For the case  $\beta = 0.001^0$  where the shape of the scatterer looks like a strip rather than a triangle, as shown in Figs. 4.38 and 4.41 general form of the far field plots is quite different.

In the polar plots of the scattered field results, it is observed that at low frequencies,  $kr_{\max} \sim 0.1$ , the pictures for all boundary geometries are almost the same in appearance and do not change with incidence angle,  $\alpha$ , hence, for all cases, the obstacles behave like point scatterers. Thus low frequency results are not useful for practical applications. However, for higher frequencies, quite remarkable differences and angular variations are observed in the structures of the plots for different boundary geometries and incidence angles.

To sum up, the T-matrix method, using only circular or spherical wave functions and removing the geometrical restriction, makes it possible to analyze the scattering of waves from inclusions of any shape. Although the completeness of the series representation of the wave fields, especially in the near field, is still a matter of discussion, the method provides a systematical and powerful computational procedure for a very wide range of wave numbers.



(a)



(b)

Figure 4.8 - Velocity potential distribution,  $|u^s/A|$ , at the boundary of a rigid circular inclusion due to the scattered wave field;  
 (a)  $ka = 0.1$ , (b)  $= 1.0$ , (c)  $ka = 5.0$

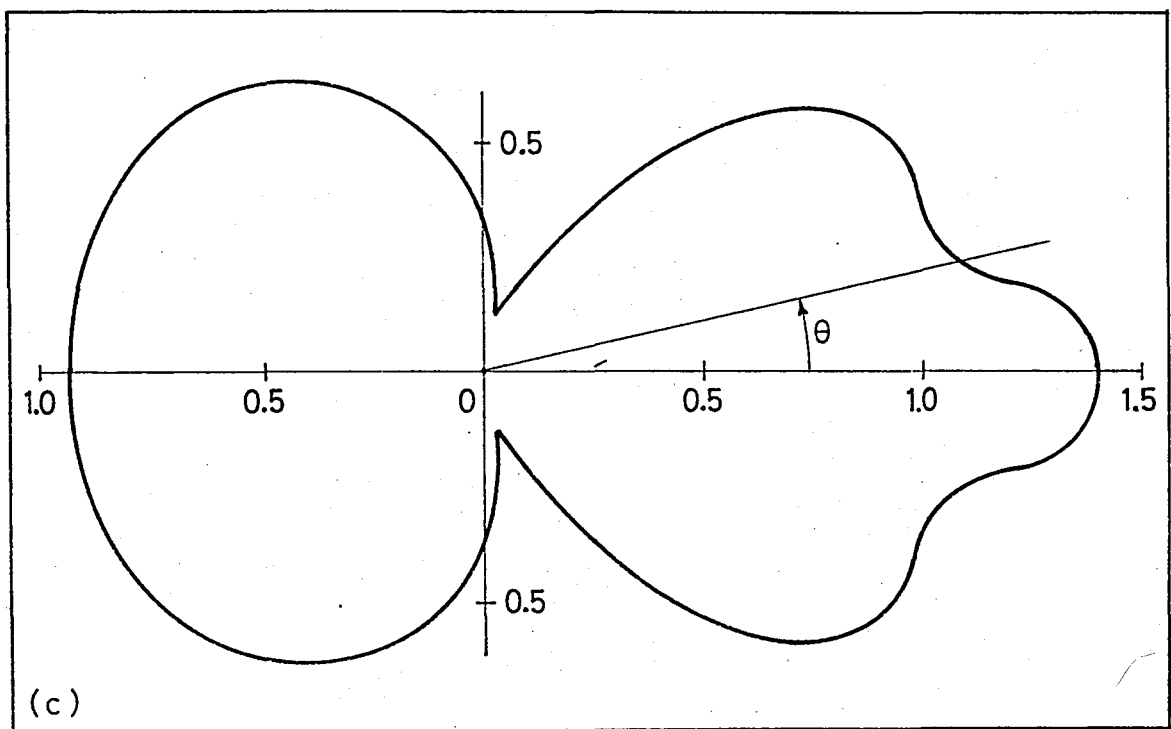


Figure 4.8 (continued).

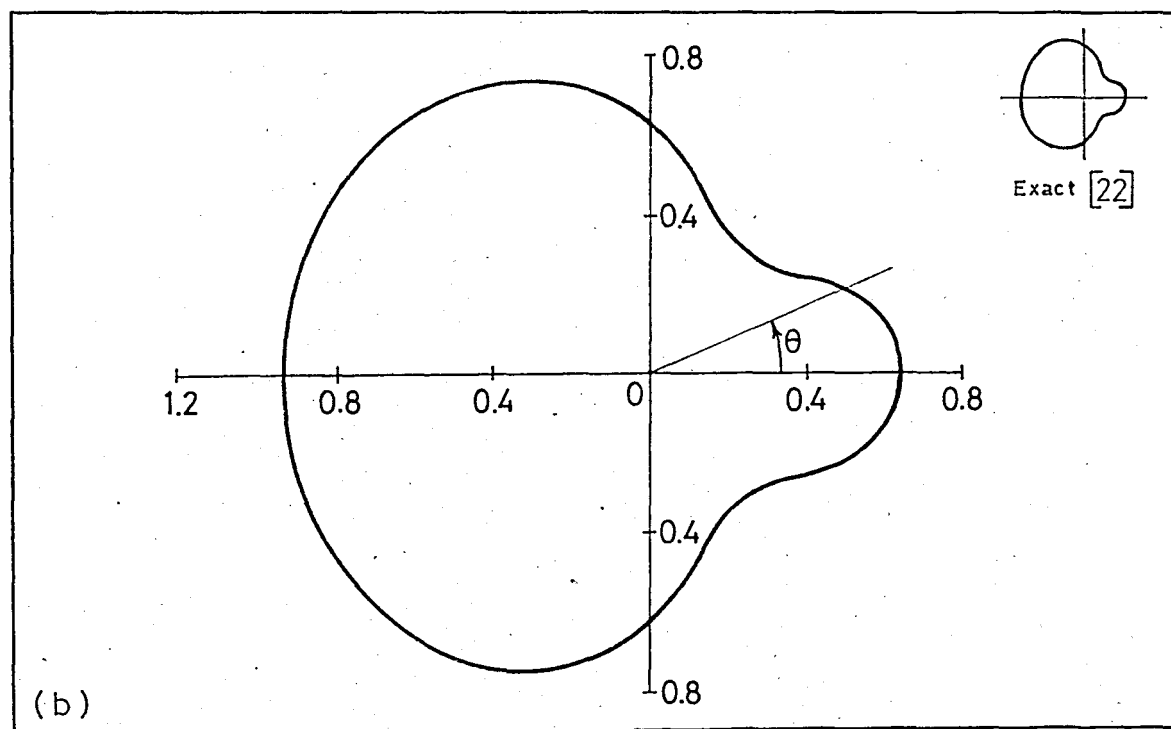
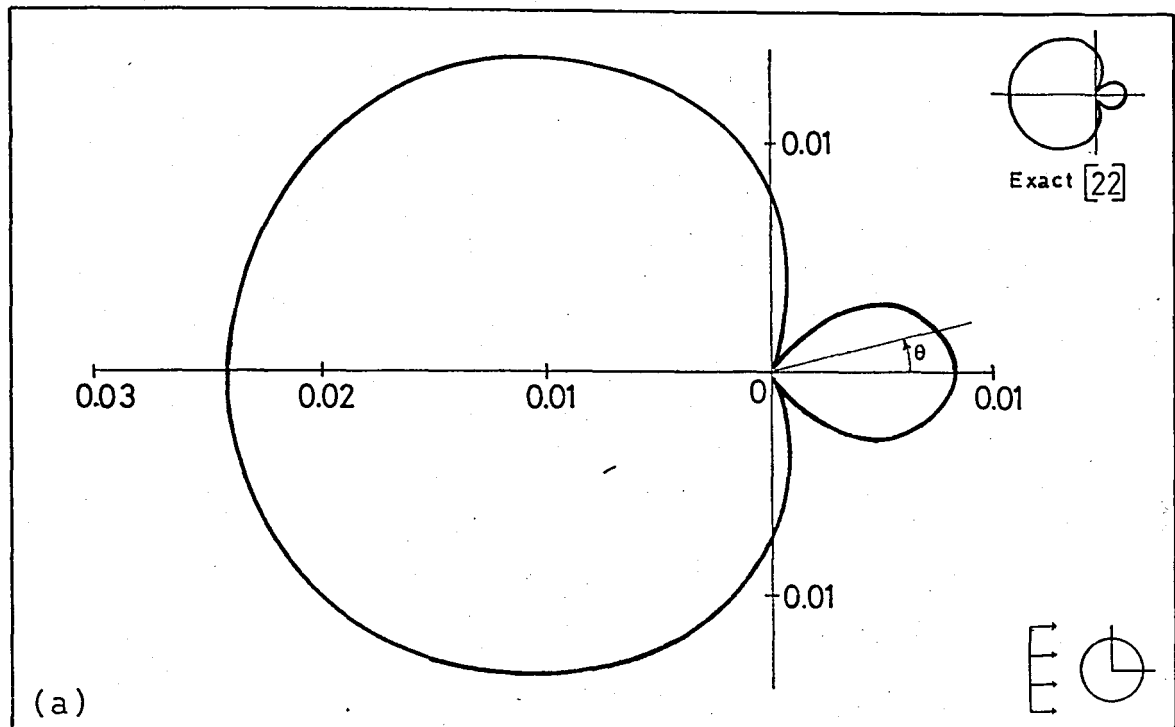


Figure 4.9 - Far field amplitude,  $|f/A|$ , due to the scattered wave field from a rigid circular inclusion;  
 (a)  $ka = 0.1$ , (b)  $ka = 1.0$ , (c)  $ka = 5.0$ .

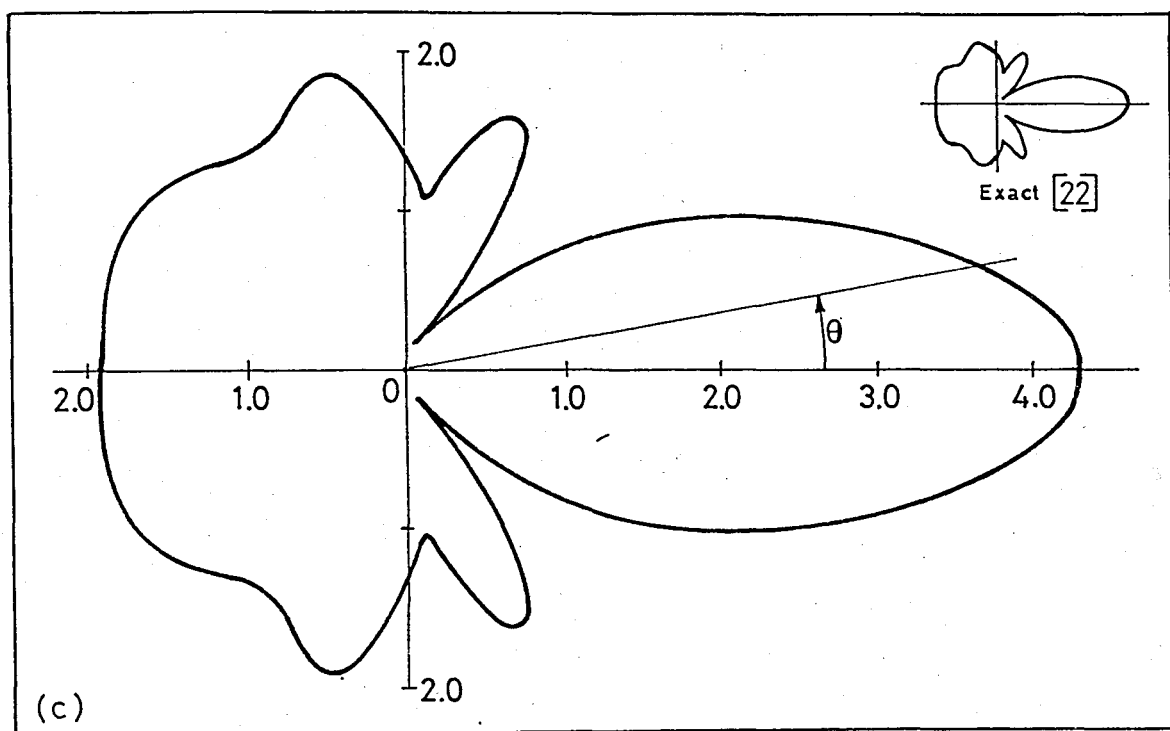


Figure 4.9 (continued).

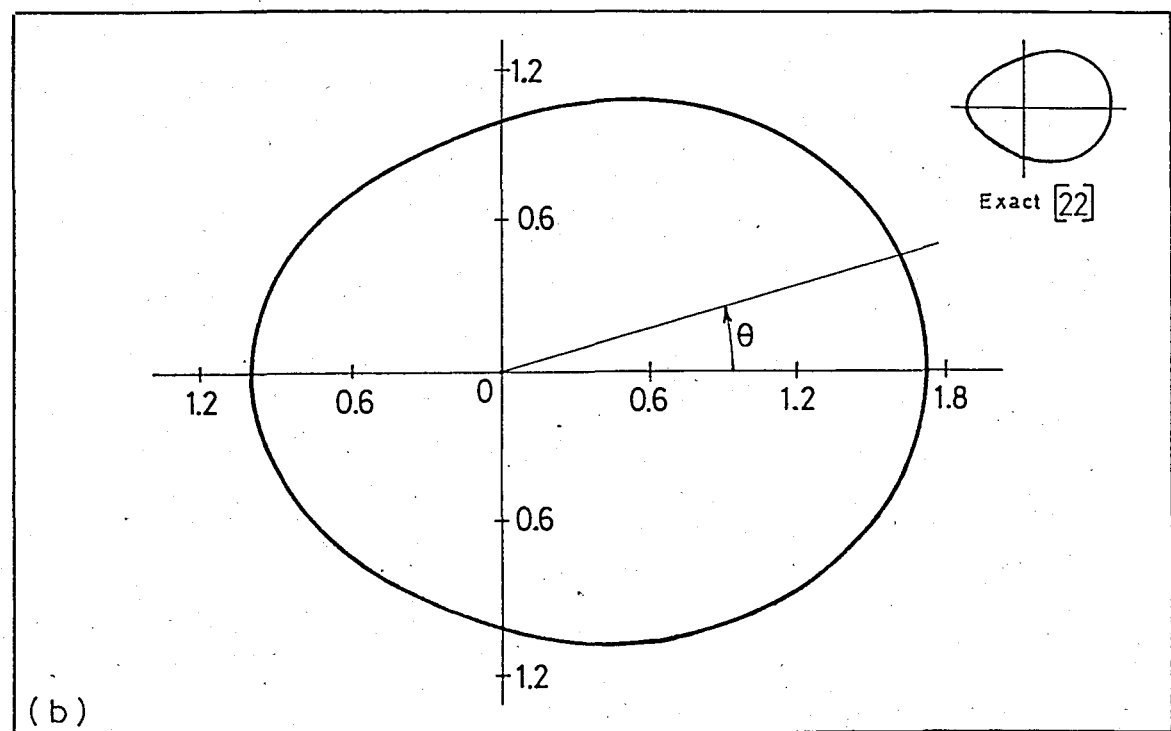
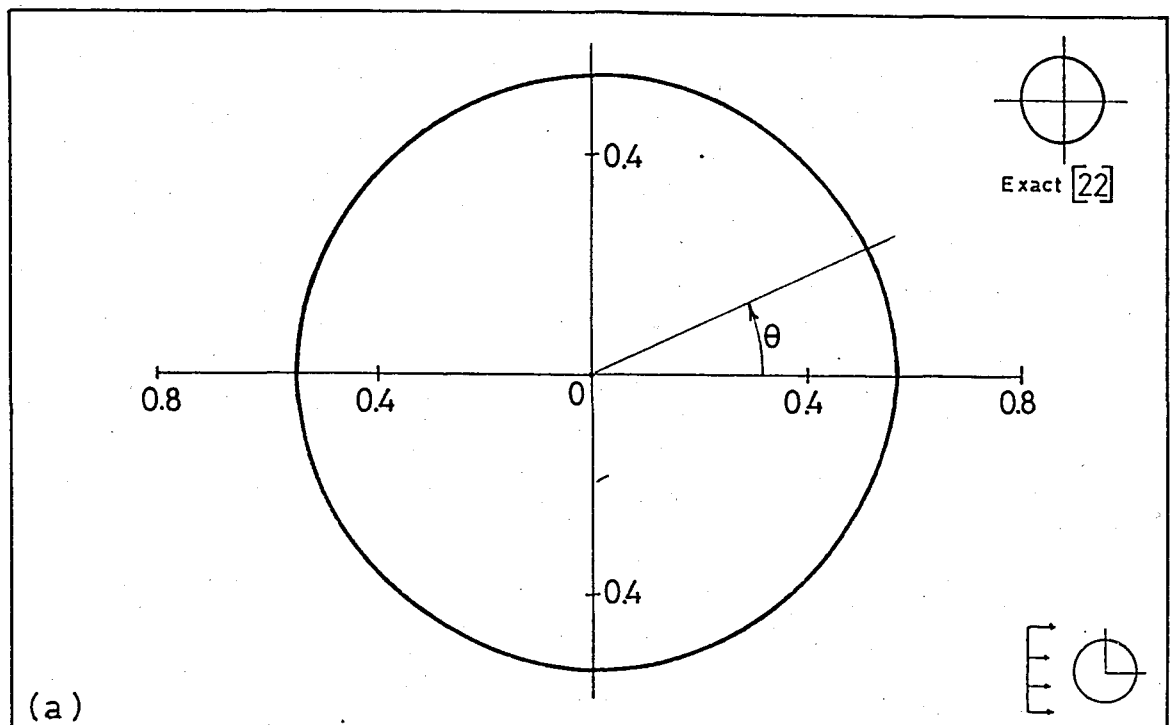


Figure 4.10 - Far field amplitude,  $|f/A|$ , due to the scattered wave field from a circular cavity;  
 (a)  $ka = 0.1$ , (b)  $ka = 1.0$ , (c)  $ka = 5.0$ .

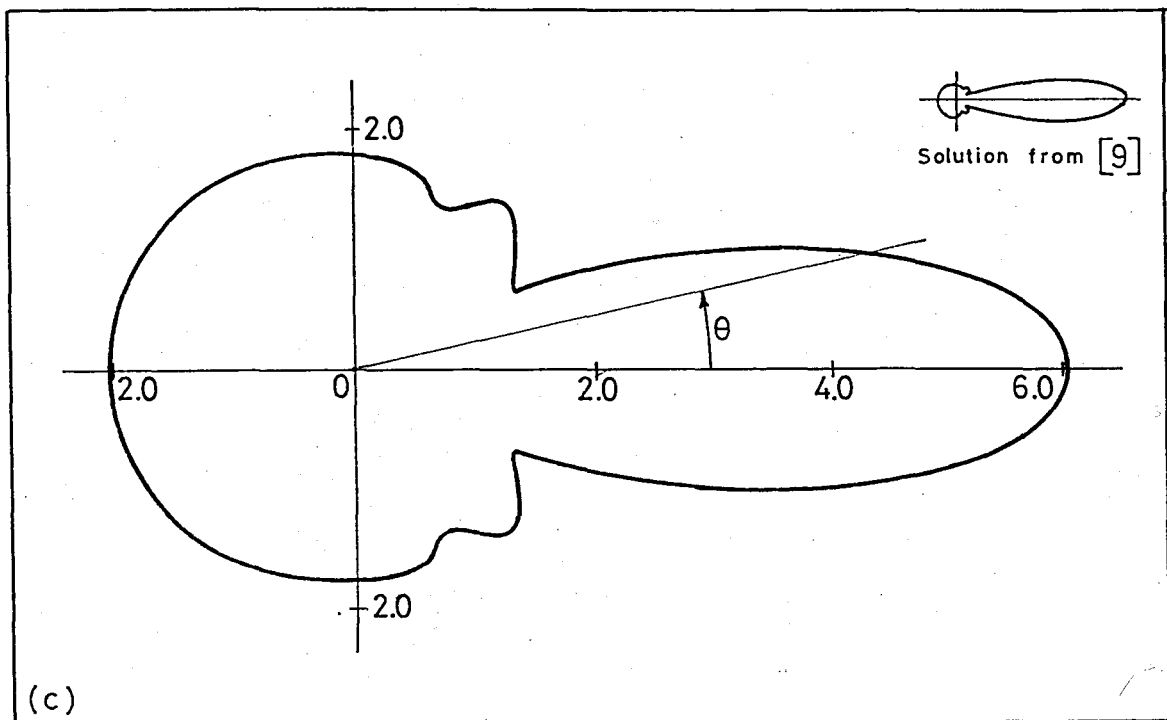


Figure 4.10 (continued).

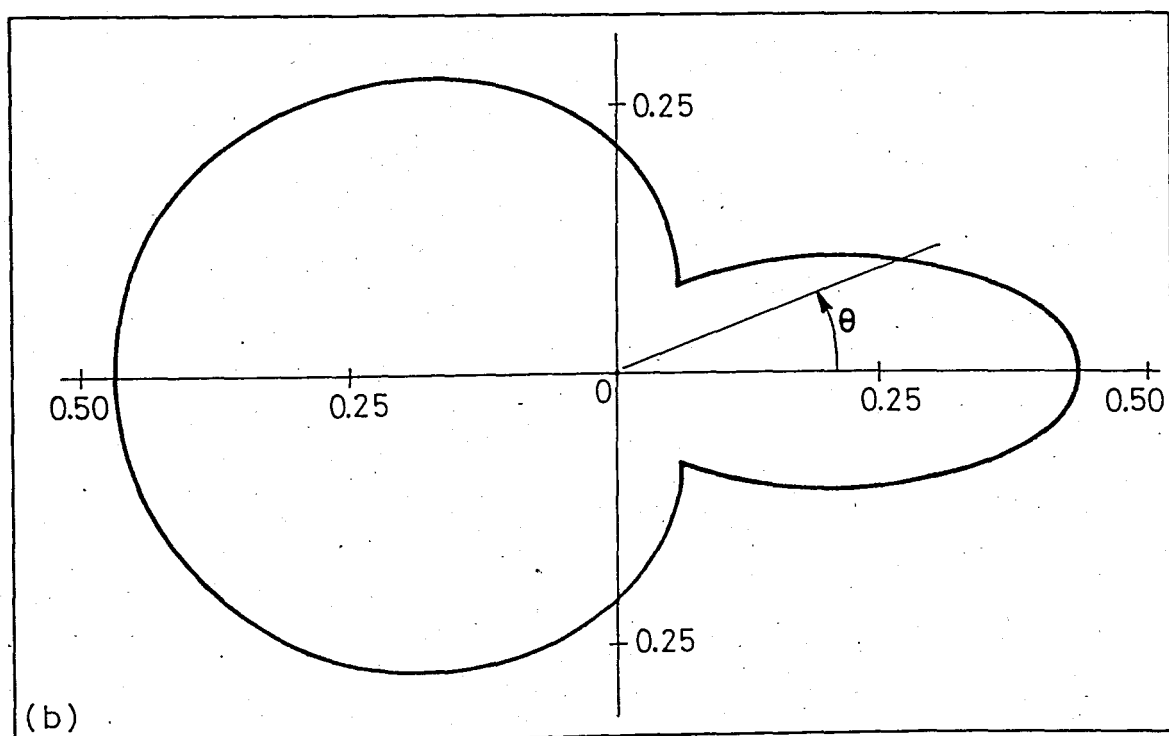
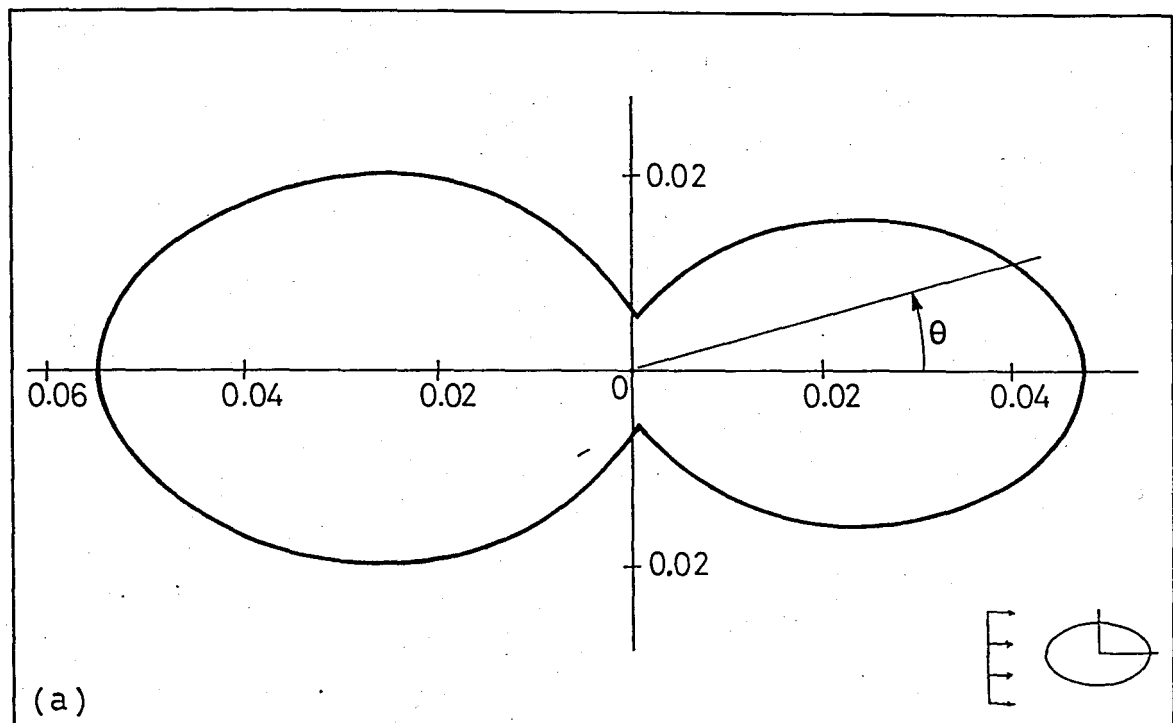


Figure 4.11 - Velocity potential distribution,  $|u^s/A|$ , at the boundary of a rigid elliptical inclusion due to the scattered wave field for  $\alpha = 0^\circ$  and  $b/a = 0.5$ ; (a)  $ka = 0.1$ , (b)  $ka = 1.0$ , (c)  $ka = 5.0$ .

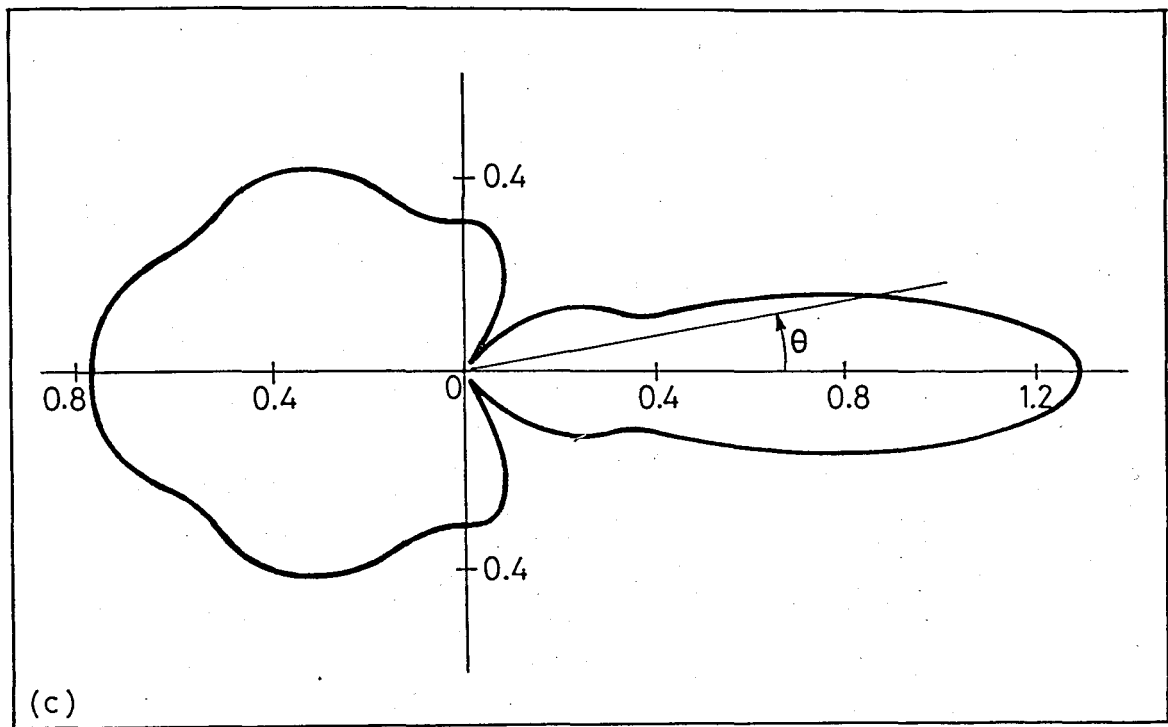


Figure 4.11 (continued).

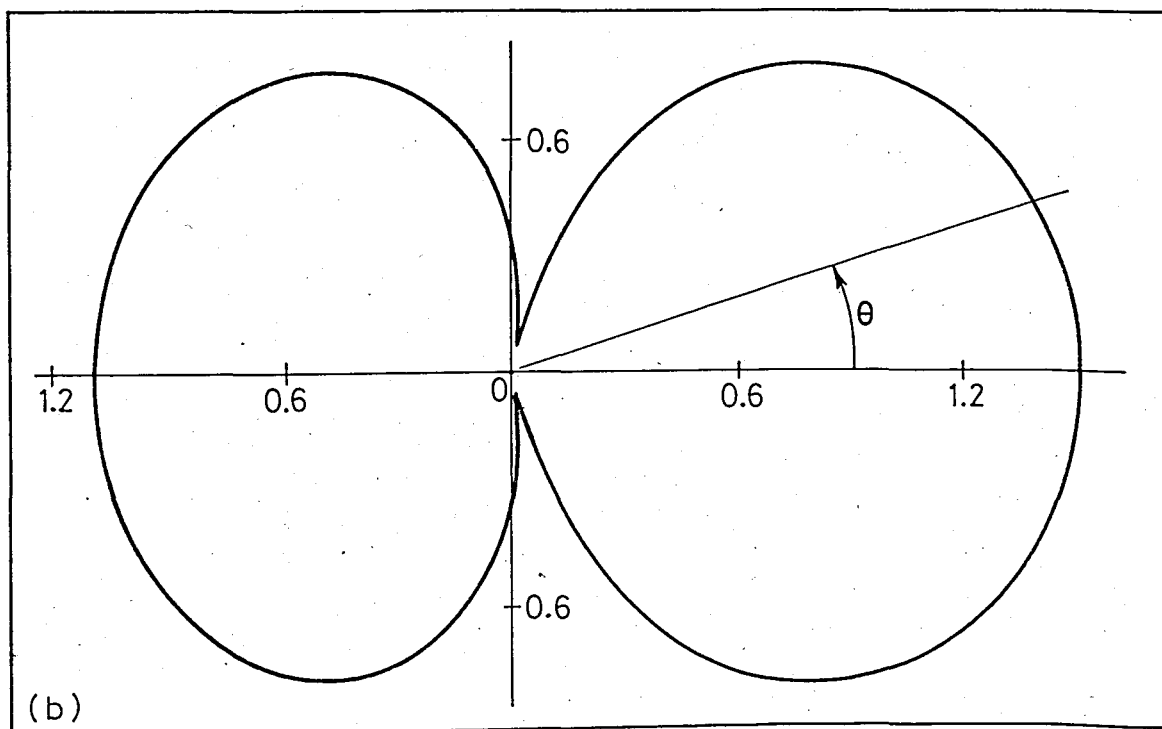
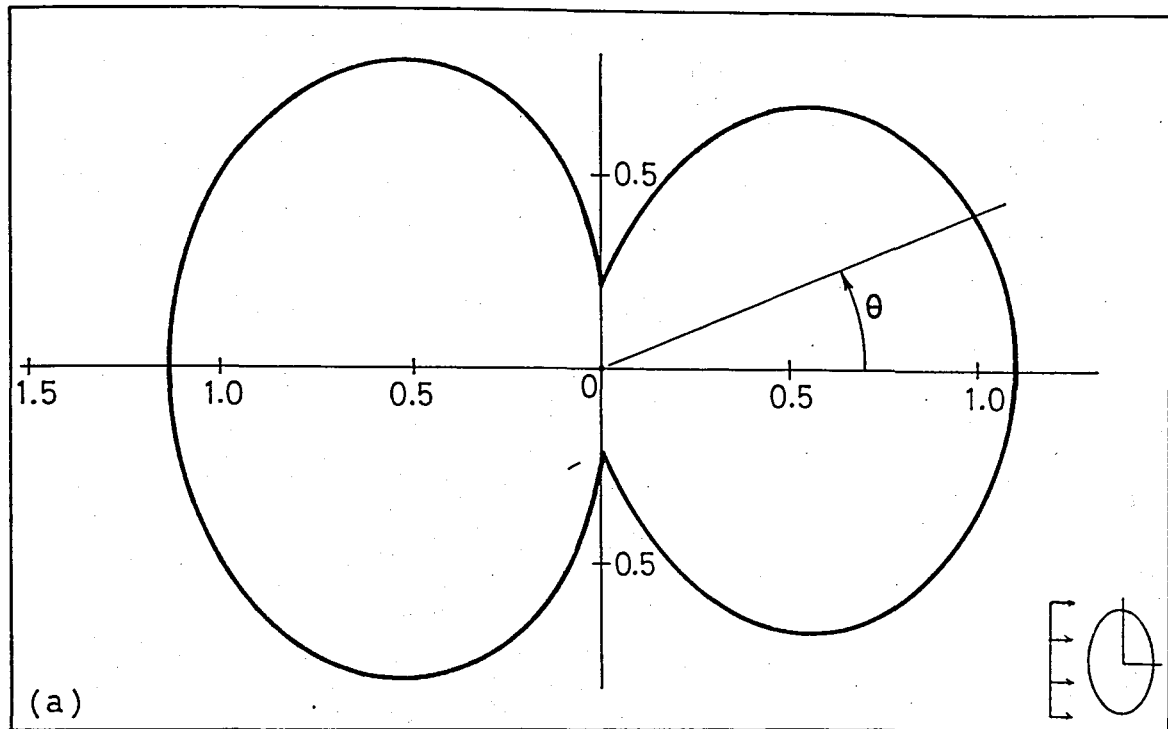


Figure 4.12 - Velocity potential distribution,  $|u^s/A|$ , at the boundary of a rigid elliptical inclusion due to the scattered wave field for  $\alpha = 0^\circ$  and  $b/a = 2.0$ ; (a)  $ka = 0.5$ , (b)  $ka = 1.0$ , (c)  $ka = 3.0$

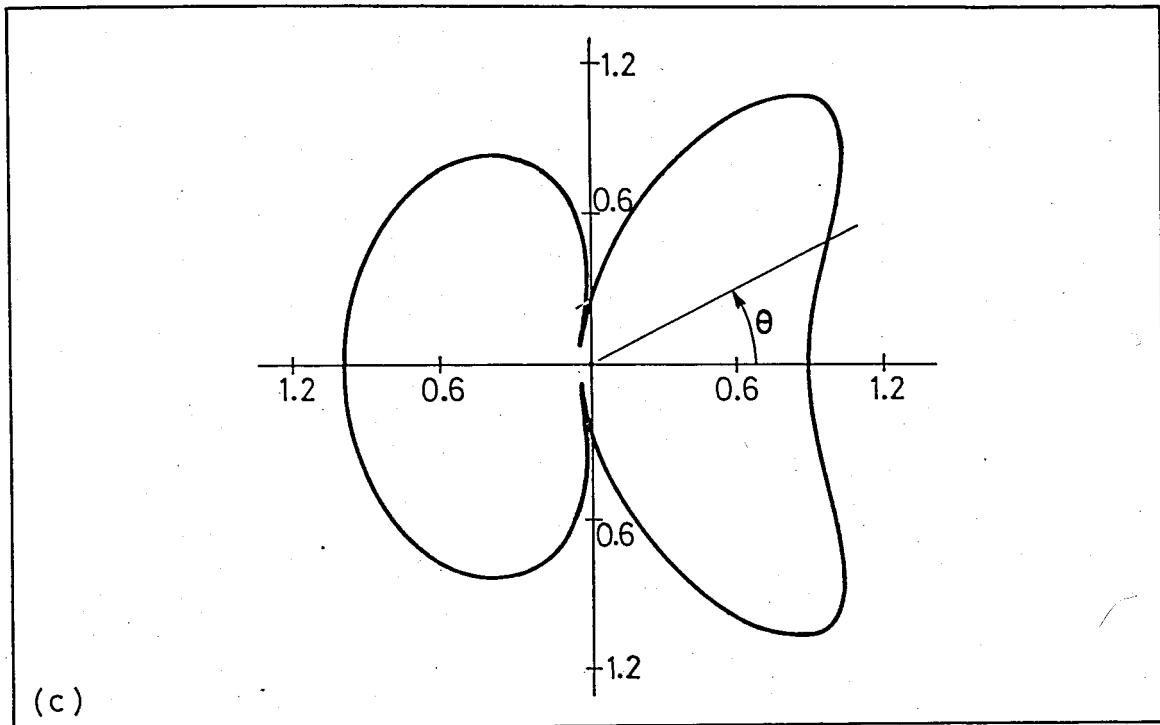


Figure 4.12 (continued).

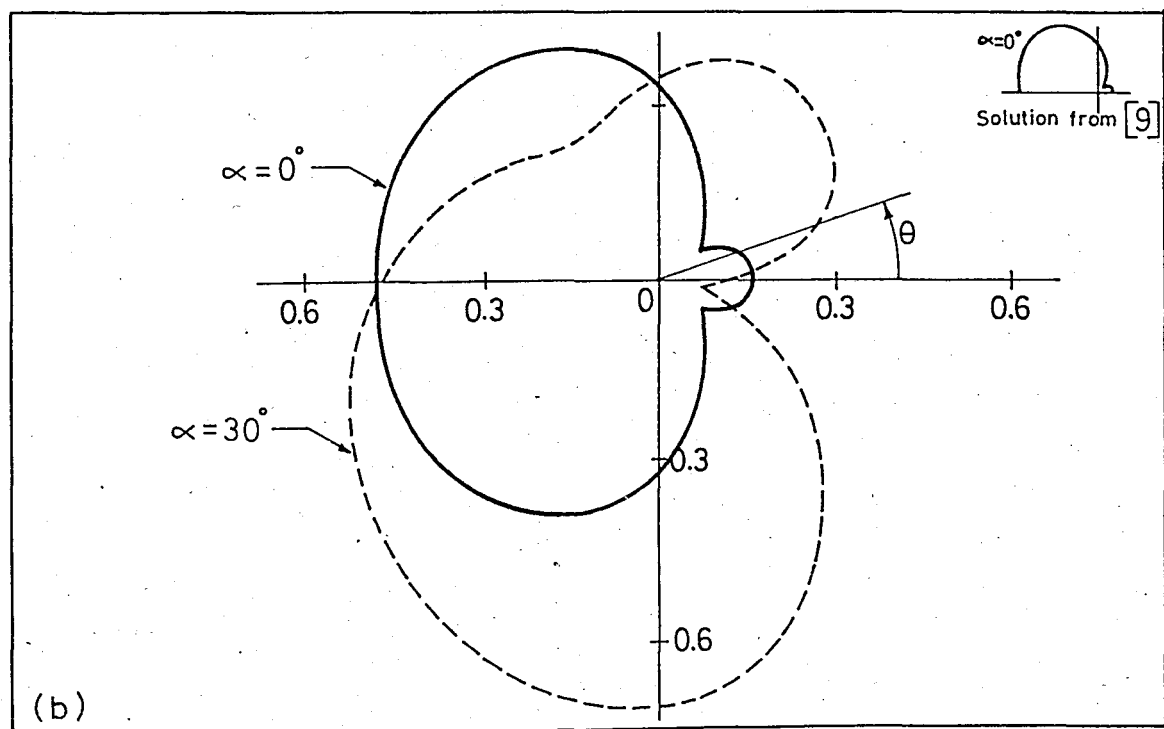
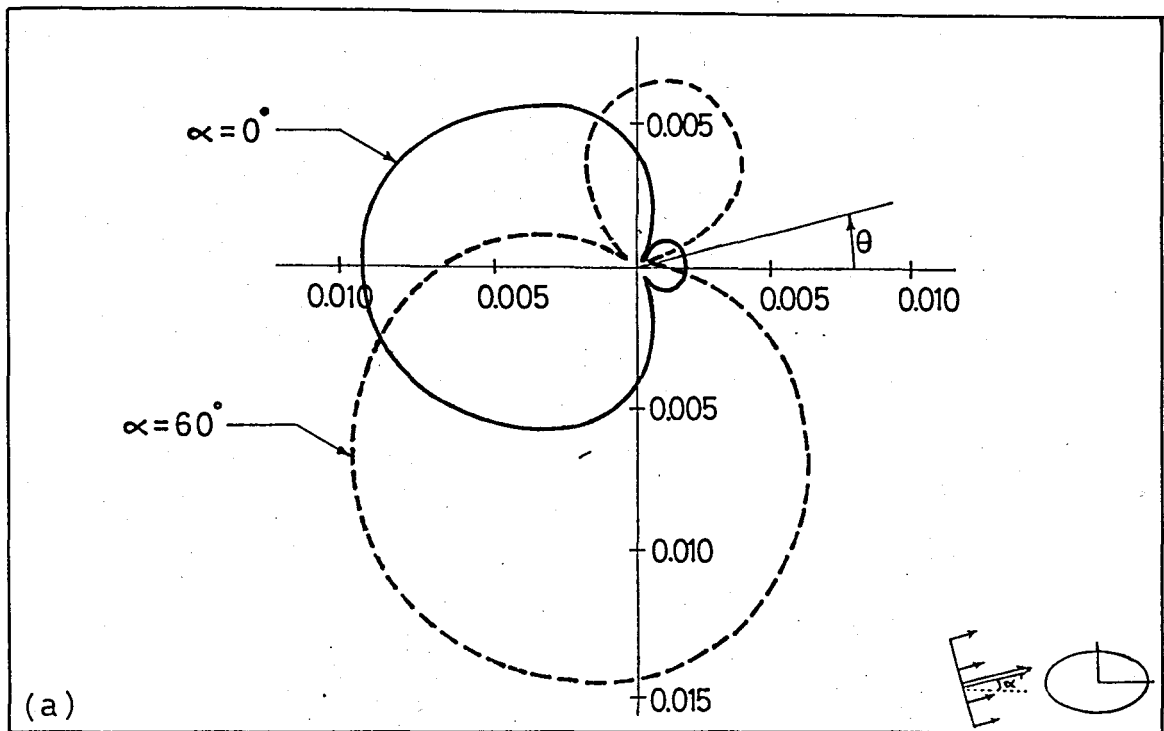


Figure 4.13 - Far field amplitude,  $|f/A|$ , due to scattered wave field from a rigid elliptical inclusion for  $b/a = 0.5$ ;  
 (a)  $ka = 0.1$ , (b)  $ka = 1.0$ , (c)  $ka = 5.0$ .

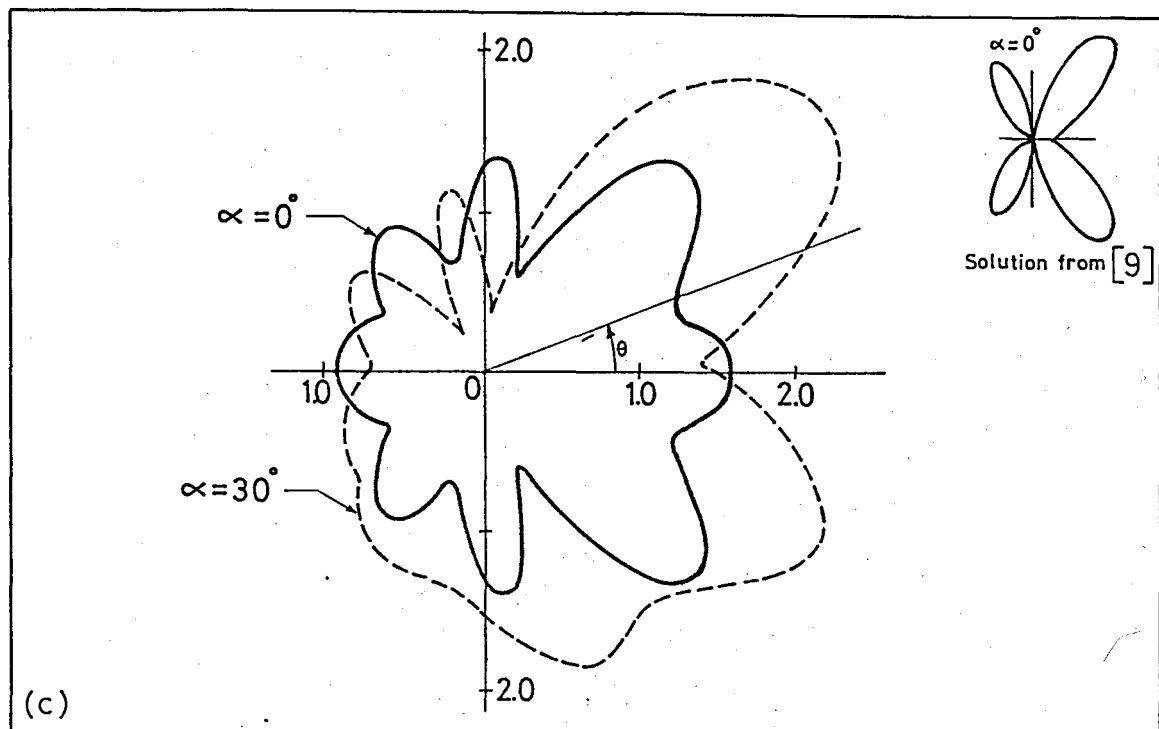


Figure 4.13 (continued).

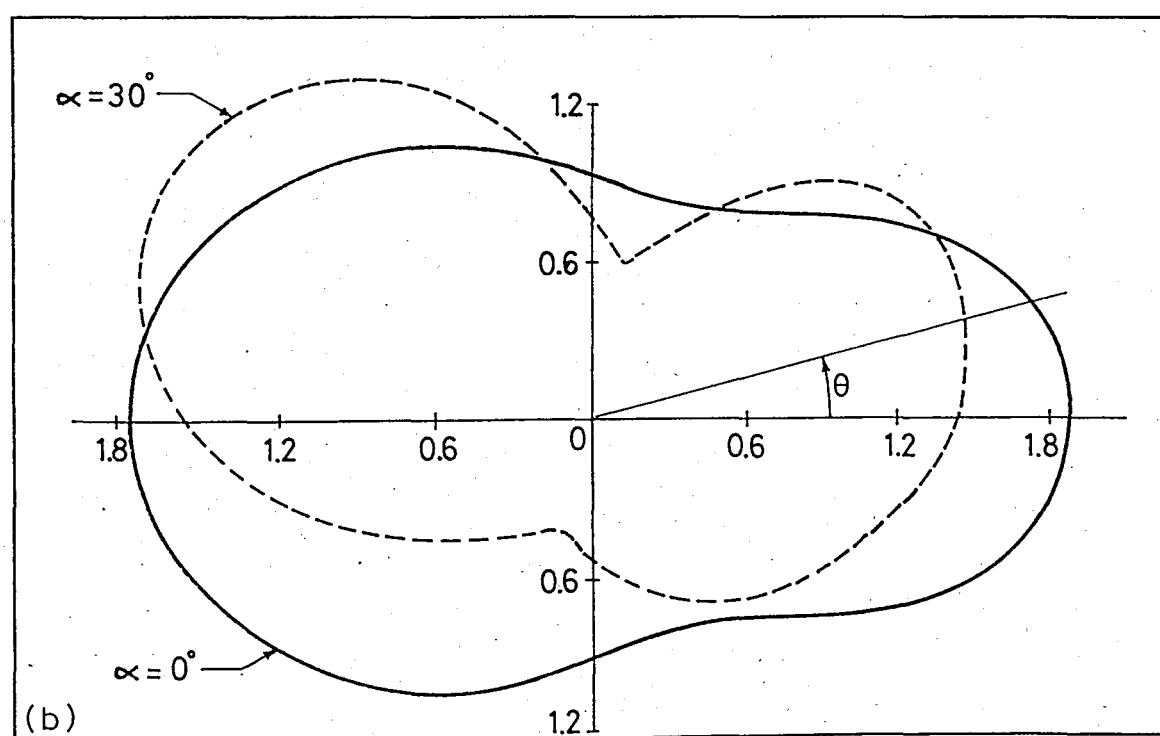
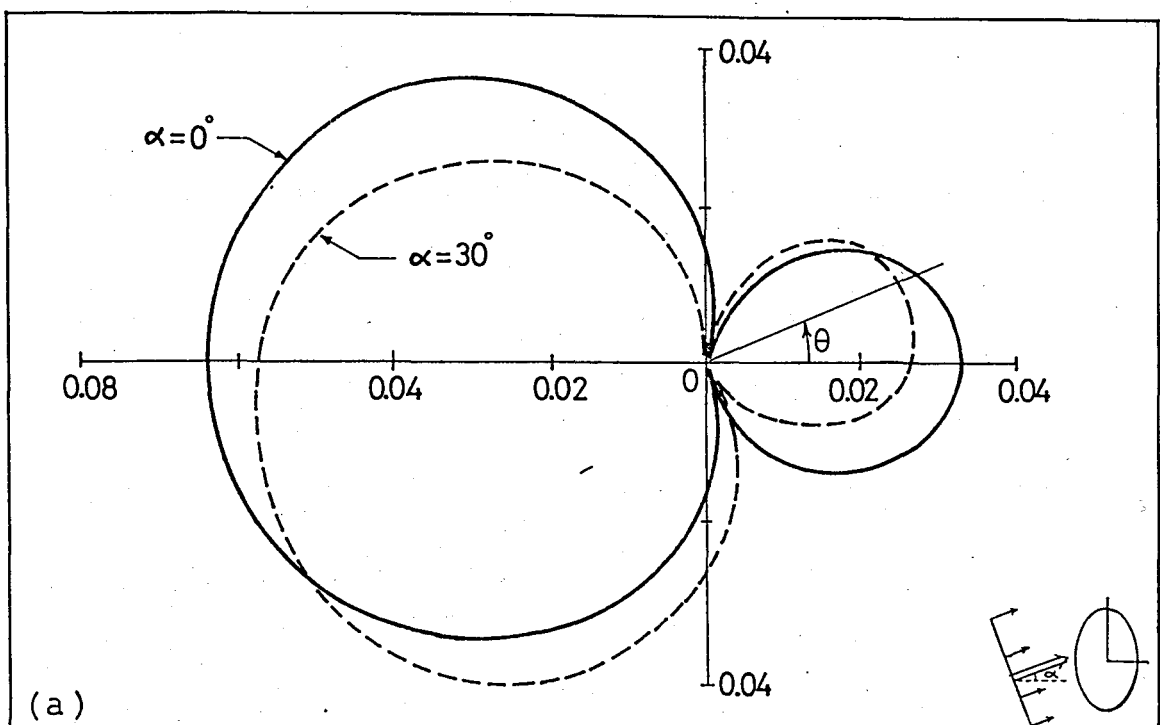


Figure 4.14 - Far field amplitude,  $|f/A|$ , due to the scattered wave field from a rigid elliptical inclusion for  $b/a = 2.0$ ;  
 (a)  $ka = 0.1$ , (b)  $ka = 1.0$ , (c)  $ka = 3.0$ .

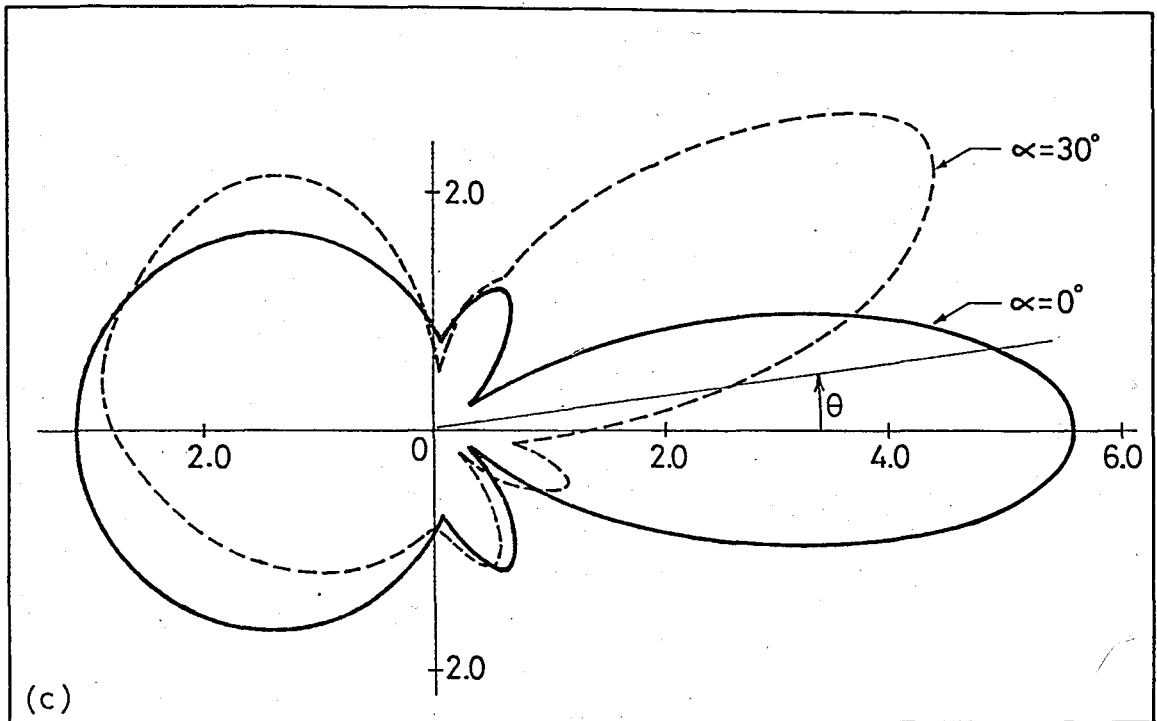


Figure 4.14 (continued).

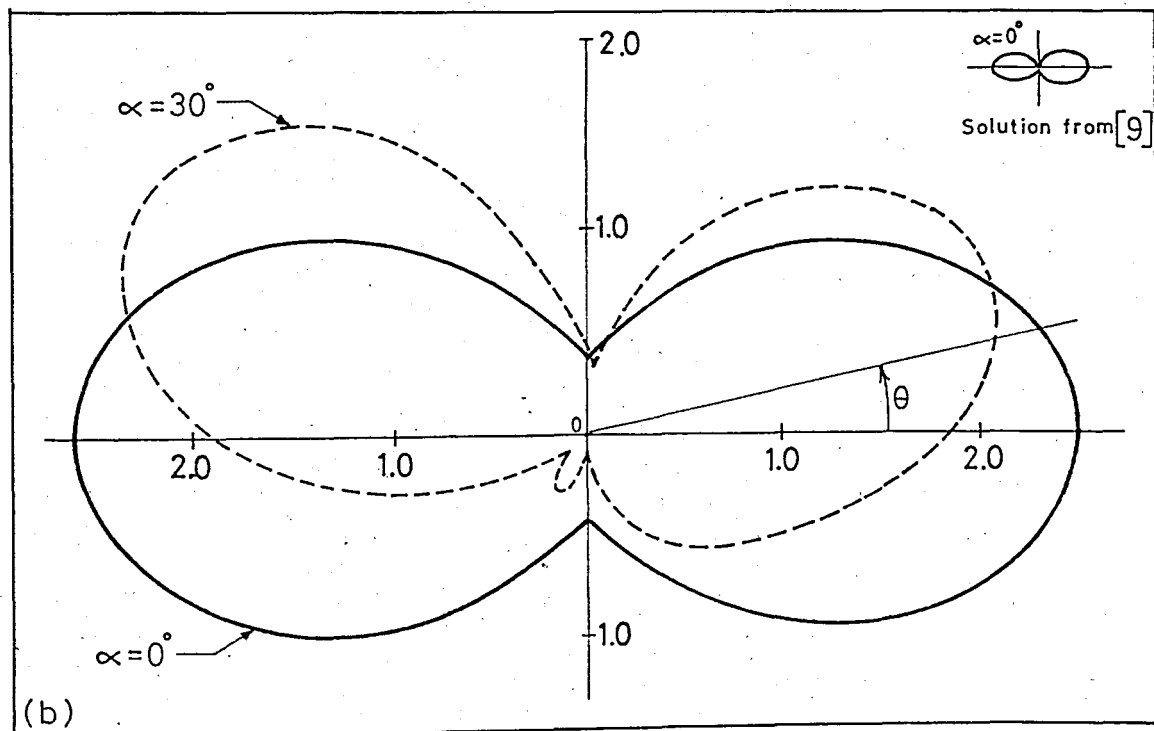
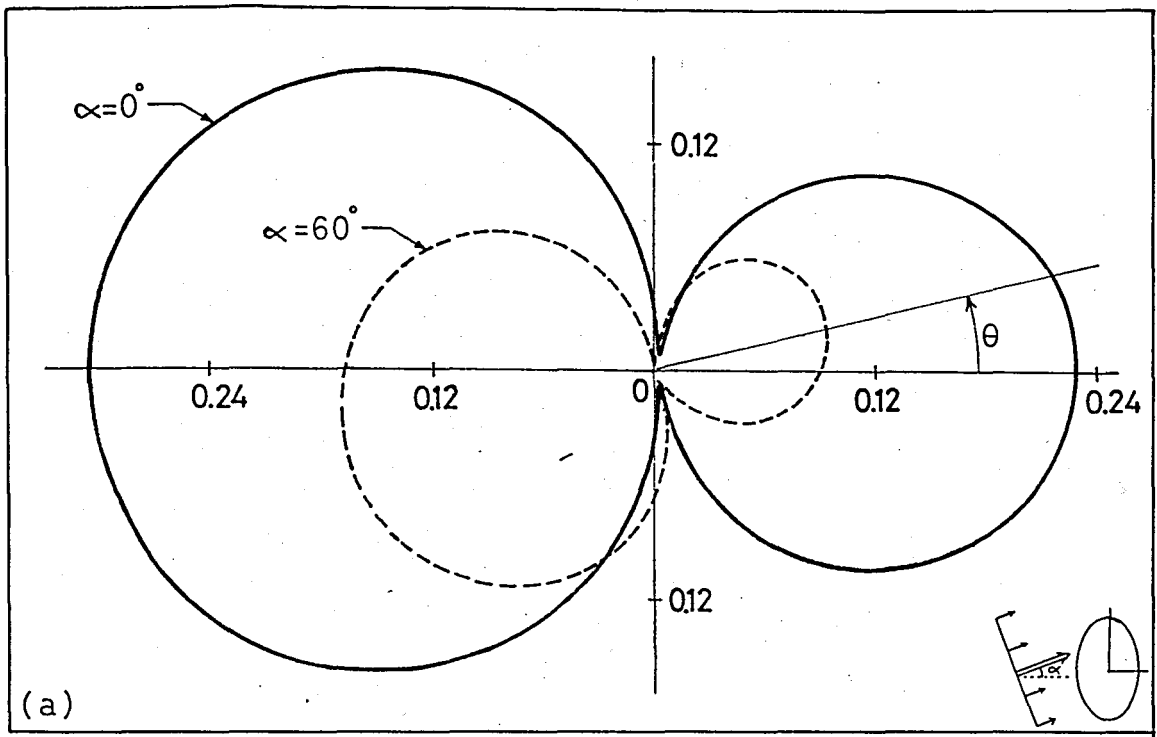


Figure 4.15 - Far field amplitude,  $|f/A|$ , due to the scattered wave field from a rigid elliptical inclusion for  $b/a = 5.0$ ;  
 (a)  $ka = 0.1$ , (b)  $ka = 0.5$ , (c)  $ka = 1.0$ .

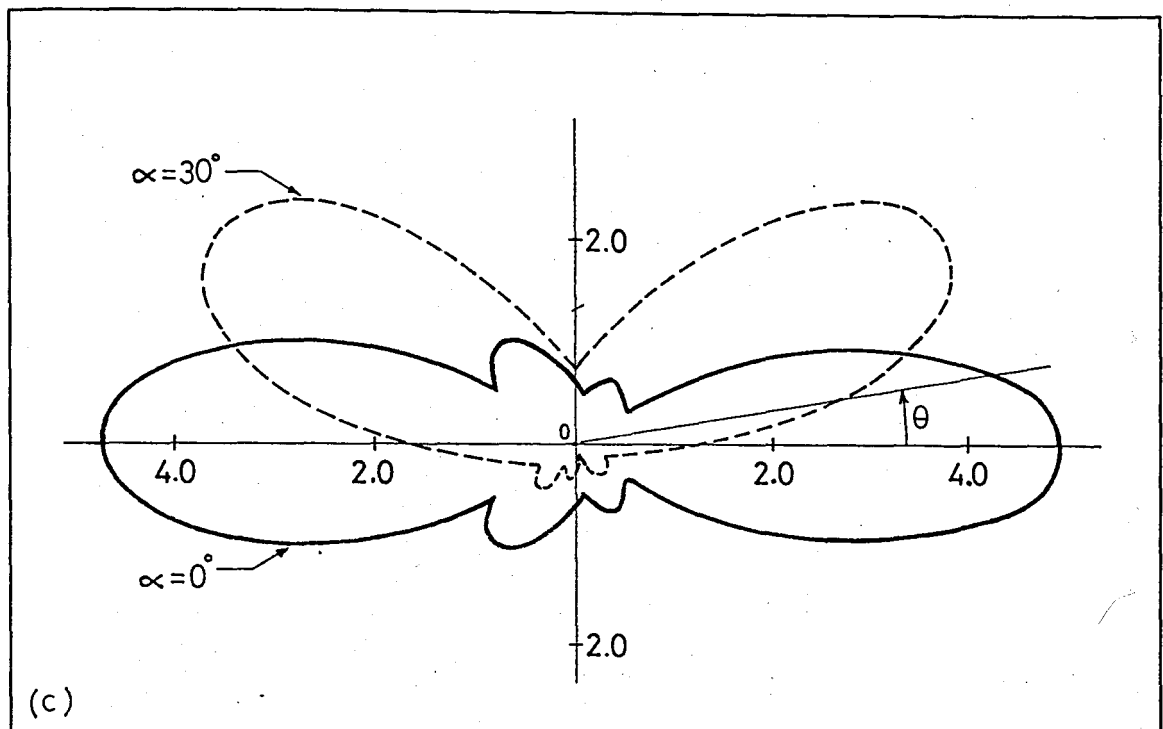


Figure 4.15 (continued).

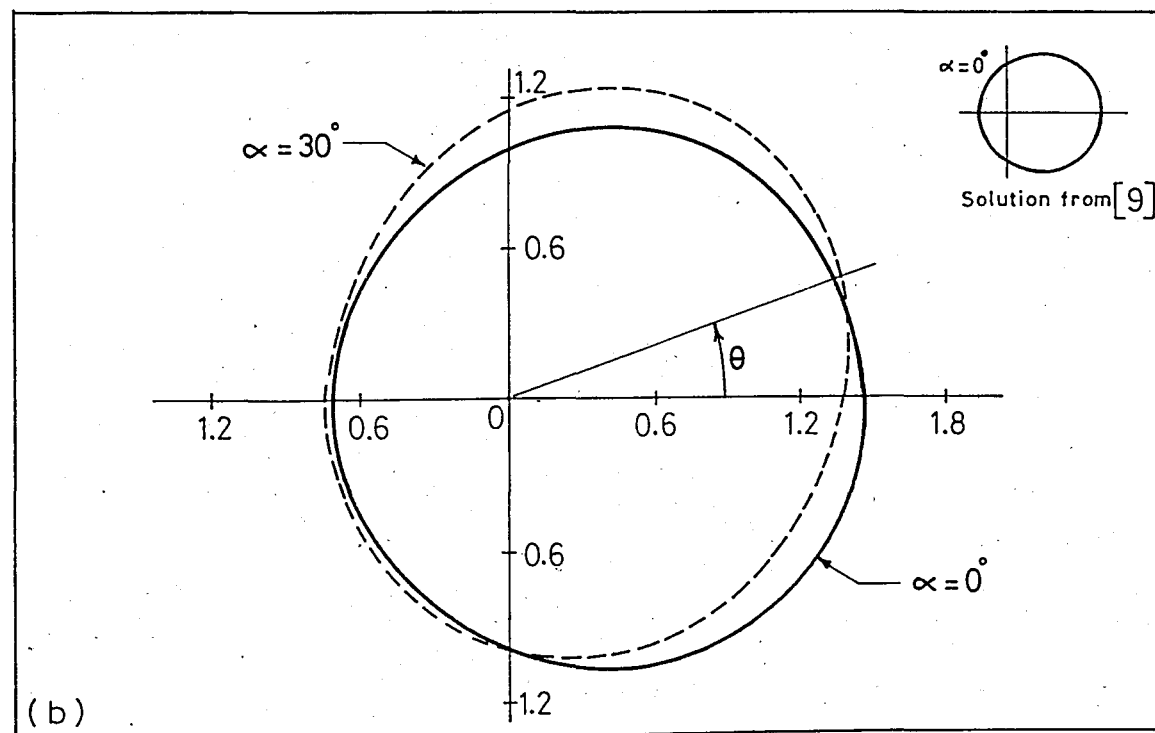
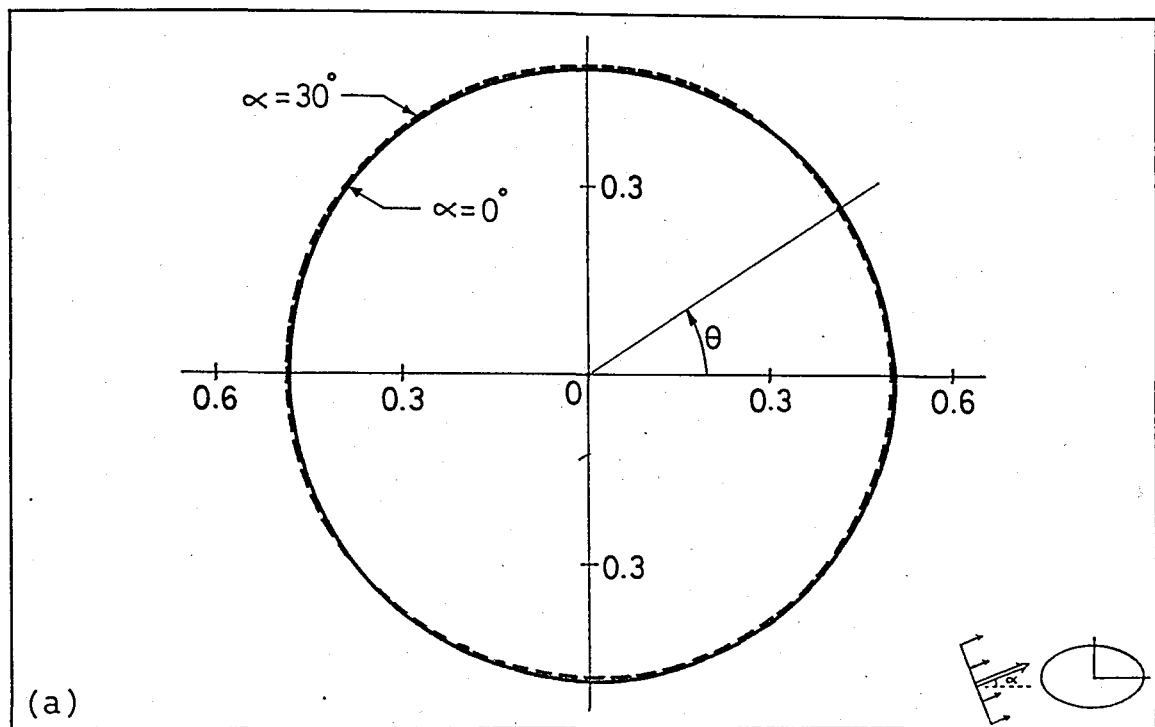


Figure 4.16 - Far field amplitude.  $|f/A|$ , due to the scattered wave field from an elliptical cavity for  $b/a = 0.5$ ;  
 (a)  $ka = 0.1$ , (b)  $ka = 1.0$ , (c)  $ka = 5.0$ .

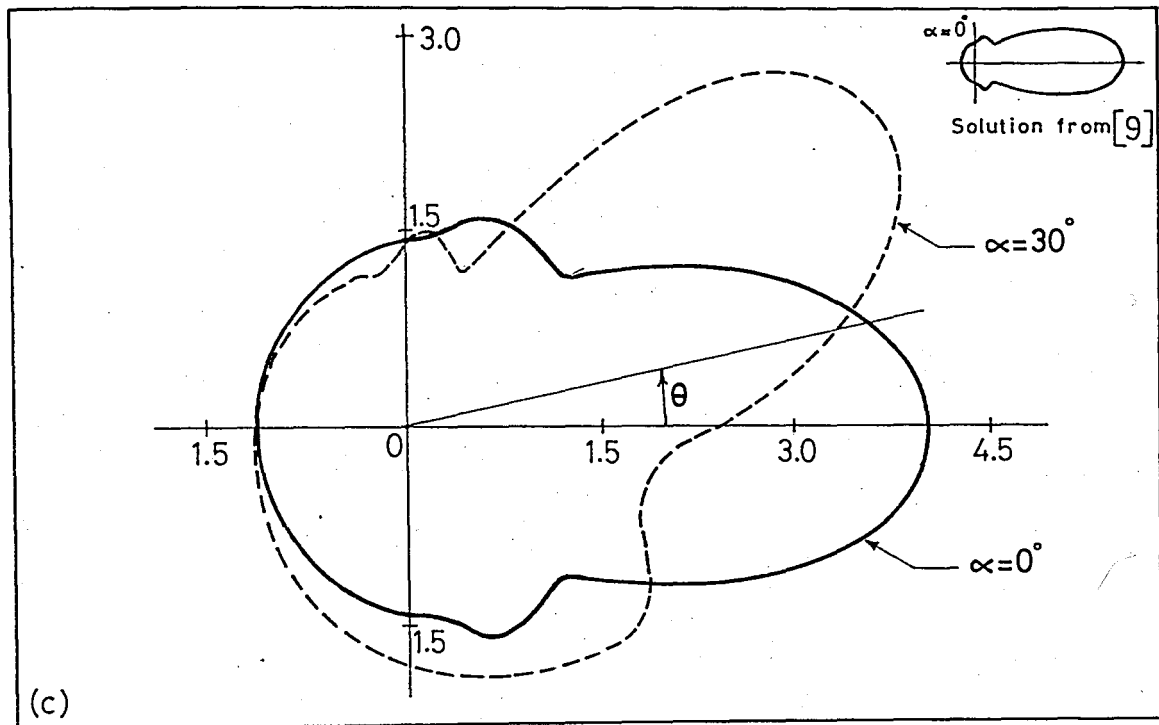


Figure 4.16 (continued).

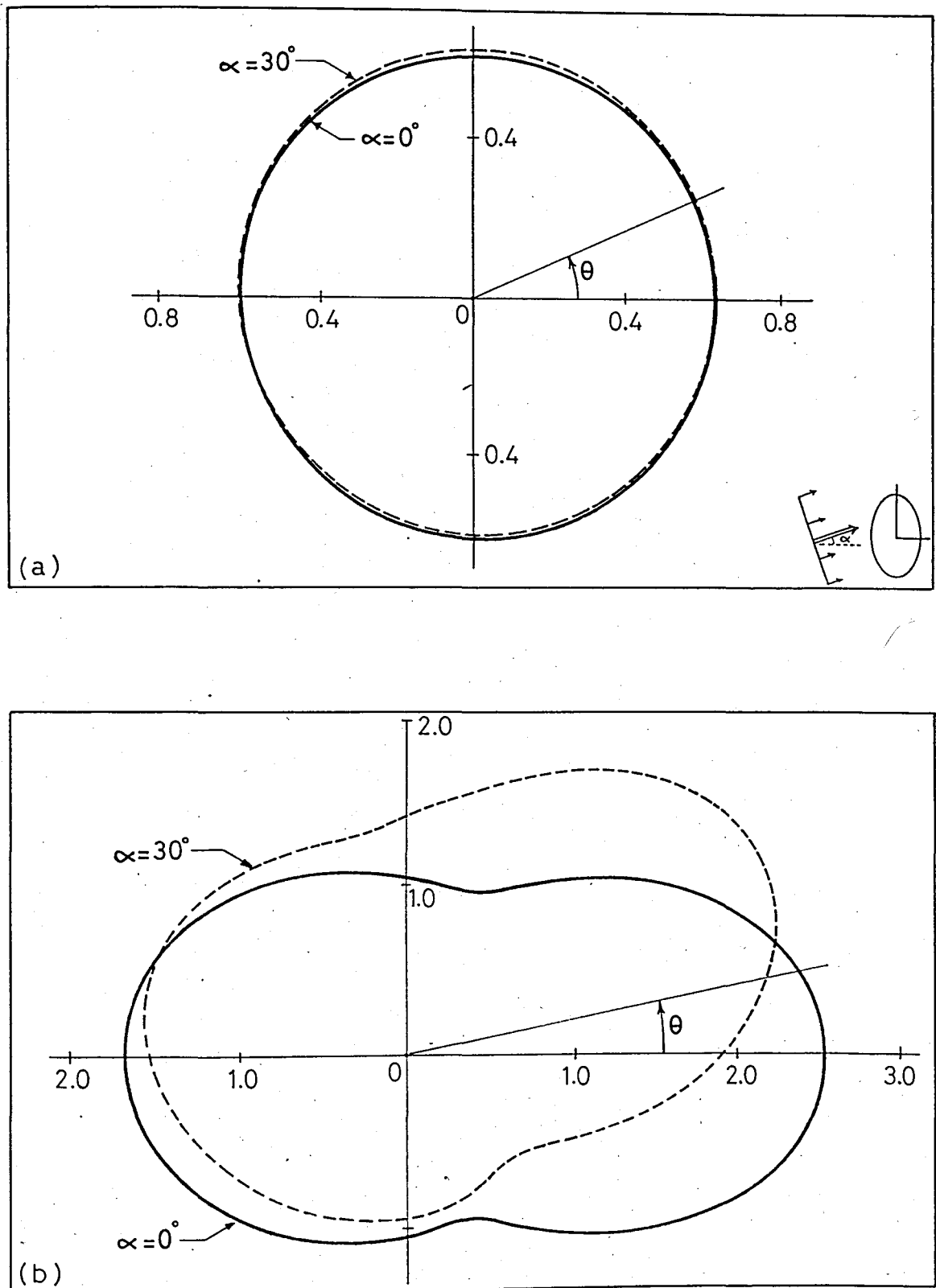


Figure 4.17 - Far field amplitude,  $|f/A|$ , due to the scattered wave field from an elliptical cavity for  $b/a = 2.0$ ;  
 (a)  $ka = 0.1$ , (b)  $ka = 1.0$ , (c)  $ka = 3.0$ .

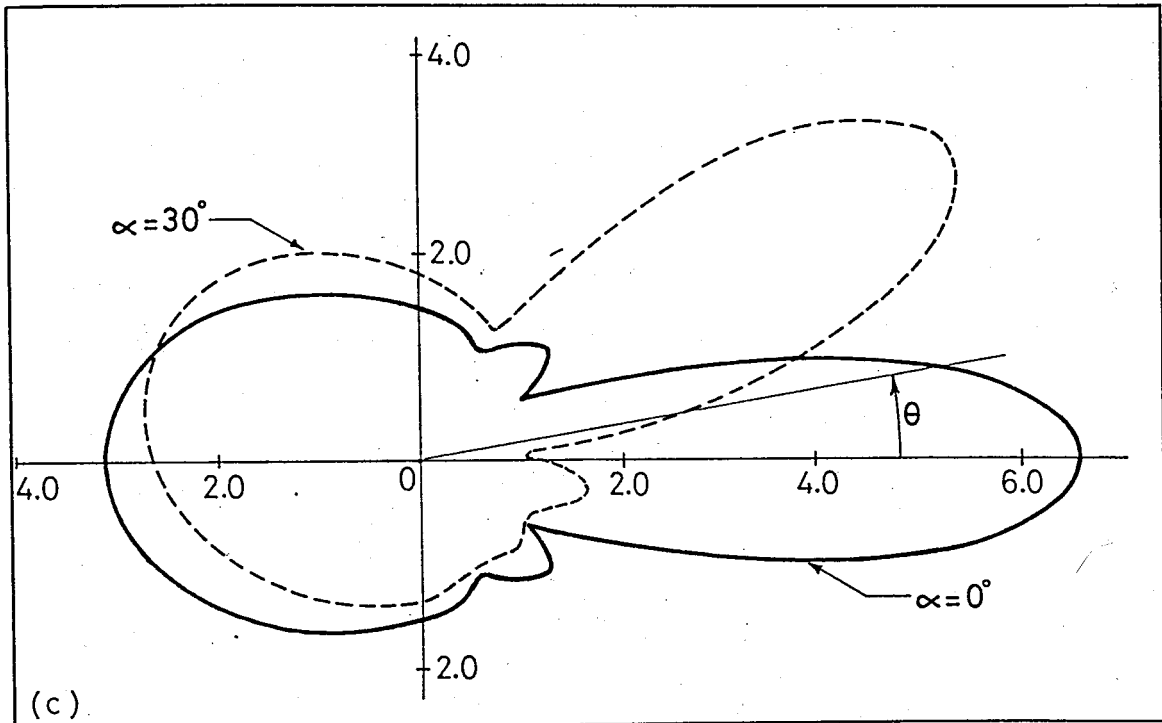


Figure 4.17 (continued).

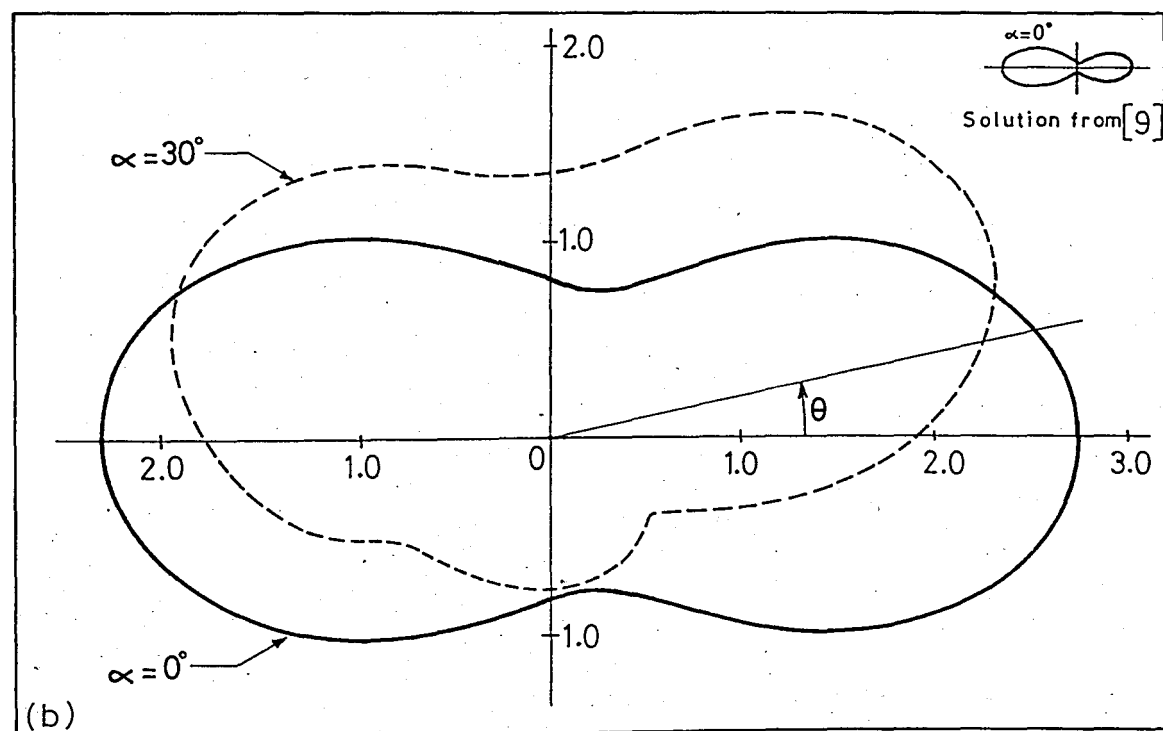
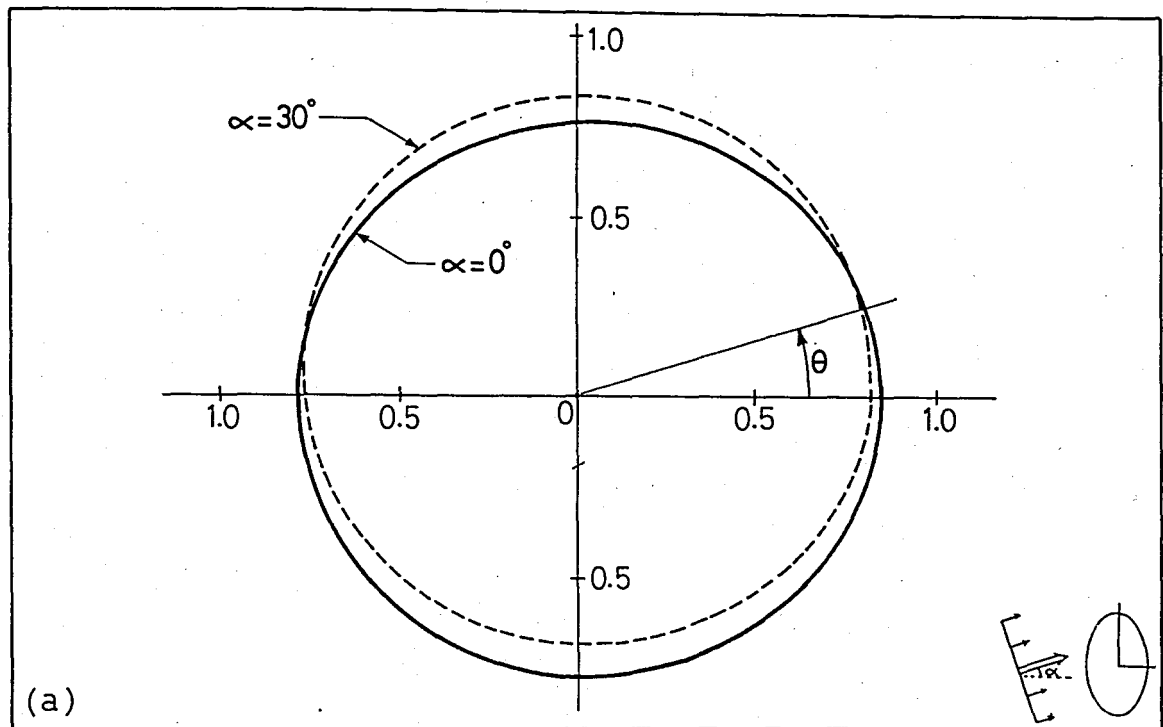


Figure 4.18 - Far field amplitude,  $|f/A|$ , due to the scattered wave field from an elliptical cavity for  $b/a = 5.0$ ;  
 (a)  $ka = 0.1$ , (b)  $ka = 0.5$ , (c)  $ka = 1.0$ .

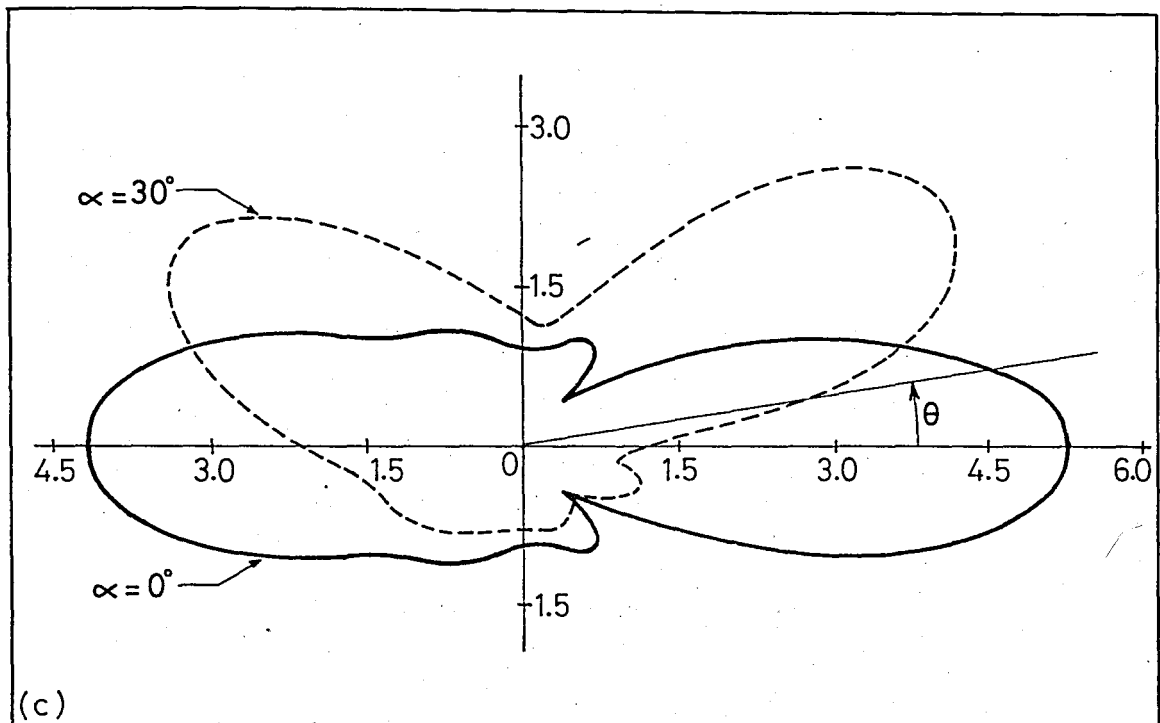


Figure 4.18 (continued).

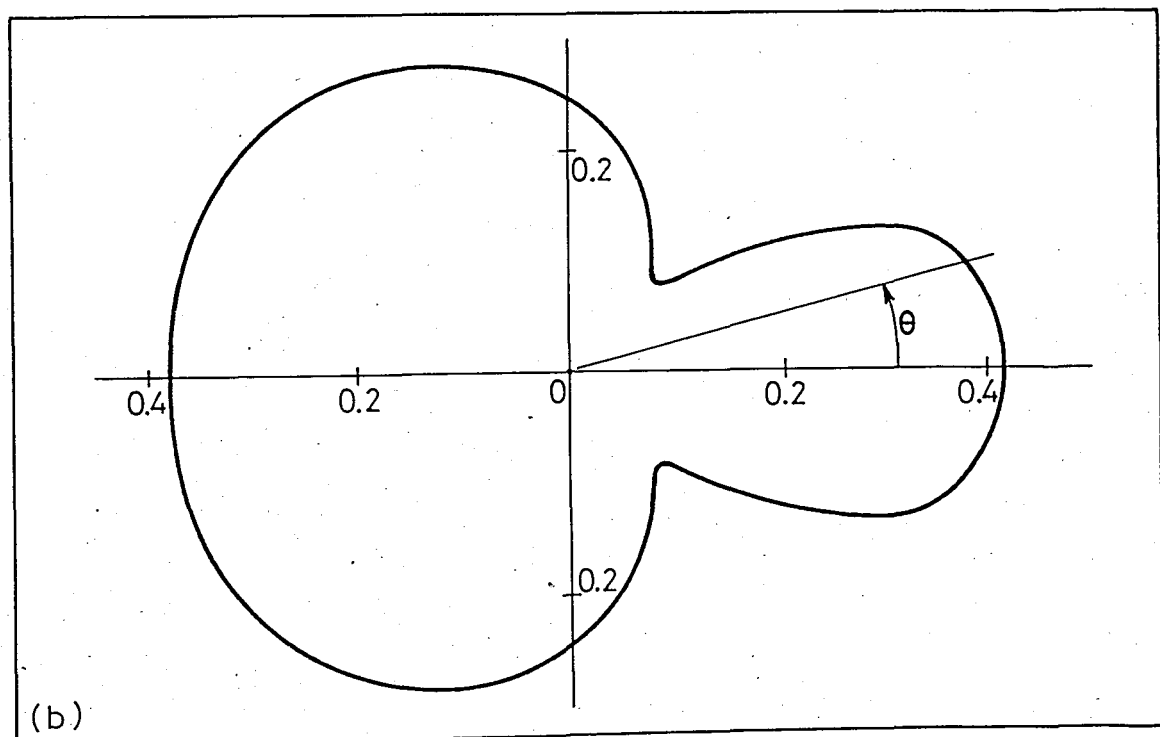
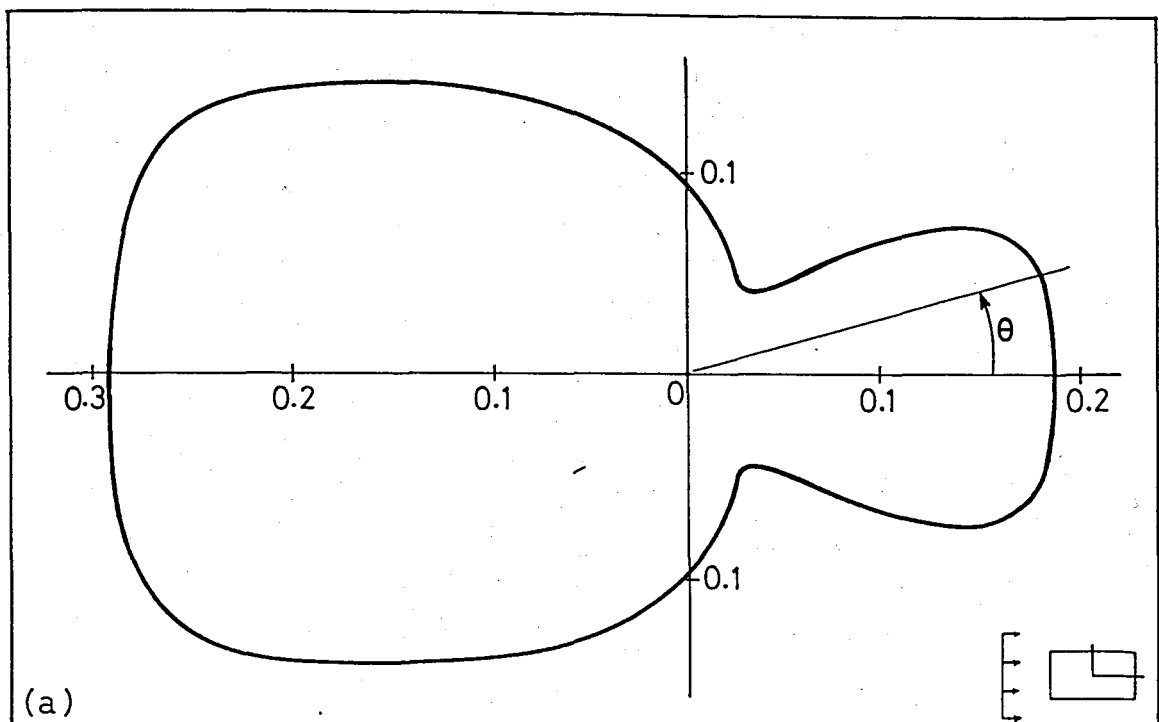


Figure 4.19 - Velocity potential distribution,  $|u^s/A|$ , at the boundary of a rigid rectangular inclusion due to scattered wave field for  $\alpha = 0^\circ$ ,  $r_c/a = 0.1$  and  $b/a = 0.5$ ;

(a)  $ka = 0.5$ , (b)  $ka = 1.0$ , (c)  $ka = 3.0$

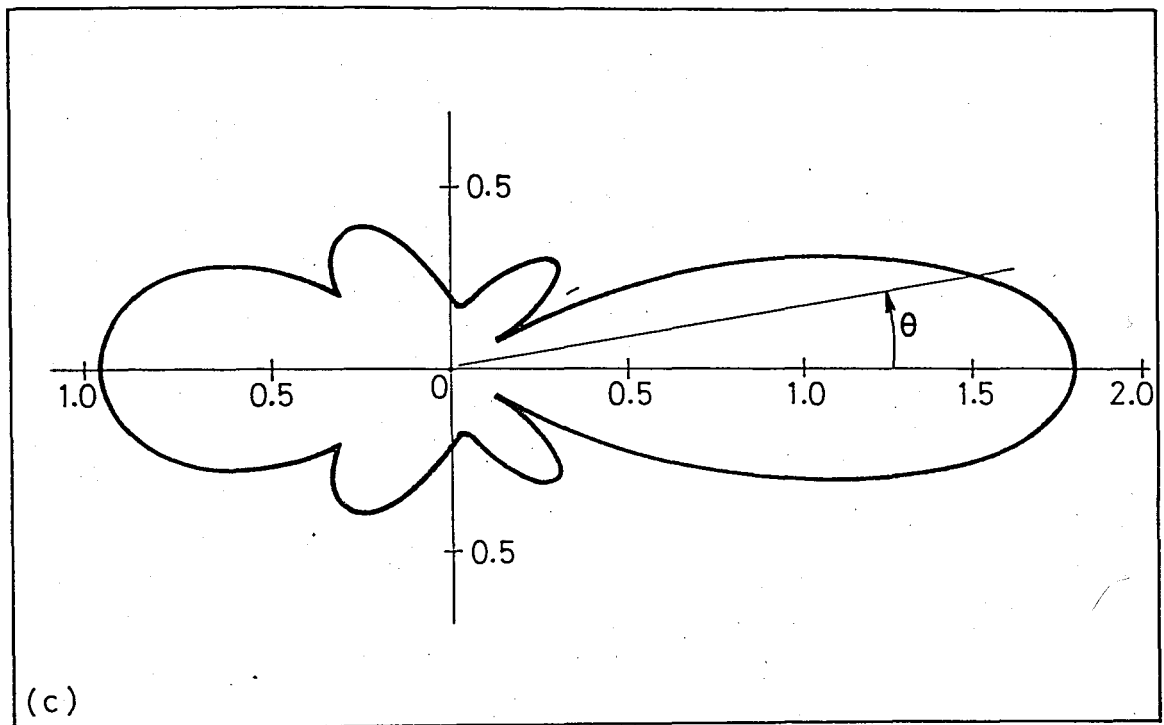


Figure 4.19 (continued).

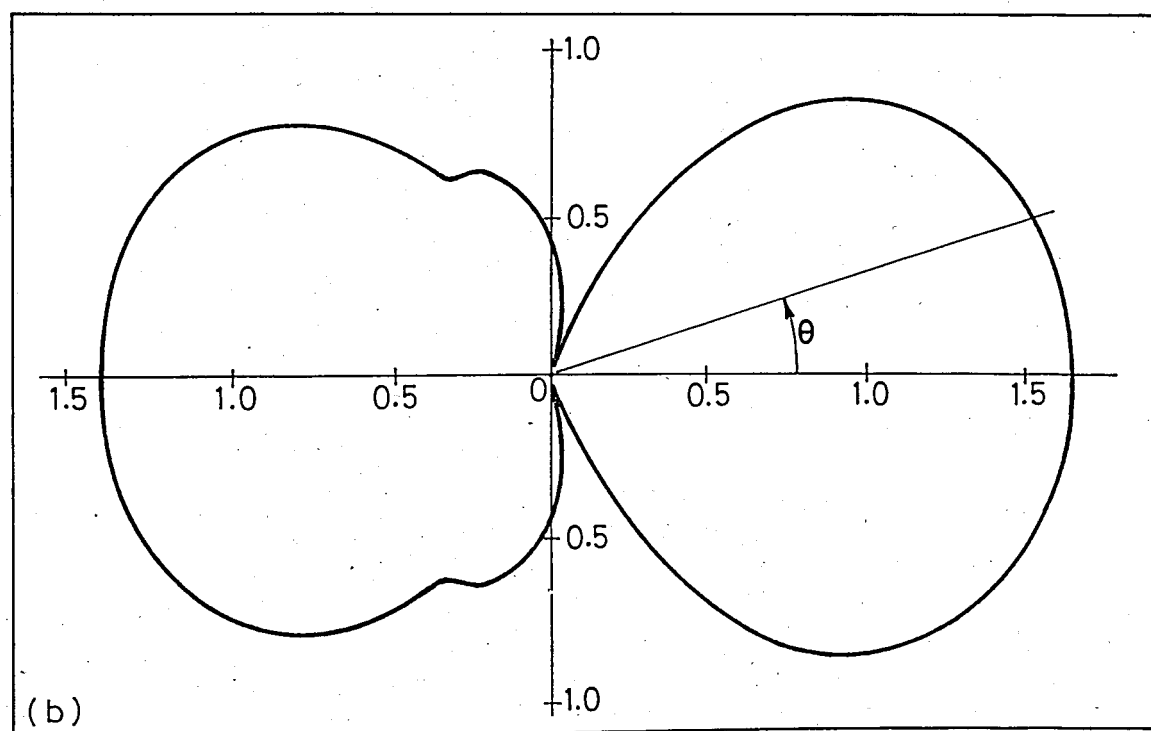
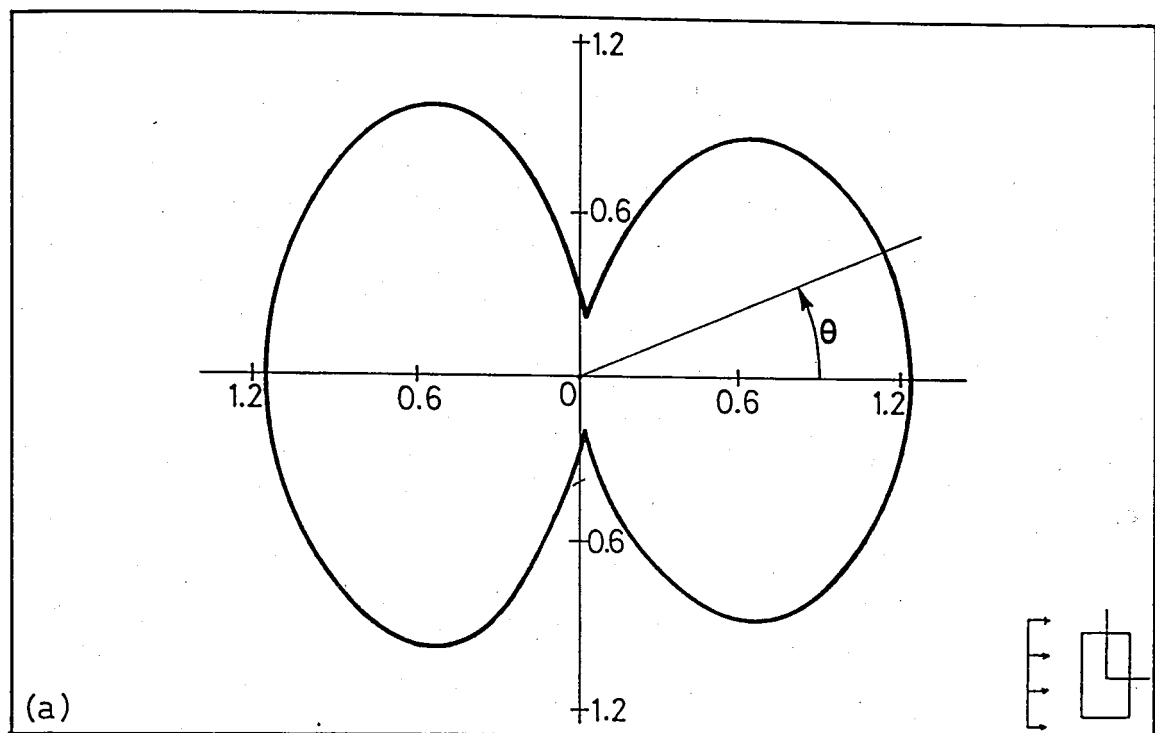


Figure 4.20 - Velocity potential distribution,  $|u^S/A|$ , at the boundary of a rigid rectangular inclusion due to the scattered wave field for  $\alpha = 0^\circ$ .  $r_c/a = 0.1$  and  $b/a = 2.0$ ; (a)  $ka = 0.5$ , (b)  $ka = 1.0$ , (c)  $ka = 3.0$ .

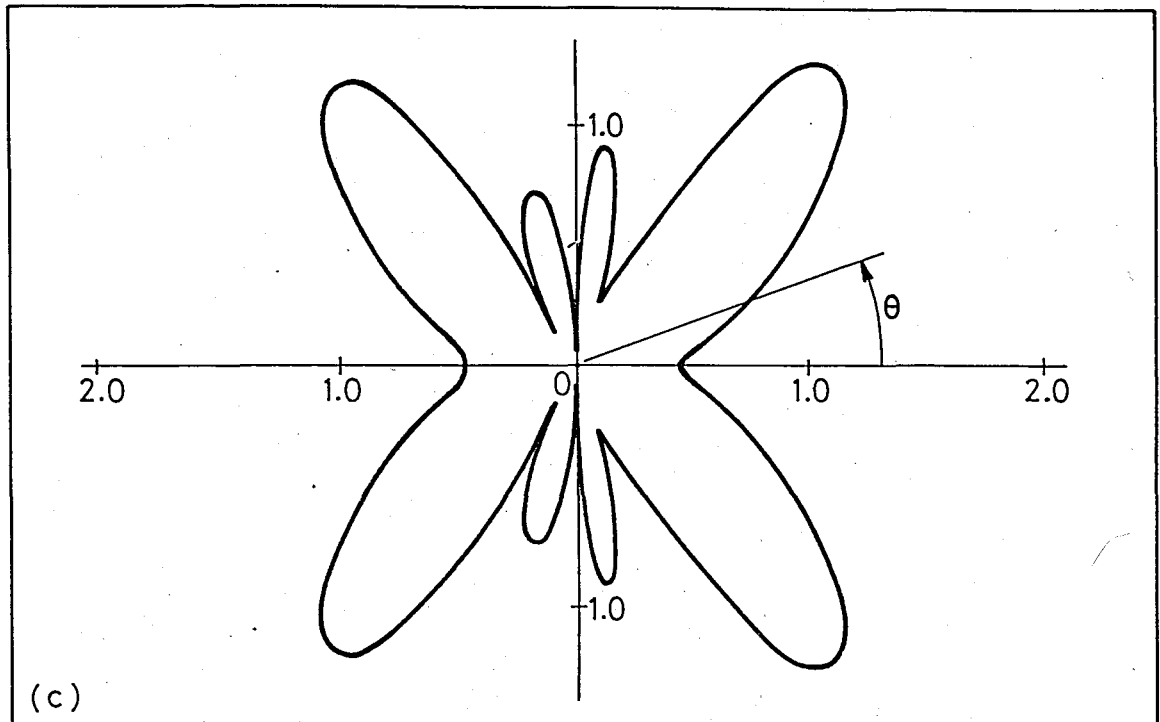


Figure 4.20 (continued).

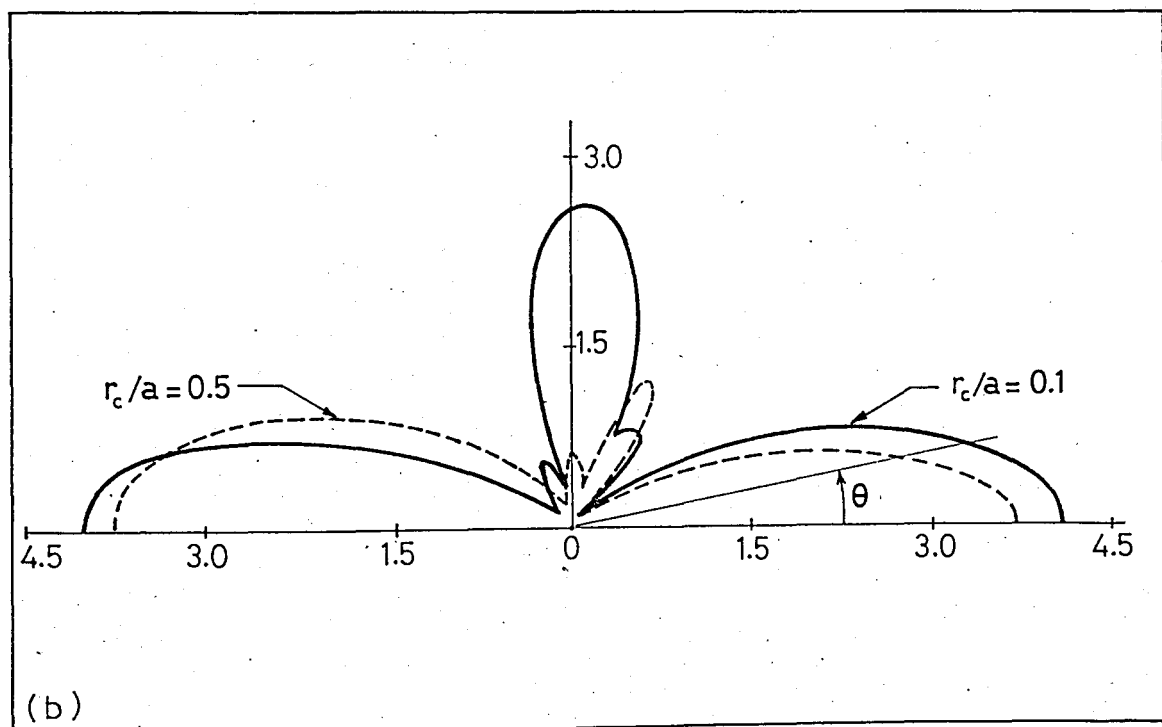
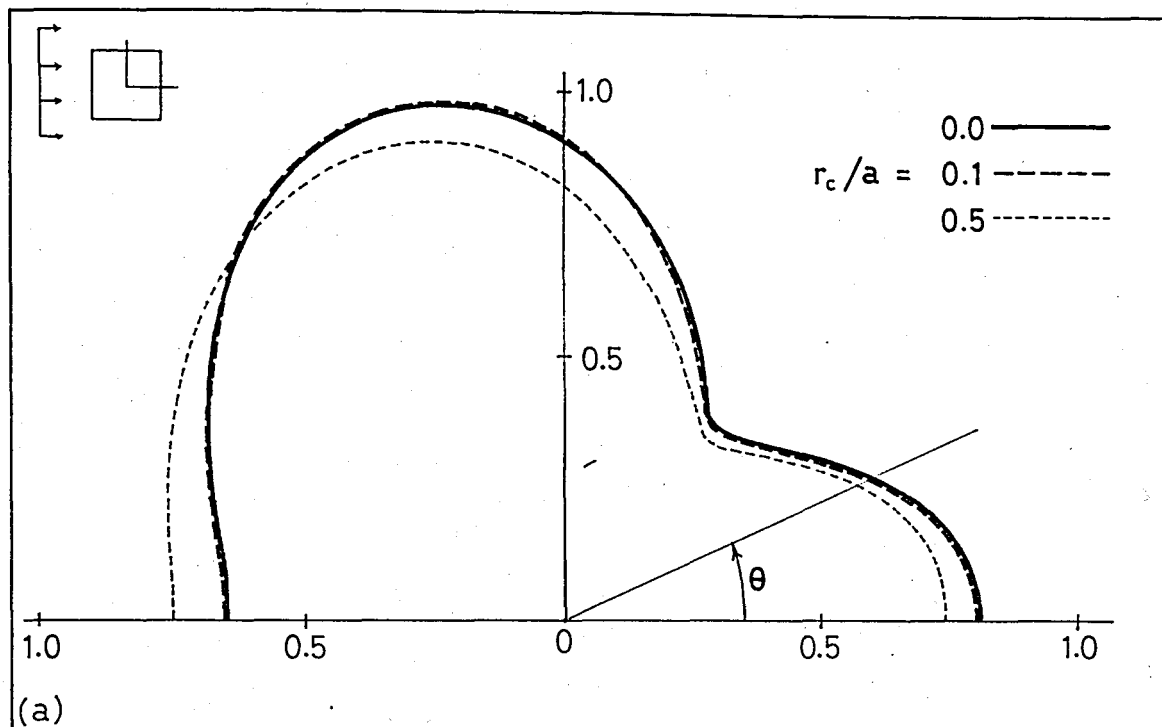


Figure 4.21 - Effect of the corner radius on the far-field amplitude,  $|f/A|$ , due to the scattered wave field from a rigid rectangular inclusion for  $\alpha = 0^\circ$  and  $b/a = 1.0$ ;  
 (a)  $ka = 1.0$ , (b)  $ka = 5.0$ .

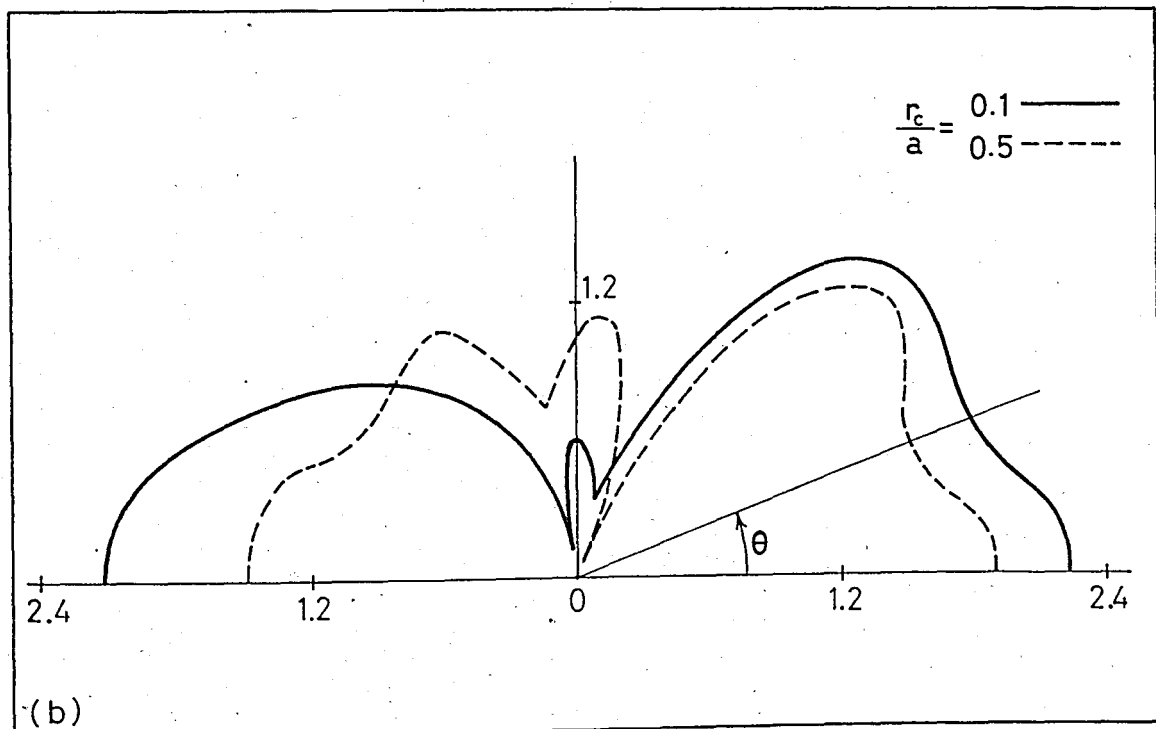
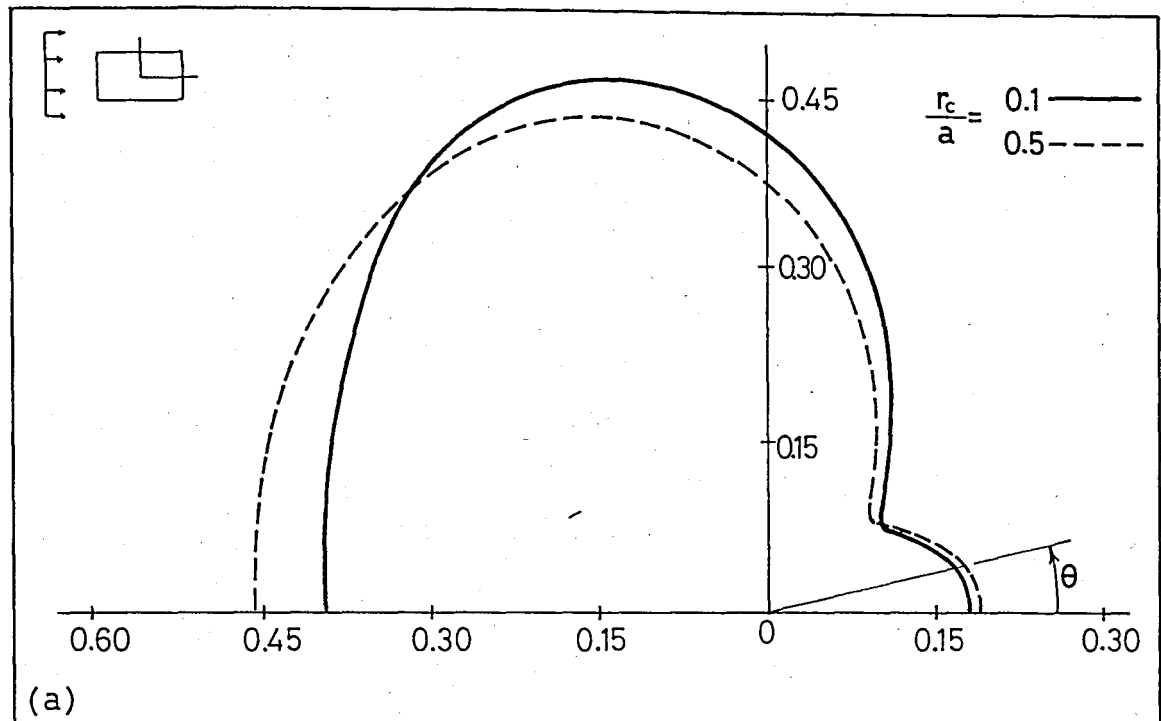


Figure 4.22 - Effect of the corner radius on the far field amplitude,  $|f/A|$ , due to the scattered wave field from a rigid rectangular inclusion for  $\alpha = 0^\circ$  and  $b/a = 0.5$ ; (a)  $ka = 1.0$ , (b)  $ka = 5.0$ .

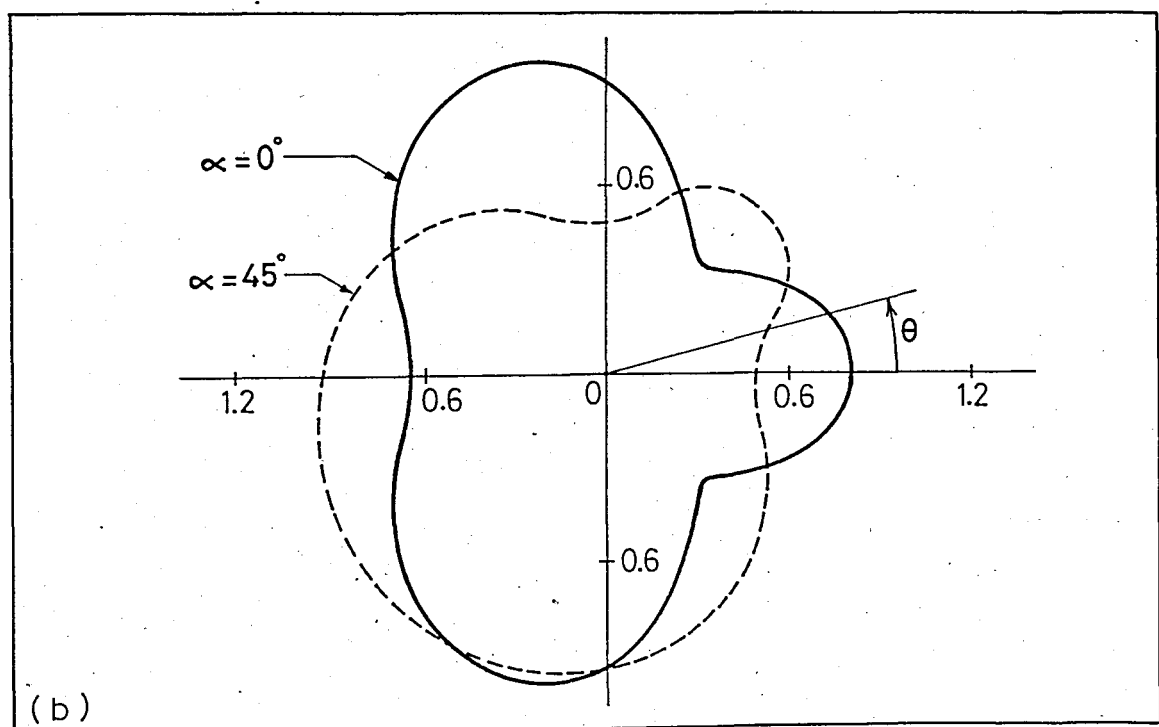
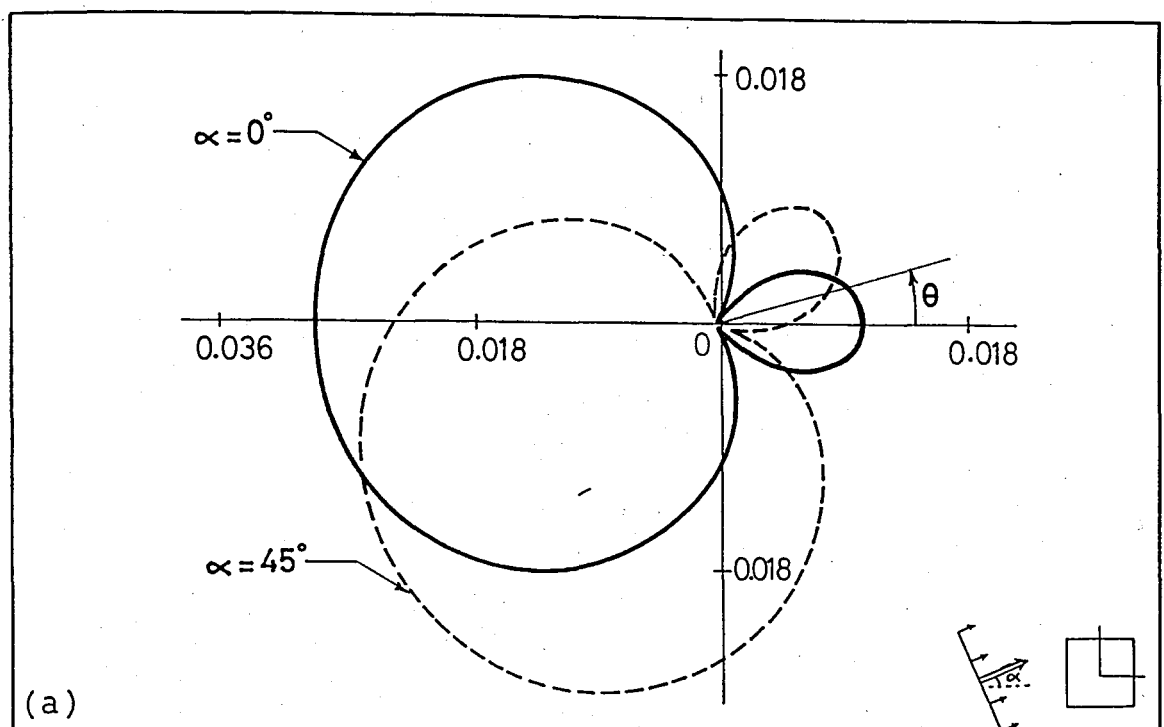


Figure 4.23 - Far field amplitude,  $|f/A|$ , due to the scattered wave field from a rigid rectangular inclusion for  $rc/a = 0.1$  and  $b/a = 1.0$ ;  
 (a)  $ka = 0.1$ , (b)  $ka = 1.0$ , (c)  $ka = 5.0$ .

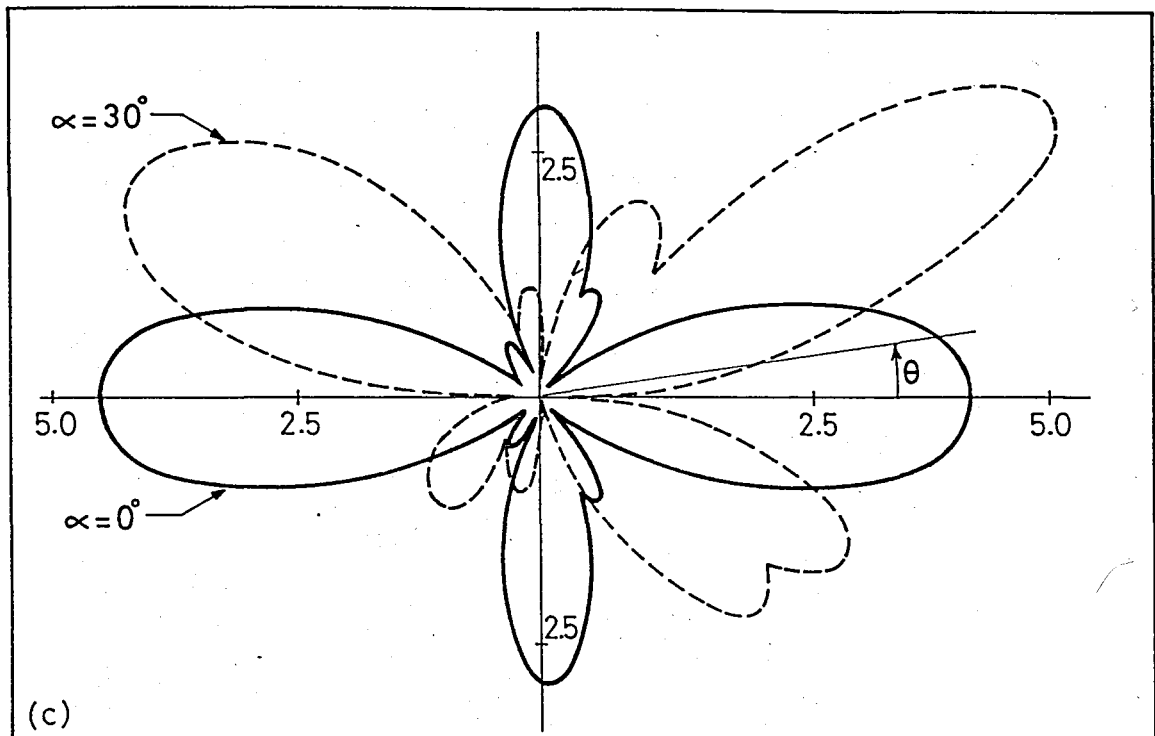


Figure 4.23 (continued).

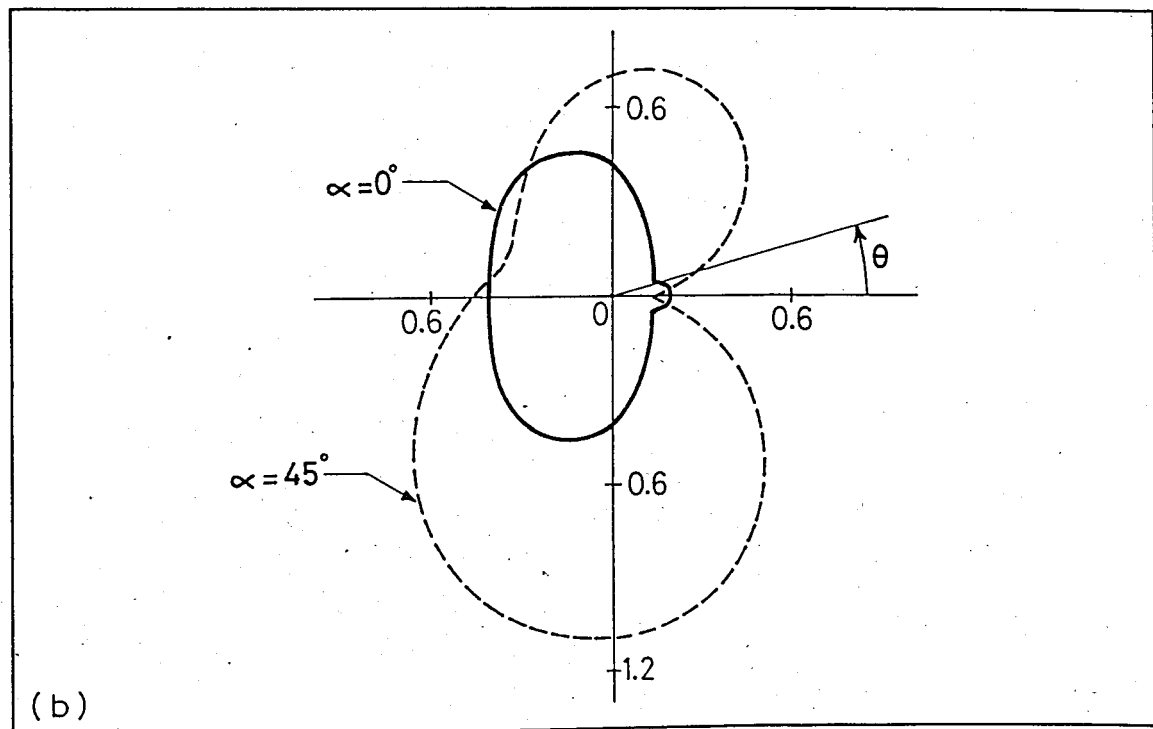
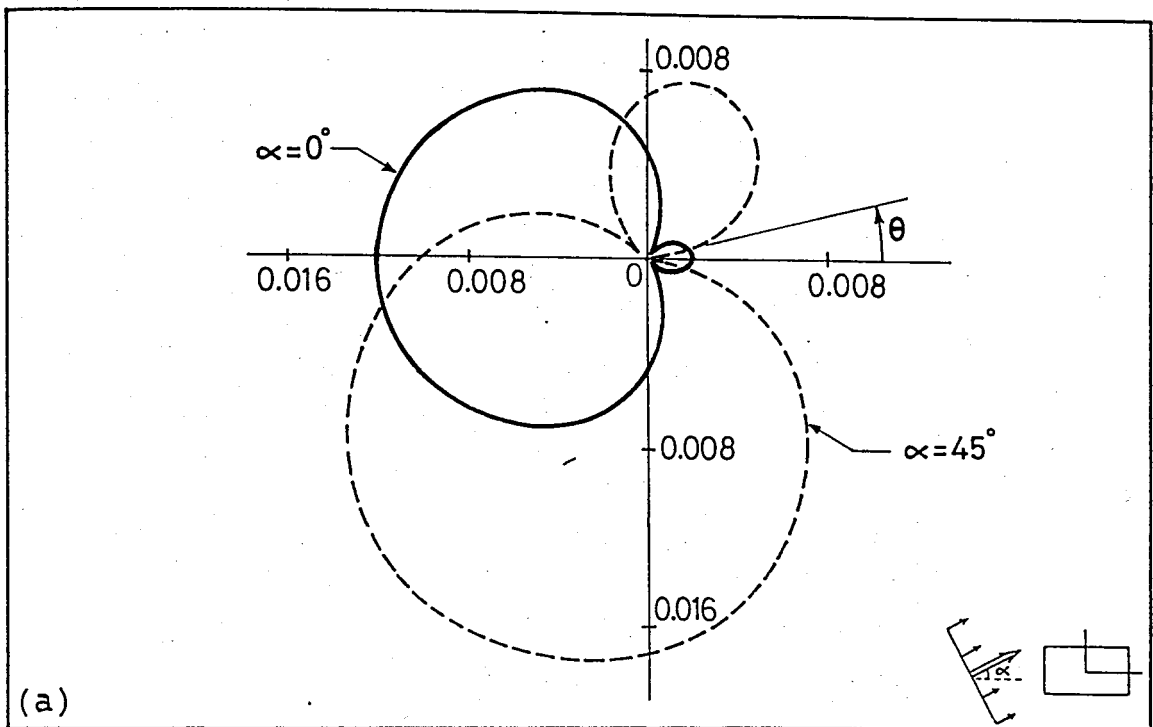


Figure 4.24 - Far field amplitude,  $|f/A|$ , due to the scattered wave field from a rigid rectangular inclusion for  $r_c/a = 0.1$  and  $b/a = 0.5$ ;  
 (a)  $ka = 0.1$ , (b)  $ka = 1.0$ , (c)  $ka = 5.0$ .

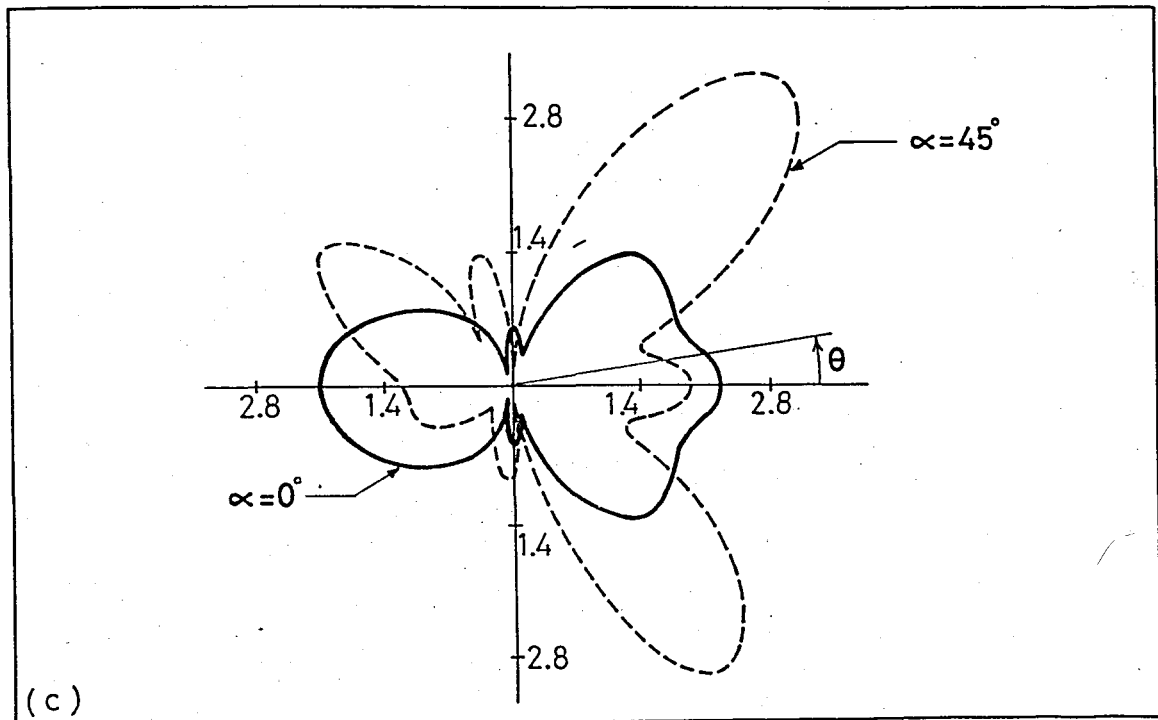


Figure 4.24 (continued).

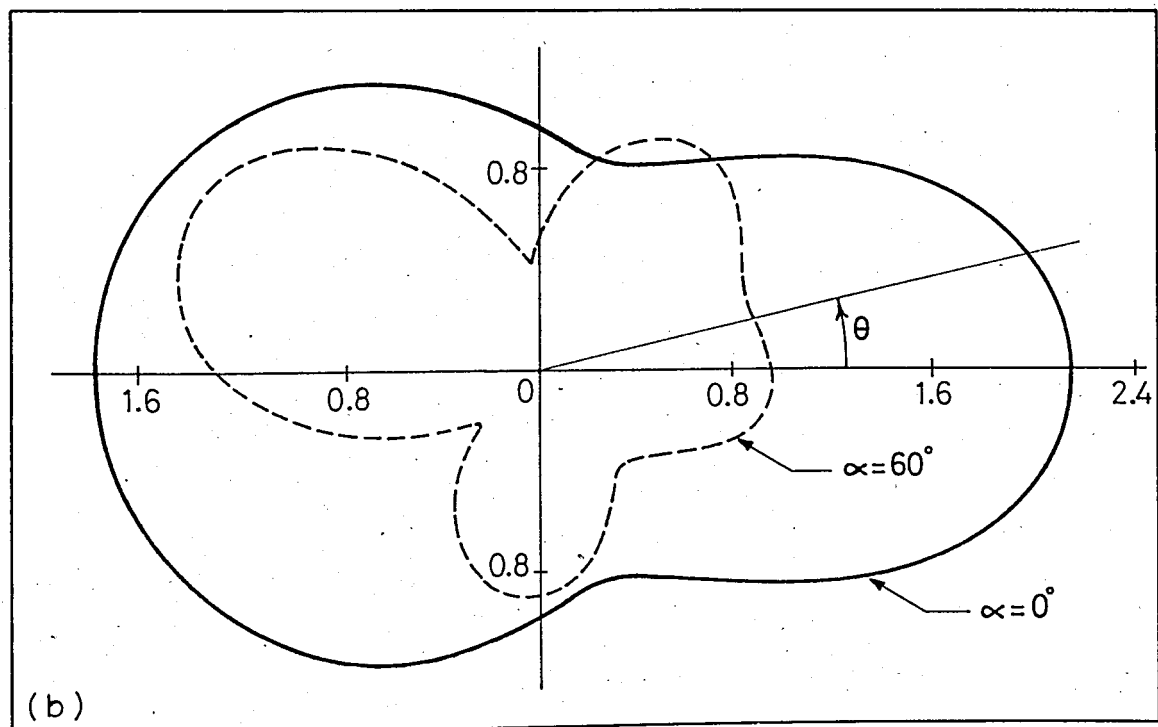
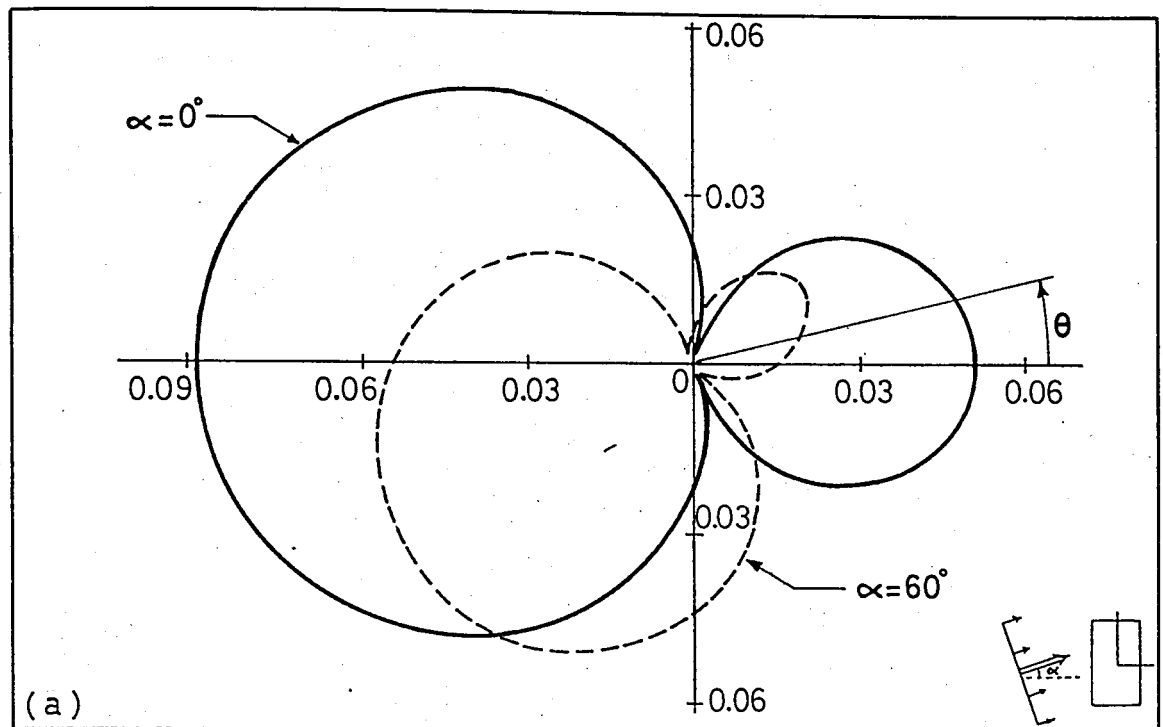


Figure 4.25 - Far field amplitude,  $|f/A|$ , due to the scattered wave field from a rigid rectangular inclusion for  $r_c/a = 0.1$  and  $b/a = 2.0$ ;  
 (a)  $ka = 0.1$ , (b)  $ka = 1.0$ , (c)  $ka = 3.0$ .

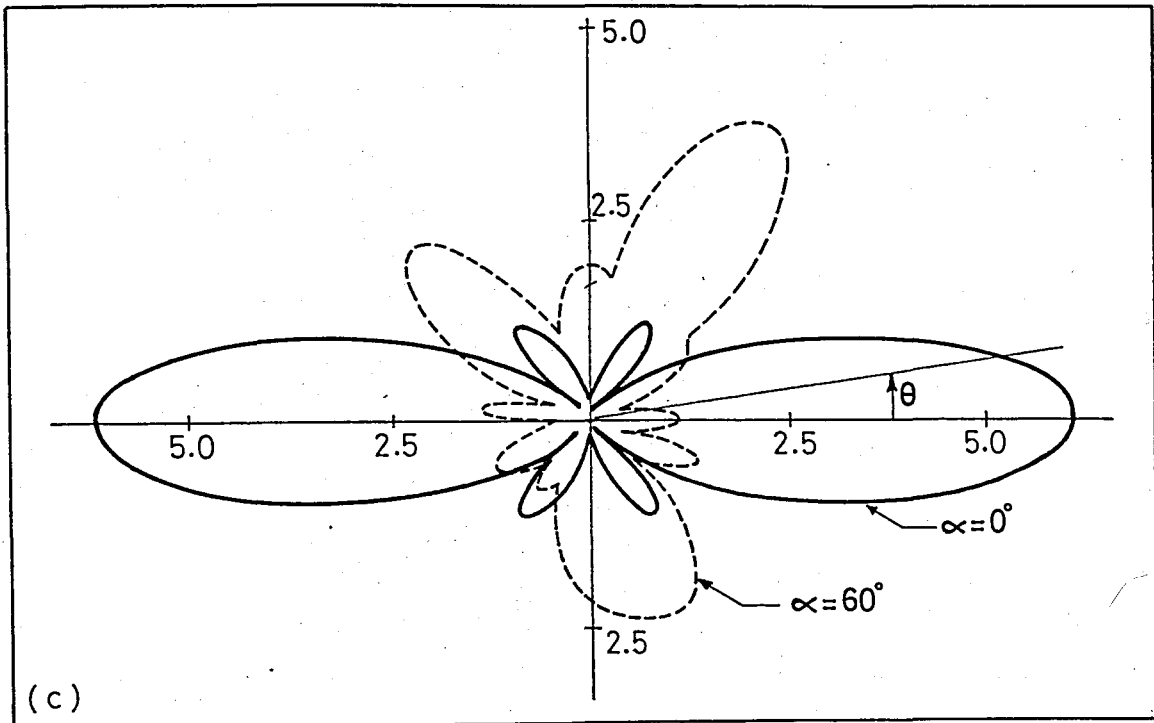


Figure 4.25 (continued).

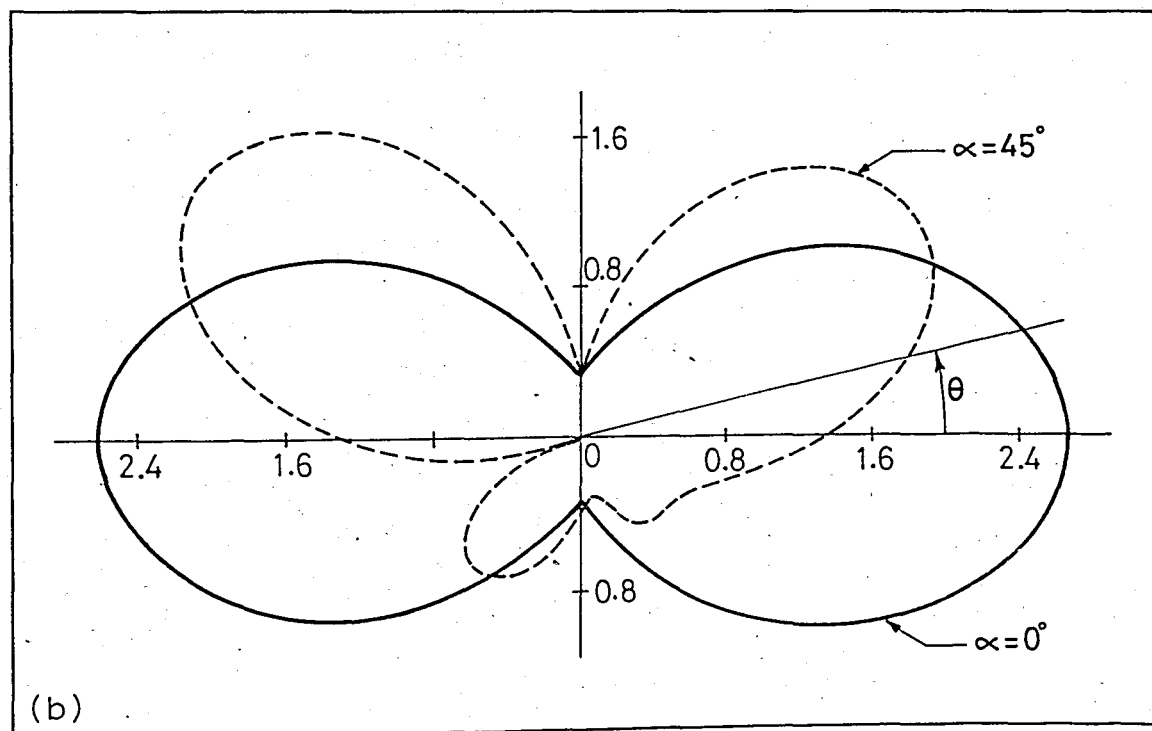
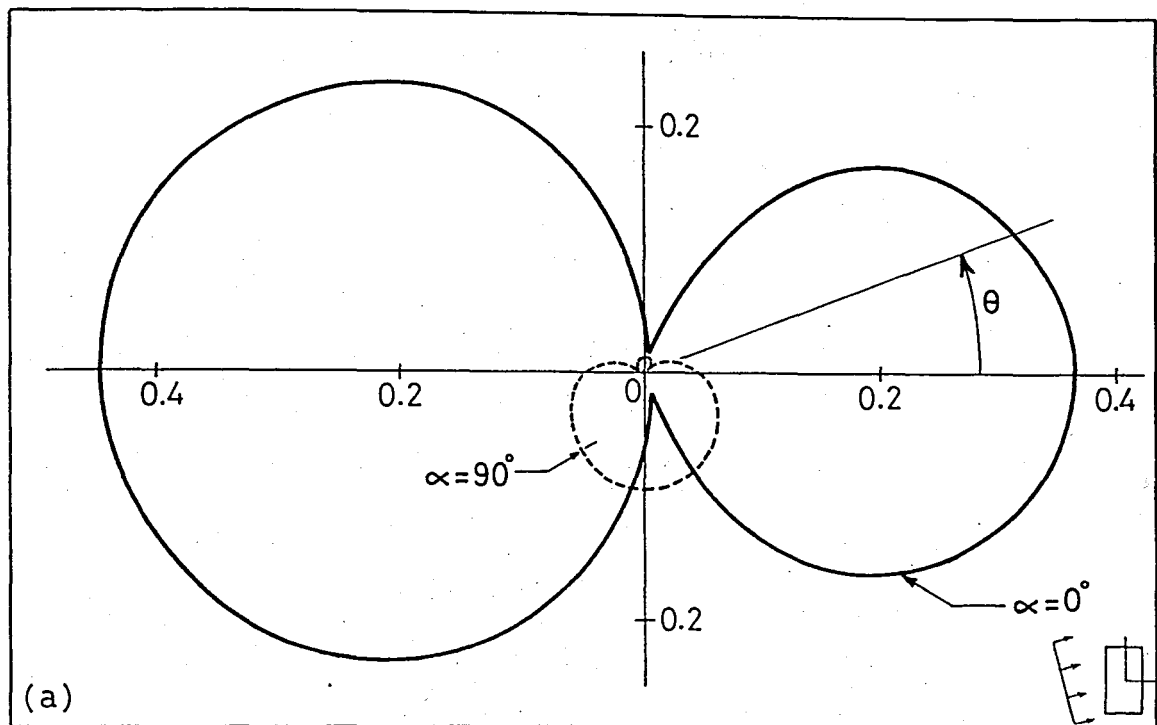


Figure 4.26 - Far field amplitude,  $|f/A|$ , due to the scattered wave field from a rigid rectangular inclusion for  $r_c/a = 0.1$  and  $b/a = 5.0$ ;  
 (a)  $ka = 0.1$ , (b)  $ka = 0.5$ , (c)  $ka = 1.0$ .

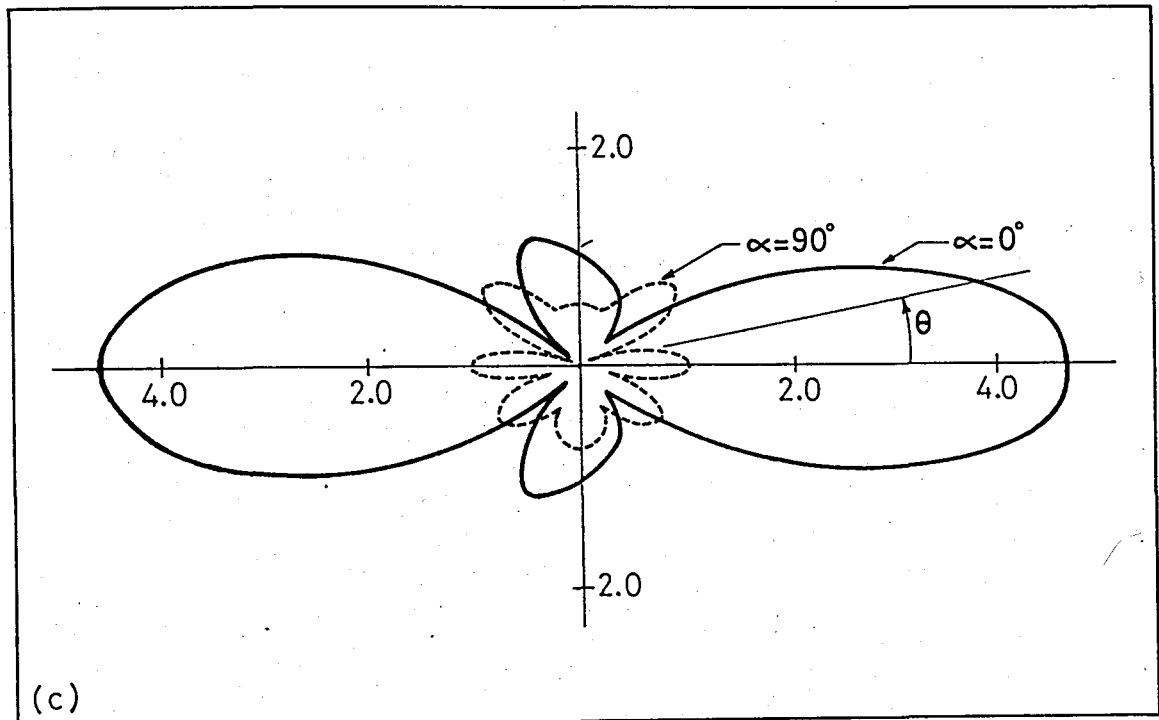


Figure 4.26 (continued).

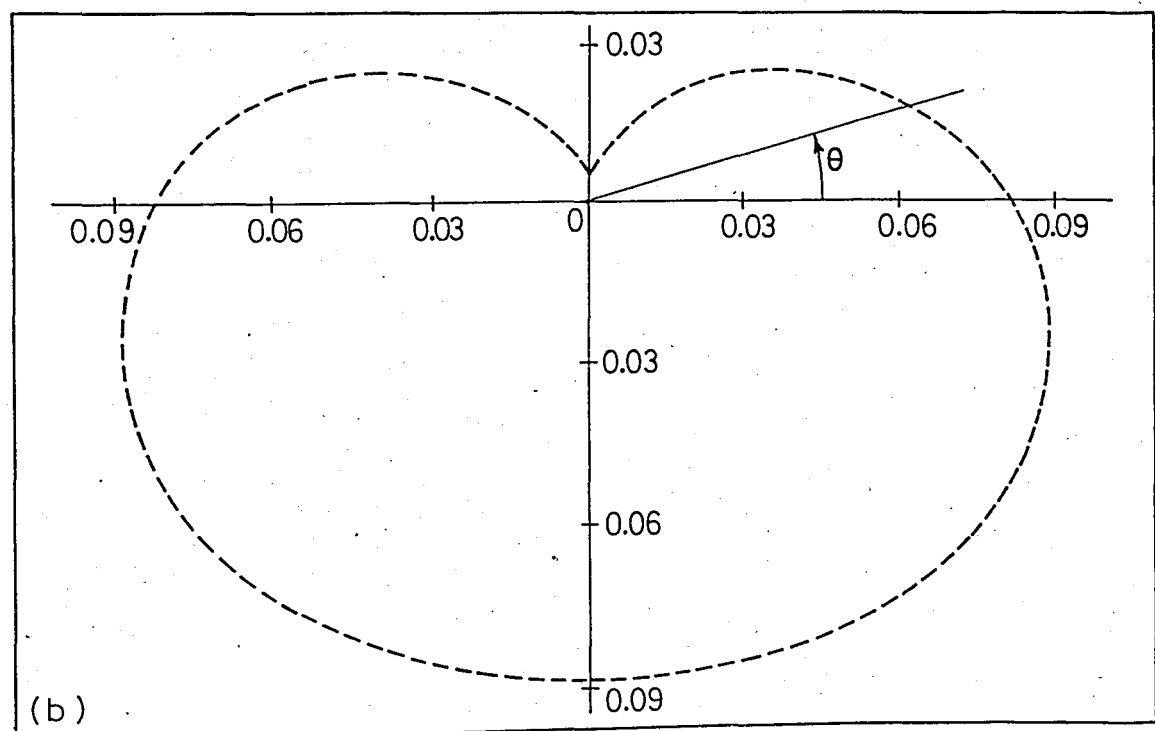
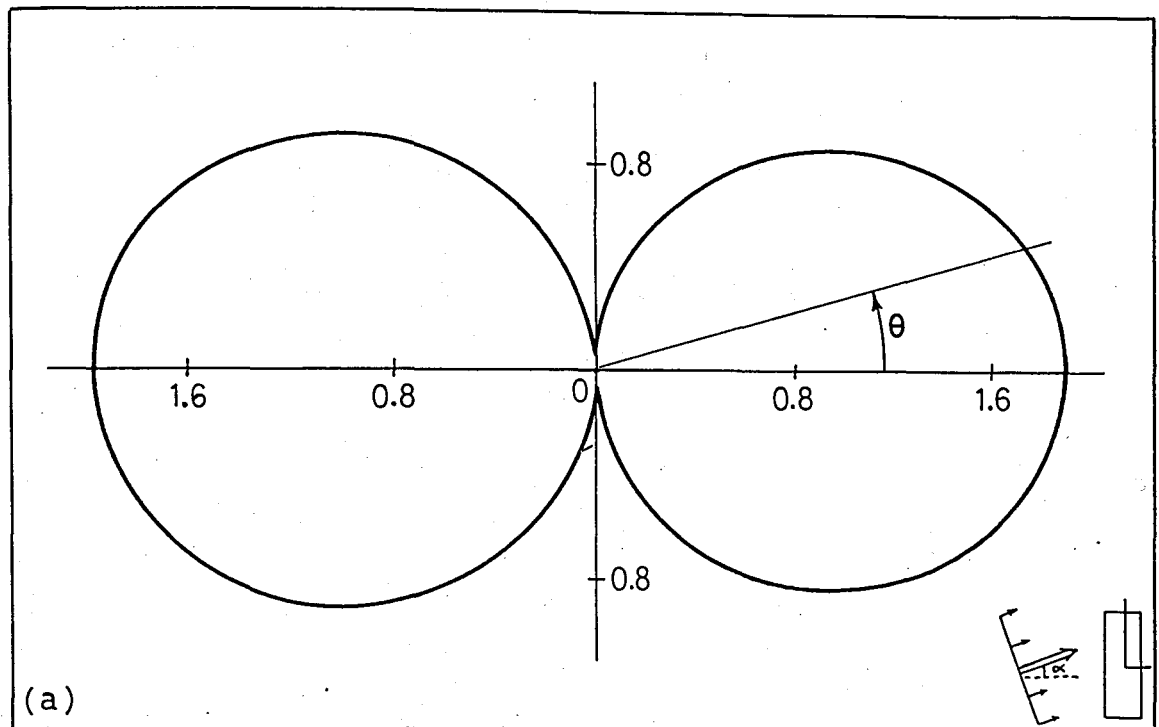


Figure 4.27 - Far field amplitude,  $|f/A|$ , due to the scattered wave field from a rigid rectangular inclusion for  $r_c/a = 0.1$  and  $b/a = 10.0$ ;

(a)  $ka = 0.1, \alpha = 0^\circ$ , (b)  $ka = 0.1, \alpha = 90^\circ$ ,  
 (c)  $ka = 0.5, \alpha = 0^\circ$ , (d)  $ka = 0.5, \alpha = 90^\circ$ .

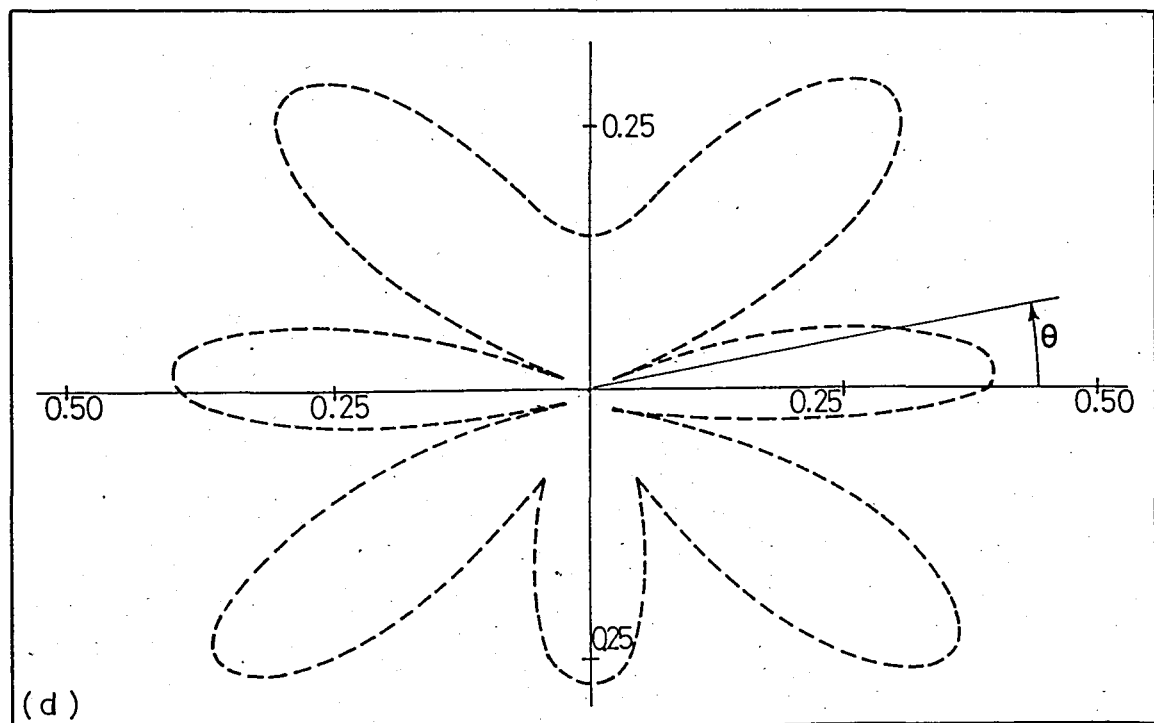
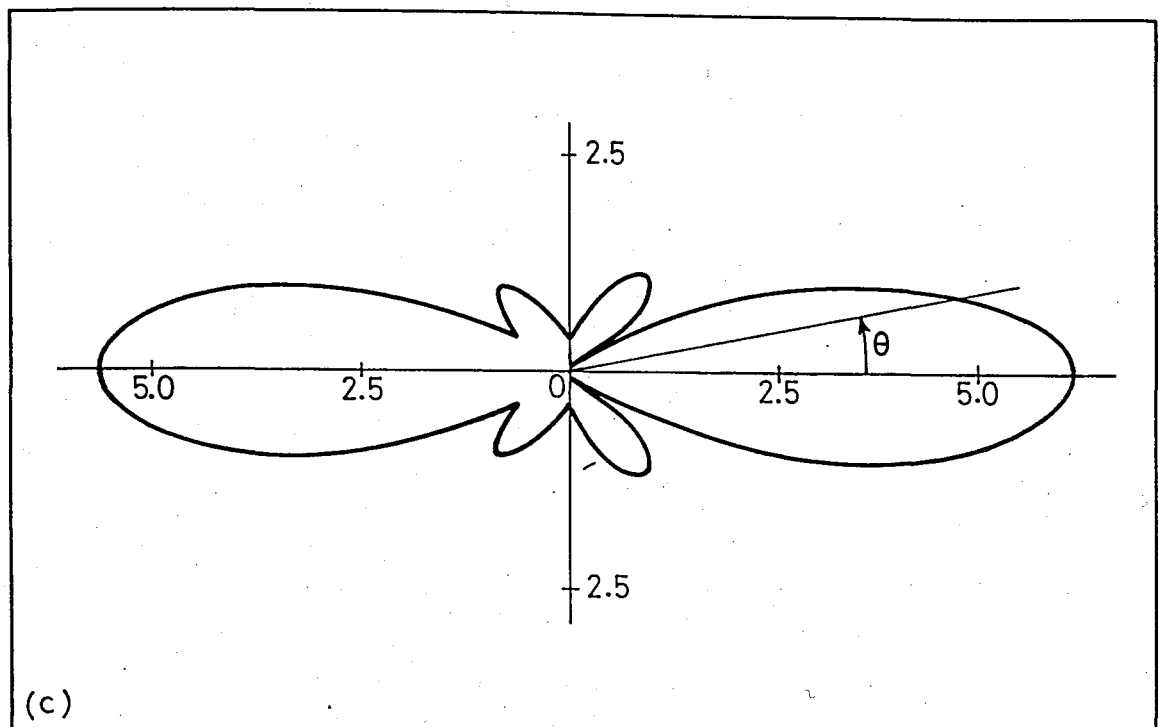


Figure 4.27 (continued).

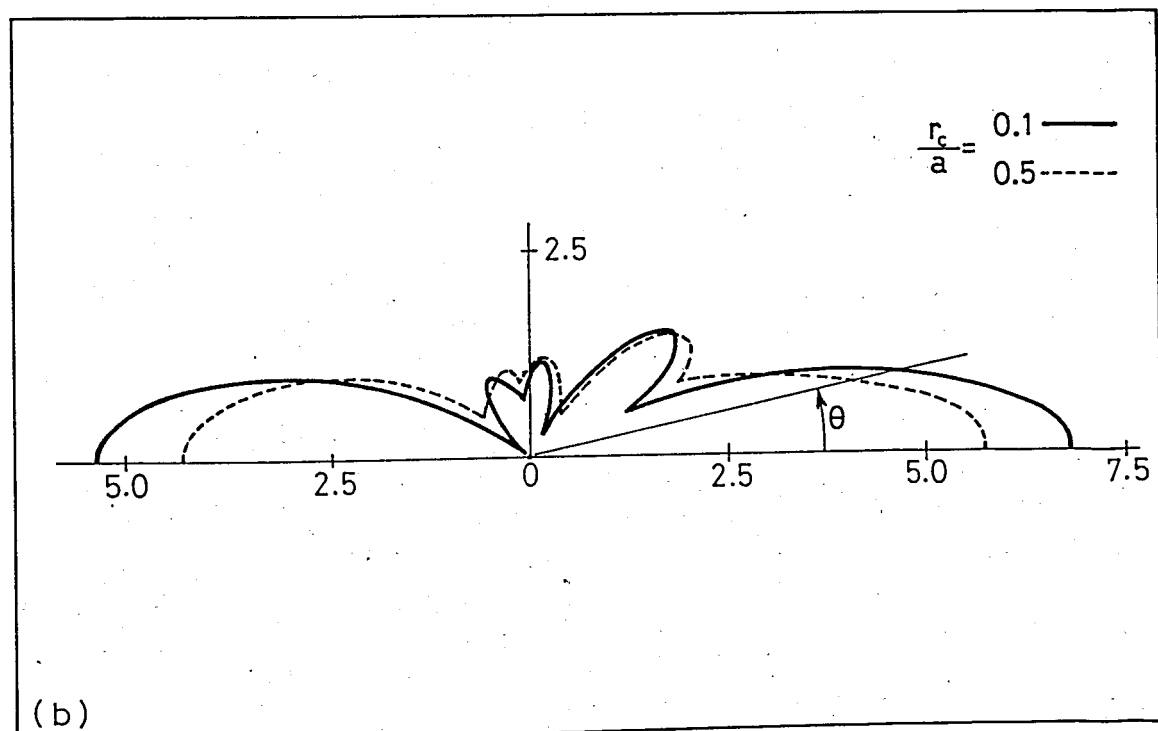
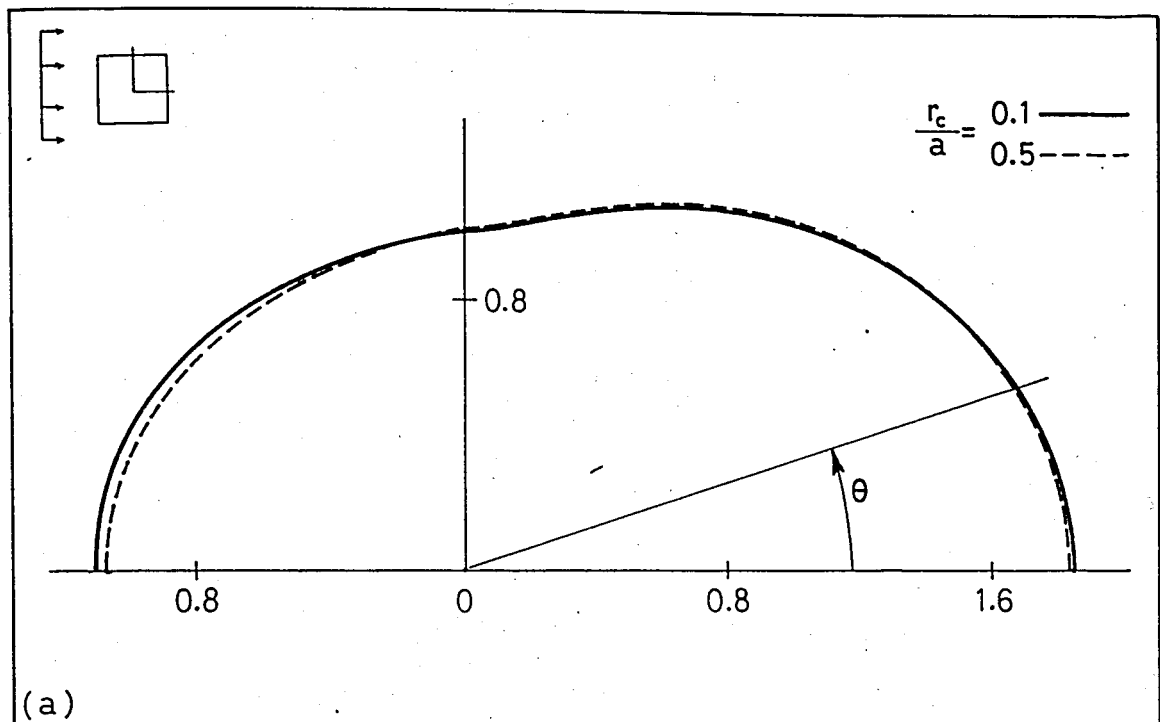
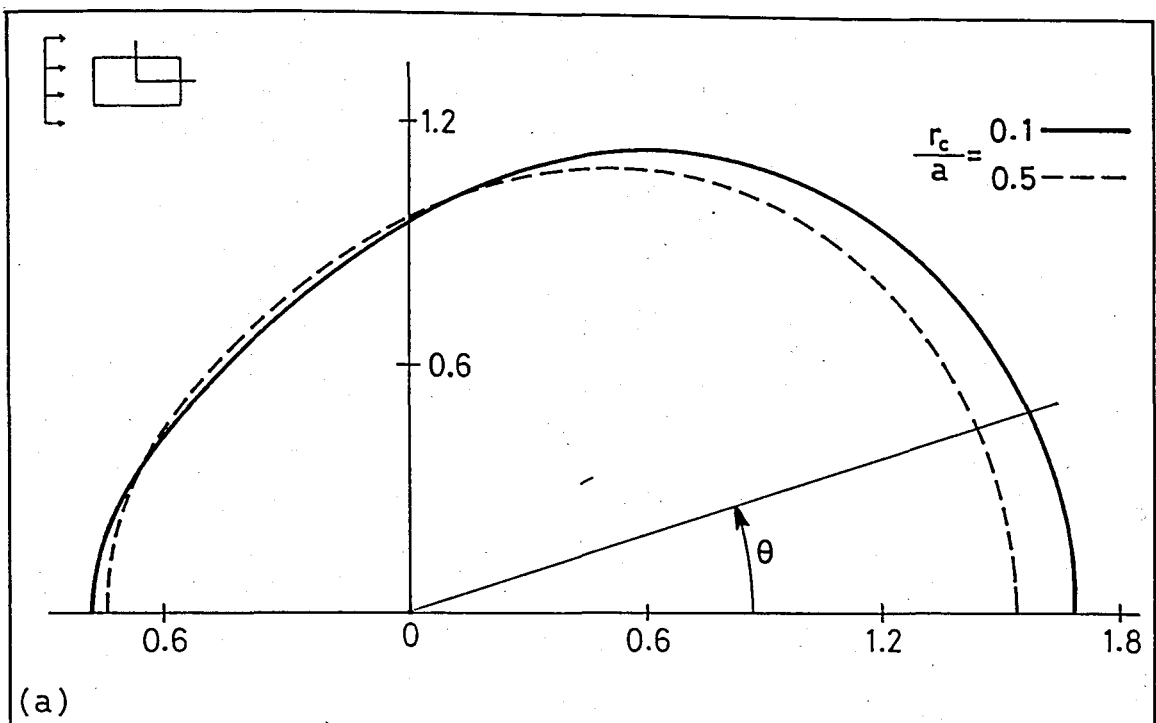
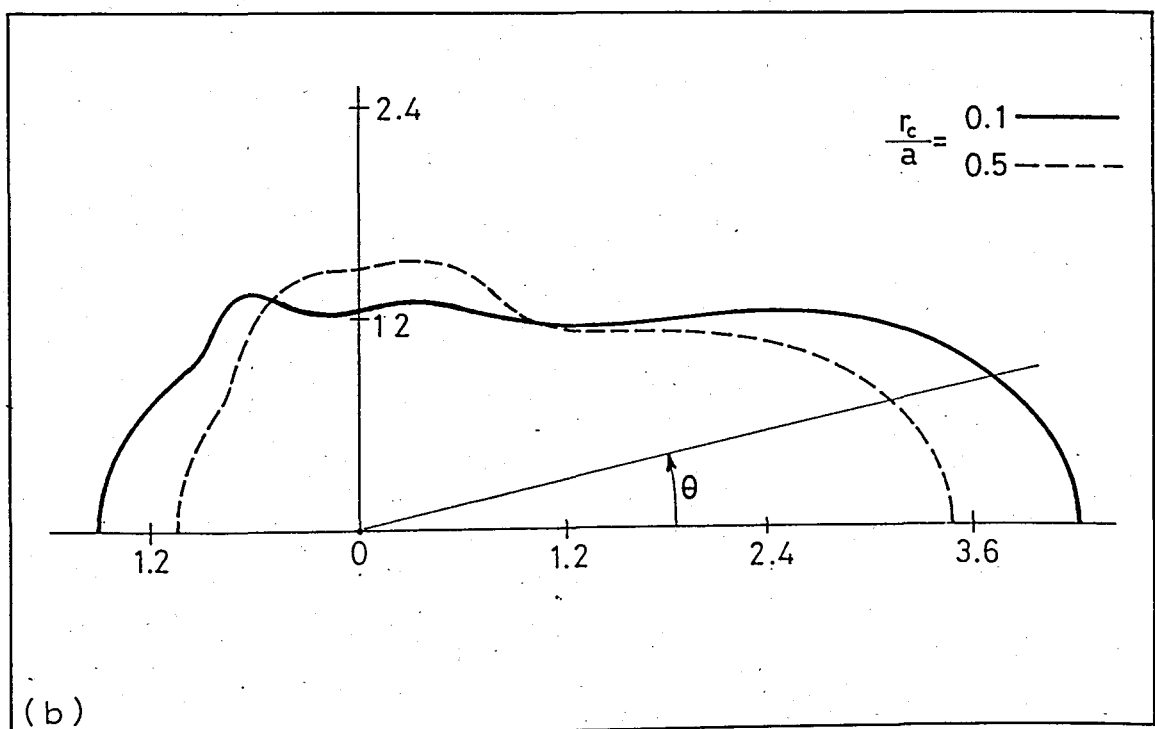


Figure 4.28 - Effect of the corner radius on the far field amplitude,  $|f/A|$ , due to the scattered wave field from a rectangular cavity for  $\alpha = 0^\circ$  and  $b/a = 1.0$ ;  
 (a)  $ka = 1.0$ , (b)  $ka = 5.0$



(a)



(b)

Figure 4.29 - Effect of the corner radius on the far field amplitude,  $|f/A|$ , due to the scattered wave field from a rectangular cavity for  $\alpha = 0^\circ$  and  $b/a = 0.5$ ;  
 (a)  $ka = 1.0$ , (b)  $ka = 5.0$ .

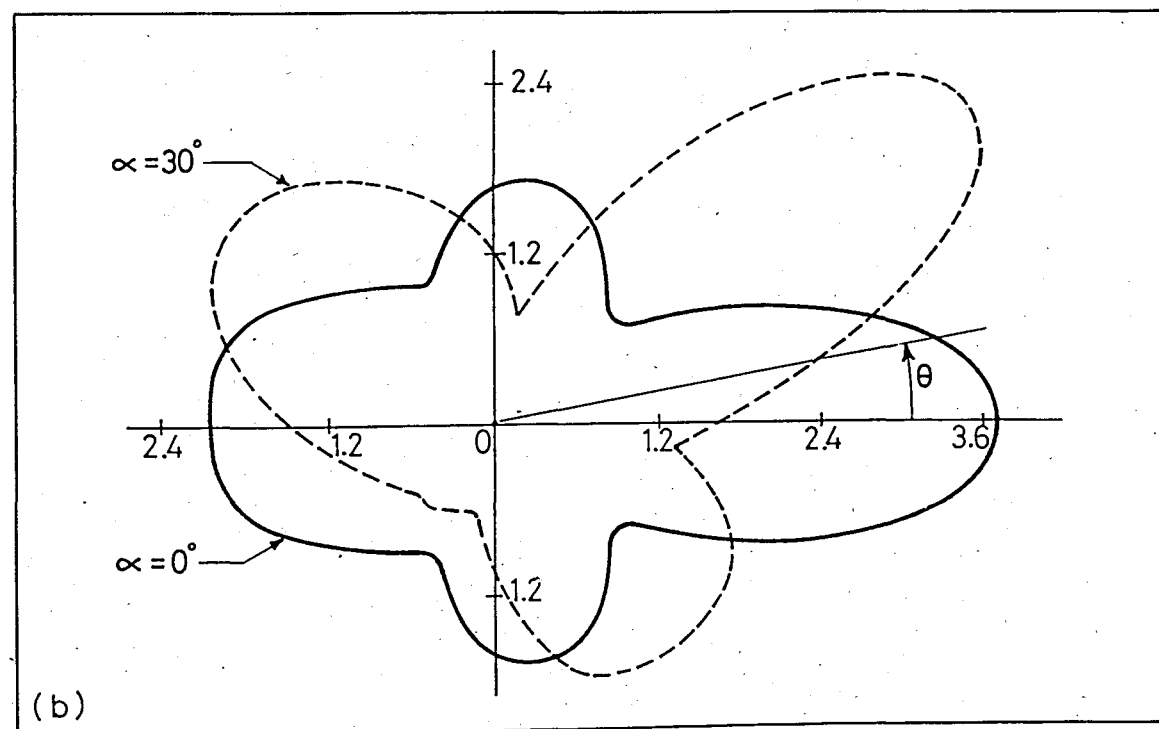
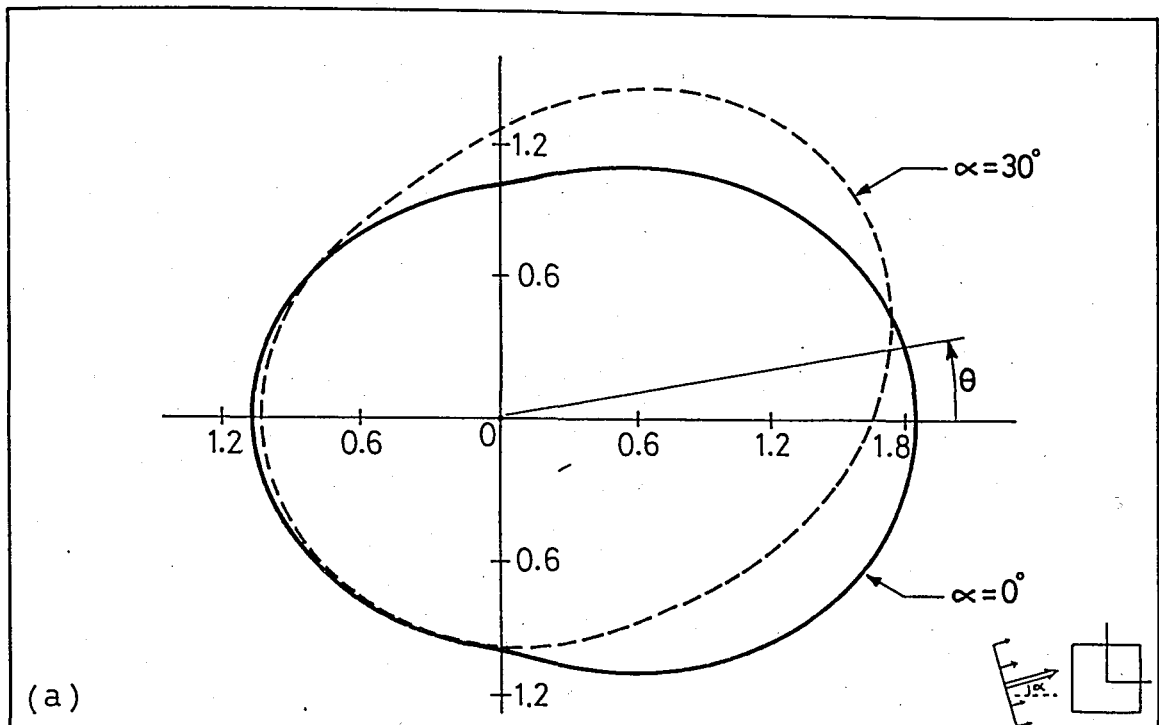


Figure 4.30 - Far field amplitude,  $|f/A|$ , due to the scattered wave field from a rectangular cavity for  $r_c/a = 0.1$  and  $b/a = 1.0$ ;  
 (a)  $ka = 1.0$ , (b)  $ka = 3.0$ , (c)  $ka = 5.0$ .

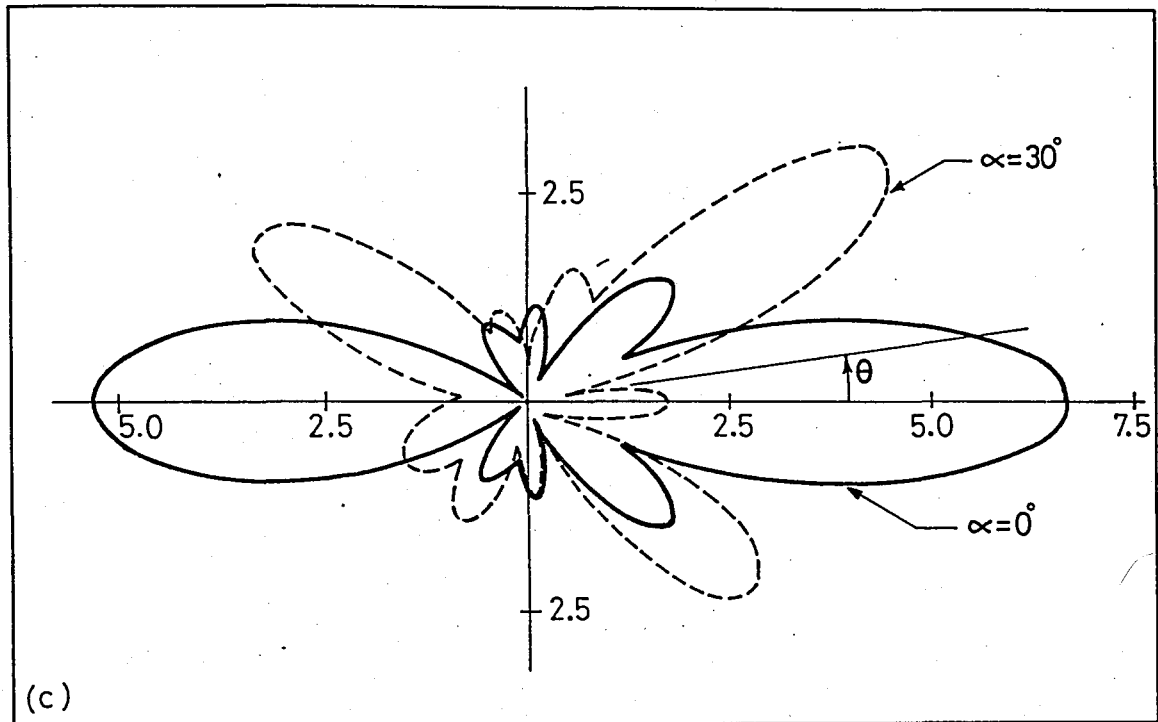


Figure 4.30 (continued).

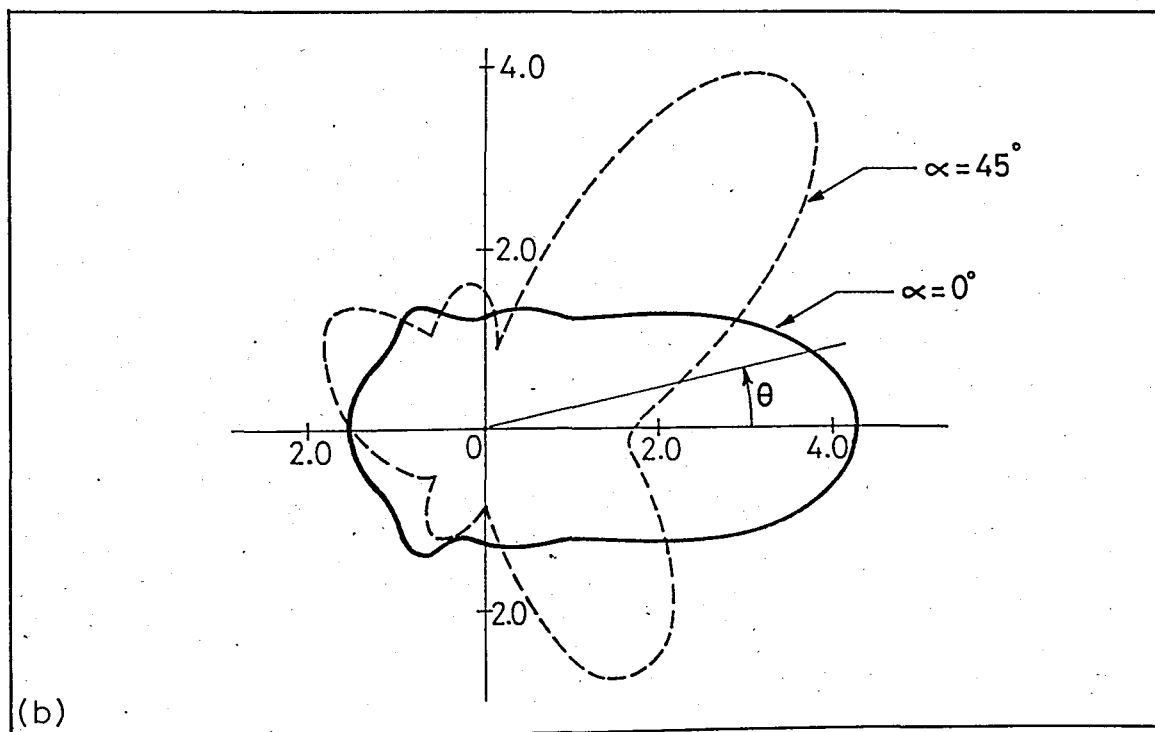
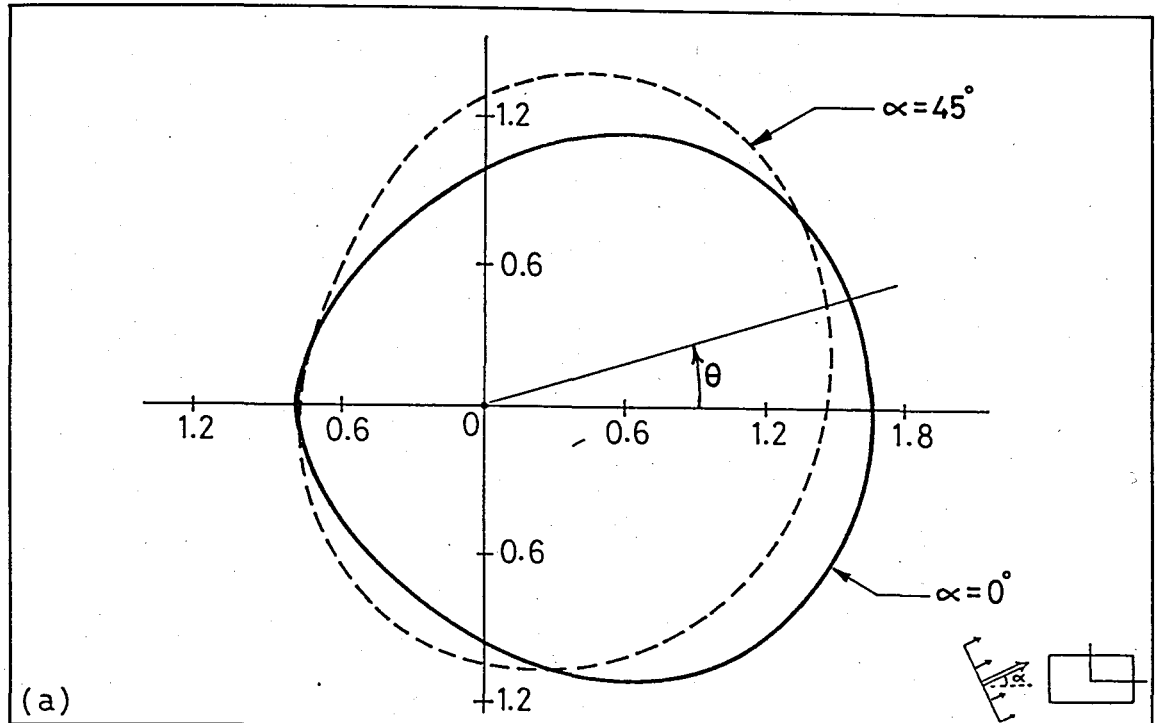


Figure 4.31. - Far field amplitude,  $|f/A|$ , due to the scattered wave field from a rectangular cavity for  $r_c/a = 0.1$  and  $b/a = 0.5$ ;  
 (a)  $ka = 1.0$ , (b)  $ka = 5.0$ .

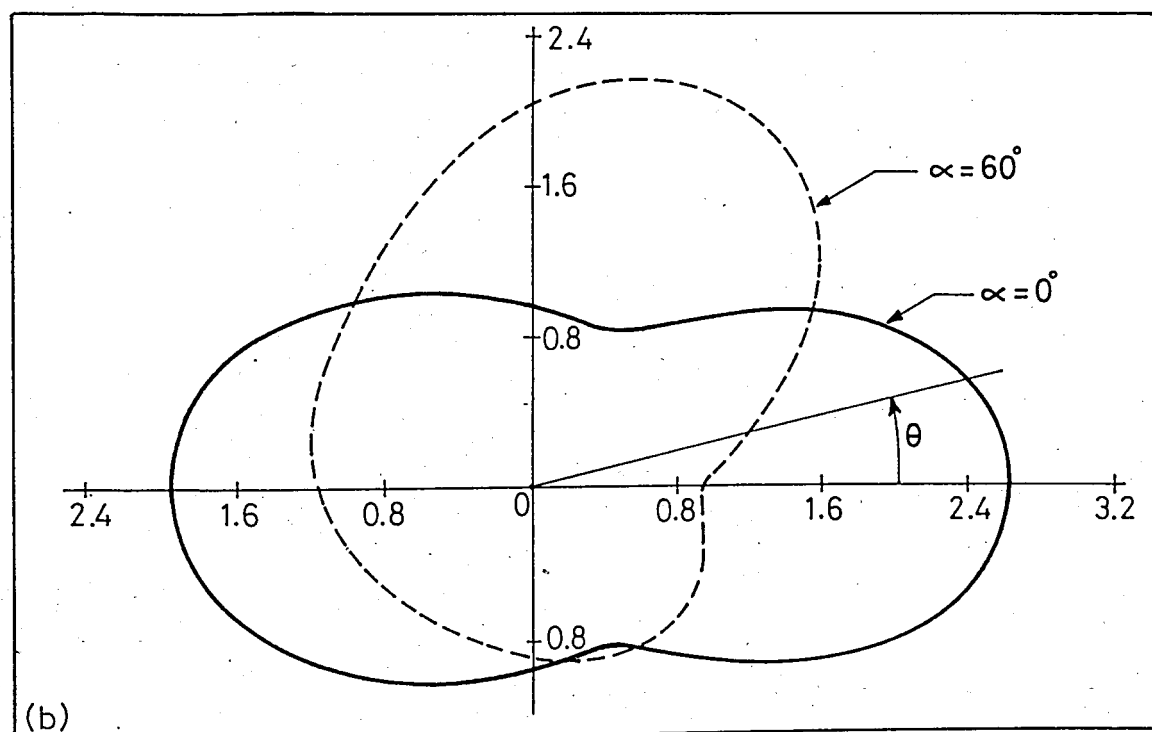
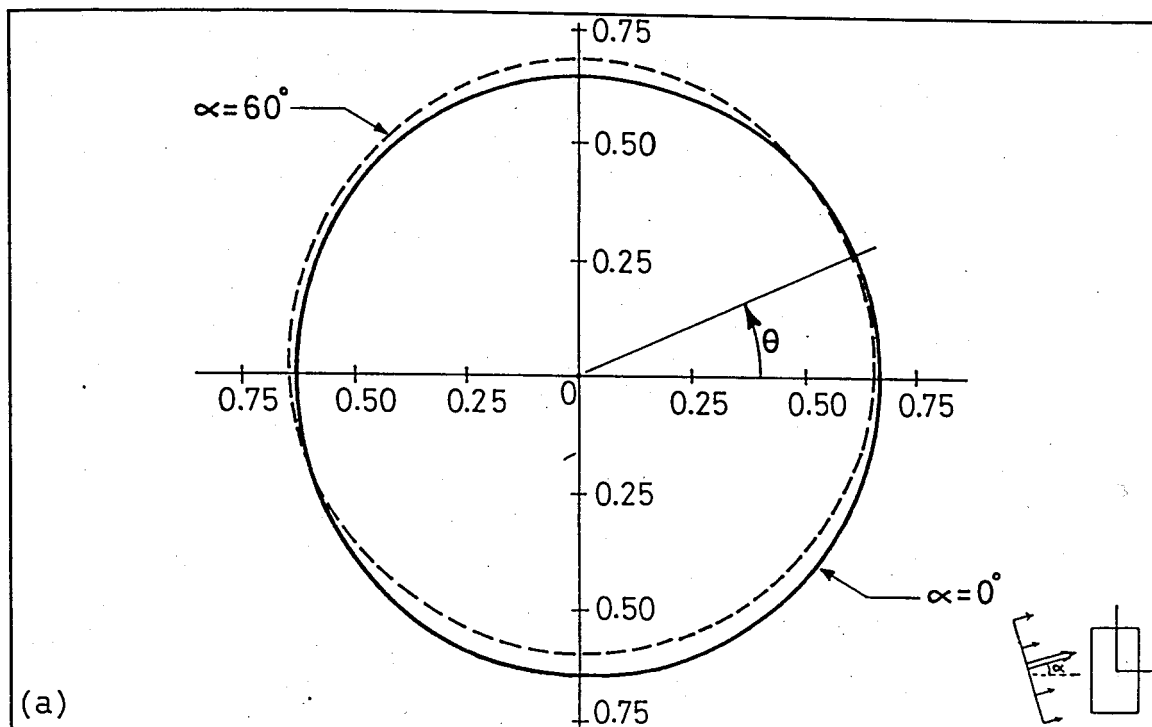


Figure 4.32 - Far field amplitude,  $|f/A|$ , due to the scattered wave field from a rectangular cavity for  $r_c/a = 0.1$  and  $b/a = 2.0$ ;  
 (a)  $ka = 0.1$ , (b)  $ka = 1.0$ , (c)  $ka = 3.0$ .

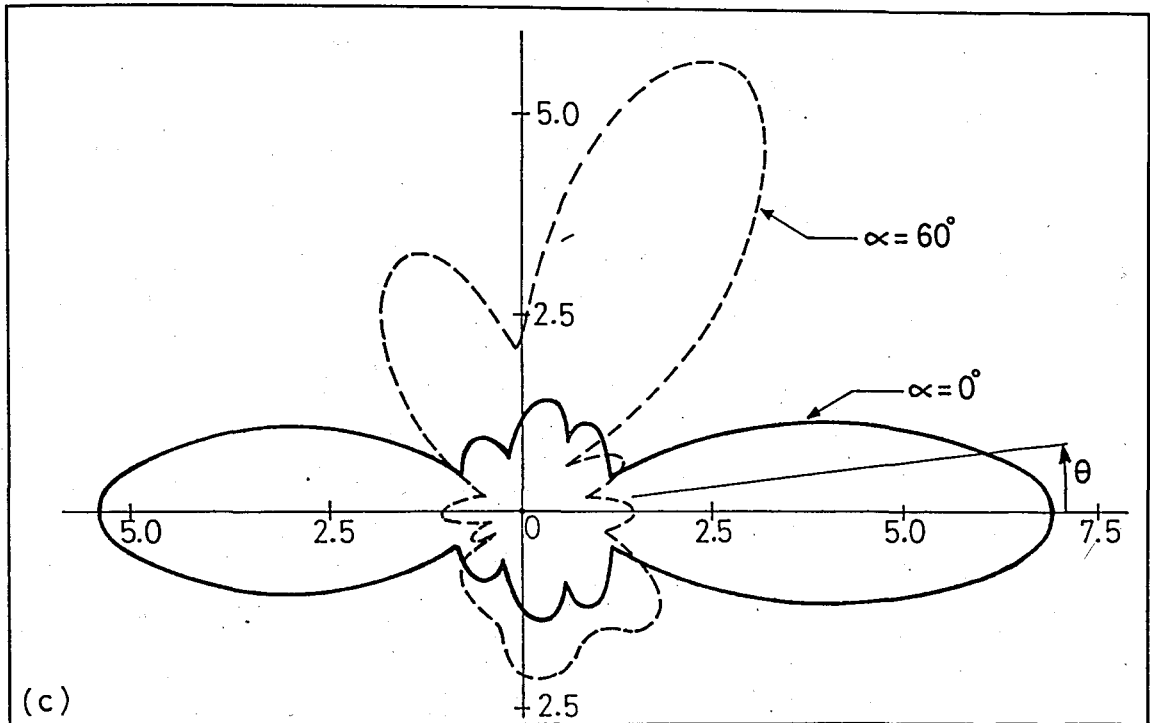


Figure 4.32 (continued).

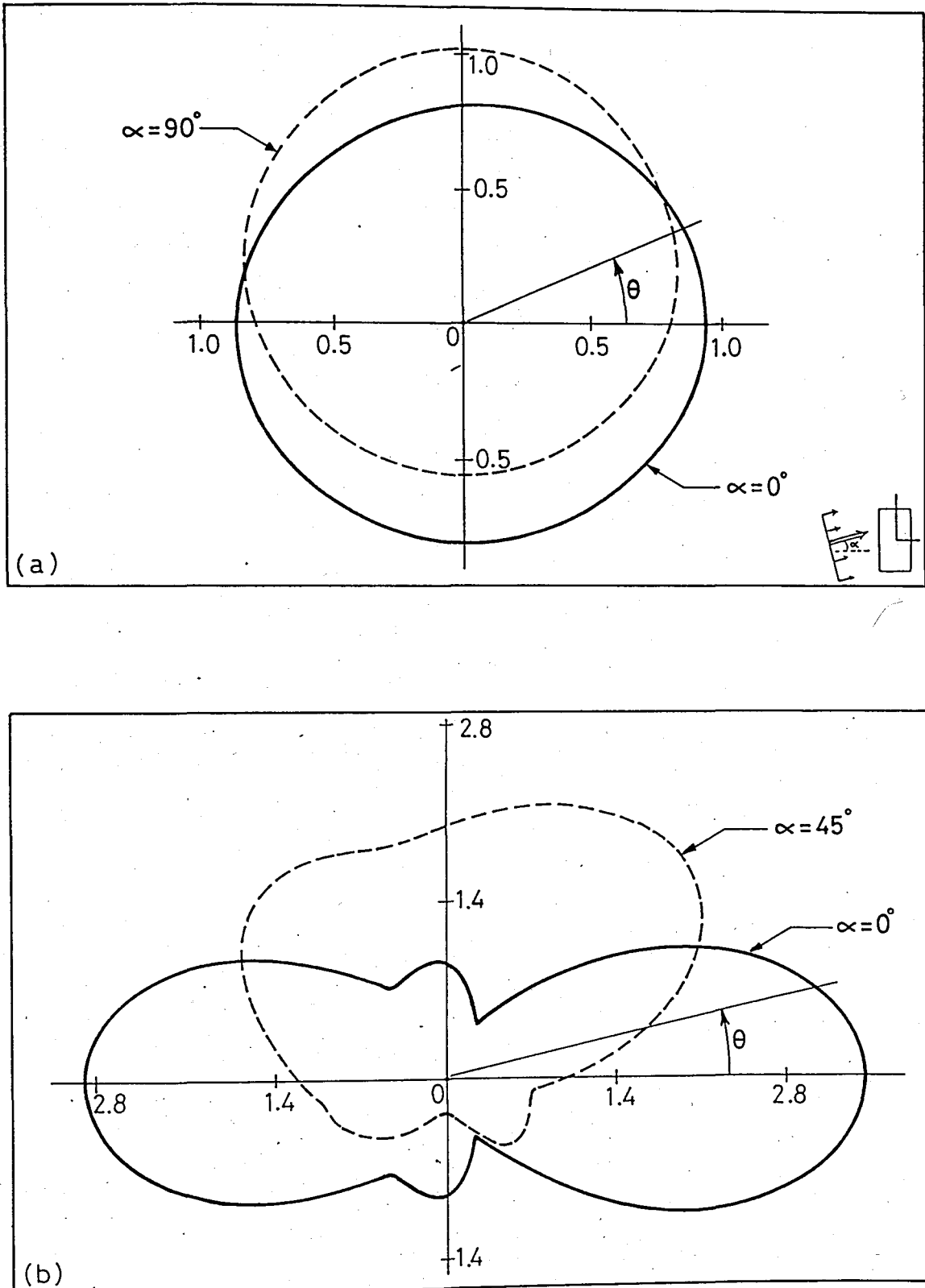


Figure 4.33 - Far field amplitude,  $|f/A|$ , due to the scattered wave field from a rectangular cavity for  $r_c/a = 0.1$  and  $b/a = 5.0$ ;  
 (a)  $ka = 0.1$ , (b)  $ka = 0.5$ , (c)  $ka = 1.0$ .

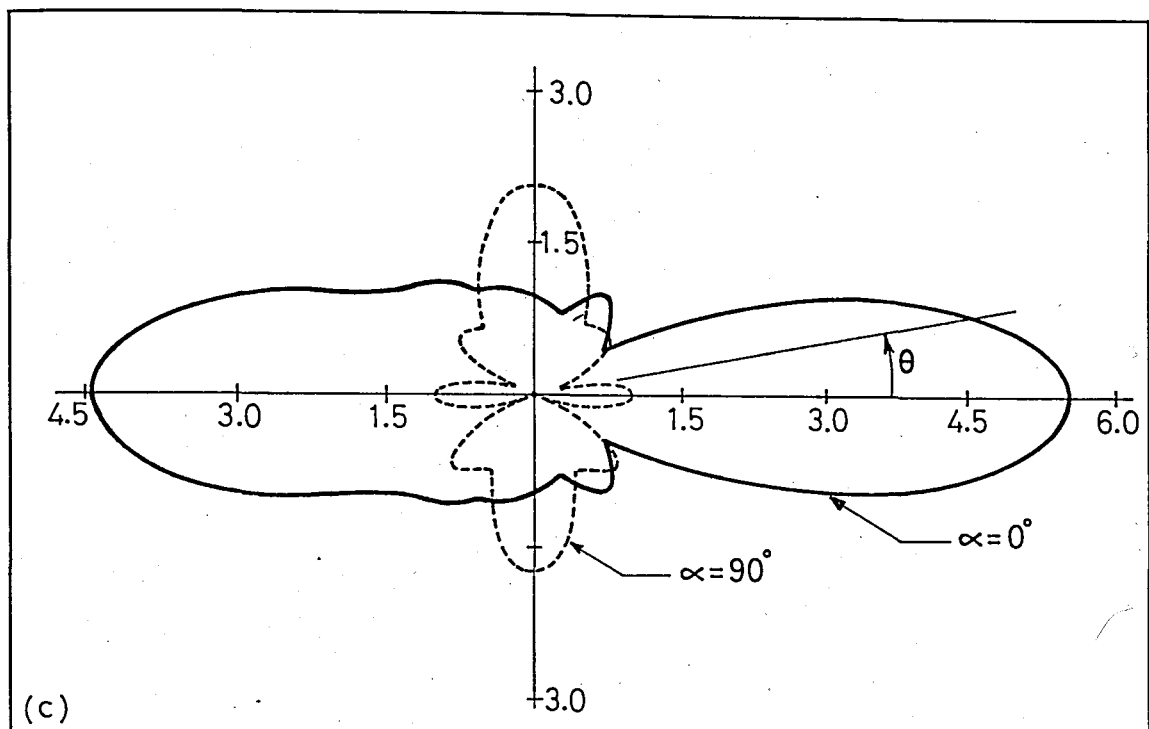


Figure 4.33 (continued).

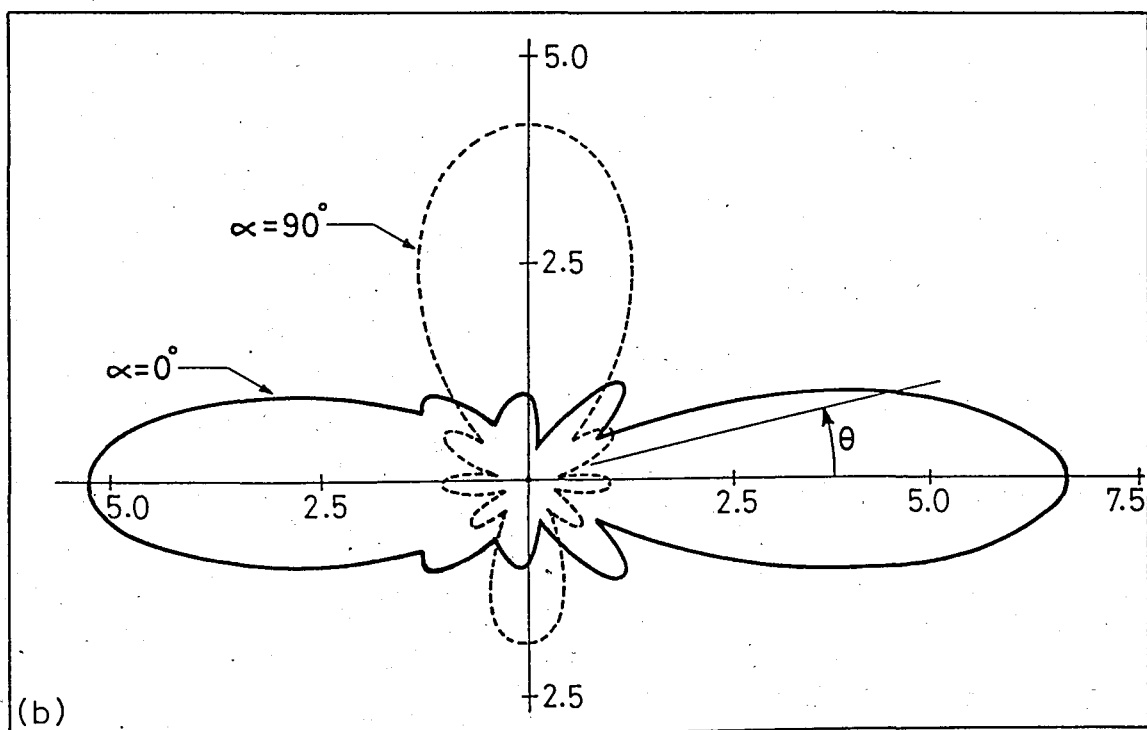
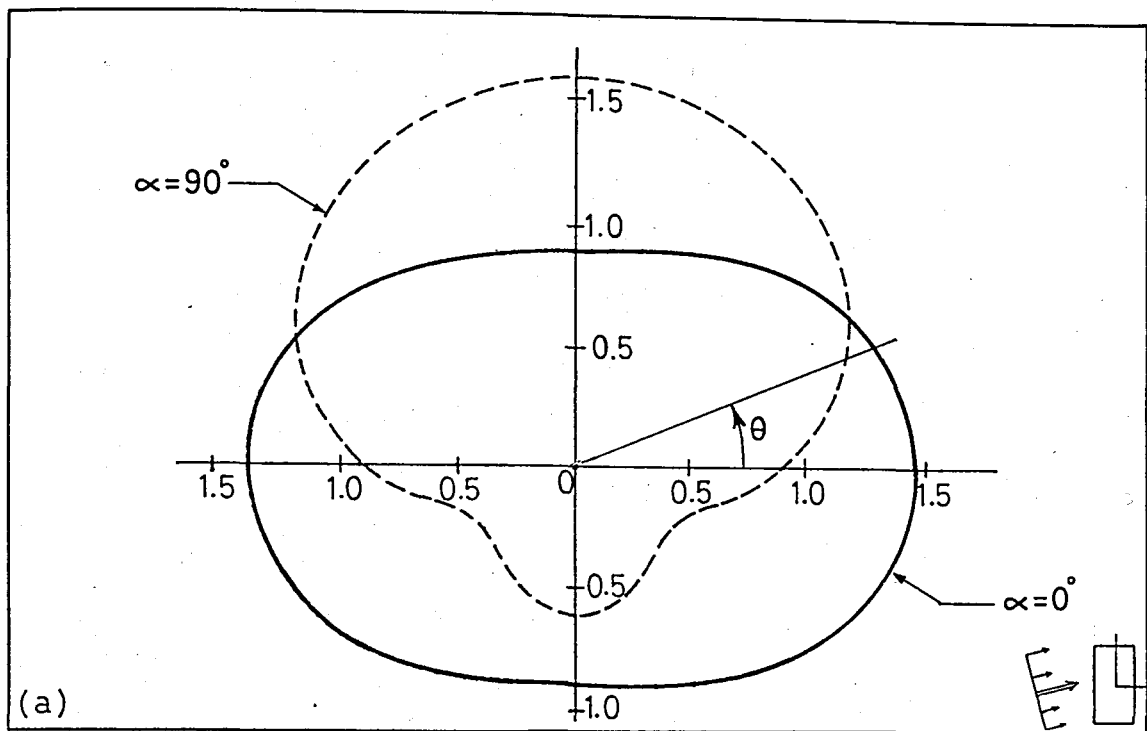


Figure 4.34 - Far field amplitude,  $|f/A|$ , due to the scattered wave field from a rectangular cavity for  $r_c/a = 0.1$  and  $b/a = 10.0$ .  
 (a)  $ka = 0.1$ , (b)  $ka = 0.5$ .

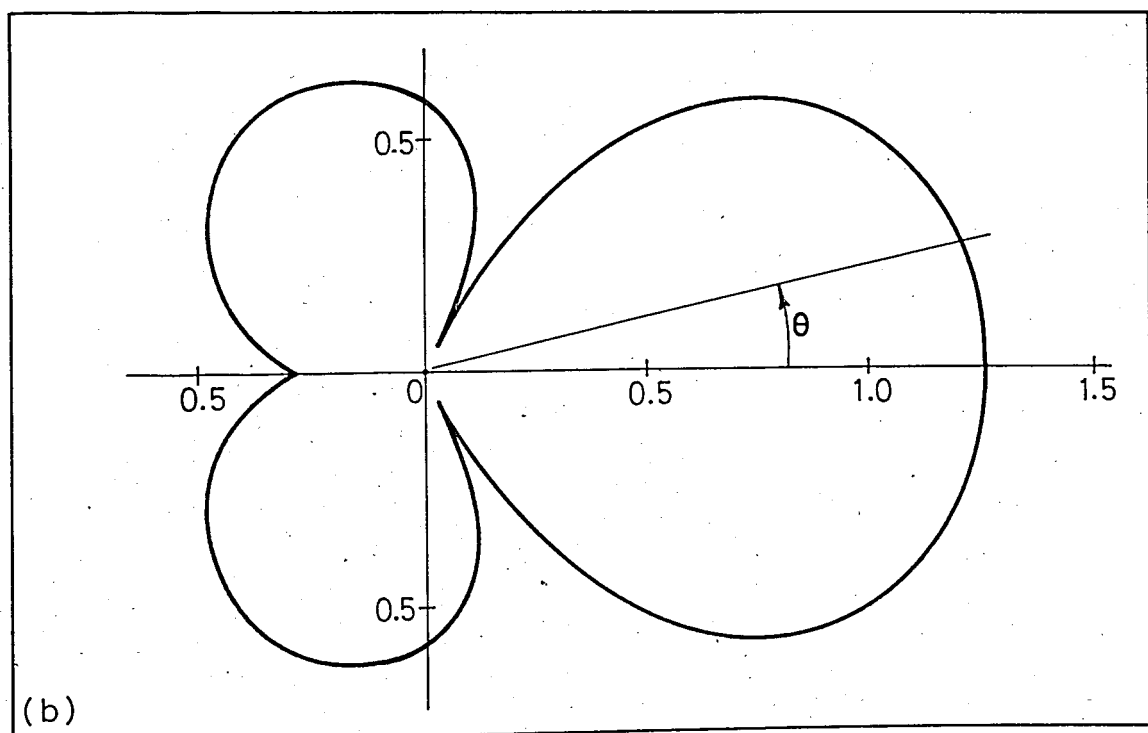
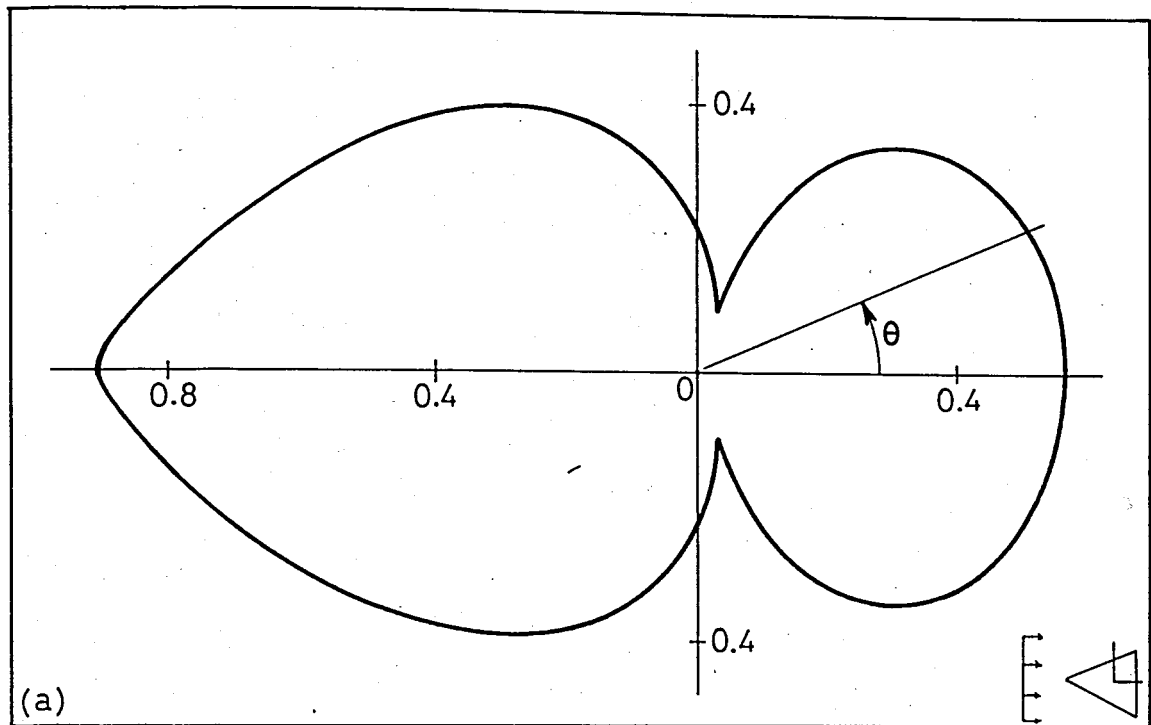


Figure 4.35 - Velocity potential distribution,  $|u^S/A|$ , at the boundary of a rigid triangular inclusion due to the scattered wave field for  $\alpha = 0^\circ$  and  $\beta = 60^\circ$ ; (a)  $kh = 1.5$ , (b)  $kh = 3.0$ , (c)  $kh = 9.0$ .

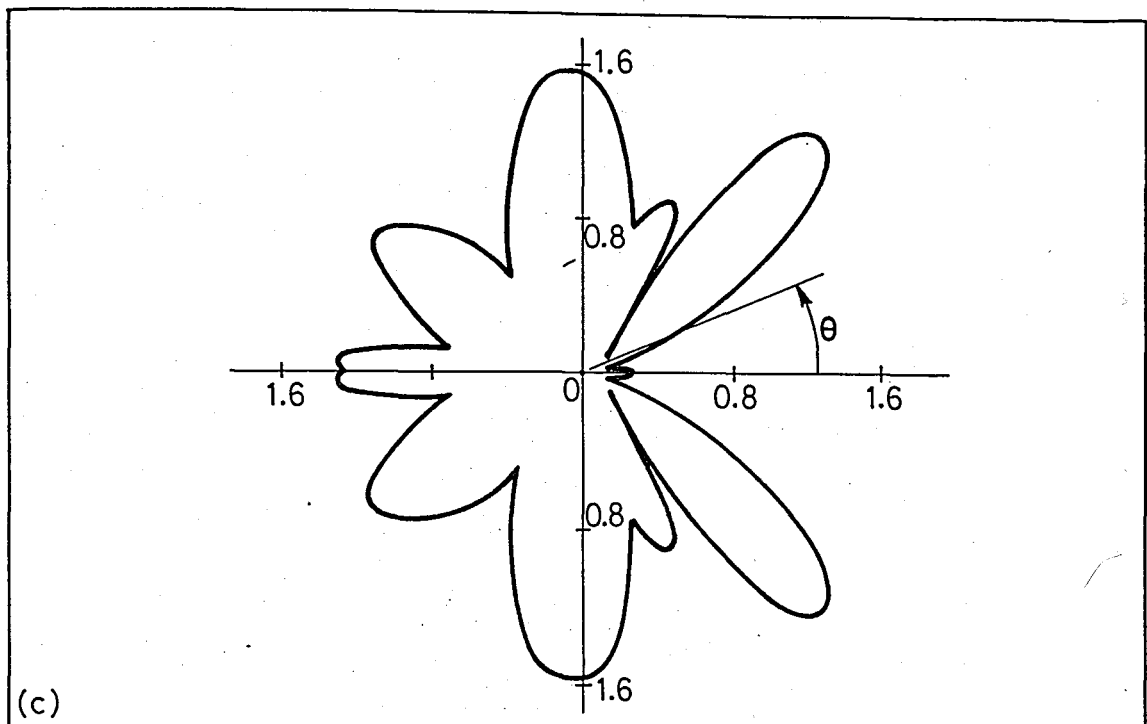


Figure 4.35 (continued).

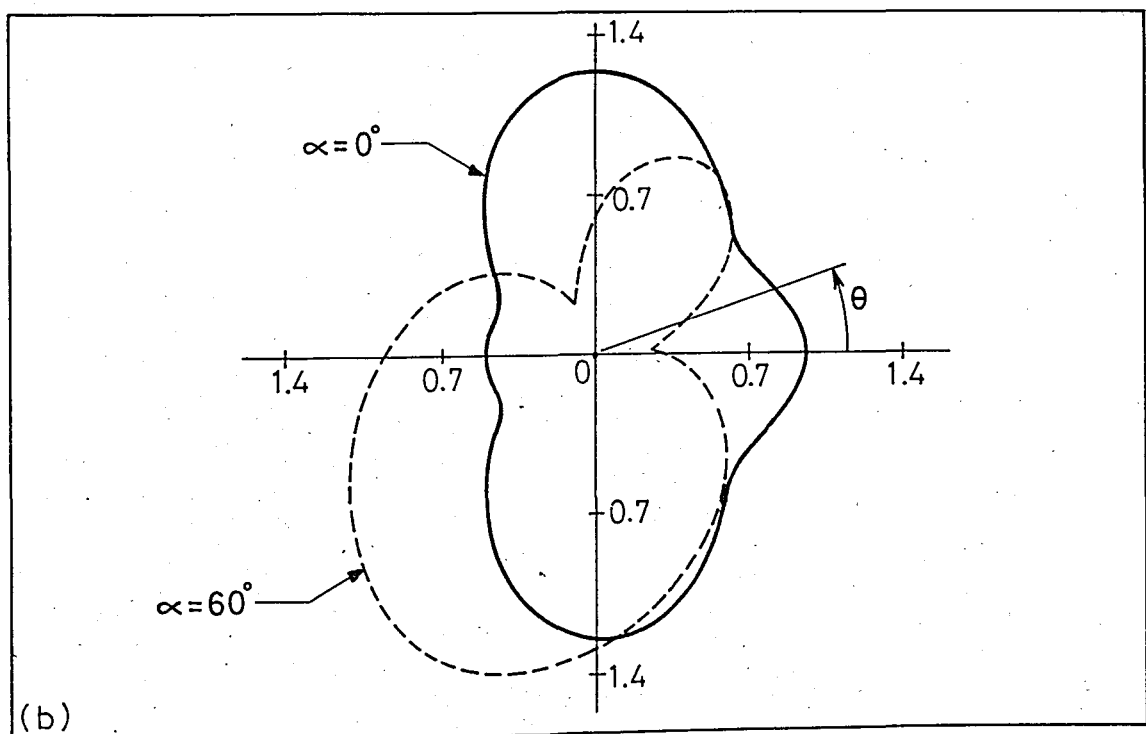
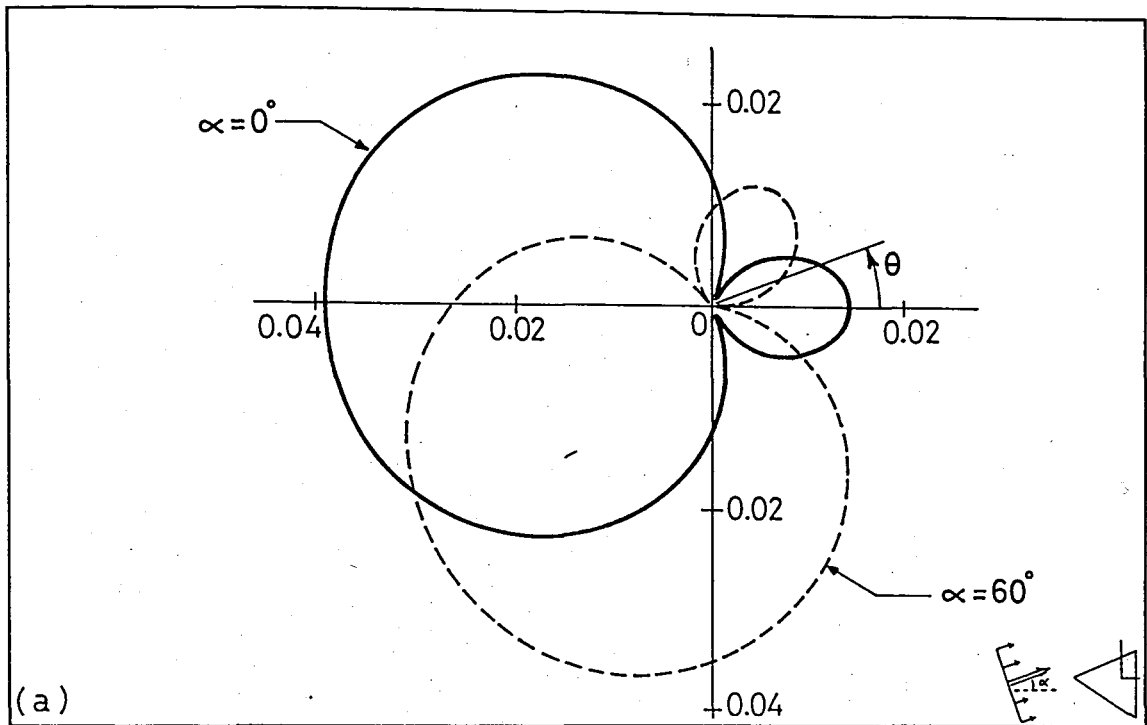


Figure 4.36 - Far field amplitude,  $|f/A|$ , due to the scattered wave field from a rigid triangular inclusion for  $\beta = 60^\circ$ ; (a)  $kh = 0.3$ , (b)  $kh = 3.0$ , (c)  $kh = 9.0$ .

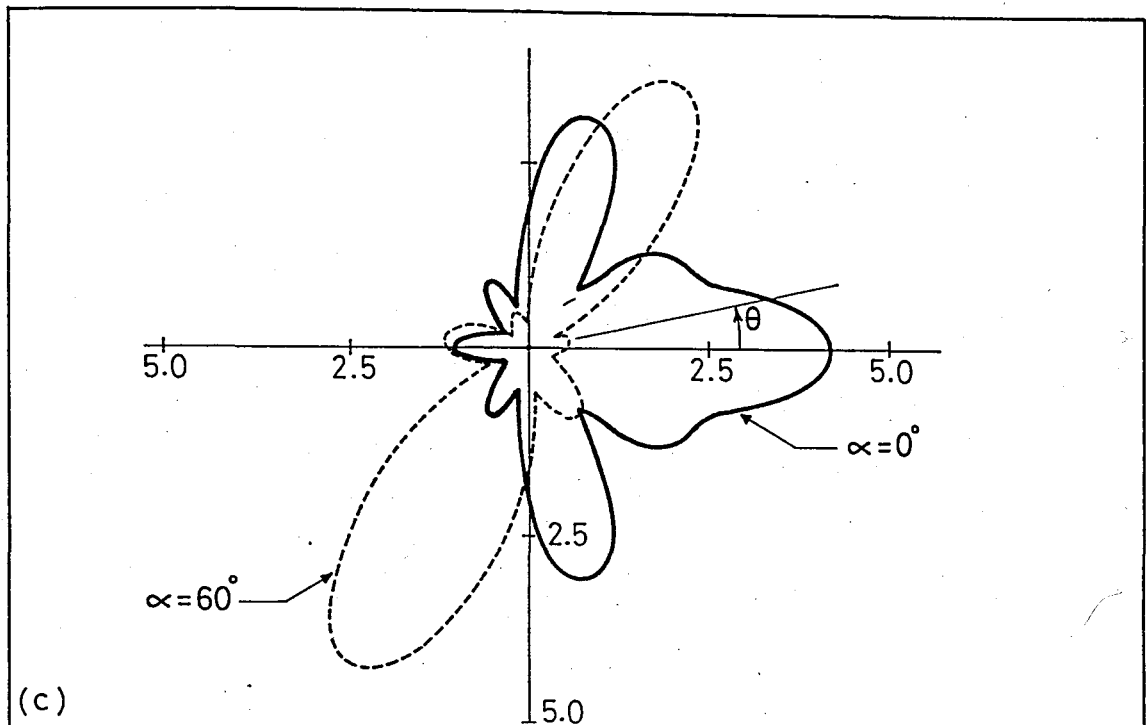


Figure 4.36 (continued).

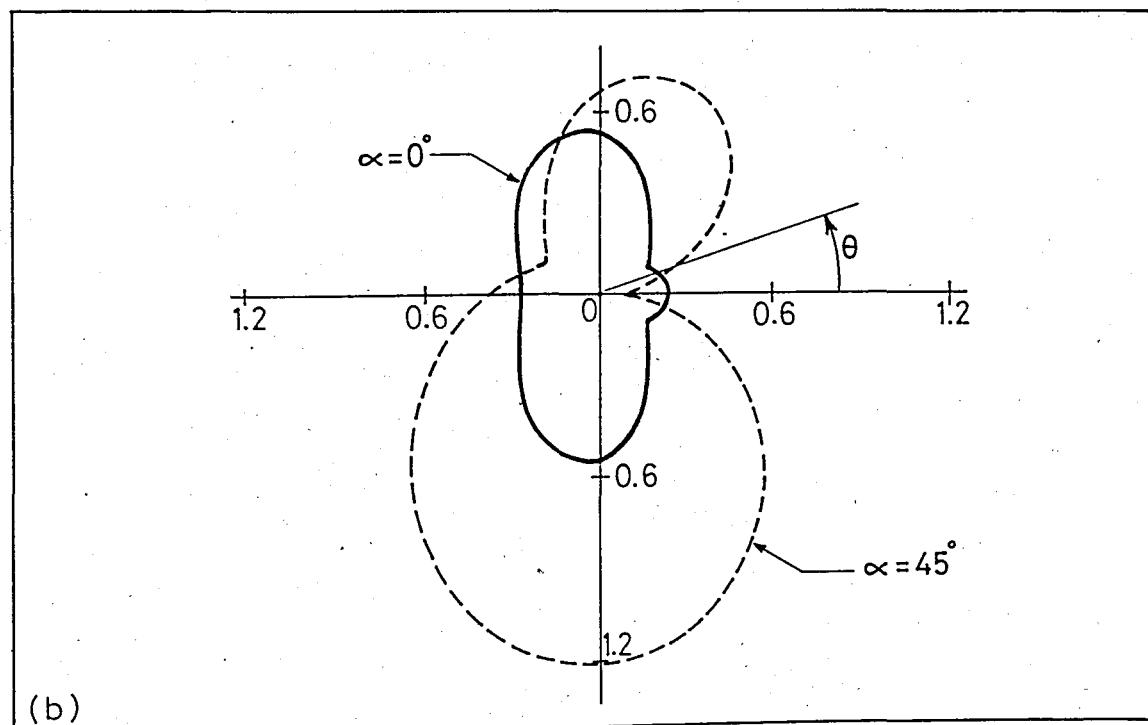
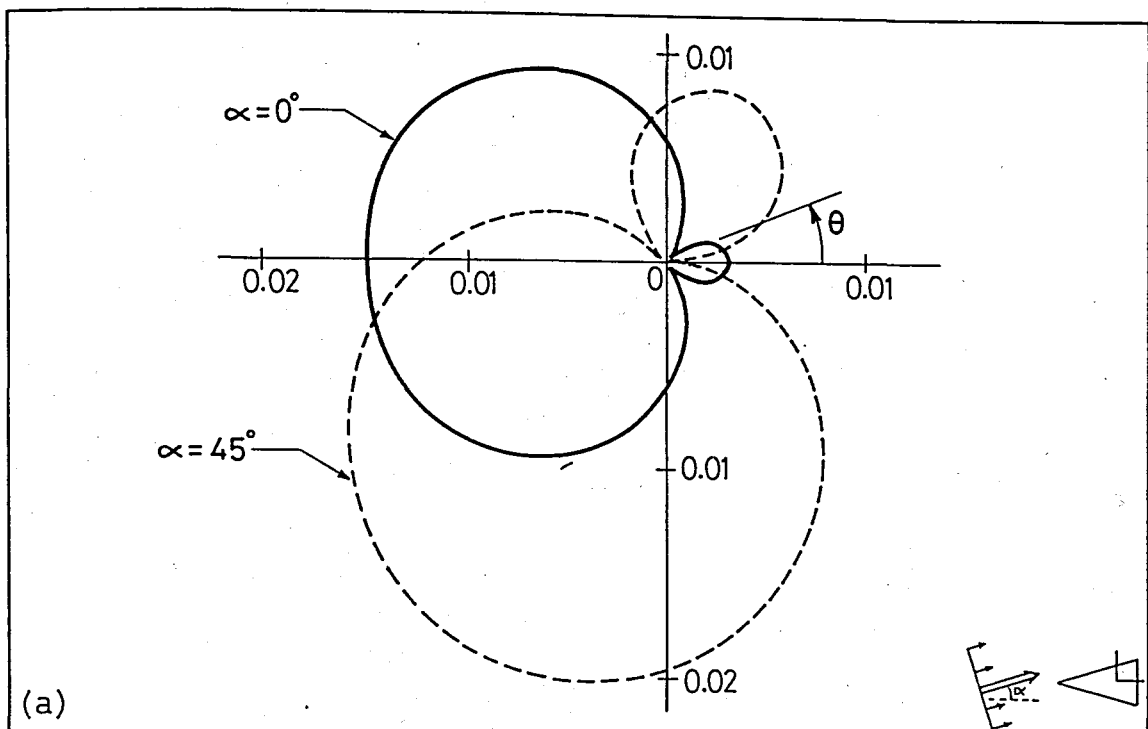


Figure 4.37 - Far field amplitude,  $|f/A|$ , due to the scattered wave field from a rigid triangular inclusion for  $\beta = 30^\circ$ ;  
 (a)  $kh = 0.3$ , (b)  $kh = 3.0$ , (c)  $kh = 9.0$ .

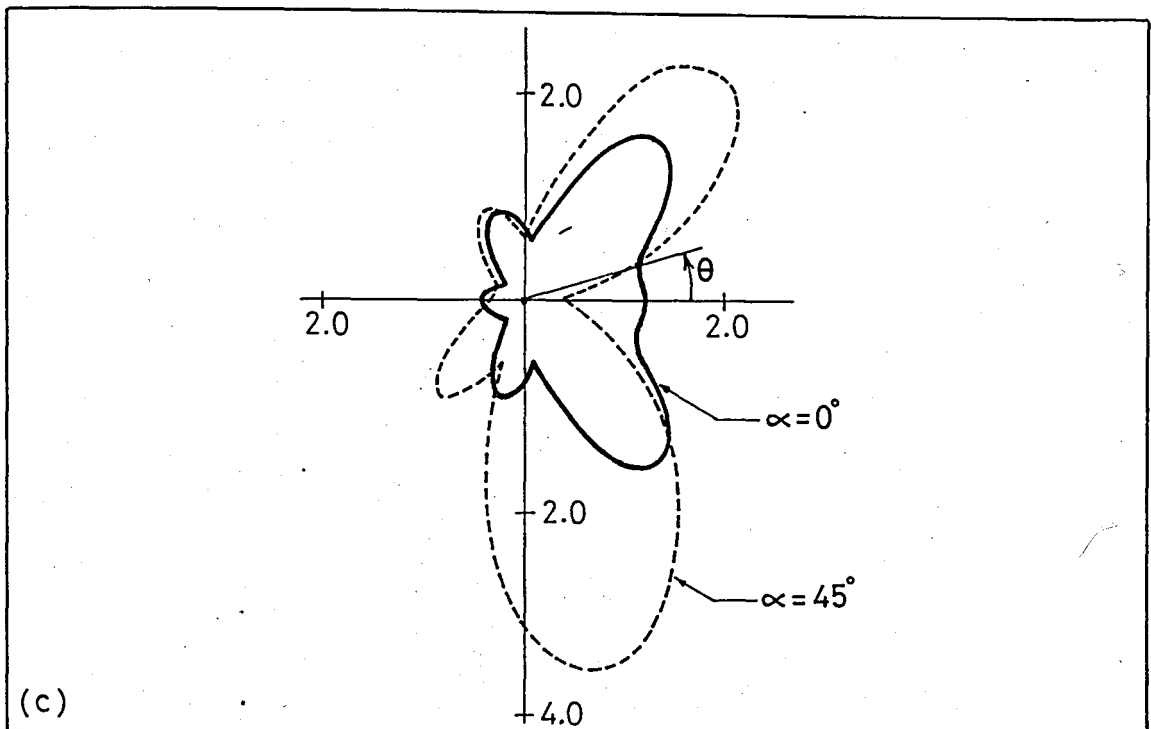


Figure 4.37 (continued).

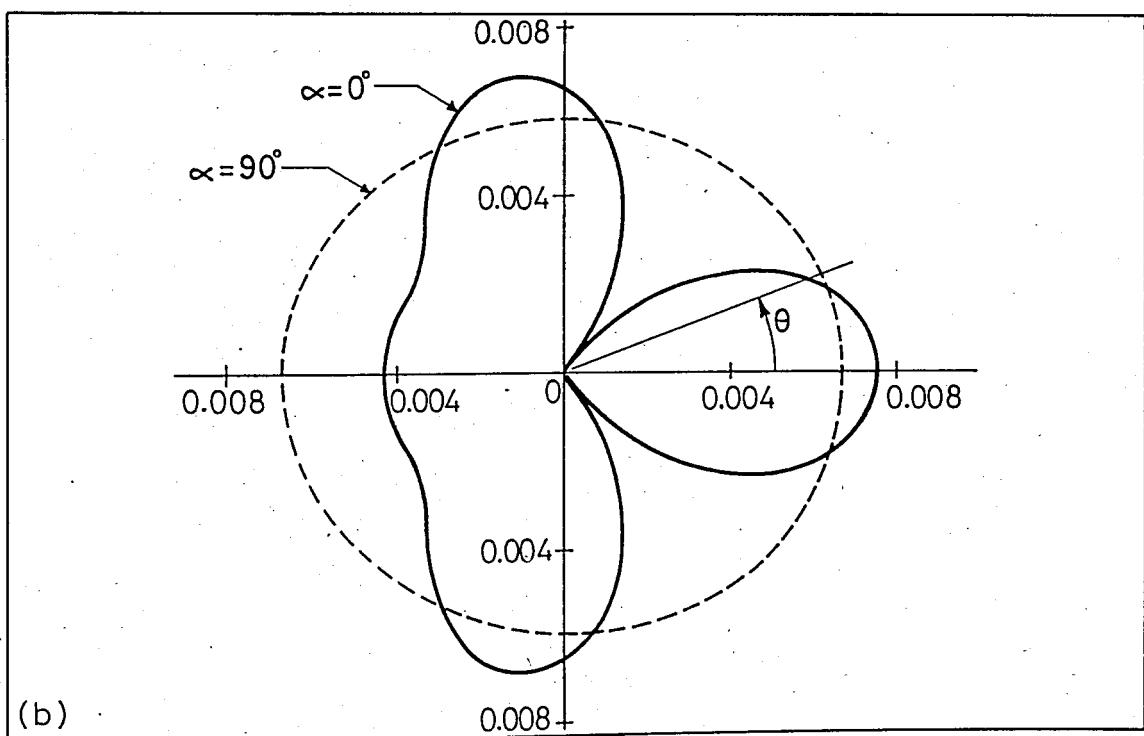
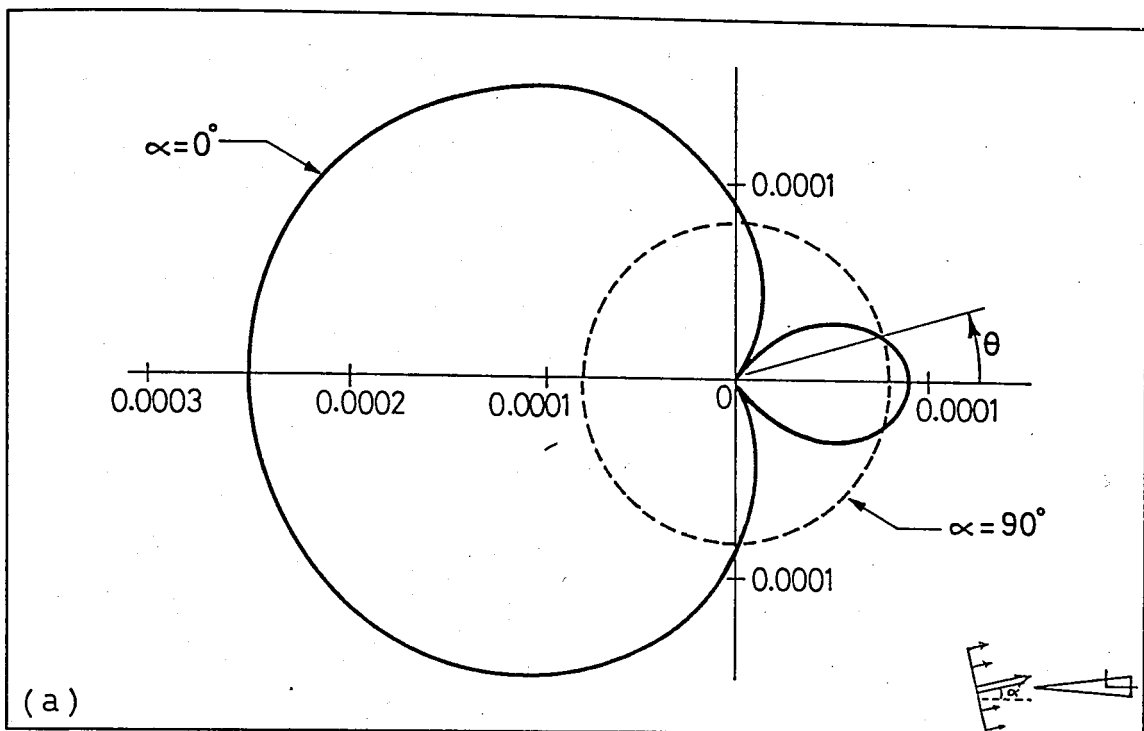


Figure 4.38 - Far field amplitude,  $|f/A|$ , due to the scattered wave field from a rigid triangular inclusion for  $\beta = 0.001^0$ ;  
 (a)  $kh = 0.3$ , (b)  $kh = 3.0$ , (c)  $kh = 9.0$ .

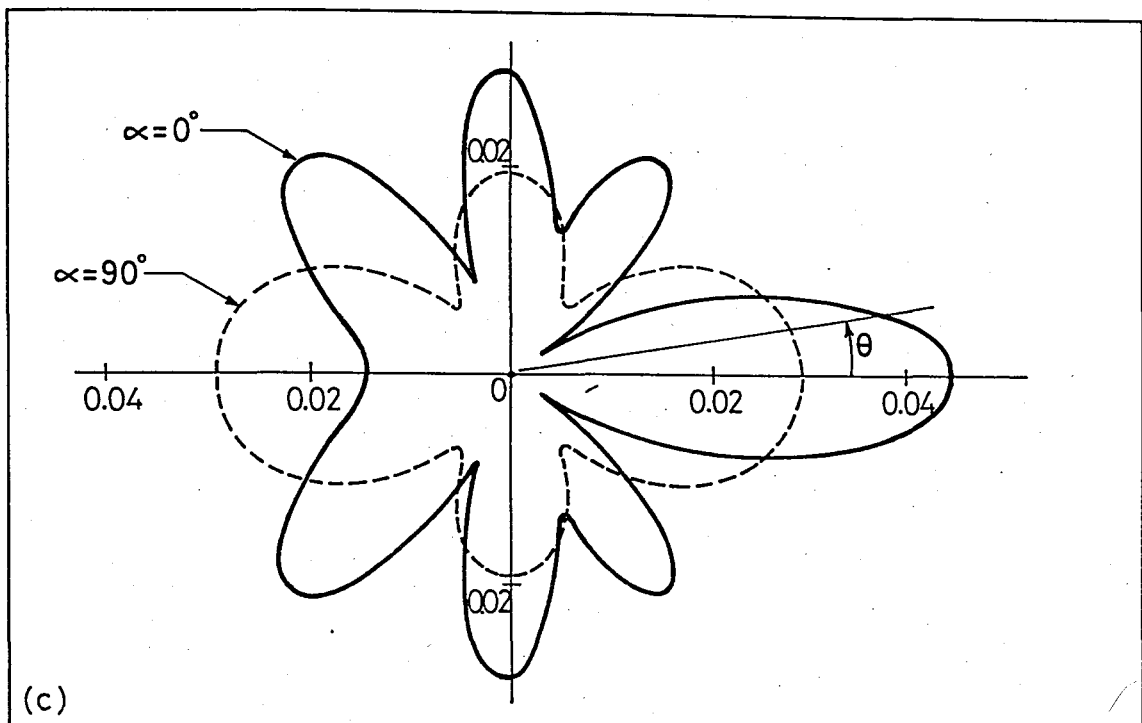


Figure 4.38 (continued).

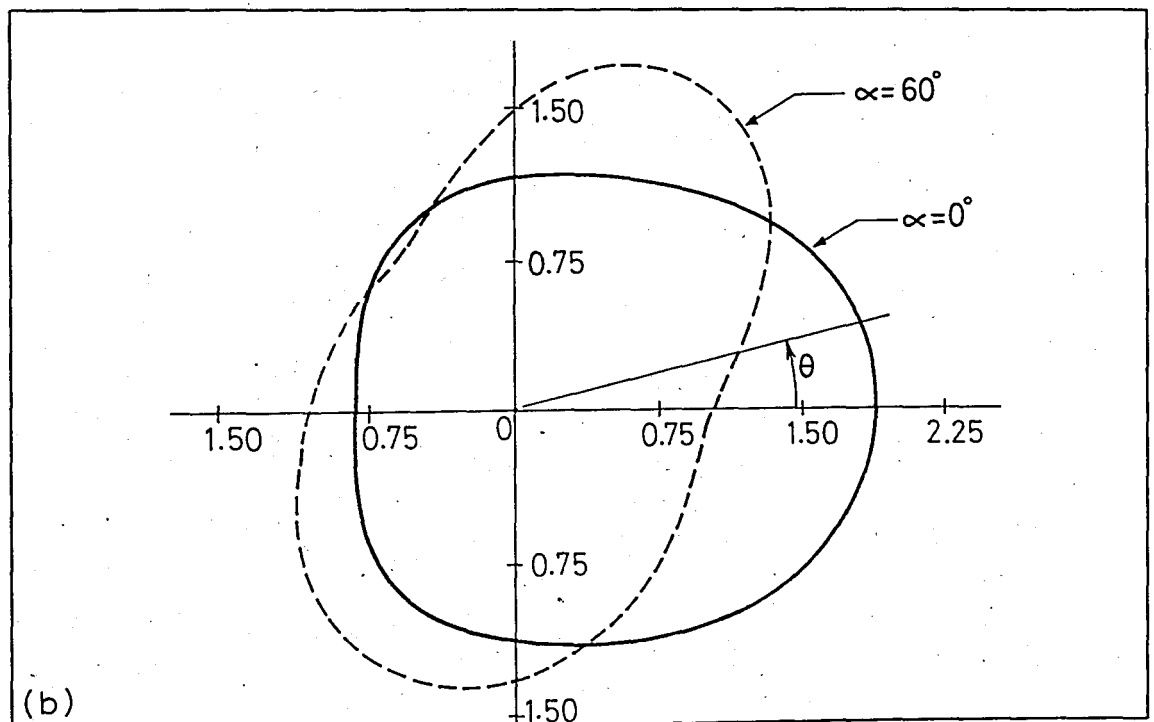
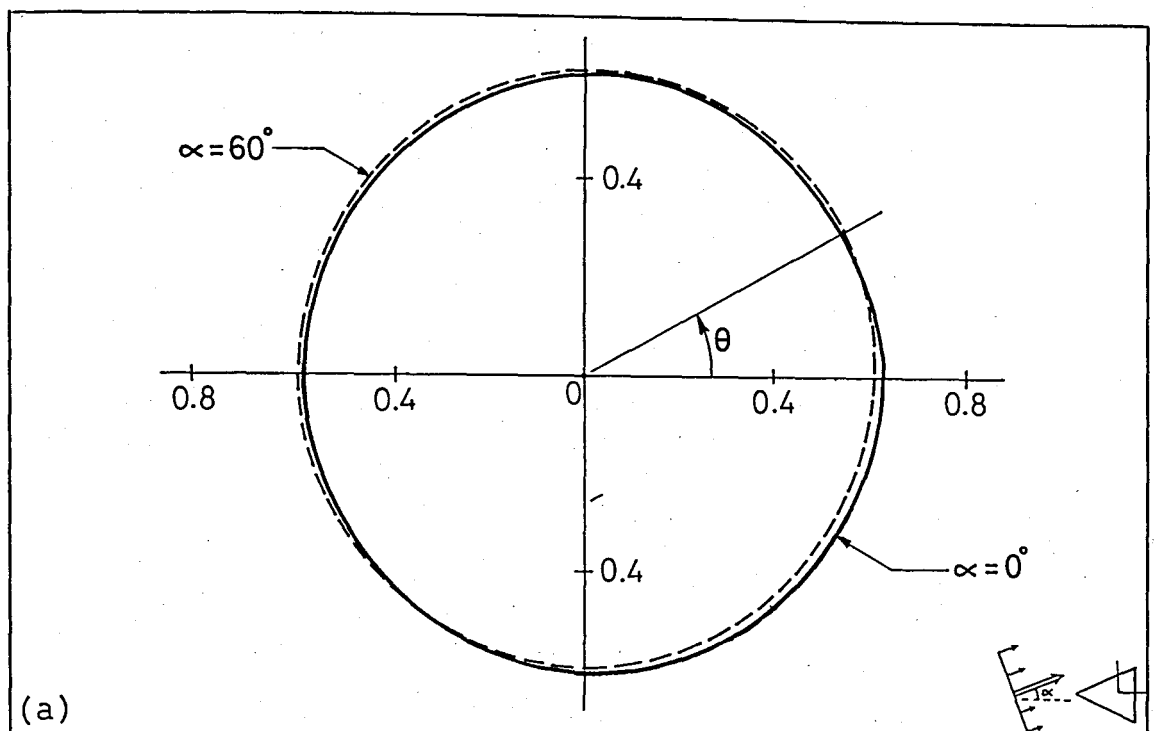


Figure 4.39 - Far field amplitude,  $|f/A|$ , due to the scattered wave field from a triangular cavity for  $\beta = 60^\circ$ ;  
 (a)  $kh = 0.3$ , (b)  $kh = 30$ , (c)  $kh = 9.0$ .

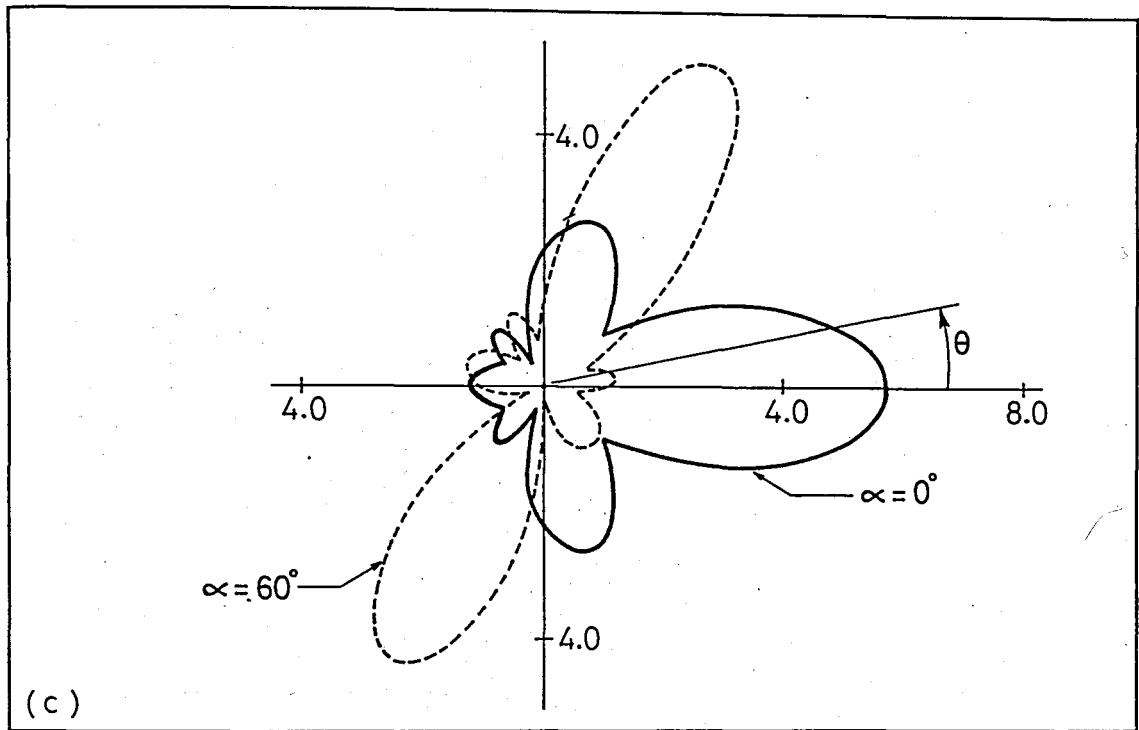


Figure 4.39 (continued).

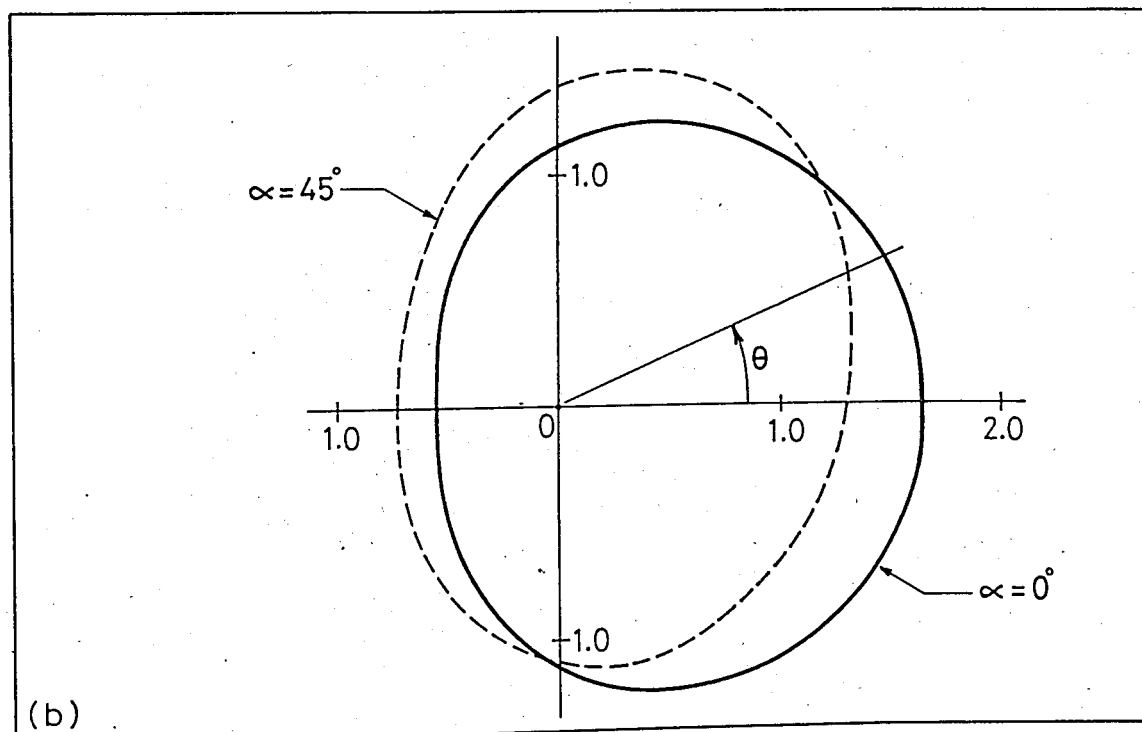
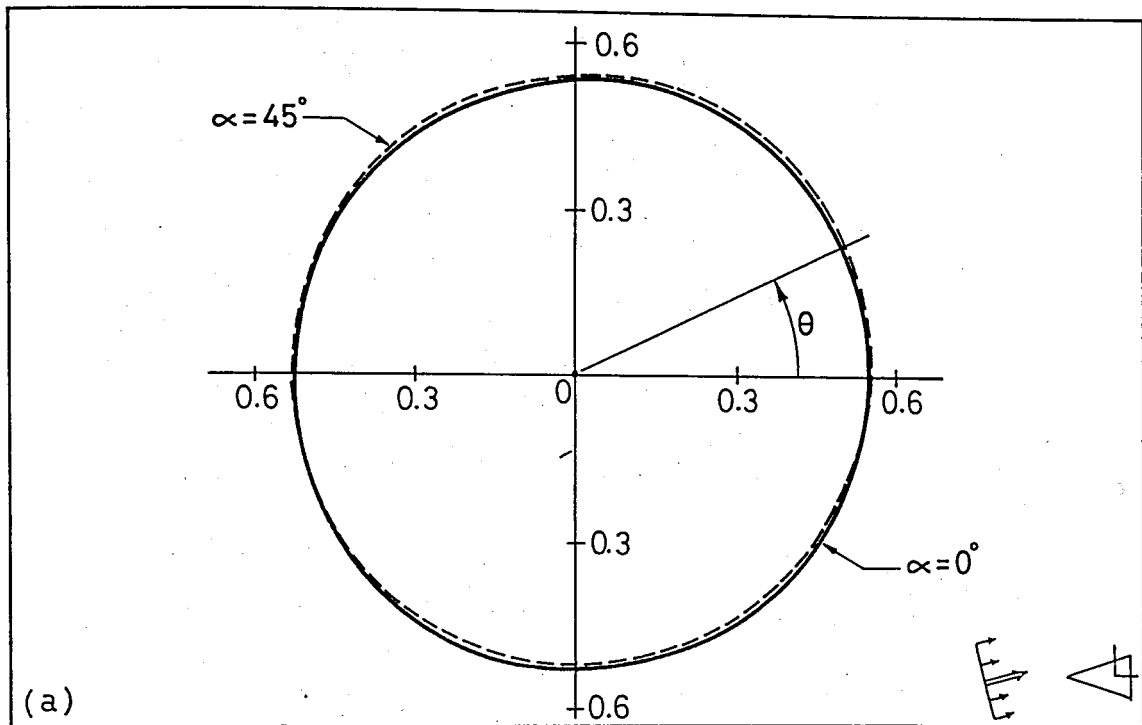
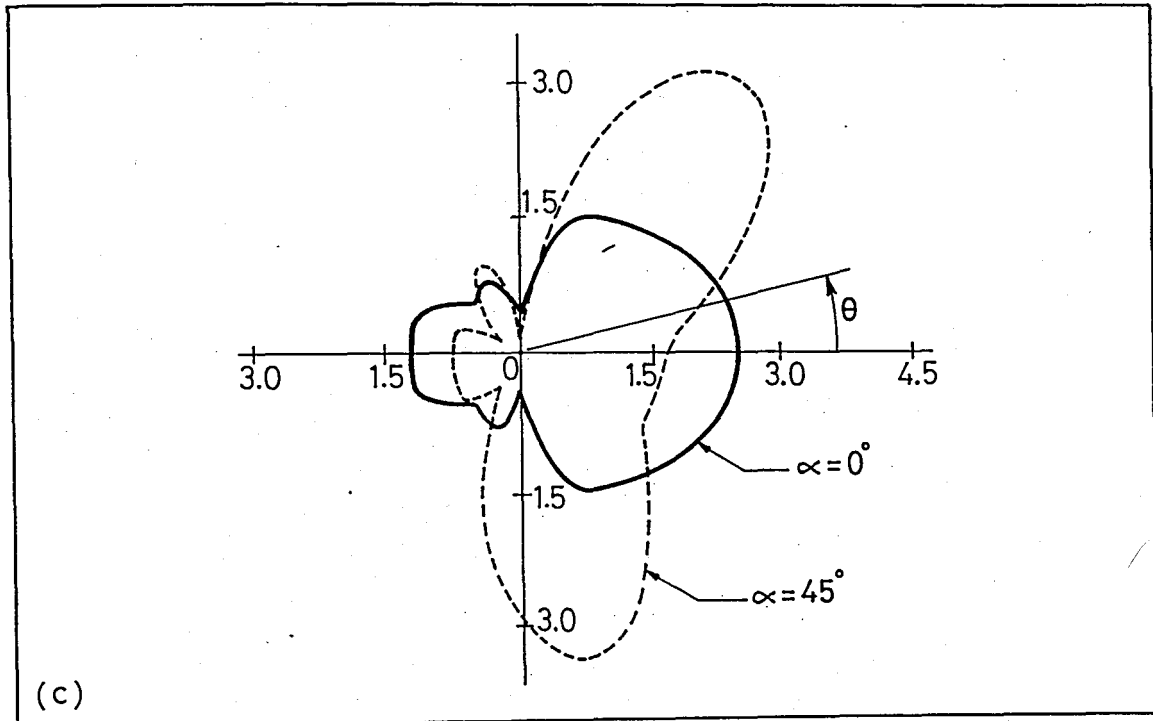


Figure 4.40 - Far field amplitude,  $|f/A|$ , due to the scattered wave field from a triangular cavity for  $\beta = 30^\circ$ ;  
 (a)  $kh = 0.3$ , (b)  $kh = 3.0$ , (c)  $kh = 9.0$ .



(c)

Figure 4.40 (continued).

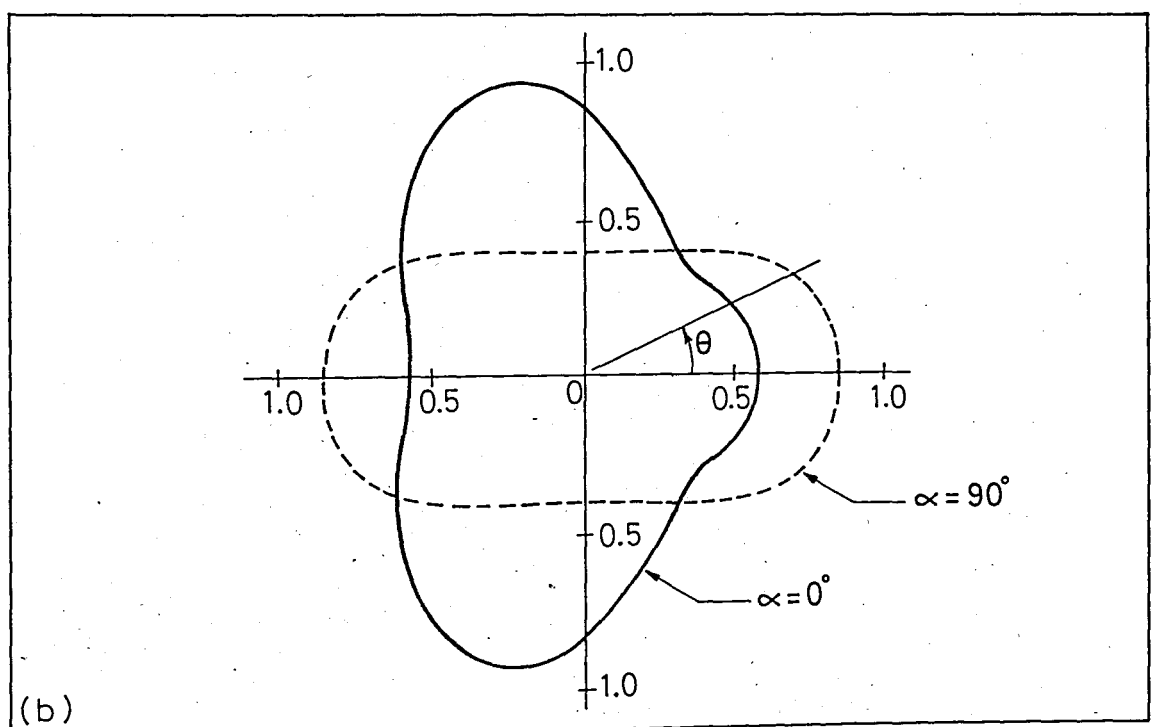
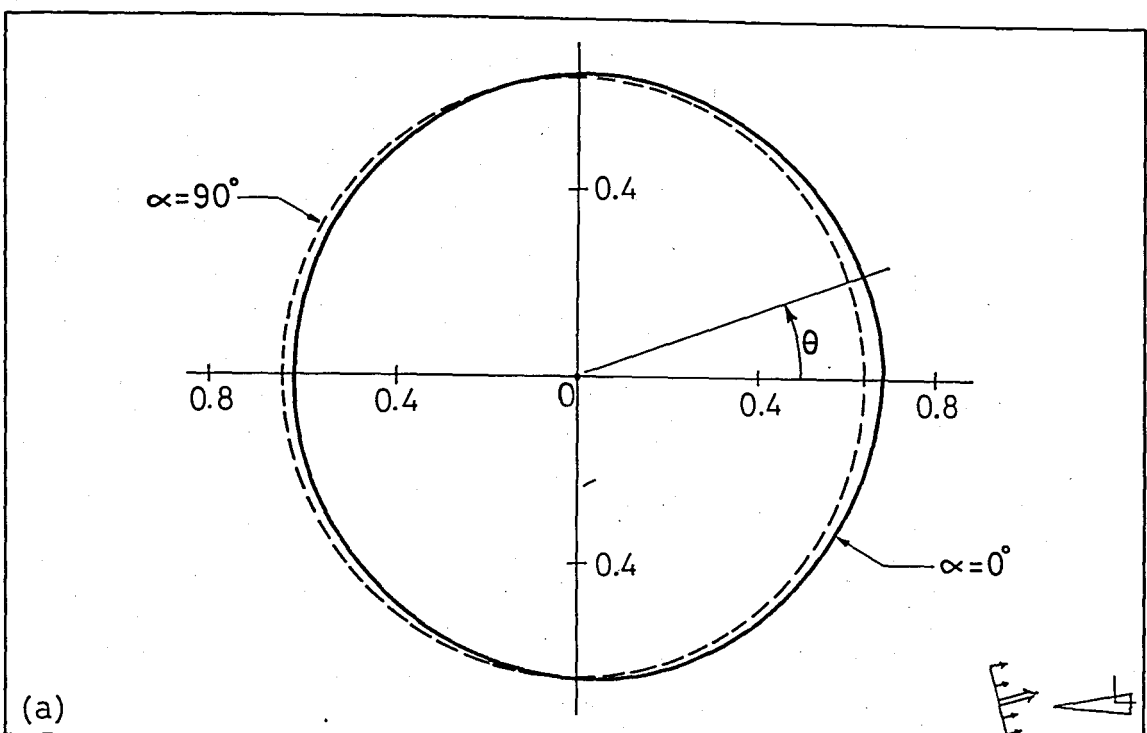


Figure 4.41 - Far field amplitude,  $|f/A|$ , due to the scattered wave field a triangular cavity for  $\beta = 0.001^0$ ;  
 (a)  $kh = 0.3$ , (b)  $kh = 3.0$ , (c)  $kh = 9.0$ .

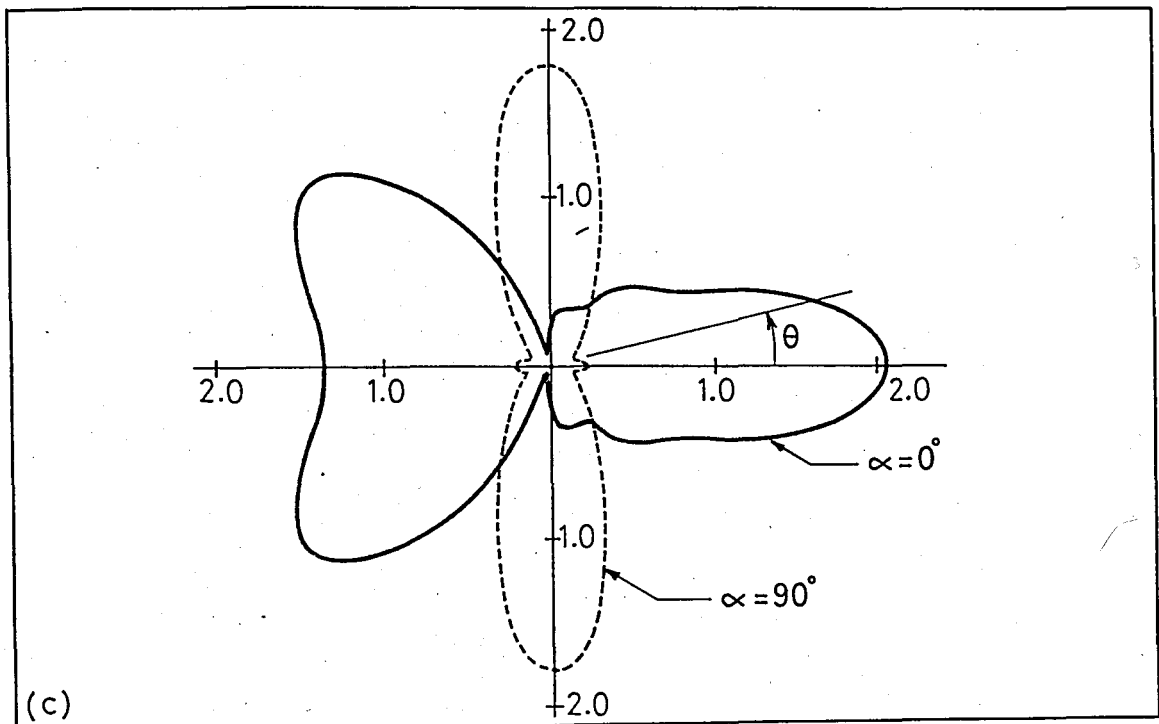


Figure 4.41 (continued).

## APPENDICES

## APPENDIX A

### SIMPSON'S APPROXIMATE INTEGRATION FORMULA

Consider an integral in the form

$$I = \int_a^b f(x)dx \quad (A.1)$$

The above integral can be evaluated approximately by using Simpson's rule which can be written as

$$\int_a^b f(x)dx \approx C_s h [w_0 f(a) + w_1 f(a+h) + w_2 f(a+2h) + \dots + w_p f(b)] , \quad (A.2)$$

where  $C_s$  is a constant factor,  $w_i$ 's are the weight factors,  $P$  is the order of the Simpson's rule used for the approximation and  $h$  is given by

$$h = (b - a)/P \quad (A.3)$$

The expression given by Eq. (A.2) may also be written in a compact form as

$$\int_a^b f(x)dx \approx C_s h \sum_{i=0}^P w_i f(a + i x h) . \quad (A.4)$$

As an example, for a fourth order Simpson's rule (Bode's formula) [19], the values of  $C_s$  and  $w_i$  are

$$C_s = 2/45, \quad w_0 = w_4 = 7, \quad w_1 = w_3 = 32, \quad w_2 = 12. \quad (A.5)$$

Thus Eq. (A.2) takes the form

$$\int_a^b f(x)dx \approx (2/45)h[7f(a) + 32f(a+h) + 12f(a+2h) \\ + 32f(a+3h) + 7f(b)], \quad (A.6)$$

where

$$h = (b - a)/4 \quad (A.7)$$

APPENDIX B  
ANALYTICAL EXPRESSIONS FOR THE  
ELEMENTS OF THE Q-MATRIX

a. Rigid Inclusion:

$$Q_{jm}^{12} = \frac{(\epsilon_j \epsilon_m)^{\frac{1}{2}}}{4} \int_0^{2\pi} d\theta \{ J_j(kr) \cos(j\theta) \} \{ [mH_m(kr) - krH_{m+1}(kr)] \sin(m\theta) \\ - \frac{m}{kr} H_m(kr) \cos(m\theta) \frac{d}{d\theta}(kr) \}. \quad (B.1)$$

$$Q_{jm}^{21} = \frac{(\epsilon_j \epsilon_m)^{\frac{1}{2}}}{4} \int_0^{2\pi} d\theta \{ J_j(kr) \sin(j\theta) \} \{ [mH_m(kr) - krH_{m+1}(kr)] \cos(m\theta) \\ + \frac{m}{kr} H_m(kr) \sin(m\theta) \frac{d}{d\theta}(kr) \}. \quad (B.2)$$

$$Q_{jm}^{22} = \frac{(\epsilon_j \epsilon_m)^{\frac{1}{2}}}{4} \int_0^{2\pi} d\theta \{ J_j(kr) \sin(j\theta) \} \{ [mH_m(kr) - krH_{m+1}(kr)] \sin(m\theta) \\ - \frac{m}{kr} H_m(kr) \cos(m\theta) \frac{d}{d\theta}(kr) \}. \quad (B.3)$$

b. Cavity:

$$Q_{jm}^{11} = - \frac{(\epsilon_j \epsilon_m)^{\frac{1}{2}}}{4} \int_0^{2\pi} d\theta \{ H_m(kr) \cos(m\theta) \} \{ [jJ_j(kr) - krJ_{j+1}(kr)] \cos(j\theta) \\ + \frac{j}{kr} J_j(kr) \sin(j\theta) \frac{d}{d\theta}(kr) \}. \quad (B.4)$$

$$Q_{jm}^{12} = - \frac{(\epsilon_j \epsilon_m)^{\frac{1}{2}}}{4} \int_0^{2\pi} d\theta \{ H_m(kr) \sin(m\theta) \} \{ [jJ_j(kr) - krJ_{j+1}(kr)] \cos(j\theta) \\ + \frac{j}{kr} J_j(kr) \sin(j\theta) \frac{d}{d\theta}(kr) \}. \quad (B.5)$$

$$Q_{jm}^{21} = - \frac{(\epsilon_j \epsilon_m)^{\frac{1}{2}}}{4} \int_0^{2\pi} d\theta \{ H_m(kr) \cos(m\theta) \} \{ [jJ_j(kr) - krJ_{j+1}(kr)] \sin(j\theta) \\ - \frac{j}{kr} J_j(kr) \cos(j\theta) \frac{d}{d\theta}(kr) \}. \quad (B.6)$$

$$Q_{jm}^{22} = - \frac{(\epsilon_j \epsilon_m)^{\frac{1}{2}}}{4} \int_0^{2\pi} d\theta \{ H_m(kr) \sin(m\theta) \} \{ [jJ_j(kr) - krJ_{j+1}(kr)] \sin(j\theta) \\ - \frac{j}{kr} J_j(kr) \cos(j\theta) \frac{d}{d\theta}(kr) \}. \quad (B.7)$$

APPENDIX C  
NUMERICAL EXPRESSIONS FOR THE  
ELEMENTS OF THE Q-MATRIX

a. Rigid Inclusion:

$$Q_{jm}^{12} \approx \frac{(\epsilon_j \epsilon_m)^{\frac{1}{2}}}{4} \cdot \frac{c_s}{P} \sum_{i=1}^N \sum_{q=0}^P (\Delta \theta_i) w_q \{ J_j(kr_{iq}) \cos(j\theta_{iq}) \}$$

$$\times \{ [mH_m(kr_{iq}) - kr_{iq}H_{m+1}(kr_{iq})] \sin(m\theta_{iq})$$

$$- \frac{m}{kr_{iq}} H_m(kr_{iq}) \cos(m\theta_{iq}) \left[ \frac{d(kr)}{d\theta} \right]_{\theta_{iq}} \} . \quad (C.1)$$

$$Q_{jm}^{21} \approx \frac{(\epsilon_j \epsilon_m)^{\frac{1}{2}}}{4} \cdot \frac{c_s}{P} \sum_{i=1}^N \sum_{q=0}^P (\Delta \theta_i) w_q \{ J_j(kr_{iq}) \sin(j\theta_{iq}) \}$$

$$\times \{ [mH_m(kr_{iq}) - kr_{iq}H_{m+1}(kr_{iq})] \cos(m\theta_{iq})$$

$$+ \frac{m}{kr_{iq}} H_m(kr_{iq}) \sin(m\theta_{iq}) \left[ \frac{d(kr)}{d\theta} \right]_{\theta_{iq}} \} . \quad (C.2)$$

$$\begin{aligned}
 Q_{jm}^{22} \simeq & \frac{(\epsilon_j \epsilon_m)^{\frac{1}{2}}}{4} \frac{c_s}{P} \sum_{i=1}^N \sum_{q=0}^P (\Delta\theta_i) w_q \{ J_j(kr_{iq}) \sin(j\theta_{iq}) \} \\
 & \times \{ [mH_m(kr_{iq}) - kr_{iq} H_{m+1}(kr_{iq})] \sin(m\theta_{iq}) \\
 & - \frac{m}{kr_{iq}} H_m(kr_{iq}) \cos(m\theta_{iq}) \left[ \frac{d(kr)}{d\theta} \right]_{\theta_{iq}} \}. \quad (C.3)
 \end{aligned}$$

b. Cavity:

$$\begin{aligned}
 Q_{jm}^{11} \simeq & - \frac{(\epsilon_j \epsilon_m)^{\frac{1}{2}}}{4} \frac{c_s}{P} \sum_{i=1}^N \sum_{q=0}^P (\Delta\theta_i) w_q \{ H_m(kr_{iq}) \cos(m\theta_{iq}) \} \\
 & \times \{ [jJ_j(kr_{iq}) - kr_{iq} J_{j+1}(kr_{iq})] \cos(j\theta_{iq}) \\
 & + \frac{j}{kr_{iq}} J_j(kr_{iq}) \sin(j\theta_{iq}) \left[ \frac{d(kr)}{d\theta} \right]_{\theta_{iq}} \}. \quad (C.4)
 \end{aligned}$$

$$\begin{aligned}
 Q_{jm}^{12} \simeq & - \frac{(\epsilon_j \epsilon_m)^{\frac{1}{2}}}{4} \frac{c_s}{P} \sum_{i=1}^N \sum_{q=0}^P (\Delta\theta_i) w_q \{ H_m(kr_{iq}) \sin(m\theta_{iq}) \} \\
 & \times \{ [jJ_j(kr_{iq}) - kr_{iq} J_{j+1}(kr_{iq})] \cos(j\theta_{iq}) \\
 & + \frac{j}{kr_{iq}} J_j(kr_{iq}) \sin(j\theta_{iq}) \left[ \frac{d(kr)}{d\theta} \right]_{\theta_{iq}} \}. \quad (C.5)
 \end{aligned}$$

$$Q_{jm}^{21} \approx -\frac{(\epsilon_j \epsilon_m)^{\frac{1}{2}}}{4} \frac{c_s}{P} \sum_{i=1}^N \sum_{q=0}^P (\Delta \theta_i) w_q \{ H_m(kr_{iq}) \cos(m \theta_{iq}) \} \\ \times \{ [j J_j(kr_{iq}) - kr_{iq} J_{j+1}(kr_{iq})] \sin(j \theta_{iq}) \\ - \frac{j}{kr_{iq}} J_j(kr_{iq}) \cos(j \theta_{iq}) [\frac{d(kr)}{d\theta}]_{\theta_{iq}} \}. \quad (C.6)$$

$$Q_{jm}^{22} \approx -\frac{(\epsilon_j \epsilon_m)^{\frac{1}{2}}}{4} \frac{c_s}{P} \sum_{i=1}^N \sum_{q=0}^P (\Delta \theta_i) w_q \{ H_m(kr_{iq}) \sin(m \theta_{iq}) \} \\ \times \{ [j J_j(kr_{iq}) - kr_{iq} J_{j+1}(kr_{iq})] \sin(j \theta_{iq}) \\ - \frac{j}{kr_{iq}} J_j(kr_{iq}) \cos(j \theta_{iq}) [\frac{d(kr)}{d\theta}]_{\theta_{iq}} \}. \quad (C.7)$$

**APPENDIX D**  
**COMPUTER PROGRAM LISTING**

```

1 C ****
2 C * SCATTERING OF ACOUSTIC WAVES *
3 C * BY THE CYLINDERS OF ARBITRARY CROSS-SECTION *
4 C * (( T-MATRIX FORMULATION )) *
5 C *
6 C ****
7 C *
8 C ****
9 C *
10 C ****
11 C
12 C *** PROGRAM-(A) ***
13 C ****
14 C THIS PROGRAM CREATES THE T-MATRIX FOR A GIVEN BOUNDARY
15 C GEOMETRY AND WAVE NUMBER, THEN, STORES THE ELEMENTS OF
16 C THE T-MATRIX INTO A DATA FILE(10) TO BE USED BY THE
17 C PROGRAM-(B) FOR EVALUATION OF THE SCATTERED FIELD.
18 C
19 C
20 C --FOLLOWING CROSS-SECTIONS FOR THE INFINITE CYLINDERS
21 C CAN BE HANDLED:
22 C     1-) CIRCULAR
23 C     2-) ELLIPTICAL
24 C     3-) RECTANGULAR (ROUND CORNERED)
25 C     4-) TRIANGULAR (ISOSCELES)
26 C
27 C
28 C
29 C
30 C ** THE PROCEDURES AND GENERAL STEPS FOLLOWED BY THE **
31 C ** PROGRAM ARE AS FOLLOWS : **
32 C
33 C
34 C --ELEMENTS OF THE Q11,Q12,Q21,Q22-MATRICES(SUBMATRICES
35 C OF THE Q-MATRIX) ARE EVALUATED BY PERFORMING THE
36 C ANGULAR INTEGRATIONS ALONG THE BOUNDARY OF THE SCATTERER.
37 C
38 C --ANGULAR INTEGRATIONS ARE EVALUATED NUMERICALLY BY THE
39 C SIMPSON'S RULE OF VARIOUS ORDER.(RECOMMENDED ORDER IS 4)
40 C
41 C
42 C --THEN, THE Q-MATRIX IS INVERTED AND THE T-MATRIX WHICH
43 C IS GIVEN BY:
44 C
45 C      -1
46 C      T=O * RE(Q)
47 C
48 C IS CONSTRUCTED, BY THE GAUSS-SCHMIDT ORTHOGONALIZATION
49 C TECHNIQUE.
50 C
51 C --FINALLY, THE T-MATRIX AND SOME PARAMETERS DESCRIBING
52 C THE BOUNDARY ARE STORED INTO A FILE(REFERRED AS UNIT. 10).
53 C
54 C
55 C * NOTE: *
56 C ****
57 C Q , ORTHOGONALIZED Q AND T-MATRICES ARE STORED
58 C ALSO INTO TWO DATA FILES(REFERRED AS UNIT 11 & 22)
59 C TO BE USED BY TWO ADDITIONAL PROGRAMS TO MAKE THE
60 C FOLLOWING CHECKS :
61 C
62 C      1-) Q * Q = I
63 C
64 C      T
65 C      2-) T * CONJ(T) = -RE(T)
66 C
67 C
68 C ****
69 C INPUT DATA
70 C ****
71 C CARD 1 :
72 C ****
73 C COLUMN 1-2: NI (READING UNIT OR FILE NO.)
74 C COLUMN 3-4: NO (WRITING UNIT OR FILE NO.)
75 C
76 C CARD 2 :
77 C ****
78 C COLUMN 1-2: NO (HALF SIZE OF THE T-MATRIX.MAX(NO)=20)
79 C COLUMN 3-4: NOSF (ORDER OF THE SIMPSON'S FORMULA.)
80 C

```

```

81 C
82 C CARD 3 :
83 C ======
84 C COLUMN 1-2: BF1 & BF2 ARE THE TWO MULTIPLICATION
85 C COLUMN 3-8: BF2 FACTORS INVOLVED IN THE SIMPSON'S
86 C FORMULA. EX: 4'TH ORDER S.F. IS GIVEN BY:
87 C INT(A TO B)F(X)*DX=2./45.*H*(7*F0+32*F1+12*F2+32*F3+7*F4)
88 C WHERE: F0=F(A) , F1=F(A+H) , F2=F(A+2H) ,..., F4=F(B)
89 C THEN, BF1=2. & BF2=45. )
90 C (*SEE CARD SET(12) FOR THE REMAINING COEFFICIENTS)
91 C
92 C CARD 4 :
93 C ======
94 C COLUMN 1-4: BCON (BOUNDARY CONDITION. ENTER:
95 C 1-) 'NEUM' FOR NEUMANN TYPE B.C.
96 C 2-) 'DRIC' FOR DIRICHLET TYPE B.C. )
97 C
98 C CARD 5 :
99 C ======
100 C COLUMN 1-4: AND (WAVE NUMBER)
101 C
102 C CARD 6 :
103 C ======
104 C COLUMN 1-6: SHAPE (CROSS-SECTONAL GEOMETRY OF THE
105 C SCATTERER. ENTER:
106 C 1-) 'CIRCLE' FOR CIRCULAR BOUNDARY
107 C 2-) 'ELLIPS' FOR ELLIPTICAL BOUNDARY
108 C 3-) 'RECTAN' FOR RECTANGULAR BOUNDARY
109 C 4-) 'TRIANG' FOR TRIANGULAR BOUNDARY
110 C
111 C CARD 7 :
112 C ======
113 C COLUMN 1-4 , 5-8 , 9-19 :
114 C FOR CIRCLE: RAD (RADIUS)
115 C FOR ELLIPSE: AA,BB (HALF MAJOR & MINOR AXES)
116 C FOR RECTANGLE: A,B (HALF MAJOR & MINOR AXES),
117 C CORRAD (CORNER RADIUS)
118 C FOR TRIANGLE: H (HEIGHT IN X-DIRECTION), BET (ANGLE
119 C BETWEEN TWO EQUAL SIDES.(IN DEGREES))
120 C
121 C CARD 8 :
122 C ======
123 C COLUMN 1-4: BGEN (TYPE OF THE ANGULAR DIVISION TO BE USED
124 C IN THE NUMERICAL EVALUATION OF THE
125 C BOUNDARY INTEGRALS. ENTER:
126 C 1-) 'AUTO' FOR EQUAL ANGULAR INTERVALS
127 C (DIVISIONS ARE MADE AUTOMATICALLY)
128 C 2-) 'MAN' FOR NON-EQUAL ANGULAR INTERVALS
129 C (DIVISIONS MUST BE GIVEN IN CARD SET(11))
130 C COLUMN 5-6: NSYM (NSYM=2 FOR THE BOUNDARIES HAVING MIRROR
131 C SYMMETRY W.R.T. X-AXIS ,THEN INTEGRATIONS
132 C ARE PERFORMED ONLY FOR HALF OF THE
133 C BOUNDARY (BETWEEN 0-180 DEGREES)
134 C NSYM=1 FOR NON-SYMMETRIC ONES)
135 C (*NOTE:# 1-) FOR THIS PROGRAM TAKE NSYM=2
136 C 2-) FOR NSYM=2, Q12(I,J) & Q21(I,J)=0.
137 C T12(I,J) & T21(I,J)=0.
138 C AND NOT TO BE PRINTED)
139 C
140 C CARD 9 :
141 C ======
142 C COLUMN 1-6: ERR (ERROR FACTOR FOR THE BESSEL FUNCTIONS.
143 C TAKE ERR=1.0-10 - 1.0-15)
144 C COLUMN 7-12: TRUNC (TRUNCATION FACTOR FOR THE O-MATRIX
145 C ELEMENTS. TAKE TRUNC=1.0-20 - 1.0-25)
146 C
147 C CARD 10 : (IF BGEN='MAN' , OMIT THIS CARD)
148 C ======
149 C COLUMN 1-3: NINTV (NUMBER OF ANGULAR INTERVALS.FOR A
150 C GOOD CONVERGENCE IN THE NUMERICAL INTEG-
151 C RATION, TAKE NINTV=72-90)
152 C (*NOTE:# NINTV SHOULD BE AN EVEN NUMBER)
153 C
154 C CARD SET 11 : (IF BGEN='AUTO', OMIT THIS CARD SET)
155 C ======
156 C # EACH CARD CONTAINS:#  

157 C COLUMN 1-3: NCIN (NO OF EQUAL SUCCESSIVE INTERVALS REPEATED)
158 C COLUMN 4-7: CIN (CORRESPONDING ANGLE FOR THE
159 C INTERVALS (IN DEGREES))
160 C (*NOTE.* CARDS MUST CONTINUE UP TO WHEN :
```

```

161 C      SUM( NCIN * CIN )=360 DEG, FOR NSYM=1
162 C      SUM( NCIN * CIN )=180 DEG, FOR NSYM=2
163 C
164 C  CARD SET 12 :
165 C  =====
166 C  #EACH CARD CONTAINS:
167 C  COLUMN 1-6: W(I) (WEIGHING COEFFICIENTS IN SIMPSON'S FORMULA.
168 C  EXAMPLE: W(1)=7. (CARD 12-1)
169 C          W(2)=32. (CARD 12-2)
170 C          W(3)=12. (CARD 12-3)
171 C          W(4)=32. (CARD 12-4)
172 C          W(5)=7. (CARD 12-5)
173 C
174 C
175 C  ***** SAMPLE DATA *****
176 C  ***** ***** ***** *****
177 C
178 C  A-) EQUAL ANGULAR INTERVALS   B-) NON-EQUAL ANG. INTERVALS
179 C
180 C  COLUMN           COLUMN
181 C  =====
182 C  CARD I123456789012   CARD I123456789012
183 C  =====
184 C  1  I 5 8           1  I 5 8
185 C  2  I 5 4           2  I10 4
186 C  3  I2. 45.         3  I2. 45.
187 C  4  INEUM          4  INEUM
188 C  5  I0.5            5  I1.0
189 C  6  ICIRCLE         6  IELLIPS
190 C  7  I1.0            7  I1.0 2.0
191 C  8  IAUTO 2         8  IMAN 2
192 C  9  I1.D-121.D-25   9  I1.D-151.D-24
193 C  10 I 72            10 I 20 4.
194 C  11 I 7.             11 I 10 6.
195 C  12 I 32.           12 I 10 4.
196 C  13 I 12.           13 I 7.
197 C  14 I 32.           14 I 32.
198 C  15 I 7.             15 I 12.
199 C
200 C
201 C
202 C
203 C***** *****
204 C
205 C
206 C  IMPLICIT REAL*8(A-H,O-Z)
207 C
208 C  REAL#8 RQ(40,40),W(10),R(10),DTDR(10),TETL(10),XI(10),CINTV(145),
209 C  & DREAL,DIMAG,DABS,CDABS,DFLOAT,DSORT,DCOS,DSIN,DATAN
210 C
211 C  COMPLEX*16 Q11(20,20),Q12(20,20),Q21(20,20),Q22(20,20),
212 C  & TM(40,40),Q(40,40),BES1(22),BES2(22),HANK(22),
213 C  & DUM1,DUM2,X1,X2,P,RR,C,D,DZ,DN,D1,D2,DCMPLX
214 C
215 C  CHARACTER*4 BCON,BGEN,WRIT(8)
216 C  CHARACTER*6 SHAPE
217 C  CHARACTER*1 LINE(132)
218 C  CHARACTER H1#12,H2#25,H3#18,H4#33,H5#8,H6#10,H7#29,H8#37,
219 C  & H9#9,H10#13,H11#28,H12#23,H13#27,MATR#8,H14#10
220 C
221 C  COMMON/INVO/Q
222 C  COMMON/REQ/RQ
223 C  COMMON/TMAT/TM
224 C  COMMON/GRAD/RAD
225 C  COMMON/GAX/AA,BB
226 C  COMMON/REC/A,B,CURRAD,TT1,TT2,TT3,TT4,ALPH,DIS
227 C  COMMON/TRIAN/H,BETA,TETA1
228 C
229 C  EQUIVALENCE (RQ(1),W(1)),(RQ(11),R(1)),(RQ(21),DTDR(1)),
230 C  & (RQ(31),TETL(1)),(RQ(41),XI(1)),(RQ(51),CINTV(1))
231 C
232 C  G(V)=V#360./(2.*PI)
233 C
234 C  DATA Q11,Q12,Q21,Q22/1600#(0.0D,0.0D)/
235 C  DATA LINE/132#='/'
236 C  DATA WRIT/'0-11','0-12','0-21','0-22','T-11','T-12','T-21','T-22'/
237 C  DATA H1,H2,H3/'B.C. TYPE : ','NEUMANN (RIGID INCLUSION)', 'DIRICHLE
238 C  & T (CAVITY)'/
239 C  DATA H4/'CROSS-SECTION OF THE SCATTERER : '/
240 C  DATA H5,H6,H7/'CIRCULAR','ELLIPICAL','RECTANGULAR (ROUND CORNER)'

```

```

241      ED)'/ DATA H8/'SYMMETRY CONDITION (WRT. X-AXIS) : '/
242      DATA H9,H10/'SYMMETRIC','NON-SYMMETRIC'
243      DATA H11/'TYPE OF BOUNDARY DIVISION : '/
244      DATA H12,H13/'EQUAL ANGULAR INTERVALS','NON-EQUAL ANGULAR INTERVAL
245      &S'/
246      DATA MATR/' MATRIX'/
247      DATA H14/'TRIANGULAR'/
248      C
249      C
250      READ(5,777) NI,NO
251      777 FORMAT(2I2)
252      READ(NI,7) NQ,NOSF,BF1,BF2
253      7 FORMAT(2I2/F2.0,F6.0)
254      NGP=NUSF+1
255      NQ2=NQ*2
256      NOT=NQ+2
257      PI=DATAN(1.00)*4.0D0
258      WRITE(NO,613)
259      613 FORMAT(1H1)
260      WRITE(NO,100)
261      100 FORMAT(//5X,47('*')/5X,'*',45X,'*',/5X,'*',8X,'SCATTERING OF ACOUS
262      ETIC WAVES',9X,'*'//5X,'*',45X,'*'//5X,'*' BY THE CYLINDERS OF ARBITRA
263      RY CROSS-SECTION '*'//5X,'*',45X,'*'//5X,'*',8X,'(( T-MATRIX FORMULA
264      EDITION ))',9X,'*'//5X,'*',45X,'*'//5X,47('*')///5X,'** PROGRAM-(A):
265      & GENERATION OF THE T-MATRIX ELEMENTS ***/5X,54(''')//)
266      READ(NI,1) BCON,ANO,SHAPE
267      1 FORMAT(A4/F4.0/A6)
268      IF(SHAPE.EQ.'CIRCLE') READ(NI,81) RAD
269      IF(SHAPE.EQ.'ELLIPS') READ(NI,81) AA,BB
270      IF(SHAPE.EQ.'RECTAN') READ(NI,81) A,B,CORRAD
271      IF(SHAPE.EQ.'TRIANG') THEN
272          READ(NI,81) H,BET
273          BET=BET*2.*PI/360.
274          TETA1=DATAN(3.*DTAN(BETA/2.))
275      END IF
276      READ(NI,82) BGEN,NSYM,ERR,TRUNC
277      82 FORMAT(A4,I2/2D6.0)
278      81 FORMAT(2F4.0,F10.0)
279      IF(BGEN.EQ.'AUTO') THEN
280          READ(NI,30) NINTV
281          30 FORMAT(I3)
282          C**** AUTOMATIC ANGULAR INTERVAL GENERATION ****
283          DO 31 I=1,NINTV/NSYM
284              31 CINTV(I)=PI*2./DFLOAT(NINTV)
285          ELSE
286          C**** MANUAL ANGULAR INTERVAL GENERATION ****
287          NINTV=0
288          KK=0
289          TOT=0.
290          DO 32 I=1,150/NSYM
291          READ(NI,33) NCIN,CIN
292          33 FORMAT(I3,F4.0)
293          DO 34 J=1;NCIN
294              K=KK+J
295              CINTV(K)=2.*PI/360.*CIN
296              34 TOT=TOT+NCIN*CIN
297              NINTV=NINTV+NSYM*NCIN
298              IF(TOT.EQ.(360./DFLOAT(NSYM))) GO TO 35
299          32 KK=KK+NCIN
300          35 END IF
301          DO 18 I=1,NGP
302              18 READ(NI,19) W(I)
303              19 FORMAT(F6.0)
304              WRITE(NO,90)
305              90 FORMAT(63('=')/)
306              IF(BCON.EQ.'NEUM') WRITE(NO,47) H1,H2
307              47 FORMAT(1X,A12,A25/)
308              IF(BCON.EQ.'DRIC') WRITE(NO,47) H1,H3
309              WRITE(NO,42) ANO
310              42 FORMAT(1X,'WAVE NUMBER : ',F4.1)
311              IF(SHAPE.EQ.'CIRCLE') WRITE(NO,43) H4,H5,RAD
312              43 FORMAT(//1X,A33,A8//1X,'RAD : ',F6.3)
313              IF(SHAPE.EQ.'ELLIPS') WRITE(NO,44) H4,H6,AA,BB
314              44 FORMAT(//1X,A33,A10//1X,'A-AXIS : ',F6.3,4X,'B-AXIS : ',F6.3)
315              IF(SHAPE.EQ.'RECTAN') WRITE(NO,45) H4,H7,A,B,CORRAD
316              45 FORMAT(//1X,A33,A29//1X,'A-AXIS : ',F6.3,'B-AXIS : ',F6.3,4X,
317              & 'CORNER RAD.:',F13.10)
318              IF(SHAPE.EQ.'TRIANG') WRITE(NO,998) H4,H14,H,BET
319              998 FORMAT(//1X,A33,A10//1X,'H : ',F6.3,' BETA : ',F7.3)

```

```

321      IF(NSYM.EQ.1) WRITE(NO,46) H8,H10
322      46 FORMAT(1X,A37,A13)
323      IF(NSYM.EQ.2) WRITE(NO,46) H8,H9
324      WRITE(NO,48) NINTV
325      48 FORMAT(//1X,'NUMBER OF BOUNDARY SEGMENTS : ',13)
326      IF(BGEN.EQ.'AUTO') THEN
327          WRITE(NO,49) H11,H12
328      ELSE
329          WRITE(NO,49) H11,H13
330      49 FORMAT(1X,A28,A27)
331      END IF
332      WRITE(NO,50) NSOF
333      50 FORMAT(1X,'ORDER OF THE SIMPSON',IH1,'S RULE USED IN NUMERICAL IN
334      &TEGRATION : ',I2)
335      WRITE(NO,51) NO2,NO2,TRUNC,ERR
336      51 FORMAT(//1X,'TOTAL DIMENSION OF THE T-MATRIX : ',I3,' X',I3//)
337      &     1X,'TRUNCATION FACTOR FOR THE Q-MATRIX ELEMENTS : ',D9.3//)
338      &     1X,'ERROR FACTOR FOR THE BESSSEL FUNCTIONS : ',D9.3//63('=/')/1H1)
339      IF(BGEN.EQ.'AUTO') GO TO 53
340      WRITE(NO,54)
341      54 FORMAT(10X,'BOUNDARY ANGULAR'/10X,'SEGMENT INTERVAL'/13X,'NO
342      &     (DEGREE)'/10X,19('='))
343      DO 55 I=1,NINTV/NSYM
344      55 WRITE(NO,56) I,G(CINTV(I))
345      56 FURMAT(12X,13,7X,F4.1/10X,19('='))
346      WRITE(NO,57)
347      57 FORMAT(1H1)
348      53 TEB=CINTV(1)
349      TEA=0.D0
350      IF(NQ.GE.13.AND.NQ.LE.18) NQT=22
351      IF(SHAPE.EQ.'RECTAN') CALL RECT
352      **** START FOR BOUNDARY INTEGRATION AND GENERATION OF ****
353      **** THE Q-MATRIX ELEMENTS ****
354      DO 2 K=1,NINTV/NSYM
355      IF(SHAPE.EQ.'ELLIPS') CALL ELLIP(TEA,TEB,R,TETL,NGP)
356      IF(SHAPE.EQ.'CIRCLE') THEN
357          TETL(1)=TEA
358          DO 999 KKK=1,NGP
359          IF(KKK.GT.1) TETL(KKK)=TETL(KKK-1)+(TEB-TEA)/DFLOAT(NGP-1)
360          999 R(KKK)=RAD
361          END.IF
362          IF(SHAPE.EQ.'TRIANG') CALL TRIAL(TEA,TEB,R,TETL,NGP,DTDR)
363          IF(SHAPE.EQ.'RECTAN') CALL RECTA1(TEA,TEB,R,TETL,NGP,DTDR)
364          IF(SHAPE.EQ.'CIRCLE'.OR.SHAP.EQ.'ELLIPS')
365          &           CALL ANGDER(SHAPE,TETL,DTDR,NGP)
366          DO 3 II=1,NGP
367          ARG=AND*R(II)
368          DZ=DCMPLX(ARG,0.D0)
369          DN=DCMPLX(0.D0,0.D0)
370          DO 4 I=1,2
371          CALL DBESS(1,DZ,DN,DUM2,BES2(I),ERR)
372          4 DN=DN+DCMPLX(1.D0,0.D0)
373          DO 5 I=3,NQT
374          5 BES2(I)=2.*(I-2)/DZ*BES2(I-1)-BES2(I-2)
375          DN=DCMPLX(((NQT-1)*1.D0),0.D0)
376          DO 40 I=1,2
377          CALL DBESS(0,DZ,DN,BES1(NQT+1-I),DUM1,ERR)
378          40 DN=DN-DCMPLX(1.D0,0.D0)
379          DO 41 I=3,NQT
380          41 BES1(NQT+1-I)=2.*(NQT+1-I)/DZ*BES1(NQT-I+2)-BES1(NQT-I+3)
381          DO 6 I=1,NQT
382          6 HANK(I)=DCMPLX(DREAL(BES1(I)),DREAL(BES2(I)))
383          DO 8 J=1,NQ+1
384          DO 8 M=1,NQ+1
385          **** SINCE, Q-MATRIX IS SYMMETRIC FOR SEPARABLE GEOMETRIES, ONLY ****
386          **** THE LOWER TRIANGULAR PART IS TO BE EVALUATED FOR CIRCLE AND ****
387          **** ELLIPSE.
388          IF((SHAPE.EQ.'CIRCLE'.OR.SHAP.EQ.'ELLIPSE').AND.
389          &           M.GT.J) GO TO 8
390          **** FOR 'CIRCLE', ( 0 ) IS A DIAGONAL MATRIX. ****
391          **** THAT IS: OIJ(J,M)=0.0 FOR ( J ) NOT EQ. TO ( M ) ****
392          **** AND NEED NOT BE EVALUATED. ****
393          IF(SHAPE.EQ.'CIRCLE'.AND.J.NE.M) GO TO 8
394          **** IF CROSS-SECTIONAL GEOMETRY OF THE SCATTERER HAS ****
395          **** A SYMMETRY W.R.T. Y-AXIS, THEN, OIJ(J,M)=0.0 FOR ****
396          **** (J+M) IS ODD, AND NEED NOT BE EVALUATED. ****
397          **** (*NOTE: TRIANGLE , LOCATED ON THE COORDINATE ****
398          **** SYSTEM SUCH THAT ITS SYMMETRY AXIS COINCIDES ****
399          **** WITH THE X-AXIS, HAS NO SYMMETRY W.R.T. Y-AXIS) ****
400          IF(SHAPE.NE.'TRIANG'.AND.((J+M)/2).NE.J+M) GO TO 8

```

```

401      EJEM=1./2.
402      IF((J.EQ.1.AND.M.NE.1).OR.(M.EQ.1.AND.J.NE.1)) EJEM=DSORT(2.)/4.0D0
403      IF(J.EQ.1.AND.M.EQ.1) EJEM=.25D0
404      P=BF1*(TEB-TEA)/DFLOAT(NGP-1)/BF2*NSYM
405      RR=P
406      IF(BCON.EQ.'NEUM') THEN
407      P=P*BES1(J)*DCOS((J-1)*TETL(II))
408      RR=RR*BES1(J)*DSIN((J-1)*TETL(II))
409      D1=HANK(M+1)
410      D2=HANK(M)
411      MM=M
412  ELSE
413      P=P*HANK(M)*DCOS((M-1)*TETL(II))
414      RR=RR*HANK(M)*DSIN((M-1)*TETL(II))
415      D1=BES1(J+1)
416      D2=BES1(J)
417      MN=J
418      EJEM=-1.D0*EJEM
419  END IF
420  C**** (X1)&(X2) ARE FUNCTION TYPE SUBPROGRAMS USED FOR *****
421  C**** CALCULATION OF THE Q-MATRIX ELEMENTS *****
422  C     X1=R(II),D1,TETL(II),DTDR(II),D2,W(II),MM,ANO,EJEM)
423  C     D=X2(R(II),D1,TETL(II),DTDR(II),D2,W(II),MM,ANO,EJEM)
424  C     IF(M.LE.NO.AND.J.LE.NO) Q11(J,M)=Q11(J,M)+C*P
425  C     IF(M.GT.1.AND.J.GT.1) Q22(J-1,M-1)=Q22(J-1,M-1)+D*RR
426  C**** IF THE BOUNDARY HAS A MIRROR SYMMETRY W.R.T. X-AXIS, *****
427  C**** THEN, ELEMENTS OF THE Q12 & Q21 MATRICES ARE ALL *****
428  C**** ZERO AND NEED NOT BE EVALUATED. *****
429  C     IF(2-NSYM) 52,8,52
430  52  IF(BCON.EQ.'NEUM') THEN
431      IF(M.GT.1.AND.J.LE.NO) Q12(J,M-1)=Q12(J,M-1)+D*D
432      IF(J.GT.1.AND.M.LE.NO) Q21(J-1,M)=Q21(J-1,M)+C*RR
433  ELSE
434      IF(M.GT.1.AND.J.LE.NO) Q12(J,M-1)=Q12(J,M-1)+C*RR
435      IF(J.GT.1.AND.M.LE.NO) Q21(J-1,M)=Q21(J-1,M)+D*D
436  END IF
437  8  CONTINUE
438  3  CONTINUE
439  IF(K-NINTV/NSYM) 58,2,2
440  58  TEA=TEA+CINTV(K)
441  TEB=TEB+CINTV(K+1)
442  C**** DISPLAY OF THE COMPLETED INTERVALS (HELPFUL IN *****
443  C**** INTERACTIVE EXECUTION OF THE PROGRAM IN TERMINAL) *****
444  2  WRITE(6,61) K
445  61  FORMAT(12X,'** ',12,' **')
446  C**** TRUNCATION OF THE Q-MATRIX ELEMENTS TO INCREASE *****
447  C**** THE ACCURACY OF THE INVERSION, AND CONSTRUCTION OF*****
448  C**** THE Q-MATRIX FROM QIJ-SUBMATRICES *****
449  CALL CTRUNC(Q11,NQ2,0,0,TRUNC,NQ)
450  CALL CTRUNC(Q12,NQ2,0,0,TRUNC,NQ)
451  CALL CTRUNC(Q21,NQ2,NQ,0,TRUNC,NQ)
452  CALL CTRUNC(Q22,NQ2,NQ,NQ,TRUNC,NQ)
453  IF(SHAPE.EQ.'RECTAN'.OR.SHAP.EQ.'TRIANG') GO TO 627
454  DO 881 I=1,NQ2
455  DO 881 J=1,NQ2
456  IF(J.GT.I) Q(I,J)=Q(J,I)
457  881 CONTINUE
458  627  WRITE(11,777) NQ,NQ2
459  NNO=NQ*13
460  NT=0
461  IF(NQ.GT.10) NNO=130
462  LL=0
463  NPRINT=2*NSYM-1
464  73  DO 71 L=1,4,NPRINT
465  NTEST=0
466  MM=1
467  NN=NQ
468  IF(L.GT.2) THEN
469      MM=NQ+1
470      NN=NQ2
471  END IF
472  IF(L.EQ.2.OR.L.EQ.4) THEN
473      K=NQ+1
474      N=NQ2
475  ELSE
476      K=1
477      N=NQ
478  END IF
479  IF(NQ.GT.10) THEN
480      N=10

```

```

481      IF(L.EQ.2.OR.L.EQ.4) N=NQ+10
482      END IF
483      WRITE(NO,65) (LINE(I),I=1,NNQ)
484      65 FORMAT(1X,130A1)
485      WRITE(NO,66) WRIT(L+LL),MATR
486      66 FORMAT(20X,A4,A8)
487      70 WRITE(No,65) (LINE(I),I=1,NNO)
488      DO 68 I=MM,NN
489      WRITE(No,67) (DREAL(Q(I,J)),J=K,N)
490      68 WRITE(No,69) (DIMAG(Q(I,J)),J=K,N)
491      67 FORMAT(/1X,100I3.5)
492      69 FORMAT(2X,10D13.5)
493      IF(NTEST.EQ.1) GO TO 71
494      IF(NQ.GT.10) THEN
495      NTEST=1
496      K=N+1
497      N=NQ
498      IF(L.EQ.2.OR.L.EQ.4) N=NQ2
499      GO TO 70
500      END IF
501      71 CONTINUE
502      IF(LL.GT.0) GO TO 74
503      IF(NT.EQ.1) GO TO 444
504      DO 76 J=1,NQ2
505      DO 76 M=1,NQ2
506      76 RQ(J,M)=DREAL(Q(J,M))*(-1.0D0)
507      WRITE(6,63)
508      63 FORMAT(//1X,'** INVERSION STARTED **')
509      C**** INVERSION OF THE Q-MATRIX AND CREATION OF THE ****
510      C**** T-MATRIX BY GAUSS-SCHMIDT ORTHOGONALIZATION ****
511      CALL PRCSSM(NQ2)
512      WRITE(6,64)
513      64 FORMAT(1X,'*** COMPLETED ***')
514      DU 122 I=1,NQ2
515      DO 122 J=1,NQ2
516      122 WRITE(11,80) Q(I,J)
517      DO 121 J=1,NQ2
518      DO 121 I=1,NQ2
519      121 WRITE(11,80) DCONEG(Q(I,J))
520      NT=NT+1
521      WRITE(No,673)
522      673 FORMAT(//5X,'** ORTHOGONALIZED Q-MATRICES **')
523      GU TO 73
524      444 DO 72 I=1,NQ2
525      DO 72 J=1,NQ2
526      72 Q(I,J)=TM(I,J)
527      LL=4
528      GO TO 73
529      C**** STORAGE OF THE RESULTS INTO THE FILES TO BE USED ****
530      C**** BY THE PROGRAM-(B) AND OTHER CHECKING PROGRAMS ****
531      74 WRITE(10,75) BCON,ANO,SHAPE
532      75 FORMAT(1X,A4,' (B.C.)'//1X,F4.1,' (WAVE NO)'//1X,A6,' (SCATTERER)')
533      IF(SHAPE.EQ.'CIRCLE') WRITE(10,93) RAD
534      IF(SHAPE.EQ.'ELLIPS') WRITE(10,77) AA,BB
535      IF(SHAPE.EQ.'RECTAN') WRITE(10,91) A,B,CORRAD
536      IF(SHAPE.EQ.'TRIANG') WRITE(10,997) H,BET
537      997 FORMAT(1X,2F6.3,' (H & BETA ) ')
538      91 FORMAT(1X,2F6.3,F13.10,' (A & B - AXES , CORNER RADIUS ) ')
539      93 FORMAT(1X,F6.3,' (RADIUS ) ')
540      77 FORMAT(1X,2F6.3,' (A & B - AXES ) ')
541      WRITE(10,78) NSYM,NQ
542      78 FORMAT(1X,I2,' (SYM. COND.)'//1X,I3,' (NO)')
543      WRITE(22,777) NQ,NQ2
544      DO 79 I=1,NQ2
545      DO 79 J=1,NQ2
546      WRITE(22,80) TM(I,J)
547      79 WRITE(10,80) TM(I,J)
548      80 FORMAT(1X,2D30.23)
549      STOP
550      END
551      C
552      C
553      C
554      C
555      C
556      SUBROUTINE ELLIP(T1,T2,R,TET,NGP)
557      C
558      C***** ****
559      C   SUBPROGRAM FOR CALCULATION OF R & TETA VALUES IN POLAR
560      C   COORDINATES FOR EACH ANGULAR INTERVAL ALONG THE

```

```

561 C ELLIPTICAL BOUNDARY.
562 C T1 : LOWER ANGLE OF THE INTERVAL
563 C T2 : UPPER ANGLE OF THE INTERVAL
564 C NGP : NUMBER OF ANGULAR DIVISION FOR THAT INTERVAL
565 C***** ****
566 C
567 IMPLICIT REAL*8(A-H,O-Z)
568 DIMENSION R(10),TET(10)
569 COMMON/GAX/A,B
570 F(T)=A*B/(DSQRT(A*A*(DSIN(T))**2+B*B*(DCOS(T))**2))
571 T3=T2-T1
572 TET(1)=T1
573 R(1)=F(T1)
574 DO 1 I=2,NGP
575 TET(I)=TET(I-1)+T3/DFLOAT(NGP-1)
576 1 R(I)=F(TET(I))
577 RETURN
578 END
579 C
580 C
581 C
582 C
583 C
584 SUBROUTINE ANGDER(SHAPE,TETL,DTDR,NGP)
585 C
586 C***** ****
587 C SUBPROGRAM FOR CALCULATION OF THE ANGULAR DERIVATIVES
588 C ( D(R)/D(TETA) ) FOR EACH INTERVAL ALONG THE
589 C CIRCULAR & ELLIPTICAL BOUNDARIES.
590 C TETL(I) : TETA VALUES OF THE INTERVAL
591 C ( I=1,NGP )
592 C DTDR(I) : CORRESPONDING ANGULAR DERIVATIVES
593 C***** ****
594 C
595 IMPLICIT REAL*8(A-H,O-Z)
596 DIMENSION TETL(10),DTDR(10)
597 CHARACTER*6 SHAPE
598 COMMON/GRAD/RAD
599 COMMON/GAX/A,B
600 F(T)=(A*B*(B*B-A*A))*DSIN(T)*DCOS(T))/DSQRT((A*A*DSIN(T)*DSIN(T)+B*B*DCOS(T)*DCOS(T))**3)
601 IF(SHAPE.EQ.'CIRCLE') GO TO 1
602 GO TO 2
603 1 DO 3 I=1,NGP
604 3 DTDR(I)=0.D0
605 RETURN
606 2 IF(SHAPE.EQ.'ELLIPS') GO TO 4
607 GO TO 5
608 4 DO 6 I=1,NGP
609 6 DTDR(I)=F(TETL(I))
610 5 RETURN
611 END
612 C
613 C
614 C
615 C
616 C
617 C
618 SUBROUTINE RECT
619 C
620 C***** ****
621 C SUBPROGRAM FOR CALCULATION OF SOME REQUIRED PARAMETERS
622 C DESCRIBING THE RECTANGULAR BOUNDARY TO BE USED
623 C THROUGHOUT THE MAIN PROGRAM
624 C INPUT DATA:( A , B , CORRAD )
625 C RETURN PARAMETERS:(T1,T2,T3,T4,ALPH,DIS)
626 C***** ****
627 C
628 IMPLICIT REAL*8(A-H,O-Z)
629 COMMON/REC/A,B,CORRAD,T1,T2,T3,T4,ALPH,DIS
630 PI=DATAN(1.00)**4.D0
631 T1=DATAN((B-CORRAD)/A)
632 IF(A.EQ.CORRAD) THEN
633 T2=PI/2.
634 ALPH=PI/2.
635 DIS=(B-CORRAD)
636 ELSE
637 T2=DATAN(B/(A-CORRAD))
638 ALPH=DATAN((B-CORRAD)/(A-CORRAD))
639 DIS=(A-CORRAD)/DCOS(ALPH)
640 END IF

```

```

641      T3=PI-T2
642      T4=PI-T1
643      RETURN
644      END
645      C
646      C
647      C
648      C
649      C
650      SUBROUTINE RECTA1(TEA,TEB,R,TETX,NGP,DTDR)
651      C
652      C*****SUBPROGRAM FOR CALCULATION OF R & TETA VALUES AND ALSO
653      C ANGULAR DERIVATIVES ( D(R)/D(TETA) ) FOR EACH ANGULAR.
654      C INTERVAL ALONG THE RECTANGULAR BOUNDARY
655      C
656      C      TEA : LOWER ANGLE OF THE INTERVAL
657      C      TEB : UPPER ANGLE OF THE INTERVAL
658      C      NGP : NUMBER OF ANGULAR DIVISION
659      C      FOR THAT INTERVAL
660      C*****SUBPROGRAM FOR CALCULATION OF R & TETA VALUES AND ALSO
661      C
662      IMPLICIT REAL*8(A-H,O-Z)
663      COMMON/REC/A,B,CORRAD,T1,T2,T3,T4,ALPH,DIS
664      DIMENSION TETL(10),R(10),DTDR(10),TETX(10)
665      F(T,X)=DIS**DCOS(T-X)+DSQRT(DIS**2*(DCOS(T-X))**2+CORRAD**2-DIS**2)
666      G(TE)=DIS**DSIN(TE)+DIS**2*DCOS(TE)*DSIN(TE)/DSQRT(DIS**2*DCOS(TE)*
667      &**2+CORRAD**2-DIS**2)
668      PI=DATAN(1.0D0)**4.0D0
669      TEC=TEB-TEA
670      TETX(1)=TEA
671      DO 1 I=2,NGP
672      1 TETX(I)=TETX(I-1)+TEC/DFLOAT(NGP-1)
673      DO 3 I=1,NGP
674      TETL(I)=TETX(I)
675      IF(TETX(I).GT.PI) TETL(I)=TETX(I)-PI
676      3 CONTINUE
677      DO 2 I=1,NGP
678      IF(TETL(I).LE.T1.OR.TETL(I).GE.T4) THEN
679      R(I)=DABS(A/DCOS(TETL(I)))
680      DTDR(I)=A**DSIN(TETL(I))/DCOS(TETL(I))**2
681      IF(TETL(I).GE.T4) DTDR(I)=-DTDR(I)
682      GO TO 2
683      END IF
684      IF(TETL(I).GT.T1.AND.TETL(I).LT.T2) THEN
685      R(I)=F(TETL(I),ALPH)
686      TET=TETL(I)-ALPH
687      DTDR(I)=-G(TET)
688      GO TO 2
689      END IF
690      IF(TETL(I).GE.T2.AND.TETL(I).LE.T3) THEN
691      R(I)=B/DSIN(TETL(I))
692      DTDR(I)=-B*DCOS(TETL(I))/DSIN(TETL(I))**2
693      GO TO 2
694      END IF
695      IF(TETL(I).GT.T3.AND.TETL(I).LT.T4) THEN
696      R(I)=F(TETL(I),PI-ALPH)
697      TET=PI-TETL(I)-ALPH
698      DTDR(I)=G(TET)
699      END IF
700      2 CONTINUE
701      RETURN
702      END
703      C
704      C
705      C
706      C
707      C
708      SUBROUTINE TRIA1(TEA,TEB,R,TETX,NGP,DTDR)
709      C
710      C*****SUBPROGRAM FOR CALCULATION OF R & TETA VALUES AND ALSO
711      C ANGULAR DERIVATIVES ( D(R)/D(TETA) ) FOR EACH ANGULAR.
712      C INTERVAL ALONG THE TRIANGULAR BOUNDARY
713      C
714      C      TEA : LOWER ANGLE OF THE INTERVAL
715      C      TEB : UPPER ANGLE OF THE INTERVAL
716      C      NGP : NUMBER OF ANGULAR DIVISION
717      C      FOR THAT INTERVAL
718      C*****SUBPROGRAM FOR CALCULATION OF R & TETA VALUES AND ALSO
719      C
720      IMPLICIT REAL*8(A-H,O-Z)

```

```

721      COMMON/TRIAN/H,BETA,TETA1
722      DIMENSION TETL(10),R(10),DTDR(10),TETX(10)
723      PI=DATAN(1.)#4.
724      TEC=TEB-TEA
725      TETX(1)=TEA
726      DO 1 I=2,NGP
727      1 TETX(I)=TETX(I-1)+TEC/DFLOAT(NGP-1)
728      DO 3 I=1,NGP
729      TETL(I)=TETX(I)
730      IF(TETX(I).GT.PI) TETL(I)=2.*PI-TETX(I)
731      3 CONTINUE
732      DO 2 I=1,NGP
733      IF(TETL(I).LE.TETA1) THEN
734      R(I)=H/3.*((1./DCOS(TETL(I)))
735      DTDR(I)=H/3.*DSIN(TETL(I))/(DCOS(TETL(I)))**2
736      IF(TETX(I).GT.PI) DTDR(I)=-DTDR(I)
737      GO TO 2
738      END IF
739      IF(TETL(I).GT.TETA1) THEN
740      R(I)=2.*H/3.*DTAN(BETA/2.)/(DSIN(TETL(I))-DCOS(TETL(I))*
741      & DTAN(BETA/2.))
742      & DTDR(I)=-2.*H/3.*DTAN(BETA/2.)*(DCOS(TETL(I))+DSIN(TETL(I))*
743      & DTAN(BETA/2.))/(DSIN(TETL(I))-DCOS(TETL(I))*
744      & DTAN(BETA/2.))**2
745      IF(TETX(I).GT.PI) DTDR(I)=-DTDR(I)
746      END IF
747      2 CONTINUE
748      RETURN
749      END

750 C
751 C
752 C
753 C
754 C
755 C      COMPLEX FUNCTION X1*16(XRL,XBESP,XTET,XDT,XBES,XW,IND,ANO,EJEM)
756 C
757 C*****SUBPROGRAM USED IN CALCULATION OF THE
758 C      Q-MATRIX ELEMENTS
759 C*****SUBPROGRAM USED IN CALCULATION OF THE
760 C      Q-MATRIX ELEMENTS
761 C
762 C      COMPLEX*16 XBESP,XBES
763 C      REAL*8 XRL,XTET,XDT,XW,DCOS,DSIN,ANO,EJEM,DFLOAT
764 C      X1=((IND-1)*XBES-ANO*XRL*XBE SP)/DCOS((IND-1)*XTET)+(IN
765 C      D-1)*DSIN((IND-1)*XTET)*XDT*XBE SP/XRL)*XW*EJEM
766 C      RETURN
767 C
768 C
769 C
770 C
771 C
772 C
773 C      COMPLEX FUNCTION X2*16(XRL2,XBESP2,XTET2,XDT2,XBES2,XW2,IND2,ANO,
774 C      & EJEM)
775 C
776 C*****SUBPROGRAM USED IN CALCULATION OF THE
777 C      Q-MATRIX ELEMENTS
778 C*****SUBPROGRAM USED IN CALCULATION OF THE
779 C      Q-MATRIX ELEMENTS
780 C
781 C      COMPLEX*16 XBESP2,XBES2
782 C      REAL*8 XRL2,XTET2,XDT2,XW2,DCOS,DSIN,EJEM,ANO
783 C      X2=((IND2-1)*XBES2-ANO*XRL2*XBE SP2)*DSIN((IND2-1)*XTET
784 C      & 2)-(IND2-1)*DCOS((IND2-1)*XTET2)*XDT2*XBE SP2/XRL2)*XW2*EJEM
785 C      RETURN
786 C
787 C
788 C
789 C
790 C
791 C
792 C      SUBROUTINE CTRUNC(OIJ,NOT,M,N,TRUNC,NO)
793 C
794 C*****THIS SUBPROGRAM IS USED IN TRUNCATION
795 C      THIS SUBPROGRAM IS USED IN TRUNCATION
796 C      CONSTRUCTION OF THE Q-MATRIX
797 C*****CONSTRUCTION OF THE Q-MATRIX
798 C
799 C      COMPLEX*16 OIJ(20,20),O(40,40),DCMPLX
800 C      COMMON/INVO/O

```

```

801      REAL*8 CDABS,TRUNC
802      DO 1 I=1,NGT/2
803      DO 1 J=1,NGT/2
804      IF(CDABS(QIJ(I,J)).LT.TRUNC) QIJ(I,J)=DCMPLX(0.0D,0.0D)
805      1  Q(I+M,J+N)=QIJ(I,J)
806      RETURN
807      END
808      C
809      C
810      C
811      C
812      C
813      SUBROUTINE PRCSSM(NBGR)
814      C
815      C*****SUBPROGRAM FOR GAUSS-SCHMIDT ORTHOGONALIZATION*****
816      C AND CREATION OF THE T-MATRIX
817      C*****C*****C*****C*****C*****C*****C*****C*****C*****C*****C
818      C*****C*****C*****C*****C*****C*****C*****C*****C*****C*****C
819      C
820      IMPLICIT REAL*8(A-H,O-Z)
821      COMPLEX*16 RI(40,40),TM(40,40),DUM
822      REAL*8 RR1(40,40),DREAL,DIMAG,TMMX(40,40),RI1(40,40)
823      COMMON/INVO/RI
824      COMMON/G/RI1
825      COMMON/TMAT/TM
826      COMMON/REQ/RR1
827      DO 1 I=1,NBGR
828      DO 1 J=1,NBGR
829      1 RI1(I,J)=DIMAG(RI(I,J))
830      C**** CONDITIONING OF THE Q-MATRIX BEFORE ORTHOGONALIZATION ****
831      CALL CNDTHO(NBGR)
832      C**** NORMALIZE THE N'TH ROW OF AN (N) BY (N) MATRIX ****
833      SUM1=0.D0
834      DO 20 K=1,NBGR
835      SUM1=RR1(NBGR,K)**2+RI1(NBGR,K)**2+SUM1
836      20 CONTINUE
837      SUM1=DSQRT(SUM1)
838      DO 28 K=1,NBGR
839      RR1(NBGR,K)=RR1(NBGR,K)/SUM1
840      RI1(NBGR,K)=RI1(NBGR,K)/SUM1
841      28 CONTINUE
842      C**** SET UP A LOOP FOR THE N-1 REMAINING ROWS. ****
843      NM1=NBGR-1
844      NROW=NBGR
845      DO 100 I=1,NMI
846      NROW=NROW-1
847      MROW=NROW
848      DO 36 K=1,NBGR
849      TMMX(1,K)=RR1(NROW,K)
850      TMMX(2,K)=RI1(NROW,K)
851      36 CONTINUE
852      DO 80 J=NROW,NMI
853      SK1=0.D0
854      SI1=0.D0
855      MROW=MROW+1
856      DO 40 K=1,NBGR
857      SR1=SR1+RR1(MROW,K)*RR1(NROW,K)+RI1(MROW,K)*RI1(NROW,K)
858      SI1=SI1+RR1(MROW,K)*RI1(NROW,K)-RI1(MROW,K)*RR1(NROW,K)
859      40 CONTINUE
860      DO 48 K=1,NBGR
861      TMMX(1,K)=TMMX(1,K)-SR1*RR1(MROW,K)+SI1*RI1(MROW,K)
862      TMMX(2,K)=TMMX(2,K)-SR1*RI1(MROW,K)-SI1*RR1(MROW,K)
863      48 CONTINUE
864      80 CONTINUE
865      SUM1=0.D0
866      DO 84 K=1,NBGR
867      SUM1=SUM1+TMMX(1,K)**2+TMMX(2,K)**2
868      84 CONTINUE
869      SUM1=DSQRT(SUM1)
870      DO 88 K=1,NBGR
871      RR1(NROW,K)=TMMX(1,K)/SUM1
872      RI1(NROW,K)=TMMX(2,K)/SUM1
873      88 CONTINUE
874      100 CONTINUE
875      DO 2 I=1,NBGR
876      DO 2 J=1,NBGR
877      2 RI(I,J)=DCMPLX(RI1(I,J),RI1(I,J))
878      2 DUM=RI(I,J)
879      DO 3 I=1,NBGR
880      3 DUM=RI(I,J).

```

```

881      RI(I,J)=RI(J,I)
882      3 RI(J,I)=DUM
883 C**** PERFORM Q-TRANSPOSE * REAL(0) TO GET T-MATRIX . *****
884      DO 160 I=1,NBGR
885      DO 152 J=1,NBGR
886      TMMX(I,J)=0.D0
887      152 CONTINUE
888      160 CONTINUE
889      DO 180 I=1,NBGR
890      DO 176 J=1,NBGR
891      DO 172 K=1,NBGR
892      TMMX(I,J)=TMMX(I,J)-RI1(K,I)*RR1(K,J)
893      172 CONTINUE
894      176 CONTINUE
895      180 CONTINUE
896      DO 196 I=1,NBGR
897      DO 192 J=1,NBGR
898      TM(I,J)=DCMPLX(0.D0,TMMX(I,J))
899      192 CONTINUE
900      196 CONTINUE
901      DO 208 I=1,NBGR
902      DO 204 J=1,NBGR
903      TMMX(I,J)=0.D0
904      204 CONTINUE
905      208 CONTINUE
906      DO 220 I=1,NBGR
907      DO 216 J=1,NBGR
908      DO 212 K=1,NBGR
909      TMMX(I,J)=TMMX(I,J)+RR1(K,I)*RR1(K,J)
910      212 CONTINUE
911      216 CONTINUE
912      220 CONTINUE
913      DO 236 I=1,NBGR
914      DO 232 J=1,NBGR
915      TM(I,J)=TM(I,J)-DCMPLX(TMMX(I,J),0.D0)
916      232 CONTINUE
917      236 CONTINUE
918      RETURN
919      END
920 C
921 C
922 C
923 C
924 C
925      SUBROUTINE CNDTNQ(NBGR)
926 C
927 C***** C SUBPROGRAM FOR CONDITIONING OF THE Q-MATRIX TO INCREASE
928 C THE ACCURACY IN THE ORTHOGONALIZATION
929 C***** C
930 C***** C
931 C
932 IMPLICIT REAL*8(A-H,O-Z)
933 REAL*8 RR1(40,40),RI1(40,40)
934 COMMON/Q/RI1
935 COMMON/REQ/RR1
936 NROW=NBGR
937 DO 60 KR=2,NBGR
938 C**** RESCALE THE CURRENT ROW *****
939 SCLE1=1.D0/RI1(NROW,NROW)
940 DO 8 LC=1,NBGR
941 RR1(NROW,LC)=SCLE1*RR1(NROW,LC)
942 RI1(NROW,LC)=SCLE1*RI1(NROW,LC)
943 8 CONTINUE
944 C**** RESCALE ALL THE ROWS UP TO THE CURRENT ROW. *****
945 MROW=NROW-1
946 DO 20 MR=1,MROW
947 RSCL1=RI1(MR,NROW)
948 DO 16 MC=1,NBGR
949 RR1(MR,MC)=RR1(MR,MC)-RSCL1*RR1(NROW,MC)
950 RI1(MR,MC)=RI1(MR,MC)-RSCL1*RI1(NROW,MC)
951 16 CONTINUE
952 20 CONTINUE
953 NROW=NROW-1
954 60 CONTINUE
955 C**** SET THE IMAGINARY ELEMENTS ABOVE THE MAIN DIAGONAL=0. ****
956 NROW=NBGR-1
957 DO 80 I=1,NROW
958 IB=I+I
959 DO 72 J=IB,NBGR
960 RI1(I,J)=0.D0

```

```

961      72 CONTINUE
962      80 CONTINUE
963      RETURN
964      END
965      C
966      C
967      C
968      C
969      C
970      SUBROUTINE DBESS(M0,DZ,DN,DB1,DB2,E)
971      C
972      C
973      C DOCUMENTATION ADDED AT CORNELL UNIVERSITY 8/5/74 FOR THE SUBROUTINE D
974      C DZ IS THE VALUE OF WHICH WE ARE TAKING THE BESSSEL FUNCTION.
975      C DN IS THE ORDER OF THE BESSSEL FUNCTION.
976      C THE VALUE OF THE BESSSEL FUNCTION IS STORED IN DB1 IF THE
977      C BESSSEL FUNCTION WAS OF THE FIRST KIND, IE. A J-BESSEL FUNCTION.
978      C THE VALUE OF THE BESSSEL FUNCTION IS STORED IN DB2 IF THE
979      C BESSSEL FUNCTION WAS OF THE SECOND KIND, IE. A Y-BESSEL FUNCTION.
980      C
981      C
982      IMPLICIT REAL*8(A-H,O-Z)
983      CCALCULATES BESSSEL FUNCTION (COMPLEX ORDER AND COMPLEX ARGUMENT) OF THE
984      CFIRST KIND IF M0=0, AND ALSO OF THE SECOND KIND (NEUMANN FUNCTION) IF
985      CM0=1
986      CCALCULATES BESSSEL FUNCTION OF COMPLEX ORDER AND COMPLEX ARGUMENT USING
987      CPOWER SERIES FOR ABS(Z) LESS THAN Z0AND ASYMPTUTIC SERIES FOR ABS(Z)
988      CGREATER THAN Z0. CHOOSES Z0=10 IF GIVEN Z0 LESS THAN 1
989      C E1 DETERMINES ROUNDOFF OF EN TO INTEGER. IF E1 LE 0., SETS TO .001
990      1002 FORMAT(45H NEITHER SERIES FOR BESSSEL FUNCTION CONVERGES)
991      1022 FORMAT(46H NEITHER SERIES FOR NEUMANN FUNCTION CONVERGES)
992      1011 FORMAT(50H THIS IS A SINGULAR POINT OF THE NEUMANN FUNCTION , ,
993      14H ZX=.1PE14.5,3X,4H ZY=.E14.5)
994      DIMENSION C(10),C1(100),C2(100),C3(100),C4(100),C5(100),T3(101)
995      DIMENSION C6(101)
996      COMPLEX#16 Z,EN,B,ARG,G,T1,EX,S1,CF,SF,T3
997      COMPLEX #16 FNS,S,T,U,V,S2,T2,SOZ,ZLG,A,A1,B1,B2,BIT,ZH,ZHS,C1
998      COMPLEX #16 X,DZ,DN,DB1,DB2,CDUM
999      REAL*8 DATANZ,DREAL,DIMAG,DLG,DFLOAT,DSIGN,DABS,CDABS
1000      COMPLEX#16 CDEXP,CDSORT,CDCOS,COSIN,DCMPLX
1001      INTEGER*4 IDINT
1002      DATA IFLAG /0/
1003      ERO=.1D-2
1004      Z=DZ
1005      X=Z
1006      ZX=DREAL(DZ)
1007      ZY=DIMAG(DZ)
1008      EN=DN
1009      ENX=DREAL(DN)
1010      ENY=DIMAG(DN)
1011      M=M0+1
1012      ABSZ=CDABS(Z)
1013      DB1=DCMPLX(0.0D,0.0D)
1014      DB2=DCMPLX(0.0D,0.0D)
1015      NFLAG=2
1016      NF=0
1017      KFLAG=1
1018      CKFLAG DENOTES QUADRANT OF Z
1019      IF((ZX.LT.0.0D.AND.ZY.GE.0.0D)KFLAG=2
1020      IF((ZX.LT.0.0D.AND.ZY.LT.0.0D)KFLAG=3
1021      IF((ZX.GE.0.0D.AND.ZY.LT.0.0D)KFLAG=4
1022      IF(KFLAG.EQ.2.OR.KFLAG.EQ.3) X=-Z
1023      CROUTINE MOVES Z FROM LEFT-HALF PLANE TO RIGHT-HALF PLANE IF ASYMPTOTIC
1024      CSERIES TO BE USED
1025      IF(IFLAG.GT.0)GO TO 2
1026      C(1)=3.141592653589793D0
1027      C(2)=C(1)/2.0D
1028      C(3)=C(2)/2.0D
1029      C(4)=1.0D/DSQRT(C(2))
1030      C(5)=DLG(2.0D)
1031      C(6)=8.0D
1032      C(7)=64.0D
1033      C(9)=2.0D*C(1)
1034      C(10)=1.0D/C(1)
1035      EUL=.5772156649015338D0-C(5)
1036      CI=DCMPLX(0.0D,2.0D)
1037      A1=DCMPLX(0.0D,C(1))
1038      C6(1)=1.0D
1039      DO 100 I=1,100
1040      EYE=I

```

```

1041      C1(I) = EYE
1042      C2(I) = 2.00*EYE
1043      C3(I) = -2.00*EYE-1.00
1044      C4(I)=(4.00*EYE-1.00)**2
1045      C6(I+1)=C6(I)+1.00/DFLOAT(I+1)
1046      100 C5(I)=(4.00*EYE-3.00)**2
1047      IFLAG=1
1048      2 ERR=.1D-07
1049      IF(E.GT.0.00)ERR=E
1050      I=0
1051      ZZ=5.00
1052      IF(DABS(ENY).LE.ERO.AND.DABS(IDINT(ENX)-ENX).LE.ERO)INFLAG=-1
1053          ITEMP=ENX+DSIGN(.5D0,ENX)
1054          TEMP=ITEMP
1055          IF(NFLAG.EQ.-1) EN=DCMPLX(ITEMP,0.00)
1056          ENX1=DREAL(EN)
1057          IF(NFLAG.EQ.-1.AND.ENX1.EQ.0.00)INFLAG=0
1058          IF(NFLAG.EQ.-1.AND.ENX1.GT.0.00)INFLAG=1
1059          CNFLAG=-1,0,+1,+2 MEANS (ENX,ENY) A NEGATIVE INTEGER,ZERO,A POSITIVE INT
1060          CEGER, AND A NON-INTEGER,RESPECTIVELY
1061          IF(NFLAG.EQ.2.AND.M.EQ.2)M=3
1062          CFOR M=3, EXPRESSES NEUMANN FUNCTION IN TERMS OF BESSEL FUNCTIONS
1063          IF(NFLAG.EQ.-1)EN=-EN
1064          3 CONTINUE
1065          JFLAG=0
1066          A=CDEXP(EN*A1)
1067          IF(ABSZ.GE.ZZ) GO TO 6
1068          IF(ENY.EQ.0.00.AND.DABS(IDINT(ENX)+0.5D0-ENX).LE.ERO) GO TO 6
1069          IF(ABSZ.NE.0.00)GO TO 8
1070          IF(M.EQ.2) WRITE(6,1011) DZ
1071          IF(NFLAG.NE.0)GO TO 16
1072          DB1=DCMPLX(1.00,0.00)
1073          16 RETURN
1074          8 CONTINUE
1075          I=1
1076          ZLG=DCMPLX(DLOG(ABSZ),DATAN2(DIMAG(Z),DREAL(Z)))
1077          CCHOOSES PRINCIPAL VALUE OF Z IN CALCULATING CLUG(Z)
1078          ARG=EN+C1(I)
1079          CALL DGAMM(ARG,G,CDUM,ERR,O)
1080          ZH=EN*(ZLG-C(5))
1081          ZHS=CDEXP(ZH)
1082          T3(1)=ZHS/G
1083          S1=T3(1)
1084          EX=CDEXP(C2(I)*(ZLG-C(5)))
1085          11 I=I+1
1086          T3(I)=-T3(I-1)*EX/((EN+C1(I-1))*C1(I-1))
1087          S1=S1+T3(I)
1088          S1S=CDABS(S1)
1089          T1S=CDABS(T3(1))
1090          IF(T1S.LE.ERR*S1S) GO TO 9
1091          IF(I.LT.10)GO TO 11
1092          IF(JFLAG.GT.0)GO TO 14
1093          JFLAG=1
1094          GO TO 6
1095          14 WRITE(6,1002)
1096          STOP
1097          81 CONTINUE
1098          JFLAG=1
1099          GO TO 6
1100          82 WRITE(6,1022)
1101          STOP
1102          9 B=S1
1103          IF(M.NE.2)GO TO 55
1104          N=DABS(ENX)
1105          U=2.00*(ZLG+EUL)
1106          S2=B*U
1107          IZZZ=1
1108          77 DO 75 J=IZZZ,1
1109          J1=J-1
1110          J1N=N+J-1
1111          IF (J1.LE.0) GO TO 200
1112          IF (J1.GT.101) GO TO 201
1113          TEMP1=C6(J1)
1114          GO TO 203
1115          200 TEMP1=0.00
1116          GO TO 203
1117          201 TEMP1=C6(101)
1118          DO 202 JJ=102,J1
1119          TEMP1=TEMP1+1.00/DFLOAT(JJ)
1120          202 CONTINUE

```

```

1121    203 CONTINUE
1122      IF( J1N.LE.0) GO TO 205
1123      IF( J1N.GT.101) GO TO 206
1124      TEMP2=C6(J1N)
1125      GO TO 208
1126      205 TEMP2=0.0D0
1127      GO TO 208
1128      206 TEMP2=C6(101)
1129      DO 207 JJ=102,J1N
1130      - TEMP2=TEMP2+1.D0/DFLOAT(JJ)
1131      207 CONTINUE
1132      208 CONTINUE
1133      T2=T3(J)*TEMP1+TEMP2
1134      T2R=DABS(DREAL(T2))
1135      T2I=DABS(DIMAG(T2))
1136      75 S2=S2-T2
1137      S2R=DABS(DREAL(S2))
1138      S2I=DABS(DIMAG(S2))
1139      IF( T2R.GT.ERR*S2R) GO TO 78
1140      IF( T2I.LE.ERR*S2I) GO TO 76
1141      78 I=I+1
1142      IF( I.GT.101.AND.JFLAG.EQ.0) GO TO 81
1143      IF( I.GT.101.AND.JFLAG.NE.0) GO TO 82
1144      T3(I)=-T3(I-1)*EX/((EN+C1(I-1))*C1(I-1))
1145      IZZZ=I
1146      GO TO 77
1147      76 B2=S2*C(10)
1148      IF( N.EQ.0) GO TO 55
1149      S1=DCMPLX(0.0D0,0.0D0)
1150      T1=-C(10)/ZHS
1151      LUP=N-1
1152      IF( LUP.EQ.0) GO TO 72
1153      DO 70 LL=1,LUP
1154      70 T1=T1*DFLOAT(LL)
1155      S1=S1+T1
1156      DO 71 LL=1,LUP
1157      T1=T1*EX/(DFLOAT(LL)*DFLOAT(LUP-LL+1))
1158      71 S1=S1+T1
1159      GO TO 73
1160      72 S1=S1+T1
1161      73 B2=B2+S1
1162      GO TO 55
1163      55 IF( NFLAG.LT.0) B=A*B
1164      BX=DREAL(B)
1165      BY=DIMAG(B)
1166      BXA=DABS(BX)
1167      BYA=DABS(BY)
1168      IF( ZX.EQ.0.0D0.OR.ZY.EQ.0.0D0) NF=1
1169      IF( NFLAG.NE.2.AND.BXA.LT.BYA.AND.NF.EQ.0.1) BX=0.0D0
1170      IF( NFLAG.NE.2.AND.BYA.LT.BXA.AND.NF.EQ.0.1) BY=0.0D0
1171      GO TO (56,57,58,59),M
1172      6 ARG=X-EN*C(2)-C(3)
1173      CF=CDCCOS(ARG)
1174      SF=C(6)*CDCSIN(ARG)
1175      FNS=C1(4)*EN*EN
1176      I=0
1177      S1=DCMPLX(1.0D0,0.0D0)
1178      S2=DCMPLX(0.0D0,0.0D0)
1179      U=DCMPLX(1.0D0,0.0D0)
1180      T1S=1.0D0
1181      S=CF
1182      18 I=I+1
1183      V=-(FNS-C5(I))/(C(7)*X*C3(I))*U
1184      U=V*(FNS-C4(I))/(C2(I)*X)
1185      US=CDABS(U)
1186      IF( US.GT.T1S) GO TO 20
1187      12 CUNTINUE
1188      T=U*CF+V*SF
1189      TR=DABS(DREAL(T))
1190      TI=DABS(DIMAG(T))
1191      S=S+T
1192      SR=DABS(DREAL(S))
1193      SI=DABS(DIMAG(S))
1194      IF( TR.GT.ERR*SR) GO TO 24
1195      IF( TI.LE.ERR*SI) GO TO 26
1196      24 T1=U
1197      T2=V
1198      S1=S1+T1
1199      S2=S2+T2
1200      T1S=US

```

```

1201      17 IF(I-100)18,25,25
1202      20 IF(I.EQ.1) GO TO 12
1203      IF(JFLAG.GT.0) GO TO 23
1204      JFLAG=1
1205      GO TO 8
1206      23 WRITE(6,1002)
1207      29 CUNTUE
1208      STOP
1209      26 CONTINUE
1210      SQZ=CDSQRT(X)
1211      IF(DREAL(SQZ).LT.0.D0)SQZ=-SQZ
1212      CCHOOSSES PROPER BRANCH FOR SQUARE ROOT
1213      B=C(4)/SQZ*S
1214      IF(KFLAG.EQ.2)B=A*B
1215      IF(KFLAG.EQ.3)B=B/A
1216      IF(M.EQ.3)M=2
1217      IF(M.NE.2)GO TO 55
1218      B2=C(4)/SQZ*(SF*(S1+U)/C(6)-CF*(S2+V)*C(6))
1219      IF(KFLAG.EQ.2)B2=(B2+CDCOS(C(1)*EN)*CI*B)/A
1220      IF(KFLAG.EQ.3)B2=(B2-CDCOS(C(1)*EN)*CI*B)*A
1221      GO TO 55
1222      25 IF(JFLAG.GT.0)GO TO 28
1223      JFLAG=1
1224      GO TO 8
1225      28 WRITE(6,1002)
1226      GO TO 29
1227      58 B1=DCMPLX(BX,BY)
1228      M=4
1229      EN=-EN
1230      GO TO 3
1231      59 B1T=DCMPLX(BX,BY)
1232      EN=-EN
1233      ARG=C(1)*EN
1234      B2=(CDCOS(ARG)*B1-B1T)/CDSIN(ARG)
1235      DB1=B1
1236      DB2=B2
1237      RETURN
1238      57 IF(NFLAG.EQ.-1)B2=A*B2
1239      DB2=B2
1240      56 DB1=DCMPLX(BX,BY)
1241      RETURN
1242      END
1243      SUBROUTINE DGAMM(DZ,DGM,DPS,ERR,JJ)
1244      CIF JJ=0,CALCULATES ONLY GAMMA FUNCTION, IF JJ=1, CALCULATES ONLY PSI
1245      CFUNCTION, IF JJ=2, CALCULATES BOTH
1246      IMPLICIT REAL*8(A-H,O-Z)
1247      COMPLEX*16 GAM,Z,DZ,DGM,DPS,DPSI
1248      COMPLEX *16 TERM1,ZT1,TERM,SUM,ZLG,ZTGAM,ZT
1249      COMPLEX*16 CDLOG,DCMPLX,CDEXP,CDSIN
1250      REAL*8 DREAL,DIMAG,DLOG,DABS
1251      INTEGER*4 IDINT
1252      DIMENSION B(10)
1253      DIMENSION C(100)
1254      DATA IFLAG /0/
1255      1001 FORMAT(1H ,//,24H SERIES DID NOT CONVERGE)
1256      1010 FORMAT(1H ,//,47H THIS IS A SINGULAR POINT OF THE GAMMA FUNCTION
1257      X,/5X,6HARG R=,E12.5,3X,6HARG I=,E12.5)
1258      IF(JJ.EQ.0)GO TO 60
1259      DPS=DPSI(DZ,ERR)
1260      IF(JJ.EQ.1)RETURN
1261      60 E=ERR
1262      IF(E.LE.0.D0)E=.1D-07
1263      ZX=DREAL(DZ)
1264      ZY=DIMAG(DZ)
1265      Z=DZ
1266      IF((ZX.LT.0.D0)Z=-Z
1267      NFLAG=2
1268      J=0
1269      CK=NUMBER OF TERMS IN SERIES
1270      IF((ZY.EQ.0.D0.AND.(IDINT(ZX)-ZX).EQ.0.D0).NFLAG=1
1271      IF(NFLAG.EQ.1.AND.ZX.LE.0.D0)NFLAG=0
1272      CNFLAG=0 MEANS Z=0 OR Z A NEGATIVE INTEGER NFLAG=1 MEANS Z A POSITIVE
1273      IF(NFLAG.NE.0)GO TO 51
1274      WRITE(6,1010) DZ
1275      DGM=DCMPLX(0.D0,0.D0)
1276      RETURN
1277      51 IF(NFLAG.EQ.2)GO TO 42
1278      IF((ZX.GT.2.0D0)) GO TO 55
1279      DGM=DCMPLX(1.D0,0.D0)
1280      RETURN

```

```

1281      55 IF(ZX.GT.20.D0)GO TO 42
1282      IF=IDINT(ZX)-1
1283      IJ=1
1284      DO 300 N=2,IF
1285      300 IJ=IJ*N
1286      DGM=IJ
1287      RETURN
1288      42 CONTINUE
1289      IF(IFLAG.NE.0)GO TO 20
1290      DO 100 I=1,100
1291      100 C(I)=1
1292      PI=3.141592653589793D0
1293      PI2=DLLOG(2.D0*PI)/2.D0
1294      B(1)=1.000/12.000
1295      B(2)=-1.000/360.000
1296      B(3)=1.000/1260.000
1297      B(4)=-1.000/1680.000
1298      B(5)=1.000/1188.000
1299      B(6)=-691.000/360360.000
1300      B(7)=1.000/156.000
1301      B(8)=-3617.000/122400.000
1302      B(9)=43867.000/244188.000
1303      B(10)=-174611.000/125400.000
1304      CB(I) ARE THE BERNOULLI COEFFICIENTS IN STIRLING'S FORMULA
1305      IFLAG=1
1306      20 ZT=Z
1307      ZT1=ZT-1.D0
1308      I=0
1309      5 IF(DREAL(ZT).GT.10.D0) GO TO 3
1310      4 I=I+1
1311      IF(I.LE.100)GO TO 30
1312      WRITE (6,1001)
1313      STOP
1314      30 CONTINUE
1315      ZT=ZT+1.D0
1316      GO TO 5
1317      3 IF=I
1318      ZLG=CDLOG(ZT)
1319      SUM=(ZT-.5 D0)*ZLG -ZT+PI2
1320      TERM1=SUM
1321      ATER1R=DABS(DREAL(TERM1))
1322      ATER1I=DABS(DIMAG(TERM1))
1323      J=0
1324      8 J=J+1
1325      TERM=B(J)*CDEXP(-(2.D0*C(J)-1.D0)*ZLG)
1326      ATERR=DABS(DREAL(TERM))
1327      ATERI=DABS(DIMAG(TERM))
1328      SUM=SUM+TERM
1329      ASUMR=DABS(DREAL(SUM))
1330      ASUMI=DABS(DIMAG(SUM))
1331      IF(ATERR.GT.ATER1R)GO TO 24
1332      IF(ATERI.GT.ATER1I)GO TO 24
1333      IF(ASUMR.EQ.0.D0)GO TO 9
1334      IF(ATERR/ASUMR.GT.E)GO TO 27
1335      9 CONTINUE
1336      IF(ASUMI.EQ.0.D0) GO TO 6
1337      IF(ATERI/ASUMI.LE.E)GO TO 6
1338      27 CONTINUE
1339      ATER1R=ATERR
1340      ATER1I=ATERI
1341      GO TO 7
1342      24 CONTINUE
1343      7 IF(J.LT.10)GO TO 8
1344      GO TO 4
1345      6 ZTGAM=SUM
1346      IF(IF.EQ.0)GO TO 31
1347      DO 200 K=1,IF
1348      200 ZTGAM=ZTGAM-CDLOG(ZT1+C(K))
1349      31 GAM=CDEXP(ZTGAM)
1350      IF(ZX.LT.0.D0)GAM=-PI/(GAM*CDSIN(PI*Z)*Z)
1351      DGM=GAM
1352      RETURN
1353      END
1354      COMPLEX FUNCTION DPSI#16(Z,E)
1355      IMPLICIT COMPLEX#16 (A-H,O-Z)
1356      COMPLEX#16 CDEXP,CDLOG,CDCOS,CDSIN,DCMPLX
1357      REAL#8 DATA2N,DFLOAT,DABS,CDABS
1358      REAL#8 E,ERR,B,ABTER,ABTER1,ABSUMI,PI,ZX,ZY,ZXI,EN,EUL,DREAL,DIMAG
1359      INTEGER#4 IOINT
1360      DIMENSION B(10)

```

```

1361      DATA IFLAG /0/
1362      ERR=E
1363      IF(ERR.LE.0.0)ERR=.1D-5
1364      ZP=Z
1365      ZT=Z
1366      ZX=DREAL(ZP)
1367      ZY=DIMAG(ZP)
1368      NI=IDINT(ZX)
1369      ZXI=DFLOAT(NI)-ZX
1370      IF(ZY.NE.0.0.D0.OR.ZX.GT.0.0.D0.OR.ZXI.NE.0.0.D0)GO TO 1
1371      DPSI=DCMLX(0.0D0,0.0D0)
1372      WRITE (6,1010) Z
1373      RETURN
1374      CCALCULATE PSI HERE IF Z IS A POSITIVE INTEGER
1375      1 IF(ZY.NE.0.0.D0.OR.ZXI.NE.0.0.D0)GO TO 2
1376      EUL=-.5772156649
1377      DPSI=EUL
1378      IF(NI.EQ.1)RETURN
1379      NF=NI-1
1380      DO 100 N=1,NF
1381      100 DPSI=DPSI+1.0D0/DFLOAT(N)
1382      RETURN
1383      2 ISIGN=0
1384      IF(ZX.LT.0.0D0)ISIGN=1
1385      IF(ISIGN.EQ.1)ZT=1.0D0-ZT
1386      CREFLECTS Z INTO 1-Z IF Z IS IN LEFT-HALF PLANE
1387      ZS=ZT
1388      NR=0
1389      IF(IFLAG.NE.0)GO TO 3
1390      PI=DATAN2(0.0D0,-1.0D0)
1391      B(1)=1.0D0/(2.0D0*6.0D0)
1392      B(2)=-1.0D0/(4.0D0*30.0D0)
1393      B(3)=1.0D0/(6.0D0*42.0D0)
1394      B(4)=-1.0D0/(8.0D0*30.0D0)
1395      B(5)=5.0D0/(10.0D0*66.0D0)
1396      B(6)=-691.0D0/(12.0D0*2730.0D0)
1397      B(7)=7.0D0/(14.0D0*6.0D0)
1398      B(8)=-3617.0D0/(16.0D0*510.0D0)
1399      B(9)=43867.0D0/(18.0D0*798.0D0)
1400      B(10)=-174611.0D0/(20.0D0*330.0D0)
1401      IFLAG=1
1402      3 IF((NR+NI).GT.10)GO TO 4
1403      NR=NR+1
1404      GO TO 3
1405      CINCREASES REAL PART OF Z UNTIL GREATER THAN 10
1406      4 ZT=ZT+DFLOAT(NR)
1407      ZL=CDLOG(ZT)
1408      TER1=.500/ZT
1409      SUM=ZL-TER1
1410      ABTER1=CDABS(TER1)
1411      N=0
1412      8 N=N+1
1413      EN=DFLOAT(N)
1414      TER=-B(N)*CDEXP(-2.0D0*EN*ZL)
1415      ABTER=CDABS(TER)
1416      IF(ABTER.LT.ABTER1)GO TO 5
1417      NR=NR+1
1418      ZT=ZS
1419      IF(NR.LT.100)GO TO 4
1420      WRITE (6,1011)
1421      RETURN
1422      5 SUM=SUM+TER
1423      ABSUM1=CDABS(DIMAG(SUM))
1424      IF(ABSUM1.NE.0.0D0)GO TO 6
1425      IF(ABTER/CDABS(SUM).LE.ERR)GO TO 7
1426      GO TO 9
1427      6 IF(DABS(DREAL(TER))/DABS(DREAL(SUM)).LE.ERR.AND.DABS(DIMAG(TER))/
1428      1 ABSUM1.LE.ERR)GO TO 7
1429      9 ABTER1=ABTER
1430      GO TO 8
1431      7 DPSI=SUM
1432      IF(NR.EQ.0) GO TO 10
1433      DO 200 N=1,NR
1434      200 DPSI=DPSI-1.0D0/(ZT-DFLOAT(N))
1435      10 IF(ISIGN.EQ.0)RETURN
1436      ARG=PI*ZP
1437      DPSI=DPSI-PI*CDCOS(ARG)/CD SIN(ARG)
1438      RETURN
1439      1010 FORMAT(1H //,45H THIS IS A SINGULAR POINT OF THE PSI FUNCTION,/,,
1440      130X,6HARG R=,1PE12.5,3X,6HARG I=,E12.5)
1441      1011 FORMAT(1H //,24H SERIES DID NOT CONVERGE)
1442      END

```

\*\*\*\*\*  
SAMPLE RUN WITH THE SAMPLE DATA-(A) GIVEN IN THE PROGRAM-(A)  
\*\*\*\*\*

\*\*\*\*\*  
\* SCATTERING OF ACOUSTIC WAVES  
\*  
\* BY THE CYLINDERS OF ARBITRARY CROSS-SECTION.  
\*  
\* (( T-MATRIX FORMULATION ))  
\*  
\*\*\*\*\*

\*\* PROGRAM-(A): GENERATION OF THE T-MATRIX ELEMENTS \*\*  
=====

B.C. TYPE : NEUMANN (RIGID INCLUSION)

WAVE NUMBER : .5

CROSS-SECTION OF THE SCATTERER : CIRCULAR

RADIUS : 1.000

SYMMETRY CONDITION (W.R.T. X-AXIS) : SYMMETRIC

NUMBER OF BOUNDARY SEGMENTS : 72

TYPE OF BOUNDARY DIVISION : EQUAL ANGULAR INTERVALS

ORDER OF THE SIMPSON'S RULE USED IN NUMERICAL INTEGRATION : 4

TOTAL DIMENSION OF THE T-MATRIX: 10 X 10

TRUNCATION FACTOR FOR THE Q-MATRIX ELEMENTS : .100-025

ERROR FACTOR FOR THE BESSEL FUNCTIONS : .100-013

## 0-11 MATRIX

```

-.17857+000 .00000 .00000 .00000 .00000
.10846+001 .00000 .00000 .00000 .00000
.00000 .86373-001 .00000 .00000 .00000
.00000 .47539+000 .00000 .00000 .00000
.00000 .00000 .28808-002 .00000 .00000
.00000 .00000 .48779+000 .00000 .00000
.00000 .00000 .00000 .30650-004 .00000
.00000 .00000 .00000 .49718+000 .00000
.00000 .00000 .00000 .00000 .16132-006
.00000 .00000 .00000 .00000 .49892+000

```

## 0-22 MATRIX

```

.86373-001 .00000 .00000 .00000 .00000
.47539+000 .00000 .00000 .00000 .00000
.00000 .28808-002 .00000 .00000 .00000
.00000 .48779+000 .00000 .00000 .00000
.00000 .00000 .30650-004 .00000 .00000
.00000 .00000 .49718+000 .00000 .00000
.00000 .00000 .00000 .16132-006 .00000
.00000 .00000 .00000 .49892+000 .00000
.00000 .00000 .00000 .00000 .50729-009
.00000 .00000 .00000 .00000 .49947+000

```

## \*\* ORTHOGONALIZED Q-MATRICES \*\*

## 0-11 MATRIX

```

.16246+000 .00000 .00000 .00000 .00000
.98672+000 .00000 .00000 .00000 .00000
.00000 -.17876+000 .00000 .00000 .00000
.00000 .98389+000 .00000 .00000 .00000
.00000 .00000 -.59057-002 .00000 .00000
.00000 .00000 .99998+000 .00000 .00000
.00000 .00000 .00000 -.61647-004 .00000
.00000 .00000 .00000 .10000+001 .00000
.00000 .00000 .00000 .00000 -.32333-006
.00000 .00000 .00000 .00000 .10000+001

```

## 0-22 MATRIX

```

.17876+000 .00000 .00000 .00000 .00000
.98389+000 .00000 .00000 .00000 .00000
.00000 -.59057-002 .00000 .00000 .00000
.00000 .99998+000 .00000 .00000 .00000
.00000 .00000 .00000 -.61647-004 .00000
.00000 .00000 .00000 .10000+001 .00000
.00000 .00000 .00000 .00000 -.32333-006
.00000 .00000 .00000 .10000+001 .00000
.00000 .00000 .00000 .00000 -.10157-008
.00000 .00000 .00000 .00000 .10000+001

```

## T-11 MATRIX

-.26392-001	.00000	.00000	.00000	.00000
-.16030+000	.00000	.00000	.00000	.00000
.00000	-.31956-001	.00000	.00000	.00000
.00000	.17588+000	.00000	.00000	.00000
.00000	.00000	-.34877-004	.00000	.00000
.00000	.00000	.59056-002	.00000	.00000
.00000	.00000	.00000	-.38004-008	.00000
.00000	.00000	.00000	.61647-004	.00000
.00000	.00000	.00000	.00000	-.10454-012
.00000	.00000	.00000	.00000	.32333-006

## T-22 MATRIX

-.31956-001	.00000	.00000	.00000	.00000
.17588+000	.00000	.00000	.00000	.00000
.00000	-.34877-004	.00000	.00000	.00000
.00000	.59056-002	.00000	.00000	.00000
.00000	.00000	-.38004-008	.00000	.00000
.00000	.00000	.61647-004	.00000	.00000
.00000	.00000	.00000	-.10454-012	.00000
.00000	.00000	.00000	.32333-006	.00000
.00000	.00000	.00000	.00000	-.10316-017
.00000	.00000	.00000	.00000	.10157-008

```

1 C ****
2 C ****
3 C *
4 C * SCATTERING OF ACOUSTIC WAVES *
5 C *
6 C * BY THE CYLINDERS OF ARBITRARY CROSS-SECTION *
7 C *
8 C * (( T-MATRIX FORMULATION )) *
9 C ****
10 C ****
11 C *** P R O G R A M - (B) ***
12 C ****
13 C EVALUATION OF THE SCATTERED WAVE FIELD AT VARIOUS DISTANCES
14 C FROM THE SCATTERER AND FOR VARIOUS INCIDENCE ANGLES OF THE
15 C ACOUSTIC PLANE WAVE ,BY USING THE T-MATRIX CREATED BY THE
16 C PROGRAM-(A).
17 C
18 C
19 C *** THE GENERAL STEPS FOLLOWED BY THE PROGRAM ARE AS FOLLOWS ***
20 C
21 C -- READING OF THE PARAMETERS DESCRIBING THE BOUNDARY OF THE
22 C SCATTERER AND ELEMENTS OF THE T-MATRIX FROM THE FILE(10)
23 C
24 C
25 C -- CREATION OF THE INCIDENT WAVE FIELD COEFFICIENTS
26 C A1(I) & A2(I) FOR A DESIRED INCIDENCE ANGLE (AINC)
27 C
28 C
29 C -- CALCULATION OF THE SCATTERED WAVE FIELD COEFFICIENTS
30 C C1(I) & C2(I) . WHERE:
31 C
32 C C1 = T11*A1 + T12*A2 C2 = T21*A1 + T22*A2
33 C
34 C (C1 & C2 ARE COLUMN VECTORS & T1J'S ARE (NO X NO) MATRICES)
35 C
36 C -- EVALUATION AND PRESENTATION OF THE FOLLOWING RESULTS
37 C BOTH IN TABULAR AND POLAR GRAPHICAL FORMS:
38 C A-1) NEAR FIELD SOLUTIONS (*ONLY FOR CIRCULAR BOUNDARY)
39 C AT DESKED REGIONS OR,ON THE BOUNDARY OF THE
40 C SCATTERER.
41 C 1-) VELOCITY POTENTIALS DUE TO SCATTERED WAVE FIELD
42 C 2-) WAVE VELOCITIES DUE TO SCATTERED WAVE FIELD
43 C B-) FAR-FIELD SCATTERED WAVE FIELD AMPLITUDES
44 C C-) TOTAL SCATTERING CROSS-SECTION (ALSO CHECK FOR
45 C CONVERGENCY)
46 C
47 C ***** IMPORTANT NOTE *****
48 C ****
49 C CONVERGENCY OF THE TOTAL SCATTERING CROSS-SECTION
50 C MUST BE CHECKED UP TO AT LEAST 1.E-3 %. IF (%1 DIFFERENCE
51 C IS GREATER THAN 1.E-3,THEN THE SIZE OF THE T-MATRIX
52 C USED MUST BE INCREASED. IN SUCH A CASE, A NEW T-MATRIX
53 C OF THE LARGER SIZE MUST BE RECREATED BY THE PROGRAM-(A).
54 C
55 C
56 C ****
57 C INPUT DATA
58 C ****
59 C CARD 1 :
60 C ****
61 C COLUMN 1-2: NI (READING UNIT OR FILE NO.)
62 C COLUMN 3-4: NO (WRITING UNIT OR FILE NO.)
63 C
64 C CARD 2 :
65 C ****
66 C COLUMN 1-3: NYAZ (ANGULAR INCREMENT IN PRINTING THE
67 C TABULAR RESULTS. EXAMPLE: IF NYAZ=10,
68 C THEN SCATTERED WAVE FIELD RESULTS
69 C VERSUS POLAR ANGLE ARE PRINTED FOR EACH
70 C 10 DEGREE INCREMENT. MIN(NYAZ)=2.
71 C (*NOTE*: NYAZ SHOULD BE AN EVEN NUMBER)
72 C COLUMN 4-6 : XAX ( XAX & YAX ARE THE SCALE PARAMETERS
73 C COLUMN 7-9 : YAX REQUIRED FOR 'SUBROUTINE GRAPH4'.
74 C TAKE XAX & YAX=6.0-11.0)
75 C (*NOTE*: 'GRAPH4' IS A LIBRARY PROGRAM IN UNIVAC-1106 SYSTEM)
76 C
77 C CARD 3 :
78 C ****
79 C COLUMN 1-2: NINC (NUMBER OF INCIDENCE ANGLES FOR WHICH
80 C THE SCATTERED FIELD SOLUTIONS ARE DESIRED)

```

```

81 C
82 C CARD SET 4 :
83 C =====
84 C *EACH CARD CONTAINS*
85 C COLUMN 1-4: DUM4 (INCIDENCE ANGLE OF THE WAVE.(IN DEGREES))
86 C (*NOTE:# NO OF CARDS IN SET(4) MUST
87 C BE EQUAL TO 'NINC'. )
88 C
89 C CARD 5 :
90 C =====
91 C COLUMN 1-2: NPOT (IF VELOCITY POTENTIALS ARE DESIRED TO
92 C BE EVALUATED NPOT=1 ,OTHERWISE NPOT=0)
93 C COLUMN 3-4: NVEL (IF WAVE VELOCITIES ARE DESIRED NVEL=1,
94 C OTHERWISE NVEL=0)
95 C . COLUMN 5-6: NFAR (IF FAR-FIELD SOLUTION IS DESIRED
96 C NFAR=1 ,OTHERWISE NFAR=0 )
97 C COLUMN 7-8:NCROS (NCROS=1 IF TOTAL SCATTERING CROSS-SECTION
98 C IS DESIRED)
99 C COLUMN 9-10: NREG (NUMBER OF REGIONS AT WHICH THE NEAR FIELD
100 C SOLUTIONS ARE DESIRED TO BE EVALUATED.
101 C (*NOTE:# IF BOTH NPOT & NVEL=0,TAKE NREG=0 )
102 C
103 C CARD SET 6 : (*IF NREG=0 ,OMIT THIS CARD SET)
104 C =====
105 C *EACH CARD CONTAINS*
106 C COLUMN 1-4: REG(I) (REGION(DISTANCE FROM THE ORIGIN OF THE
107 C POLAR COORDINATE SYSTEM))
108 C (*NOTE:# 1-) TAKE REG(I)=0. ,IF THE NEAR FIELD
109 C SOLUTIONS ARE DESIRED TO BE
110 C EVALUATED ON THE BOUNDARY OF
111 C THE SCATTERER.
112 C (2-) I=1,NREG
113 C
114 C
115 C
116 C ****
117 C SAMPLE DATA
118 C ****
119 C ( A ) ( B )
120 C
121 C COLUMN COLUMN
122 C ===== =====
123 C CARD I1234567890 CARD I1234567890
124 C ===== =====
125 C 1 I 5 6 1 I 5 6
126 C 2 I 10 5. 5. 2 I 10 9. 7.
127 C 3 I 1 3 I 2
128 C 4 10. 4 130.
129 C 5 I 1 0 1 1 2 5 145.
130 C 6 10. 6 I 0 0 1 1 0
131 C 7 15.
132 C
133 C
134 C ****
135 C
136 C
137 IMPLICIT REAL*8(A-H,O-Z)
138 C
139 DIMENSION AINC(10),REG(10)
140 C
141 COMPLEX*16 T11(20,20),T12(20,20),T21(20,20),T22(20,20),
142 E BES1(22),BES2(22),HANK(22),DUM1,DUM2,DZ,DN,CPART,
143 E A1(20),A2(20),C1(20),C2(20),BASF(20),
144 E USPOT(190),USVEL(190),USFAR(190)
145 C
146 COMMON/REC/A,B,CORRAD,T1,T2,T3,T4,ALPH,DIS
147 COMMON/TRIAN/H,BETA,TETA1
148 C
149 REAL*4 X(190),Y(190),XAX,YAX
150 C
151 CHARACTER BCN*4,SHAPE*6,H1*12,H2*25,H3*18,H4*33,H8*37,
152 E H5*8,H6*10,H7*34,H9*9,H10*13,H11*10
153 C
154 G(V)=V*360./(2.*PI)
155 F(U)=U*2.*PI/360.
156 C
157 DATA H1,H2,H3/'B.C. TYPE : ','NEUMANN (RIGID INCLUSION)', 'DIRICHLE'
158 ET (CAVITY)'/
159 DATA H4/'CROSS-SECTION OF THE SCATTERER : '/
160 DATA H8/'SYMMETRY CONDITION (W.R.T. X-AXIS) : '/

```

```

161      DATA H5,H6,H7/'CIRCULAR','ELLIPTICAL','RECTANGULAR (WITH ROUNDED C
162      &ORNERS)'/
163      DATA H9,H10/'SYMMETRIC','NON-SYMMETRIC'/
164      DATA H11/'TRIANGULAR'/
165  C
166      READ(5,10) NI,NO,NYAZ,XAX,YAX
167      10 FORMAT(2I2/I3,2F3.0)
168      WRITE(NO,613)
169      613 FORMAT(1H1)
170      WRITE(NO,100)
171      100 FORMAT(//5X,47('*')/5X,'*',45X,'*'/*5X,'*',8X,'SCATTERING OF ACOUS
172      ETIC WAVES',9X,'*'/*5X,'*',45X,'*'/*5X,'*',BY THE CYLINDERS OF ARBITRA
173      ERY CROSS-SECTION '*'/*5X,'*',45X,'*'/*5X,'*',8X,'(( T-MATRIX FORMULA
174      & EQUATION ))',9X,'*'/*5X,'*',45X,'*'/*5X,47('*')////*5X,'** PROGRAM-(B):'
175      & EVALUATION OF THE NEAR AND FAR FIELD SOLUTIONS ***/5X,65('=')//)
176      PI=DATAN(1.0D0)*4.0D0
177  C**** READING OF THE DATA,CREATED BY THE PROGRAM-(A) AND ****
178  C**** STORED INTO THE FILE(10) ****
179      READ(10,1) BCUN,ANO,SHAPE
180      1 FORMAT(1X,A4/1X,F4.1/1X,A6)
181      IF(SHAPE.EQ.'CIRCLE') READ(10,2) RAD
182      IF(SHAPE.EQ.'ELLIPS') READ(10,2) AA,BB
183      IF(SHAPE.EQ.'RECTAN') READ(10,2) A,B,CORRAD
184      IF(SHAPE.EQ.'TRIANG') THEN
185          READ(10,2) H,BET
186          BETA=F(BET)
187          TETA1=DATAN(3.*DTAN(BETA/2.))
188      END IF
189      2 FORMAT(1X,2F6.3,F13.10)
190      READ(10,4) NSYM,NO
191      4 FORMAT(1X,I2/1X,13)
192      NO2=NO*2
193      NOT=NO+2
194      IF(NQ.GE.13. AND.NO.LE.18) NOT=22
195      DO 5 I=1,NO
196      DO 6 J=1,NO
197      6 READ(10,7) T11(I,J)
198      DO 5 J=1,NO
199      5 READ(10,7) T12(I,J)
200      DO 8 I=1,NO
201      DO 9 J=1,NO
202      9 READ(10,7) T21(I,J)
203      DO 8 J=1,NO
204      8 READ(10,7) T22(I,J)
205      7 FORMAT(1X,2D30.23)
206      WRITE(NO,11)
207      11 FORMAT(63('=')/)
208      IF(BCON.EQ.'NEUM') WRITE(NO,12) H1,H2
209      12 FORMAT(1X,A12,A25)
210      IF(BCON.EQ.'DRIC') WRITE(NO,12) H1,H3
211      IF(SHAPE.EQ.'CIRCLE') WRITE(NO,13) H4,H5,RAD
212      13 FORMAT(1X,A33,A8//1X,'RADIUS : ',F6.3)
213      IF(SHAPE.EQ.'ELLIPS') WRITE(NO,14) H4,H6,AA,BB
214      14 FORMAT(1X,A33,A10//1X,'A-AXIS : ',F6.3,4X,'B-AXIS : ',F6.3)
215      IF(SHAPE.EQ.'RECTAN') WRITE(NO,15) H4,H7,A,B,CORRAD
216      15 FORMAT(1X,A33,A34//1X,'A-AXIS:',F6.3,4X,'B-AXIS:',F6.3,4X,
217      & 'CORNER RAD.:',F13.10)
218      IF(SHAPE.EQ.'TRIANG') WRITE(NO,998) H4,H11,H,BET
219      998 FORMAT(1X,A33,A10//1X,'H:',F6.3,', BETA:',F7.3)
220      IF(NSYM.EQ.1) WRITE(NO,16) H8,H10
221      16 FORMAT(1X,A37,A13)
222      IF(NSYM.EQ.2) WRITE(NO,16) H8,H9
223      WRITE(NO,17) ANO,NO2,NO2
224      17 FORMAT(//1X,'WAVE TYPE : ACOUSTIC PLANE WAVE//1X,'WAVE NO : ',
225      & F4.1//1X,'TOT.DIM. OF THE T-MATRIX USED : ',I3,'X',I3//63('='))
226      READ(NI,18) NINC
227      DO 19 I=1,NINC
228      READ(NI,20) DUM4
229      19 AINC(I)=F(DUM4)
230      18 FORMAT(I2)
231      20 FORMAT(F4.0)
232      READ(NI,21) NPOT,NVEL,NEAR,NCROS,NREG
233      21 FORMAT(5I2)
234      IF(SHAPE.EQ.'RECTAN') CALL RECT
235      IF(NREG.EQ.0) GO TO 23
236      DO 22 I=1,NREG
237      22 READ(NI,20) REG(I)
238      23 DO 24 II=1,NINC
239      WRITE(NO,46) II,GAINC(II)
240      46 FORMAT(//6X,I2,'- ANGLE OF INCIDENCE : ',F4.0,'(DEGREES)'/45('=

```

```

241      E1)
242 C**** CCREATION OF THE INCIDENT WAVE FIELD COEFFICIENTS ****
243      A1(1)=(1.00,0.00)
244      DO 25 I=1,NQ
245      IF(NQ-I) 26,27,26
246      26 A1(I+1)=DSORT(2.0D0)*(0.0D0,1.0D0)**I*DCOS(I*AINC(I))
247      27 A2(I)=DSORT(2.0D0)*(0.0D0,1.0D0)**I*DSIN(I*AINC(I))
248      25 CONTINUE
249 C**** CALCULATION OF THE SCATTERED WAVE FIELD COEFFICIENTS ****
250      CALL MULVEC(T11,A1,C1,NQ)
251      IF(NSYM-2) 28,29,28
252      28 CALL MULVEC(T12,A2,C2,NQ)
253      DO 30 I=1,NQ
254      30 C1(I)=C1(I)+C2(I)
255      29 CALL MULVEC(T22,A2,C2,NQ)
256      IF(NSYM-2) 31,32,31
257      31 CALL MULVEC(T21,A1,BASF,NQ)
258      DO 33 I=1,NQ
259      33 C2(I)=C2(I)+BASF(I)
260      32 TEB=PI*4.0D0/360.
261      I=1
262      IF(NREG) 64,65,64
263      64 DO 34 I=1,NREG
264      65 TEA=0.0D0
265 C**** CALCULATION OF THE NEAR & FAR-FIELD SOLUTIONS ****
266      DO 35 J=1,181
267      IF(NREG.EQ.0) GO TO 36
268      REGION=REG(I)
269      DTDR=0.0D0
270      IF(REG(I).EQ.0.) THEN
271          IF(SHAPE.EQ.'CIRCLE') REGION=RAD
272          IF(SHAPE.EQ.'ELLIPS') THEN
273              REGION=AA*BB/DSORT(AA*AA*(DSIN(TEA))**2+BB*BB*(DCOS(TEA))**2)
274              DTDR=(AA*BB*(BB*BB-AA*AA)*DSIN(TEA)*DCOS(TEA))/DSORT((AA*AA*DSIN(TEA))**2+BB*BB*DCOS(TEA))**2)**3
275          END IF
276          IF(SHAPE.EQ.'RECTAN') CALL RECTA2(TEA,REGION,DTDR)
277          IF(SHAPE.EQ.'TRIANG') CALL TRIA2(TEA,REGION,DTDR)
278      END IF
279      DZ=DCMPLX((ANU*REGION),0.0D0)
280      DN=(0.0D0,0.0D0)
281      DO 37 K=1,2
282      CALL DBESS(1,DZ,DN,DUM2,BES2(K),1.0-15)
283      37 DN=DN+(1.0D0,0.0D0)
284      DO 38 K=3,NQ+1
285      38 BES2(K)=2.0*(K-2)/DZ*BES2(K-1)-BES2(K-2)
286      DN=DCMPLX(((NQ-1)*1.0D0),0.0D0)
287      DO 70 K=1,2
288      CALL DBESS(0,DZ,DN,BES1(NQ+1-K),DUM1,1.0-15)
289      70 DN=DN-(1.0D0,0.0D0)
290      DO 71 K=3,NQ
291      71 BES1(NQ+1-K)=2.0*(NQ+1-K)/DZ*BES1(NQ-K+2)-BES1(NQ-K+3)
292      DO 39 K=1,NQ+1
293      39 HANK(K)=DCMPLX(DREAL(BES1(K)),DREAL(BES2(K)))
294      USPOT(J)=0.0D0,0.0D0
295      USVEL(J)=0.0D0,0.0D0
296      USFAR(J)=0.0D0,0.0D0
297      DO 40 N=1,NQ
298      EJEM=1.0D0
299      IF(N.GT.1) EJEM=DSQRT(2.0D0)
300      IF(N.EQ.1) THEN
301          CPART=C1(N)*DCOS((N-1)*TEA)
302          IF(N.EQ.1) THEN
303              CPART=C1(N)*DCOS((N-1)*TEA)
304              GO TO 414
305          END IF
306          CPART=C1(N)*DCOS((N-1)*TEA)+C2(N-1)*DSIN((N-1)*TEA)
307          414 IF(NPOT) 41,42,41
308          41 USPOT(J)=USPOT(J)+CPART*HANK(N)*EJEM
309          42 IF(NVEL) 43,44,43
310          43 USVEL(J)=USVEL(J)+EJEM*((N-1)*HANK(N)-DZ*HANK(N+1))*CPART+(N-1)/
311          EREGION*HANK(N)*(C1(N)*DSIN((N-1)*TEA)-C2(N)*DCOS(N*TEA))*DTDR
312          44 IF(I.GT.1) GO TO 40
313          IF(NFAR) 45,40,45
314          45 USFAR(J)=USFAR(J)+CPART*EJEM*(0.0D0,1.0D0)**(1-N)
315          40 CONTINUE
316          35 TEA=TEA+TEB
317          IF(I.GT.1) GO TO 49
318          IF(NFAR) 91,50,91
319          91 WRITE(NO,47)
320          47 FORMAT(//1X,63(' ')//6X,'# FAR-FIELD SCATTERED FIELD AMPLITUDE #')

```

```

321      6/1X,63('=')) WRITE(NO,48)
322      48 FORMAT(1/1X,'REAL',7X,'IMAGINARY ',6X,'PEAK VALUE'/3X,'ANGLE',10X,
323      6'PART',9X,'PART',13X,!/(NORM)'/1X,63('=')) CALL GRAFIK(NO,USFAR,PI,NSYM,NYAZ,XAX,YAX,AINC(II))
324      50 IF(NCROS) 51,490,51
325      51 WRITE(NO,52)
326      52 FORMAT(//1X,36('=')/,2X,'CHECK FOR THE CONVERGENCE OF THE'/3X,'TOT
327      &AL SCATTERING CROSS-SECTION'/37('='),/,1X,'ORDER TOT.S.C.SECTION (
328      &%) DIFFERENCE'/37('=')) USC=0.D0
329      331 C**** CALCULATION OF THE TOTAL SCATTERING CROSS-SECTION *****
330      332 DO 53 N=1,NQ
331      333 PRC=USC
332      334 USC=USC+CDABS(C1(N))**2+CDABS(C2(N))**2
333      335 IF(N.EQ.1) THEN
334      336 WRITE(NO,54) N,USC
335      337 GO TO 53
336      338 ELSE
337      339 PERDIF=DABS(USC-PRC)/DABS(PRC)*100.D0
338      340 WRITE(NO,54) N,USC,PERDIF
339      341
340      342 C
341      343 END IF
342      344 53 CONTINUE
343      345 54 FORMAT(1X,14,D16.7,D14.7)
344      346 WRITE(NO,55)
345      347 55 FORMAT(1H1)
346      348 490 IF(NREG.EQ.0) GO TO 24
347      349 IF(REG(I).EQ.0.) THEN
348      350   WRITE(NO,56)
349      351   ELSE
350      352   WRITE(NO,57) REG(I)
351      353 END IF
352      354 56 FORMAT(//6X,'REGION : *BOUNDARY*'/6X,19('='))
353      355 57 FORMAT(//6X,'REGION : ',F4.1/6X,10('='))
354      356 IF(INPUT) 58,59,58
355      357 58 WRITE(NO,60)
356      358 60 FORMAT(//1X,63('=')/8X,'** VELOCITY POTENTIALS DUE TO SCATTERED FI
357      359 &ELD **'/1X,63('='))
358      360 WRITE(NO,48)
359      361 CALL GRAFIK(NO,USPOT,PI,NSYM,NYAZ,XAX,YAX,AINC(II))
360      362 59 IF(NVEL) 61,34,61
361      363 61 WRITE(NO,63)
362      364 63 FORMAT(//1X,63('=')/8X,'** WAVE VELOCITIES DUE TO SCATTERED FIELD
363      365 &**'/1X,63('='))
364      366 WRITE(NO,48)
365      367 CALL GRAFIK(NO,USVEL,PI,NSYM,NYAZ,XAX,YAX,AINC(II))
366      368 34 CONTINUE
367      369 24 CONTINUE
368      370 STOP
369      371
370      371 END
371      372 C
372      373 C
373      374 C
374      375 SUBROUTINE MULVEC(A,B,C,N)
375      376 C
376      377 C*****SUBROUTINE MULVEC*****
377      378 C SUBPROGRAM FOR MATRIX & VECTOR MULTIPLICATION
378      379 C*****SUBROUTINE MULVEC*****
379      380 C
380      381 COMPLEX*16 A(20,20),B(20),C(20),T
381      382 DO 1 I=1,N
382      383 T=(0.D0,0.D0)
383      384 DO 2 J=1,N
384      385 2 T=T+A(I,J)*B(J)
385      386 1 C(I)=T
386      387 RETURN
387      388 END
388      389 C
389      390 C
390      391 C
391      392 C
392      393 C
393      394 SUBROUTINE RECT
394      395 C
395      396 C*****SUBROUTINE RECT*****
396      397 C SUBPROGRAM FOR CALCULATION OF SOME REQUIRED PARAMETERS
397      398 C DESCRIBING THE RECTANGULAR BOUNDARY TO BE USED
398      399 C THROUGHOUT THE MAIN PROGRAM
399      400 C INPUT DATA:( A , B , CORRAD )

```

```

401 C      RETURN PARAMETERS:(T1,T2,T3,T4,ALPH,DIS)
402 C***** ****
403 C
404 IMPLICIT REAL*8(A-H,O-Z)
405 COMMON/REC/A,B,CORRAD,T1,T2,T3,T4,ALPH,DIS
406 PI=DATAN(1.0D0)*4.0D0
407 T1=DATAN((B-CORRAD)/A)
408 IF(A.EQ.CORRAD) THEN
409   T2=PI/2.
410   ALPH=PI/2.
411   DIS=(B-CORRAD)
412 ELSE
413   T2=DATAN(B/(A-CORRAD))
414   ALPH=DATAN((B-CORRAD)/(A-CORRAD))
415   DIS=(A-CORRAD)/DCOS(ALPH)
416 END IF
417 T3=PI-T2
418 T4=PI-T1
419 RETURN
420 END
421 C
422 C
423 C
424 C
425 C
426 SUBROUTINE RECTA2(TEX,R,DTDR)
427 C
428 C***** ****
429 C      SUBPROGRAM FOR CALCULATION OF R & D(R)/D(TETA)
430 C      VALUES FOR A GIVEN ANGLE(TETA) ALONG THE
431 C      RECTANGULAR BOUNDARY
432 C***** ****
433 C
434 IMPLICIT REAL*8(A-H,O-Z)
435 COMMON/REC/A,B,CORRAD,T1,T2,T3,T4,ALPH,DIS
436 F(T,X)=DIS*DCOS(T-X)+DSQRT(DIS**2*(DCOS(T-X))**2+CORRAD**2-DIS**2)
437 G(T)=DIS*DSIN(TE)+DIS**2*DCOS(TE)*DSIN(TE)/DSQRT(DIS**2*DCOS(TE)*
438   &**2+CORRAD**2-DIS**2)
439 PI=DATAN(1.0D0)*4.0D0
440 TET=TEX
441 TETL=TET
442 IF(TET.GT.PI) TETL=TET-PI
443 IF(TETL.LE.T1.OR.TETL.GE.T4) THEN
444   R=DABS(A/DCOS(TETL))
445   DTDR=A*DSIN(TETL)/DCOS(TETL)**2
446   IF(TETL.GE.T4) DTDR=-DTDR
447 RETURN
448 END IF
449 IF(TETL.GT.T1.AND.TETL.LT.T2) THEN
450   R=F(TETL,ALPH)
451   TET=TETL-ALPH
452   DTDR=-G(TET)
453 RETURN
454 END IF
455 IF(TETL.GE.T2.AND.TETL.LE.T3) THEN
456   R=B/DSIN(TETL)
457   DTDR=-B*DCOS(TETL)/DSIN(TETL)**2
458 RETURN
459 END IF
460 IF(TETL.GT.T3.AND.TETL.LT.T4) THEN
461   R=F(TETL,PI-ALPH)
462   TET=PI-TETL-ALPH
463   DTDR=G(TET)
464 END IF
465 RETURN
466 END
467 C
468 C
469 C
470 C
471 C
472 SUBROUTINE TRIA2(TEX,R,DTDR)
473 C
474 C***** ****
475 C      SUBPROGRAM FOR CALCULATION OF R & D(R)/D(TETA)
476 C      VALUES FOR A GIVEN ANGLE(TETA) ALONG THE
477 C      TRIANGULAR BOUNDARY
478 C***** ****
479 C
480 IMPLICIT REAL*8(A-H,O-Z)

```

```

481      COMMON/TRIAN/H,BETA,TETA1
482      PI=DATAN(1.)*4.
483      TET=TEX
484      TETL=TET
485      IF(TET.GT.PI) TETL=2.*PI-TET
486      IF(TETL.LE.TETA1) THEN
487          R=H/3.*(1./DCOS(TETL))
488          DTDR=H/3.*DSIN(TETL)/(DCOS(TETL))**2
489          IF(TEX.GT.PI) DTDR=-DTDR
490          RETURN
491      END IF
492      IF(TETL.GT.TETA1) THEN
493          R=2.*H/3.*DTAN(BETA/2.)/(DSIN(TETL)-DCOS(TETL))
494          E=DTAN(BETA/2.)
495          DTDR=-2.*H/3.*DTAN(BETA/2.)*(DCOS(TETL)+DSIN(TETL)*
496          E-DTAN(BETA/2.))/(DSIN(TETL)-DCOS(TETL)*
497          E-DTAN(BETA/2.))**2
498          IF(TEX.GT.PI) DTDR=-DTDR
499      END IF
500      RETURN
501  END
502 C
503 C
504 C
505 C
506 C
507      SUBROUTINE GRAFIKING(US,PI,NSYM,NYAZ,XAX,YAX,AINC)
508 C
509 C*****SUBPROGRAM FOR PRESENTATION OF THE RESULTS
510 C
511 C IN TABULAR AND POLAR GRAPHICAL FORMS
512 C*****SUBROUTINE GRAFIKING(US,PI,NSYM,NYAZ,XAX,YAX,AINC)
513 C
514      COMPLEX#16 US(190),DCMPLX
515      REAL#8 DIMAG,DREAL,CDABS,PI,TG,T
516      REAL#4 X(190),Y(190),XAX,YAX
517      T=0.
518      K=NYAZ/2
519      DO 1 I=1,181
520      IF(K.EQ.(NYAZ/2+1)) K=1
521      TG=T/360.D0*2.D0*PI
522 C***DATA TO BE PRESENTED IN GRAPHS, ARE STORED INTO X(I) & Y(I) ARRAYS
523 C***(*NOTE: FIRST, POLAR TO RECTANGULAR CONVERSION IS NECESSARY
524 C***      FOR 'GRAPH4')
525      X(I)=CDABS(US(I))*DCOS(TG)
526      Y(I)=CDABS(US(I))*DSIN(TG)
527      IF(NSYM.EQ.2.AND.I.GT.91.AND.AINC.EQ.0.) GO TO 1
528      IF(K.EQ.NYAZ/2) WRITE(NO,2) T,DREAL(US(I)),DIMAG(US(I)),CDABS(US(I))
529      E)
530      K=K+1
531      2 FORMAT(4X,F4.0,8X,F8.5,4X,F8.5,9X,F8.5)
532      1 T=T+2.D0
533      CALL GRAPH4(XAX,YAX,181,X,Y)
534 C***'GRAPH4' IS A LIBRARY PROGRAM IN UNIVAC-1106 SYSTEM ****
535      WRITE(NO,3)
536      3 FORMAT(1H1)
537      RETURN
538  END
539 C
540 C
541 C
542 C
543 C
544      SUBROUTINE DBESS(M0,DZ,DN,DB1,DB2,E)
545 C
546 C
547 C DOCUMENTATION ADDED AT CORNELL UNIVERSITY 8/5/74 FOR THE SUBROUTINE D
548 C DZ IS THE VALUE OF WHICH WE ARE TAKING THE BESSSEL FUNCTION.
549 C DN IS THE ORDER OF THE BESSSEL FUNCTION.
550 C THE VALUE OF THE BESSSEL FUNCTION IS STORED IN DB1 IF THE
551 C BESSSEL FUNCTION WAS OF THE FIRST KIND, IE. A J-BESSSEL FUNCTION.
552 C THE VALUE OF THE BESSSEL FUNCTION IS STORED IN DB2 IF THE
553 C BESSSEL FUNCTION WAS OF THE SECOND KIND, IE. A Y-BESSSEL FUNCTION.
554 C
555 C
556      IMPLICIT REAL#8(A-H,O-Z)
557      CCALCULATES BESSSEL FUNCTION (COMPLEX ORDER AND COMPLEX ARGUMENT) OF THE
558      CFIRST KIND IF M0=0, AND ALSO OF THE SECOND KIND (NEUMANN FUNCTION) IF
559      CM0=1
560      CCALCULATES BESSSEL FUNCTION OF COMPLEX ORDER AND COMPLEX ARGUMENT USING

```

```

561 CPOWER SERIES FOR ABS(Z) LESS THAN ZO AND ASYMPTOTIC SERIES FOR ABS(Z)
562 CGREATER THAN ZO. CHOOSES ZO=10 IF GIVEN ZO LESS THAN 1
563 C E1 DETERMINES ROUNDOFF OF EN TO INTEGER. IF E1 LE 0., SETS TO .001
564 1002 FORMAT(45H NEITHER SERIES FOR BESSEL FUNCTION CONVERGES)
565 1022 FORMAT(46H NEITHER SERIES FOR NEUMANN FUNCTION CONVERGES)
566 1011 FORMAT(50H THIS IS A SINGULAR POINT OF THE NEUMANN FUNCTION)
567 14H ZX=,1PE14.5,3X,4H ZY=,E14.5)
568 DIMENSION C(10),C1(100),C2(100),C3(100),C4(100),C5(100),T3(101)
569 DIMENSION CG(101)
570 COMPLEX*16 Z,EN,B,ARG,G,T1,EX,S1,CF,SF,T3
571 COMPLEX *16 FNS,S,T,U,V,S2,T2,SOZ,ZLG,A,A1,B1,B2,B1T,ZH,ZHS,CI
572 COMPLEX *16 X,DZ,DN,DB1,DB2,CDUM
573 REAL*8 DATAN2,DREAL,DIMAG,DLOG,DFLOAT,DSIGN,DABS,CDABS
574 COMPLEX*16 CDEXP,CDSQRT,CDCOS,COSIN,DCMPLX
575 INTEGER*4 IDINT
576 DATA IFLAG /0/
577 ERO=.1D-2
578 Z=DZ
579 X=Z
580 ZX=DREAL(DZ)
581 ZY=DIMAG(DZ)
582 EN=DN
583 ENX=DREAL(DN)
584 ENY=DIMAG(DN)
585 M=MD+1
586 ABSZ=CDABS(Z)
587 DB1=DCMPLX(0.0D,0.0D)
588 DB2=DCMPLX(0.0D,0.0D)
589 NFLAG=2
590 NF=0
591 KFLAG=1
592 CKFLAG DENOTES QUADRANT OF Z
593 IF(ZX.LT.0.0D.AND.ZY.GE.0.0D)KFLAG=2
594 IF(ZX.LT.0.0D.AND.ZY.LT.0.0D)KFLAG=3
595 IF(ZX.GE.0.0D.AND.ZY.LT.0.0D)KFLAG=4
596 IF(KFLAG.EQ.2.OR.KFLAG.EQ.3)X=-Z
597 CROUTINE MOVES Z FROM LEFT-HALF PLANE TO RIGHT-HALF PLANE IF ASYMPTOTIC
598 CSERIES TO BE USED
599 IF(IFLAG.GT.0)GO TO 2
600 C(1)=3.141592653589793D0
601 C(2) =C(1) /2.0D
602 C(3)=C(2)/2.0D
603 C(4) =1.0D/DSQRT(C(2))
604 C(5)=DLG(2.0D)
605 C(6)=8.0D
606 C(7)=64.0D
607 C(9)=2.0D*C(1)
608 C(10)=1.0D/C(1)
609 EUL=.5772156649015338D0-C(5)
610 C1=DCMPLX(0.0D,2.0D)
611 A1=DCMPLX(0.0D,C(1))
612 C6(1)=1.0D
613 DO 100 I=1,100
614 EYE=I
615 C1(I) =EYE
616 C2(I) =2.0D*EYE
617 C3(I) =2.0D*EYE-1.0D
618 C4(I)=(4.0D*EYE-1.0D)*#2
619 C6(I+1)=C6(I)+1.0D/DFLOAT(I+1)
620 100 C5(I)=(4.0D*EYE-3.0D)*#2
621 IFLAG=1
622 2 ERR=.1D-07
623 IF(E.GT.0.0D)ERR=E
624 I=0
625 ZZ=5.0D
626 IF(DABS(ENY).LE.ERO.AND.DABS(IDINT(ENX)-ENX).LE.ERO)NFLAG=-1
627 ITMP=ENX+DSIGN(.5D0,ENX)
628 TEMP=ITMP
629 IF(NFLAG.EQ.-1) EN=DCMPLX(TEMP,0.0D)
630 ENX1=DREAL(EN)
631 IF(NFLAG.EQ.-1.AND.ENX1.EQ.0.0D)NFLAG=0
632 IF(NFLAG.EQ.-1.AND.ENX1.GT.0.0D)NFLAG=1
633 CNFLAG=-1,0,+1,+2 MEANS (ENX,ENY) A NEGATIVE INTEGER,ZERO,A POSITIVE INT
634 CEGER, AND A NON-INTEGER,RESPECTIVELY
635 IF(NFLAG.EQ.2.AND.M.EQ.2)M=3
636 CFOR M=3, EXPRESSES NEUMANN FUNCTION IN TERMS OF BESSEL FUNCTIONS
637 IF(NFLAG.EQ.-1)EN=-EN
638 3 CONTINUE
639 JFLAG=0
640 A=CDEXP(EN#A1)

```

```

641      IF(ABSZ.GE.ZZ) GO TO 6
642      IF(ENY.EQ.0.D0.AND.DABSTIDINT(ENX)+0.5D0-ENX).LE.ERO) GO TO 6
643      IF(ABSZ.NE.0.D0)GO TO 8
644      IF(M.EQ.2) WRITE(6,1011) DZ
645      IF(INFLAG.NE.0)GO TO 16
646      DB1=DCMPLX(1.D0,0.D0)
647      16 RETURN
648      8 CONTINUE
649      I=1
650      ZLG=DCMPLX(DLOG(ABSZ),DATAN2(DIMAG(Z),DREAL(Z)))
651      CCHOSES PRINCIPAL VALUE OF Z IN CALCULATING CLOG(Z)
652      ARG=EN+C1(1)
653      CALL DGAMM(ARG,G,CDUM,ERR,0)
654      ZH=EN*(ZLG-C(5))
655      ZHS=CDEXP(ZH)
656      T3(1)=ZHS/G
657      S1=T3(1)
658      EX=CDEXP(C2(1)*(ZLG-C(5)))
659      11 I=I+1
660      T3(I)=-T3(I-1)*EX/((EN+C1(I-1))*C1(I-1))
661      S1=S1+T3(I)
662      S1S=CDABS(S1)
663      T1S=CDABS(T3(I))
664      IF(T1S.LE.ERR*S1S) GO TO 9
665      IF(I.LT.101)GO TO 11
666      IF(JFLAG.GT.0)GO TO 14
667      JFLAG=1
668      GO TO 6
669      14 WRITE(6,1002)
670      STOP
671      81 CONTINUE
672      JFLAG=1
673      GO TO 6
674      82 WRITE(6,1022)
675      STOP
676      9 B=S1
677      IF(M.NE.2)GO TO 55
678      N=DABS(ENX1)
679      U=2.D0*(ZLG+EUL)
680      S2=B*U
681      IZZZ=1
682      77 DO 75 J=IZZZ,I
683      J1=J-1
684      J1N=N+J-1
685      IF (J1.LE.0) GO TO 200
686      IF (J1.GT.101) GO TO 201
687      TEMP1=C6(J1)
688      GO TO 203
689      200 TEMP1=0.D0
690      GO TO 203
691      201 TEMP1=C6(101)
692      DO 202 JJ=102,J1
693      TEMP1=TEMP1+1.D0/DFLOAT(JJ)
694      202 CONTINUE
695      203 CONTINUE
696      IF (J1N.LE.0) GO TO 205
697      IF (J1N.GT.101) GO TO 206
698      TEMP2=C6(J1N)
699      GO TO 208
700      205 TEMP2=0.D0
701      GO TO 208
702      206 TEMP2=C6(101)
703      DO 207 JJ=102,J1N
704      TEMP2=TEMP2+1.D0/DFLOAT(JJ)
705      207 CONTINUE
706      208 CONTINUE
707      T2=T3(J)*(TEMP1+TEMP2)
708      T2R=DABS(DREAL(T2))
709      T2I=DABS(DIMAG(T2))
710      75 S2=S2-T2
711      S2R=DABS(DREAL(S2))
712      S2I=DABS(DIMAG(S2))
713      IF(T2K.GT.ERR*S2K) GO TO 78
714      IF(T2I.LE.ERR*S2I) GO TO 76
715      78 I=I+1
716      IF(I.GT.101.AND.JFLAG.EQ.0)GO TO 81
717      IF(I.GT.101.AND.JFLAG.NE.0)GO TO 82
718      T3(I)=-T3(I-1)*EX/((EN+C1(I-1))*C1(I-1))
719      IZZZ=I
720      GO TO 77

```

```

721      76 B2=S2*C(10)
722      IF(N.EQ.0) GO TO 55
723      S1=DCMPLX(0.0D,0.0D)
724      T1=-C(10)/ZHS
725      LUP=N-1
726      IF(LUP.EQ.0) GO TO 72
727      DO 70 LL=1,LUP
728      70 T1=T1*DFLOAT(LL)
729      S1=S1+T1
730      DO 71 LL=1,LUP
731      T1=T1*EX/(DFLOAT(LL)*DFLOAT(LUP-LL+1))
732      71 S1=S1+T1
733      GO TO 73
734      72 S1=S1+T1
735      73 B2=B2+S1
736      GO TO 55
737      55 IF(NFLAG.LT.0)B=A*B
738      BX=DREAL(B)
739      BY=DMAG(B)
740      BXA=DABS(BX)
741      BYA=DABS(BY)
742      IF(ZX.EQ.0.D0.OR.ZY.EQ.0.D0)NF=1
743      IF(NFLAG.NE.2.AND.BXA.LT.BYA.AND.NF.EQ.1) BX=0.D0
744      IF(NFLAG.NE.2.AND.BYA.LT.BXA.AND.NF.EQ.1)BY=0.D0
745      GO TO(56,57,58,59),N
746      6 ARG=X-EN*C(2)-C(3)
747      CF=CDCOS(ARG)
748      SF=C(6)*CDCSIN(ARG)
749      FNS=C1(4)*EN*EN
750      I=0
751      S1=DCMPLX(1.0D,0.0D)
752      S2=DCMPLX(0.0D,0.0D)
753      U=DCMPLX(1.0D,0.0D)
754      T1S=1.D0
755      S=CF
756      18 I=I+1
757      V=-(FNS-C5(I))/(C(7)*X*C3(I))*U
758      U=V*(FNS-C4(I))/(C2(I)*X)
759      US=CDABS(U)
760      IF(US.GT.T1S) GO TO 20
761      12 CONTINUE
762      T=U*CF+V*SF
763      TR=DABS(DREAL(T))
764      TI=DMAG(DIMAG(T))
765      S=S+T
766      SR=DABS(DREAL(S))
767      SI=DABS(DIMAG(S))
768      IF(TR.GT.ERR*SR) GO TO 24
769      IF(TI.LE.ERR*SI) GO TO 26
770      24 T1=U
771      T2=V
772      S1=S1+T1
773      S2=S2+T2
774      T1S=US
775      17 IF(I-100)18,25,25
776      20 IF(I.EQ.1) GO TO 12
777      IF(JFLAG.GT.0) GO TO 23
778      JFLAG=1
779      GO TO 8
780      23 WRITE(6,1002)
781      29 CONTINUE
782      STOP
783      26 CONTINUE
784      SQZ=CDSSQRT(X)
785      IF(DREAL(SQZ).LT.0.D0)SQZ=-SQZ
786      CCHOSES PROPER BRANCH FOR SQUARE ROOT
787      B=C(4)/SQZ*S
788      IF(KFLAG.EQ.2)B=A*B
789      IF(KFLAG.EQ.3)B=B/A
790      IF(M.EQ.3)M=2
791      IF(M.NE.2)GO TO 55
792      B2=C(4)/SQZ*(SF*(S1+U)/C(6)-CF*(S2+V)*C(6))
793      IF(KFLAG.EQ.2)B2=(B2+CDCOS(C(1)*EN)*CI*B)/A
794      IF(KFLAG.EQ.3)B2=(B2-CDCSIN(C(1)*EN)*CI*B)*A
795      GO TO 55
796      25 IF(JFLAG.GT.0)GO TO 28
797      JFLAG=1
798      GO TO 8
799      28 WRITE(6,1002)
800      GO TO 29

```

```

801      58 B1=DCMPLX(BX,BY)
802      M=4
803      EN=-EN
804      GO TO 3
805      59 B1T=DCMPLX(BX,BY)
806      EN=-EN
807      ARG=C(1)*EN
808      B2=(CDCOS(ARG)*B1-B1T)/CDSIN(ARG)
809      DB1=B1
810      DB2=B2
811      RETURN
812      57 IF(NFLAG.EQ.-1)B2=A*B2
813      DB2=B2
814      56 DB1=DCMPLX(BX,BY)
815      RETURN
816      END
817      SUBROUTINE DGAMM(DZ,DGM,DPS,ERR,JJ)
818      CIF JJ=0, CALCULATES ONLY GAMMA FUNCTION, IF JJ=1, CALCULATES ONLY PSI
819      CFUNCTION, IF JJ=2, CALCULATES BOTH
820      IMPLICIT REAL*8(A-H,O-Z)
821      CCOMPLEX#16 GAM,Z,DZ,DGM,DPS,DPSI
822      COMPLEX #16 TERM1,ZT1,TERM,SUM,ZLG,ZTGAM,ZT
823      COMPLEX#16 CDLOG,DCMPLX,CDEXP,COSIN
824      REAL#8 DREAL,DIMAG,DLOG,DABS
825      INTEGER#4 IDINT
826      DIMENSION B(10)
827      DIMENSION C(100)
828      DATA IFLAG /0/
829      1001 FORMAT(1H //,,24H SERIES DID NOT CONVERGE)
830      1010 FORMAT(1H //,,47H THIS IS A SINGULAR POINT OF THE GAMMA FUNCTION)
831      X,,5X,6HARG R=,E12.5,3X,6HARG I=,E12.5)
832      IF(JJ.EQ.0)GO TO 60
833      DPS=DPS1(DZ,ERR)
834      IF(JJ.EQ.1)RETURN
835      60 E=ERR
836      IF(E.LE.0.D0)E=.1D-07
837      ZX=DREAL(DZ)
838      ZY=DIMAG(DZ)
839      Z=0Z
840      IF(ZX.LT.0.D0)Z=-Z
841      NFLAG=2
842      J=0
843      CK=NUMBER OF TERMS IN SERIES
844      IF(ZY.EQ.0.D0.AND.(IDINT(ZX)-ZX).EQ.0.D0) NFLAG=1
845      IF(NFLAG.EQ.1.AND.ZX.LE.0.D0)NFLAG=0
846      CNFLAG=0 MEANS Z=0 OR Z A NEGATIVE INTEGER NFLAG=1 MEANS Z A POSITIVE
847      IF(NFLAG.NE.0)GO TO 51
848      WRITE(6,1010) DZ
849      DGM=DCMPLX(0.0D0,0.0D0)
850      RETURN
851      51 IF(NFLAG.EQ.2)GO TO 42
852      IF(ZX.GT.2.0D0) GU TO 55
853      DGM=DCMPLX(1.0D0,0.0D0)
854      RETURN
855      55 IF(ZX.GT.20.0D0)GU TO 42
856      IF=IDINT(ZX)-1
857      IJ=1
858      DO 300 N=2,IF
859      300 IJ=IJ+N
860      DGM=IJ
861      RETURN
862      42 CONTINUE
863      IF(IFLAG.NE.0)GU TO 20
864      DO 100 I=1,100
865      100 C(I)=I
866      PI=3.141592653589793D0
867      PI2=DLOG(2.0D0*PI)/2.0D0
868      B(1)=1.0D0/12.0D0
869      B(2)=-1.0D0/360.0D0
870      B(3)=1.0D0/1260.0D0
871      B(4)=-1.0D0/1680.0D0
872      B(5)=1.0D0/1188.0D0
873      B(6)=-691.0D0/360360.0D0
874      B(7)=1.0D0/156.0D0
875      B(8)=-3617.0D0/122400.0D0
876      B(9)=43867.0D0/244188.0D0
877      B(10)=-174611.0D0/125400.0D0
878      CB(I) ARE THE BERNOULLI COEFFICIENTS IN STIRLING'S FORMULA
879      IFLAG=1
880      20 ZT=Z

```

```

881      ZT1=ZT-1.00
882      I=0
883      5 IF(DREAL(ZT).GT.10.0D0) GO TO 3
884      4 I=I+1
885      IF(I.LE.100) GO TO 30
886      WRITE (6,1001)
887      STOP
888      30 CONTINUE
889      ZT=ZT+1.00
890      GO TO 5
891      3 IF=I
892      ZLG=CDLOG(ZT)
893      SUM=(ZT-.5 D0)*ZLG -ZT+PI2
894      TERM1=SUM
895      ATER1R=DABS(DREAL(TERM1))
896      ATERII=DABS(DIMAG(TERM1))
897      J=0
898      8 J=J+1
899      TERM=B(J)*CDEXP(-(2.0D0*C(J)-1.0D0)*ZLG)
900      ATERR=DABS(DREAL(TERM))
901      ATERI=DABS(DIMAG(TERM))
902      SUM=SUM+TERM
903      ASUHR=DABS(DREAL(SUM))
904      ASUM1=DABS(DIMAG(SUM))
905      IF(ATERR.GT.ATER1R)GO TO 24
906      IF(ATERI.GT.ATERII)GO TO 24
907      IF(ASUHR.EQ.0.0D0)GO TO 9
908      IF(ATERR/ASUHR.GT.E1)GO TO 27
909      9 CONTINUE
910      IF(ASUM1.EQ.0.0D0) GO TO 6
911      IF(ATERI/ASUM1.LE.E1)GO TO 6
912      27 CONTINUE
913      ATER1R=ATERR
914      ATERII=ATERI
915      GO TO 7
916      24 CONTINUE
917      7 IF(J.LT.10)GO TO 8
918      GO TO 4
919      6 ZTGAM=SUM
920      IF(IF.EQ.0)GO TO 31
921      DO.200 K=1,IF
922      200 ZTGAM=ZTGAM-CDLOG(ZT1+C(K))
923      31 GAM=CDEXP(ZTGAM)
924      IF(ZX.LT.0.D0)GAM=-PI/(GAM*CDSIN(PI*Z)*Z)
925      DGM=GAM
926      RETURN
927      END
928      COMPLEX FUNCTION DPSI#16(Z,E)
929      IMPLICIT COMPLEX#16 (A-H,O-Z)
930      COMPLEX#16 CDEXP,CDLOG,COCOS,CDSIN,DCMPLX
931      REAL#8 DATAN2,DFLOAT,DABS,CDABS
932      REAL#8 E,ERR,B,ABTER,ABTER1,ABSUMI,PI,ZX,ZY,ZXI,EN,EUL,DREAL,DIMAG
933      INTEGER#4 IDINT
934      DIMENSION B(10)
935      DATA IFLAG /0/
936      ERR=E
937      IF(ERR.LE.0.D0)ERR=.1D-5
938      ZP=Z
939      ZT=Z
940      ZX=DREAL(ZP)
941      ZY=DIMAG(ZP)
942      NI=IDINT(ZX)
943      ZXI=DFLOAT(NI)-ZX
944      IF(ZY.NE.0.0D0.OR.ZX.GT.0.0D0.OR.ZXI.NE.0.0D0)GO TO 1
945      DPSI=DCMPLX(0.0D0,0.0D0)
946      WRITE (6,1010) Z
947      RETURN
948      CCALCULATE PSI HERE IF Z IS A POSITIVE INTEGER
949      1 IF(ZY.NE.0.0D0.OR.ZXI.NE.0.0D0)GO TO 2
950      EUL=-.5772156649
951      DPSI=EUL
952      IF(NI.EQ.1)RETURN
953      NF=NI-1
954      DO 100 N=1,NF
955      100 DPSI=DPSI+1.0D0/DFLOAT(N)
956      RETURN
957      2 ISIGN=0
958      IF(ZX.LT.0.D0)ISIGN=1
959      IF(ISIGN.EQ.1)ZT=1.0D0-ZT
960      CREFLECTS Z INTO 1-Z IF Z IS IN LEFT-HALF PLANE

```

```

961      ZS=ZT
962      NR=0
963      IF(IFLAG.NE.0)GO TO 3
964      PI=DATAN2(0.0D0,-1.0D0)
965      B(1)=1.0D0/(2.0D0*6.0D0)
966      B(2)=-1.0D0/(4.0D0*30.0D0)
967      B(3)=1.0D0/(6.0D0*42.0D0)
968      B(4)=-1.0D0/(8.0D0*30.0D0)
969      B(5)=5.0D0/(10.0D0*66.0D0)
970      B(6)=-691.0D0/(12.0D0*2730.0D0)
971      B(7)=7.0D0/(14.0D0*6.0D0)
972      B(8)=-3617.0D0/(16.0D0*510.0D0)
973      B(9)=43867.0D0/(18.0D0*798.0D0)
974      B(10)=-174611.0D0/(20.0D0*330.0D0)
975      IFLAG=1
976      3 IF((NR+NI).GT.10)GO TO 4
977      NR=NR+1
978      GO TO 3
979      CINCREASES REAL PART OF Z UNTIL GREATER THAN 10
980      4 ZT=ZT+DFLOAT(NR)
981      ZL=CDLOG(ZT)
982      TER1=.5D0/ZT
983      SUM=ZL-TER1
984      ABTER1=CDABS(TER1)
985      N=0
986      8 N=N+1
987      EN=DFLOAT(N)
988      TER=-B(N)*CDEXP(-2.0D0*EN*ZL)
989      ABTER=CDABS(TER)
990      IF(ABTER.LT.ABTER1)GO TO 5
991      NR=NR+1
992      ZT=ZS
993      IF(NR.LT.100)GO TO 4
994      WRITE(6,1011)
995      RETURN
996      5 SUM=SUM+TER
997      ABSUMI=DABS(DIMAG(SUM))
998      IF(ABSUMI.NE.0.0D0)GO TO 6
999      IF(ABTER/CDABS(SUM).LE.ERR)GO TO 7
1000     GO TO 9
1001     6 IF(DABS(DREAL(TER))/DABS(DREAL(SUM)).LE.ERR.AND.DABS(DIMAG(TER))/
1002         1ABSUMI.LE.ERR)GO TO 7
1003     9 ABTER1=ABTER
1004     GO TO 8
1005     7 DPSI=SUM
1006     IF(NR.EQ.0) GO TO 10
1007     DO 200 N=1,NR
1008     200 DPSI=DPSI-1.0D0/(ZT-DFLOAT(N))
1009     10 IF(ISIGN.EQ.0)RETURN
1010     ARG=PI*ZP
1011     DPSI=DPSI-PI*CDCOS(ARG)/CDSIN(ARG)
1012     RETURN
1013     1010 FORMAT(1H ,/,45H THIS IS A SINGULAR POINT OF THE PSI FUNCTION,/,,
1014     130X,6HARG R=,1PE12.5,3X,6HARG I=,E12.5)
1015     1011 FORMAT(1H ,/,24H SERIES DID NOT CONVERGE)
1016     END

```

\*\*\*\*\*  
SAMPLE RUN WITH THE SAMPLE DATA-(A) GIVEN IN THE PROGRAM-(B)  
\*\*\*\*\*

\* SCATTERING OF ACOUSTIC WAVES \*  
\* BY THE CYLINDERS OF ARBITRARY CROSS-SECTION \*  
\* (( T-MATRIX FORMULATION )) \*

\*\* PROGRAM-(B): EVALUATION OF THE NEAR AND FAR FIELD SOLUTIONS \*\*

B.C. TYPE : NEUMANN (RIGID INCLUSION)

CROSS-SECTION OF THE SCATTERER : CIRCULAR

RADIUS : 1.000

SYMMETRY CONDITION (W.R.T. X-AXIS) : SYMMETRIC

WAVE TYPE : ACOUSTIC PLANE WAVE

WAVE NO : .5

TOT.DIM. OF THE T-MATRIX USED : 10 X 10

1- ANGLE OF INCIDENCE: 0. (DEGREES)

\*\* FAR-FIELD SCATTERED FIELD AMPLITUDE \*\*

ANGLE	REAL PART	IMAGINARY PART	PEAK VALUE (NORM)
0.	-.09037	.20340	.22257
10.	-.08940	.19733	.21663
20.	-.08650	.17936	.19913
30.	-.08178	.15024	.17106
40.	-.07536	.11116	.13430
50.	-.06746	.06365	.09275
60.	-.05831	.00955	.05909
70.	-.04820	-.04914	.06883
80.	-.03742	-.11038	.11655
90.	-.02632	-.17211	.17411
100.	-.01523	-.23242	.23292
110.	-.00448	-.28955	.28958
120.	.00560	-.34196	.34201
130.	.01470	-.38835	.38863
140.	.02255	-.42765	.42825
150.	.02892	-.45903	.45994
160.	.03361	-.48186	.48303
170.	.03648	-.49572	.49707
180.	.03745	-.50037	.50177

• 63+000+

二〇

—

28

卷之三

+ 0

100

— 1 —

- 1 -

I  
21-222

10

I

四  
三

卷之三

1

卷之三

I

-21+000+

卷一

I

- .42 +000 +

10

— 1 —

10

CHECK FOR THE CONVERGENCE OF THE  
TOTAL SCATTERING CROSS-SECTION

**ORDER TOT.S.C SECTION (%) DIFFERENCE**

1	.2639208-001	
2	.9030308-001	.2421598+003
3	.9037284-001	.7724488-001
4	.9037284-001	.8410429-005
5	.9037284-001	.2313573-009

REGION : \*BOUNDARY\*

\*\* VELOCITY POTENTIALS DUE TO SCATTERED FIELD \*\*

ANGLE	REAL PART	IMAGINARY PART	PEAK VALUE (NORM)
0.	-0.33923	.35750	.49283
10.	-0.33271	.35061	.48334
20.	-0.31365	.32998	.45526
30.	-0.28357	.29578	.40975
40.	-0.24481	.24841	.34877
50.	-0.20040	.18868	.27524
60.	-0.15368	.11792	.19371
70.	-0.10805	.03809	.11457
80.	-0.06651	.04822	.08215
90.	-0.03143	-.13796	.14150
100.	-0.00426	-.22779	.22783
110.	.01458	-.31436	.31470
120.	.02558	-.39458	.39541
130.	.03006	-.46583	.46680
140.	.02984	-.52608	.52692
150.	.02693	-.57393	.57456
160.	.02325	-.60852	.60897
170.	.02037	-.62941	.62974
180.	.01930	-.63638	.63668

.72+000+

I  
I  
I  
I  
I  
I

.48+000+

I  
I  
I  
I  
I  
I

\*\*\*\*\*

.24+000+

I  
I  
I  
I  
I  
I

\*\* \*\*

.12-007+

I  
I  
I  
I  
I  
I

\* \* \*

-.24+000+

I  
I  
I  
I  
I  
I

\* \* \*

-.48+000+

I  
I  
I  
I

\* \* \*

-----+-----+-----+-----+-----+-----+-----+-----+

-.64+000 - .32+000 - .37-008 .32+000 .64+000 .96+000

REGION : 5.0

## \*\* VELOCITY POTENTIALS DUE TO SCATTERED FIELD \*\*

ANGLE	REAL PART	IMAGINARY PART	PEAK VALUE (NORM)
0.	-.08886	-.09388	.12926
10.	-.08608	-.09226	.12620
20.	-.07785	-.08758	.11718
30.	-.06448	-.08000	.10275
40.	-.04648	-.06992	.08396
50.	-.02453	-.05780	.06279
60.	.00056	-.04420	.04420
70.	.02790	-.02967	.04073
80.	.05656	-.01480	.05847
90.	.08559	-.00009	.08559
100.	.11408	.01397	.11493
110.	.14118	.02701	.14374
120.	.16615	.03871	.17060
130.	.18832	.04886	.19455
140.	.20716	.05730	.21494
150.	.22224	.06393	.23125
160.	.23323	.06869	.24313
170.	.23991	.07155	.25035
180.	.24215	.07251	.25277

.25+000+

I

I

I

I

I

I

I

I

I

I

I

I

I

I

I

I

I

I

I

I

I

I

I

I

I

I

I

I

I

I

I

I

I

I

I

I

I

I

I

I

I

I

I

I

I

I

I

I

I

I

I

I

I

I

I

I

I

I

I

I

I

I

I

I

I

I

I

I

I

I

I

I

I

I

I

I

I

I

I

I

I

I

I

I

I

I

I

I

I

I

I

I

I

I

I

I

I

I

I

I

I

I

I

I

I

I

I

I

I

I

I

I

I

I

I

I

I

I

I

I

I

I

I

I

I

I

I

I

I

I

I

I

I

I

I

I

I

I

I

I

I

I

I

I

I

I

I

I

I

I

I

I

I

I

I

I

I

I

I

I

I

I

I

I

I

I

I

I

I

I

I

I

I

I

I

I

I

I

I

I

I

I

I

I

I

I

I

I

I

I

I

I

I

I

I

I

I

I

I

I

I

I

I

I

I

I

I

I

I

I

I

I

I

I

I

I

I

I

I

I

I

I

I

I

I

I

I

I

I

I

I

I

I

I

I

I

I

I

I

I

I

I

I

I

I

I

I

I

I

I

I

I

I

I

I

I

I

I

I

I

I

I

I

I

I

I

I

I

I

I

I

I

I

I

I

I

I

I

I

I

I

I

I

I

I

I

I

I

I

I

I

I

I

I

I

I

I

I

I

I

I

I

I

I

I

I

I

I

I

I

I

I

I

I

I

I

I

I

I

I

I

I

I

I

I

I

I

I

I

I

I

I

I

I

I

I

I

I

I

I

I

I

I

I

I

I

## BIBLIOGRAPHY

1. Waterman, P.C., "New Formulation of Acoustic Scattering", J. Acoust. Soc. Amer., Vol. 45, pp. 1417-1429, 1969.
2. Morse, P.M. and Feshbach, H., Methods of Theoretical Physics. New York: McGraw-Hill Book Co., 1953.
3. Bouwkamp, C.J., "Diffraction Theory", Reports on Progress in Physics, Vol. 17, pp. 35-100, 1954.
4. Yeh, C., "Scattering of Acoustic Waves by Penetrable Prolate Spheroids", J. Acoust. Soc. Amer., Vol. 42, pp. 518-521, 1967.
5. Burke, J.E., "Scattering by Penetrable Spheroids", J. Acoust. Soc. Amer., Vol. 43, pp. 871-875, 1968.
6. Harrington, R.F., Field Computation by Moment Methods. New York: The MacMillan Co., 1968, pp. 1-21.
7. Gerjuoy, E., and Saxon, D.S., "Variational Principles for the Acoustic Field", The Physical Review, Vol. 94, pp. 1445-1458, 1954.
8. Hildebrand, F.B., Methods of Applied Mathematics, 2nd ed., Englewood Cliffs, N.J.: Prentice-Hall Inc., 1965, pp. 222-294.
9. Banaugh, R.P., and Goldsmith, W., "Diffraction of Steady Acoustic Waves by Surfaces of Arbitrary Shape", J. Acoust. Soc. Amer., Vol. 35, pp. 1590-1601, 1963.
10. Andreasen, M.G., "Scattering From Parallel Metallic Cylinders With Arbitrary Cross Sections", IEEE Trans. Antennas Propagation, Vol. 12, pp. 746-754, 1964.
11. Andreasen, M.G., "Scattering From Bodies of Revolution", IEEE Trans. Antennas Propagation, Vol. 13, pp. 303-310, 1965.
12. Pao, Y.-H. in Off-Prints From Modern Problems in Elastic Wave Propagation. (Edited by Miklowitz, J. and Achenbach, J.D.) New York: John Wiley and Sons Inc., 1978, pp. 123-144.

13. Varadan, V.V., "Scattering Matrix for Elastic Waves II. Application to Elliptic Cylinders", J. Acoust. Soc. Amer., Vol. 63, pp. 1014-1024, 1978.
14. Varadan, V.V., and Varadan, V.K., "Low-Frequency Expansion for Acoustic Wave Scattering Using Waterman's T-Matrix Method", J. Acoust. Soc. Amer., Vol. 66, pp. 586-589, 1979.
15. Su, J.-H., Varadan, V.V., and Varadan, V.K., "Acoustic Wave Scattering by a Finite Elastic Cylinder in Water", J. Acoust. Soc. Amer., Vol. 68, pp. 686-691, 1980.
16. van den Berg, P.M., "Transition Matrix in Acoustic Scattering by a Strip", J. Acoust. Soc. Amer., Vol. 70, pp. 615-619, 1981.
17. Rudenko, O.V., and Soluyan, S.I., Theoretical Foundations of Nonlinear Acoustics. New York: Consultants Bureau, 1977, pp. 5-7.
18. Sokolnikoff, I.S., and Redheffer, R.M., Mathematics of Physics and Modern Engineering. New York: McGraw-Hill Book Co., 1966, p. 399.
19. Abramowitz, M., and Stegun, I.A., Handbook of Mathematical Functions. New York: Dover Publications, Inc., 1965, p. 360, p. 886.
20. Waterman, P.C., "Matrix Theory of Elastic Wave Scattering", J. Acoust. Soc. Amer., Vol. 60, pp. 567-580, 1976.
21. Waterman, P.C. in Computer Techniques for Electromagnetics. (Edited by Mittra, R.) Oxford: Pergamon Press, 1973, pp. 97-157.
22. Chu, L.L., Aşkar, A. and Çakmak, A.S., "An Approximate Method for Scattering in Elastodynamics - the Born Approximation II: SH-Waves in Infinite and Half Space", Soil Dynamics and Earthquake Engineering, Vol. 1, No. 3, pp. 102-116, 1982.

## REFERENCES NOT CITED

- Baker, B.B., and Copson, E.T., The Mathematical Theory of Huygens' Principle. London: Oxford University Press, 1950.
- Datta, S.K., "Diffraction of SH-Waves by an Elliptic Elastic Cylinder", Int. J. Solids Struct., Vol. 10, pp. 123-133, 1974.
- Lindsay, R.B., Mechanical Radiation. New York: McGraw-Hill Book Co., 1960.
- McLachlan, N.W., Bessel Functions For Engineers. London: Oxford University-Clarendon Press, 1955.
- Pao, Y.-H. and Mow, C.C., Diffraction of Elastic Waves and Dynamic Stress Concentrations. New York: Crane and Russak Co., 1973.
- Tsao, S.J., Varadan, V.V., and Varadan, V.K., "T-Matrix Approach to Scattering of Elastic (SH) Waves by an Inclined Surface Void", J. App. Mech., 1983, Vol. 50, pp. 143-148.
- Varatharajulu, V., "Reciprocity Relations and Forward Amplitude Theorems for Elastic Waves", J. Mathematical Physics, Vol. 18, pp. 537-543, 1977.